Design, synthesis and biological evaluation of new polyamine derivatives as antikinetoplastid agents

Elodie Jagu

NNT : 2016SACLS589

THESE DE DOCTORAT
DE
L'UNIVERSITE PARIS-SACLAY
PREPAREE A
L'UNIVERSITE PARIS-SUD

ECOLE DOCTORALE N°571
Sciences chimiques : molécules, matériaux, instrumentation et biosystèmes (2MIB)
Spécialité de doctorat : Chimie

Par

Mlle Elodie Jagu

Design, synthesis and biological evaluation of new polyamine derivatives as antikinetoplastid agents

Thèse codirigée par Casimir Blonski[1], présentée et soutenue à Orsay, le 25 Novembre 2016 :
[1]Directeur de Recherche, ICMMO, Université Paris-Sud

Composition du Jury :

Mme Delphine Joseph, Professeure, Université Paris-Sud	Présidente
Mme Elisabeth Davioud-Charvet, Directeur de Recherche, Université de Strasbourg	Rapporteur
M. Patrice Le Pape, Professeur, Université de Nantes	Rapporteur
M. Olivier Russo, Docteur, Laboratoires Servier	Examinateur
M. Jean-Christophe Cintrat, Docteur CEA Saclay	Examinateur
M. Philippe Loiseau, Professeur, Université Paris-Sud	Directeur de thèse
M. Raphaël Labruère, Docteur, Université Paris-Sud	Invité

DOCTORAL THESIS OF THE UNIVERSITE PARIS-SACLAY

Design, synthesis and biological evaluation of new polyamine derivatives as antikinetoplastid agents

By Elodie JAGU

Doctoral thesis of:
Organic Chemistry, Medicinal Chemistry

Ecole doctorale n°571:
Sciences chimiques : molécules, matériaux, instrumentation et biosystèmes

Thesis committee members:

Prof. Elisabeth DAVIOUD-CHARVET Reviewer
Prof. Patrice LE PAPE Reviewer
Prof. Delphine JOSEPH Examiner
Dr. Olivier RUSSO Examiner
Dr. Jean-Christophe CINTRAT Examiner
Prof. Philippe LOISEAU Thesis co-supervisor
Dr. Raphaël LABRUERE Thesis co-supervisor

Table of contents

List of abbreviations

^{13}C-NMR	Carbon Nuclear Magnetic Resonance
^{1}H-NMR	Proton Nuclear Magnetic Resonance
AdoMet	S-adenosylmethionine
AdoMetDC	S-adenosylmethionine decarboxylase
Boc	*tert*-Butyloxycarbonyl
BOC-ON	2-(*tert*-butoxycarbonyloxyimino)-2-phenylacetonitrile
Cbz	Carboxybenzyl
CHO	Chinese hamster ovary
CoA	Coenzyme A
CP	Cysteine protease
AZ	Antizyme
DAB	1,4-diaminobutan-2-one
DBS	Dibenzosuberyl
DCC	*N,N'*-Dicyclohexylcarbodiimide
DCM	dichloromethane
DFMO	α-difluoromethylornithine
DMF	dimethylformamide
DNA	Deoxyribonucleic acid
Fmoc	Fluorenylmethoxycarbonyl
GR	Gluthatione reductase
HAT	Histone acetyltransferase
HOBt	Hydroxybenzotriazole
IC_{50}	Half maximal inhibitory concentration
K_i	Inhibitory constant
LdHAT1	Histone acetyltransferase from *Leishmania donovani*
MANT	(2'-(or-3')-O-(N-Methylanthraniloyl)

CPM	7-diethylamino-3-(4’maleimidylphenyl)-4-methylcoumarin
NADPH	Nicotinamide adenine dinucleotide phosphate
DTNB	5,5'-dithiobis-(2-nitrobenzoic acid)
NTD	Neglected tropical diseases
ODC	Ornithine decarboxylase
NTB	2-nitro-5-thiobenzoate
PAO	Polyamine oxidase
Pmc	2,2,5,7,8-pentamethyl-chromane-6-sulphonyl
PSV	Polyamine sequestred vesicle
PTS	Polyamine transport system
Put	Putrescine
RNA	Ribonucleic acid
rt	room temperature
SSAT	spermine N^1-acetyltransferase
SI	Selectivity Index
SOD	Superoxide dismutase
Spd	Spermidine
Spm	Spermine
THF	Tetrahydrofurane
THTT	1,3,5-thiadiazinane-2-thione
TryR	Trypanothione reductase
TryS	Trypanothione synthetase
TS_2	Trypanothione disulfide form
$T(SH)_2$	Trypanothione dithiol form
SpdS	Spermidine synthetase
SpmS	Spermine synthetase

Résumé de thèse

Ce projet d'interface Chimie/Biologie repose sur les expertises complémentaires de deux équipes. D'une part le laboratoire de Chimie Bioorganique et Bioinorganique de l'Institut de Chimie Moléculaire et des Matériaux d'Orsay et d'autre part le laboratoire de Chimiothérapie antiparasitaire de la Faculté de Pharmacie Châtenay-Malabry. Lors de cette thèse, les deux équipes ont participé à la conception, la synthèse, l'étude et le développement d'inhibiteurs dirigés contre les Kinétoplastidés (trypanosomes, leishmanies). Ces protozoaires sont des parasites pathogènes de l'homme transmis par le biais d'une piqure d'insecte. Ils provoquent respectivement la trypanosomose et la leishmaniose et sont responsables d'environ 120 000 morts par an à travers le monde. Les médicaments actuellement utilisés sont en nombre limité et sont, pour la plupart, à un haut niveau de toxicité. De plus, les parasites présentent de plus en plus de résistances aux composés utilisés. Il est donc urgent de développer de nouvelles stratégies thérapeutiques pour répondre à la chimiorésistance et à la toxicité des médicaments actuellement utilisés contre ces parasites. Ces dernières années, il a été démontré que le métabolisme des polyamines chez les Kinétoplastidés était essentiel, il constitue donc une cible thérapeutique d'intérêt.

Cette thèse décrit dans une partie bibliographique, l'ensemble des dérivés polyamines synthétisés à ce jour comme agents antikinétoplastides potentiels, ainsi que leurs activités biologiques. Le projet intègre l'élaboration et la synthèse de nouveaux dérivés putrescine, spermidine ou spermine. Dans un premier temps, la protection sélective des polyamines est effectuée par un groupement protecteur *tert*-butylcarbonate (Boc). Puis les différentes polyamines protégées sont couplées à des conjugués de type Acyl- ou Aryl- via des procédures de couplage variées. Les composés synthétisés sont évalués sur des modèles *in vitro* de leishmaniose et de trypanosomose africaine pour déterminer leur activité biologique. D'autre part, une évaluation enzymatique spécifique des parasites, pourra permettre une éventuelle identification de la cible. L'histone acétyltransférase de *Leishmania donovani*, identifiée comme cible potentielle a été produite au laboratoire et a montré une activité, cependant les critères

de pureté pour une étude enzymologique n'ont pas été atteints. Par ailleurs, l'activité des composés a été évaluée sur la trypanothione reductase (TryR) de trypanosome, grâce à la collaboration de l'équipe du Professeur Luise Krauth-Siegel à Heidelberg. En effet, cette enzyme est une cible fréquente des dérivés polyamines retrouvées dans la littérature. Enfin, l'adressage intraparasitaire de polyamines a été abordé *via* les transporteurs des polyamines. En effet, l'équipe développe des sondes polyamines fluorescentes afin de mettre au point un essai de compétition avec les composés utilisant le transporteur de polyamine chez ces parasites. Cinq sondes polyamine portant un motif fluorophore nitrobenzoxadiazole ont donc été synthétisées. Ces sondes ont ensuite été étudiées en microscopie fluorescente dans le laboratoire du Professeur Michael Barett à Glasgow. Et enfin essais de compétition entre ces composés et de la spermidine radiomarquée au tritium ont été effectués au CEA de Saclay dans l'équipe du Dr Jean-Christophe Cintrat. La dernière partie de ce manuscrit présente donc la stratégie mise en œuvre et l'avancée des travaux sur ce sujet.

Au total, cinquante-quatre dérivés polyamines ont été synthétisés et évalués *in vitro*. Certains présentent des activités de l'ordre du micromolaire contre *Trypanosoma brucei gambiense* et une sélection du composé le plus prometteur a été effectuée afin de l'évaluer ultérieurement *in vivo* sur souris infectées par des trypanosomes. D'autre part, chez *Leishmania donovani*, quelques composés ont démontré une efficacité contre les formes amastigotes intramacrophagiques de l'ordre de 3 µM, ce qui est encourageant pour le développement de ces dérivés. Les études enzymatiques sur la Trypanothione Réductase ont permis d'apporter des élements de pistes pour l'identification de la cible potentielle de ces composés. Les retombées sociétales concernent à la fois la santé humaine et animale par le développement potentiel de nouveaux médicaments antiparasitaires.

Introduction

This project is at the interface of chemistry and biology and relies on the complementary expertise of two different teams. On one hand, the laboratoire de Chimie Bioorganique et Bioinorganique of the Institut de Chimie Moléculaire et des Matériaux d'Orsay, and on the other hand, the laboratoire de Chimiothérapie antiparasitaire of the Faculté de Phamarcie Châtenay-Malabry. In this thesis, the two components are involved in the design, synthesis, study and development of inhibitors directed against Kinetoplastid (trypanosomes, leishmania). The protozoan parasites are the causative agents of severe diseases such as African trypanosomiasis, Chagas disease or Leishmaniasis. These are devastating infections that carry a considerable health burden on poor population. Treatment of trypanosome and leishmania relies on a small number of drugs which mostly have a limited efficacy and high level of toxicity. It is therefore urgent to develop new therapeutic strategies to address drug resistance and toxicity of currently used drugs. In recent years, the study of polyamines in medicinal chemistry for drug discovery against Kinetoplastid has been intensified. Indeed, it has been shown that the metabolism and transport of polyamines was essential in parasites, these are therapeutic targets of interest against the Kinetoplastids.

This PhD manuscript has been organized into five chapters. The first chapter of this manuscript introduces the targeted Kinetoplastid. This chapter will be the major content of a review, which will be submitted shortly. In this chapter, I gathered all the polyamine derivatives which have been reported for antikinetoplastids activity in the literature. In particular, we have decided to maintain the compounds described in this PhD in this introductive chapter. Although this choice may appear rather singular in the context of a PhD introduction, we considered that it was compulsory to legitimate the organization of the review. To facilitate its location in the text, our own work will appear highlighted in another color in this chapter. It begins with an introduction on Kinetoplastids, the diseases caused and the treatment currently used. Then, it is organized around three main parts which are diamine, triamine and tetramine derivatives. Each part includes the description of the series of molecules, the IC_{50} of the best, and in vivo results when

available. We have additionally discussed in this part the structure-activity relationships of these derivatives.

The second chapter of this PhD manuscript describes the project from the origin and the main objectives of this work are presented. Each series of designed molecules are shown as well as the biological analysis carried out.

The third chapter of this PhD manuscript includes the main text of the published article: Elodie Jagu, Rachid Djilali, Sébastien Pomel, Florence Ramiandrasoa, Stéphanie Pethe, Raphaël Labruère, Philippe M Loiseau, Casimir Blonski. Design, synthesis and in vitro antikinetoplastid evaluation of *N*-acylated putrescine, spermidine and spermine derivatives. *Bioorganic and Medicinal Chemistry Letter* **2015**, *25*, 207. This article is preceded by the description of the synthesis of selectively protected polyamines which are not included in the publication.

The fourth chapter of this PhD manuscript reports the two different series of aryl-polyamine that we have prepared. The first part of this chapter is about the hydroxybenzotriazole derivatives which are the object of an accepted publication: Elodie Jagu, Sébastien Pomel, Alba Diez-Martinez, Florence Ramiandrasoa, Stéphanie Pethe, Casimir Blonski, Raphaël Labruère, Philippe M Loiseau. Synthesis and in vitro antikinetoplastid activity of polyamine-hydroxybenzotriazole conjugates. *Bioorganic and Medicinal Chemistry*. The second part presents a series of bisbenzyl-polyamines compound that we have designed as potent antikinetoplastids.

The fifth chapter of this PhD manuscript addresses the development of a novel method for the determination of polyamine derivatives uptake *via* the polyamine transporter. This chapter introduces: i) literature on polyamine transporter into Kinetoplastids and principle of the assay; ii) the synthesis of fluorescent polyamine probes; iii) experiments performed with fluorescence or radiolabelled assays. Indeed, a fluorescent assay could be beneficial since it is a straight forward method to quantify uptake of polyamine derivatives through active transport.

This PhD manuscript ends up with a general conclusion and the evocation of the perspectives of this work.

Chapter 1: Antikinetoplastid chemotherapy and the place of polyamine-based analogs as antikinetoplastid agents.

I. Introduction

1. *Kinetoplastidae and current therapy*

The Kinetoplastids represent a class of parasitic protists responsible for three distinct human diseases: African Trypanosomiasis (African sleeping sickness), Chagas disease, and the different forms of leishmaniasis. The main distinguishing feature of this group is a subcellular structure known as the kinetoplast. The kinetoplast is a mitochondrial structure containing circular DNA.[1] At least one stage in the life cycle of all members of this group is represented by a slender and highly flexible cell equipped with one or two flagella. The size of the kinetoplastid cell varies from about 10 to 100 micrometers in length, and never exceeds 20 micrometers in width.

Human African Trypanosomiasis also known as sleeping sickness, is transmitted to human host by the bite of tsetse fly which has been infected before from infected humans or animals. This disease is caused by two subspecies of *Trypanosoma brucei* and mostly present in the rural areas of the sub-Saharan Africa. The region is economically depressed and politically unstable making difficult the estimation of the total number of cases.[2] Parasite develops in the blood and provokes fevers, headaches. After few weeks, the parasite attacks the central nervous system, and confusion, poor coordination and sleep disturbance appear as the main symptoms, hence called as sleeping sickness. The disease is fatal if untreated, and five drugs are clinically available, melarsoprol, suramin, pentamidine, eflornithine (α-difluoromethylornithine) and nifurtimox (Figure 1). The first three were discovered more than half a century ago. Melarsoprol

[1] Povelones, M. L. *Mol. Biochem. Parasitol.* **2014**, *196*, 53–60.

[2] Auty, H.; Morrison, L. J.; Torr, S. J.; Lord, J. *Trends Parasitol.* **2016**, *32*, 608–621

is the only compound existing for late-stage infection, it is an arsenic derivative with a high toxicity and only administrable by injection which is painful for the patient and fatal encephalopathy occurs in up to 5% of individuals getting this drug.[3]

Chagas disease (South American Trypanosomiasis) is caused by *Trypanosoma cruzi* and is prevalent in south of America where *Triatominae* or kissing bugs, are the insect vectors. The disease is composed of two stages, an acute stage directly after infection and a chronic stage which could develop over many years. Often, the first stage is asymptomatic or displays non specific symptoms like fever, headache, and fatigue. The chronic stage affects the nervous system, digestive system and heart causing cardiomyopathy, severe weight loss and mental disruption. The drugs currently used are limited to benznidazole and nifurtimox (Figure 1). However, it has been shown that treatments are more effective in acute stage.[4] However, both of these drugs produce significant side effects that can include anorexia, vomiting, neuropathy or psychic disturbances.

Leishmaniasis is caused by different species of *Leishmania* responsible for three clinic forms: visceral leishmaniasis, cutaneous leishmaniasis, and mucocutaneous leishmaniasis.[5] Visceral form represents the severest form of the disease since it affects the internal organs, and is caused by *L. infantum* and *L. donovani*. It has been reported that more than 90% of these cases of infection are found in India and Sudan.[6] When untreated, it is fatal in almost all cases. Visceral leishmaniasis is present in South Europe.[7] *Leishmania amazonensis* and *Leishmania mexicana* are responsible for the cuteanous form. *Leishmania* has two developmental stages, the promastigote form which replicates in the gut of the insect and the amastigote form which infect macrophages in the mammalian host.[8] Axenic amastigotes can be obtained in culture by

[3] Singh Grewal, A.; Pandita, D.; Bhardwaj, S.; Lather, V. *Curr. Top. Med. Chem.* **2016**, *16*, 2245–2265.
[4] Paucar, R.; Moreno-Viguri, E.; Pérez-Silanes, S. *Curr. Med. Chem.* **2016.**
[5] Van Assche, T.; Deschacht, M.; da Luz, R. A. I.; Maes, L.; Cos, P. *Free Radic. Biol. Med.* **2011**, *51*, 337–351.
[6] Singh, V. P.; Ranjan, A.; Topno, R. K.; Verma, R. B.; Siddique, N. A.; Ravidas, V. N.; Kumar, N.; Pandey, K.; Das, P. *Am. J. Trop. Med. Hyg.* **2010**, *82*, 9–11.
[7] Dujardin, J.-C.; Campino, L.; Cañavate, C.; Dedet, J.-P.; Gradoni, L.; Soteriadou, K.; Mazeris, A.; Ozbel, Y.; Boelaert, M. *Emerg. Infect. Dis.* **2008**, *14*, 1013–1018.
[8] Liévin-Le Moal, V.; Loiseau, P. M. *FEBS J.* **2016**, *283*, 598–607.

exposing promastigotes in vitro to high temperature and acidic pH.[9] Their transformation into amastigote-like parasites can be brought about with cellular changes, and these changes include expression of specific stage proteins on their surface, for example, amastin. Some drugs are available to treat leishmaniasis, including pentavalent antimonials such as meglumine antimoniate, sodium stibogluconate, amphotericin B, miltefosine, paromomycin, and pentamidine (Figure 1).[10] Most of these treatments produce serious side effects including vomiting, anaemia, anorexia, renal failure. In addition, drug resistance represents a major challenge in fighting *Leishmania* parasites and is a cause of serious concern. From 5 to 70% of patients in endemic areas do not respond to the aforementioned drugs.

[9] D Zilberstein; Shapira, and M. *Annu. Rev. Microbiol.* **1994**, *48*, 449–470.

[10] Hussain, H.; Al-Harrasi, A.; Al-Rawahi, A.; Green, I. R.; Gibbons, S. *Chem. Rev.* **2014**, *114*, 10369–10428.

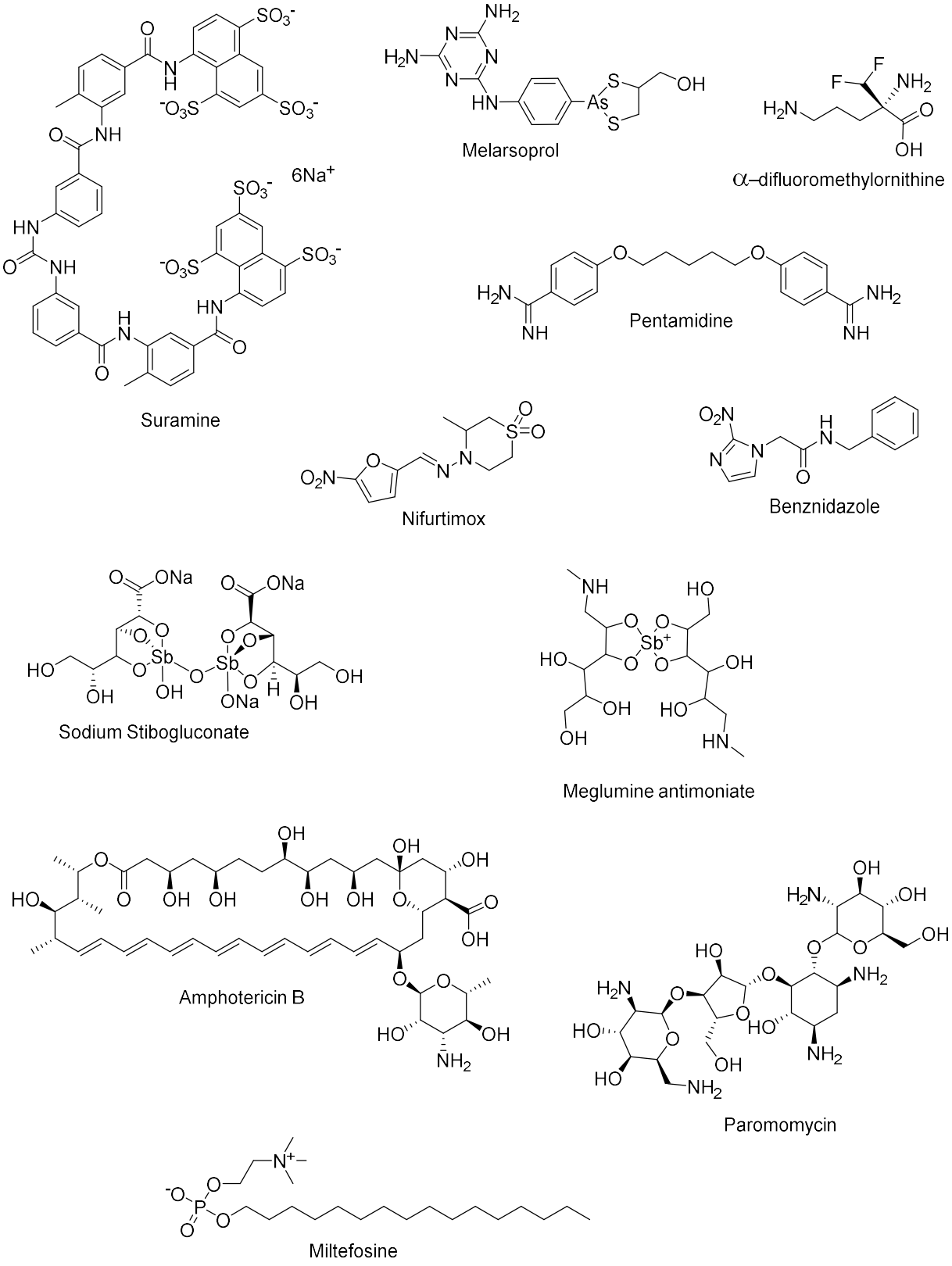

Figure 1: Present antikinetoplastids drugs.

2. *Biological targets for chemotherapy*

The present therapies rely on a small number of drugs, most of which are inadequate because of severe host toxicity.[11] In addition, the development of new treatments is necessary due to the emergence of drug resistance.[12,13] These parasitic diseases are part of Neglected Tropical Diseases (NTDs). NTDs affect hundreds of millions of people worldwide, and they are called neglected diseases because they primarily affect poor people in poor regions of the world. Therefore, they are unattractive to the pharmaceutical industry in discovering and developing new drugs because they do not represent viable economic entities. Nevertheless, the lack of any potential for a "blockbuster drug" has resulted in major challenges to government, academic and nonprofit agencies dedicated to the discovery, development and launch of new therapy for neglected diseases. In drug discovery, the identification of pertinent drug targets in a biological pathway plays a key role for the development of new and original leads. While many molecular targets had been tested, identified and validated, or eliminated, new technological advancements have allowed the screening of large libraries that will lead up to new structurally diverse compounds and will help identifying new critical targets.

Some of these kinetoplastid targets are listed below:

Kinases. Typanosomatids genomes encode for a large number of protein kinases. Therefore, the kinases family represents a rich family of potential biological targets for antikinetoplastid agents provided that there are enough differences with those from the host.[14]

Sterol Biosynthetic Pathway. The sterol biosynthetic pathway can also include promising targets because some sterols such as ergosterol are present in Kinetoplastids and absent in the mammalian host.[15]

---

[11] Metcalf, B. W.; Bey, P.; Danzin, C.; Jung, M. J.; Casara, P.; Vevert, J. P. *J. Am. Chem. Soc.* **1978**, *100*, 2551–2553.

[12] Stijlemans, B.; Caljon, G.; Van Den Abbeele, J.; Van Ginderachter, J. A.; Magez, S.; De Trez, C. *Front. Immunol.* **2016**, *7*, 233.

[13] Medina, N. P.; Mingala, C. N. *Ann. Parasitol.* **2016**, *62*, 11–15.

[14] Merritt, C.; Silva, L. E.; Tanner, A. L.; Stuart, K.; Pollastri, M. P. *Chem. Rev.* **2014**, *114*, 11280–11304.

[15] Lepesheva, G. I.; Waterman, M. R. *Curr. Top. Med. Chem.* **2011**, *11*, 2060–2071.

Purine Salvage Pathway. The parasitic protozoa, lack the enzymes to synthesize purine nucleotides de novo, therefore, they have to be contingent of the purine salvage system to use purine bases from their mammalian hosts. Nucleoside transporters uptake these metabolites through the parasite cell surface.[16]

Proteinases. There are four types of proteinases: aspartate, cysteine, serine, and metalloenzymes. In parasitic protozoa, the cysteine proteineases (CPs) are the most carefully identified and characterized. These enzymes have an important role in host cell-parasite interactions and are structurally different enough from their mammalian homologues to be used for the design of inhibitors.[17]

Folate Biosynthesis. The folate pathway is a drug target for antileishmanial agents. It is important for parasite growth, and enzymes such as thymidylate synthase and dihydrofolate reductase are involved in their biosynthesis and have obvious relevance as drug targets. These two enzymes are also implicated in the synthesis of thymine and deoxythymidine monophosphate (dTMP) and some compounds have been identified as inhibitors.[18]

Topoisomerases. DNA topoisomerases are enzymes who play an important role in many essential processes, like DNA transcription, replication, repair, and recombination. For this reason, topoisomerases represent a valuable potential as drug target.[19] DNA topoisomerase I have been characterized in *L. donovani* and *T. cruzi*, and some inhibitors of this enzyme exist such as, camptothecin, sodium stibogluconate and urea stibamine.

Superoxide dismutase (SOD). In order to detoxify the reactive oxygen species, Kinetoplastids could use different enzymatic mechanisms. The super oxide dismutase (SOD) has been found in a high level in Leishmania promastigote.[20] Moreover, SOD has been demonstrated as essential

[16] Chawla, B.; Madhubala, R. *J. Parasit. Dis. Off. Organ Indian Soc. Parasitol.* **2010**, *34*, 1–13.
[17] O'Brien, T. C.; Mackey, Z. B.; Fetter, R. D.; Choe, Y.; O'Donoghue, A. J.; Zhou, M.; Craik, C. S.; Caffrey, C. R.; McKerrow, J. H. *J. Biol. Chem.* **2008**, *283*, 28934–28943.
[18] Hardy, L. W.; Matthews, W.; Nare, B.; Beverley, S. M. *Exp. Parasitol.* **1997**, *87*, 157–169.
[19] Das, B. B.; Ganguly, A.; Majumder, H. K. *Adv. Exp. Med. Biol.* **2008**, *625*, 103–115.
[20] Meshnick, S. R.; Eaton, J. W. *Biochem. Biophys. Res. Commun.* **1981**, *102*, 970–976.

for parasite infection and growth.[21,22] Thus, development of selective inhibitors of this enzyme can be achieved since parasite's SOD is different from its host enzyme.

Trypanothione pathway. Trypanothione plays a key role against oxidative stress in Kinetoplastids, as it is vital in maintaining the cellular redox potential and thus it is essential for parasite survival. Trypanothione synthesis and its regeneration are catalyzed by two enzymes, namely, trypanothione synthetase (TryS) and trypanothione reductase (TryR). TryS catalyzes trypanothione synthesis from two molecules of glutathione and one spermidine. Trypanothione is then maintained in its reduced form by the enzyme TryR in the presence of NADPH. Thus, trypanothione pathway is a promising target against parasite and many lead compounds that inhibit TryR have been identified including polyamine derivatives as it will be described in this chapter.

Polyamine Pathway. As discussed above, the synthesis of trypanothione required spermidine molecule as precursor. Indeed, polyamines are essential for parasitic growth and survival and it have been proved that polyamine homoeostasis may also be an important drug target.[23] Parasites are able to biosynthesize them or uptake them from extracellular space by transport system, as a function of the parasite species.

3. *Kinetoplastid polyamine metabolism as a drug target*

Polyamines are low molecular weight aliphatic polycations, highly charged and ubiquitously present in all living cells. Interest has been increasing during the last 30 years in the naturally abundant polyamines *putrescine* **1** (diamine), *spermidine* **2** (triamine) and *spermine* **3** (tetramine), which were demonstrated to be involved in a large number of cellular processes (Figure 2). For example, polyamines participate in modulation of chromatin structure, gene transcription and translation, DNA stabilization, signal transduction, cell growth and proliferation, migration, membrane stability, functioning of ion channels and receptor-ligand

[21] Ghosh, S.; Goswami, S.; Adhya, S. *Biochem. J.* **2003**, *369*, 447–452.
[22] Longoni, S. S.; Sánchez-Moreno, M.; López, J. E. R.; Marín, C. *Comp. Immunol. Microbiol. Infect. Dis.* **2013**, *36*, 499–506.
[23] Birkholtz, L.-M.; Williams, M.; Niemand, J.; Louw, A. I.; Persson, L.; Heby, O. *Biochem. J.* **2011**, *438*, 229–244.

interactions. There is equilibrium between polyamines that are bound to different polyanionic molecules (mainly DNA and RNA) and free polyamines. Only the free intracellular polyamines are available for immediate cellular need and therefore are subject to strict regulation. This regulation is achieved at four levels: *de novo* synthesis, interconversion, terminal degradation and transport. Putrescine, spermidine and spermine are the polyamines contained in mammalian and kinetoplastids tissue but a wider spectrum of natural polyamines exists in other organisms.

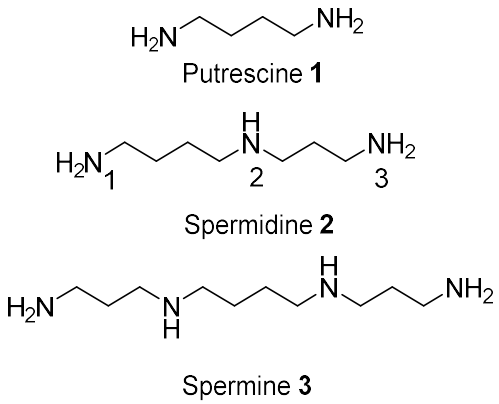

Figure 2: Most important natural polyamines.

Even if the mechanism of polyamine transport is poorly understood, the polyamine biosynthetic enzymes from the human have been well characterized at the biochemical and structural levels.[24,25] Because of the necessity to the tumor cell to use profusely polyamines, their metabolism and transport have been studied in the search for anticancer compounds. However, the success of polyamine conjugates in anticancer therapeutic approaches has been limited, with no drug accepted for clinical use. Clinical trials have been undertaken with only a few compounds. The most famous one is DFMO (α-difluoromethylornithine or eflornithine), an inhibitor of ornithine decarboxylase (ODC). Unfortunately, this inhibitor was ineffective when used alone. This was probably due to the sophisticated regulatory mechanisms enabling cells to

[24] Wallace, H. M.; Fraser, A. V.; Hughes, A. *Biochem. J.* **2003**, *376*, 1–14.
[25] Thomas, T.; Thomas, T. J. *Cell. Mol. Life Sci. CMLS* **2001**, *58*, 244–258.

adapt to considerable changes of extra and intracellular polyamines concentrations.[26] The difficulties encountered in interfering with polyamine metabolism of mammalian cells are a source of optimism for parasitologists involved in drug discovery. Polyamine metabolism in mammalian cells and in parasites showed marked differences (Figure 3), making this pathway a good target for the development of new active compounds against trypanosomatids.[27] Although DFMO is unapplicable in cancer therapy, this compound is approved for the treatment of African trypanosomiasis in combination therapy (nifurtimox) only against *T. b. gambiense*.[28]

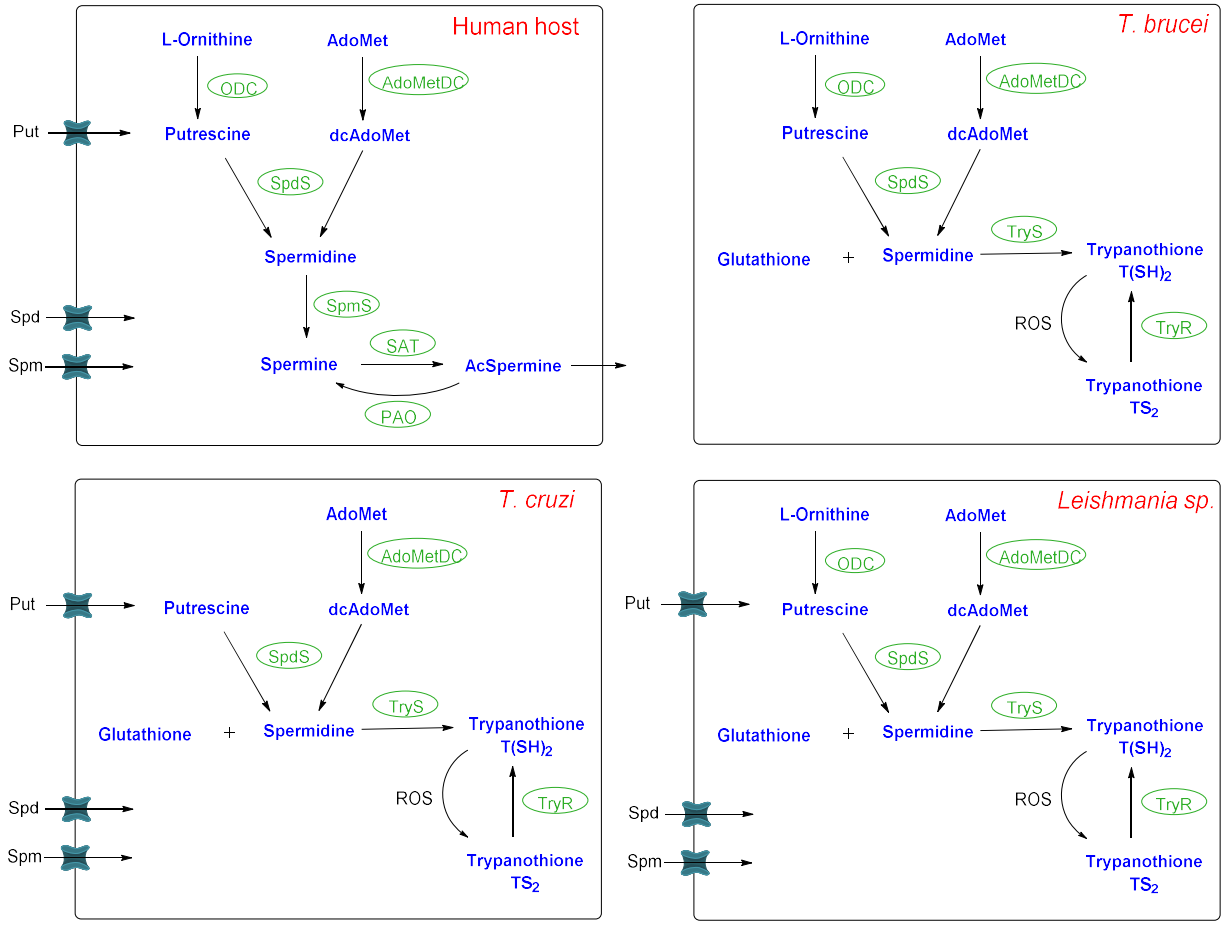

Figure 3: Polyamine metabolism and polyamine transport in Kinetoplastids compared to those in the human host. AcSpermine: acetylated spermine; AdoMet: S-adenosylmethionine; AdoMetDC: S-adenosylmethionine decarboxylase; dcAdoMet: decarboxylated S-adenosylmethionine; ODC: ornithine decarboxylase; PAO: polyamine oxidase; Put: putrescine; ROS: reactive oxygen species; SAT: spermine N^1-acetyltransferase; Spd: spermidine; SpdS: spermidine synthetase; Spm: spermine; SpmS; spermine synthetase; TryR: trypanothione reductase; TryS: trypanothione synthetase; $T(SH)_2$: reduced trypanothione; TS_2: oxidized trypanothione.

[26] Seiler, N.; Heby, O. *Acta Biochim. Biophys. Hung.* **1988**, *23*, 1–35.

[27] Heby, O.; Persson, L.; Rentala, M. *Amino Acids* **2007**, *33*, 359–366.

[28] Wang, C. C. *Annu. Rev. Pharmacol. Toxicol.* **1995**, *35*, 93–127.

Putrescine is synthesized in parasites from L-ornithine by ornithine decarboxylase (ODC) (except for *T. cruzi*). Then, putrescine gives spermidine via spermidine synthase (SpdS) and S-adenosylmethionine decarboxylase (AdoMetDC). Association of two glutathione molecules with a molecule of spermidine leads to trypanothione under dithiol form via the trypanothione synthetase (TryS). The enzyme spermine synthetase (SpmS) is not present in Kinetoplastids, whereas it allows to synthetize spermine de novo in humans.[29] Trypanosomatids have a unique thiol-based redox metabolism, depending on trypanothione as their principal thiol, in contrast with their human host, which utilizes glutathione.[30] Structural analogs are considered to be compounds with high potential for interfering with polyamine metabolism with expected application in the treatment of diseases caused by parasitic Kinetoplastids.

II. Putrescine and diamine derivatives

Putrescine is one of the first substrate in the biosynthetic pathway of polyamines, making it an important molecule for Kinetoplastid and an interesting starting point for drug research. Specific organisms also contain other natural diamine such as 1,3-diaminopropane and cadaverine (1,5-diaminopentane). In this part, putrescine analogs are gathered with unnatural diamines having shorter or longer carbon chain displaying antikinetoplastid activity. Numerous putrescine and other diamines derivatives have been studied for their trypanocidal activity.

1. Alkyl- and acyl-diamines analogs

The putrescine analog, 1,4-diaminobutan-2-one (DAB, Figure 4) **4**, inhibited *T. cruzi* epimastigotes proliferation in vitro with an IC_{50} of 118 µM and produced remarkable mitochondrial destruction and cell architecture disorganization.[31] The mitochondria seems to be the main target of **4**, and **4** possibly binds to the polyamine transporter at the parasite surface. The putrescine transport and, its subsequent metabolism to spermidine and trypanothione are essential for the conservation of mitochondrial structure and function. This ketone derivative

[29] Bacchi, C. J.; Nathan, H. C.; Hutner, S. H.; McCann, P. P.; Sjoerdsma, A. *Science* **1980**, *210*, 332–334.
[30] Fairlamb, A. H.; Cerami, A. *Annu. Rev. Microbiol.* **1992**, *46*, 695–729.
[31] Menezes, D.; Valentim, C.; Oliveira, M. F.; Vannier-Santos, M. A. *Parasitol. Res.* **2006**, *98*, 99–105.

showed in vitro activity on *Leishmania amazonensis* at a concentration of 144 µM and reduced by 50% concentration of the putrescine into the parasite.[32] Likewise, **4**-treated parasites showed severe damage of their mitochondria structure and function. **4** inhibited ODC activity and putrescine uptake, however, pre-treatment of 24h with **4** led to compensatory intracellular putrescine concentration, which could be due to an adaptive mechanism in parasites. Aside from that, diamines having a central chain ranging from 2 to 6 carbons were linked at only one extremity to different alkyl moieties.[33] The *N*-dodecyl-putrescine analog **5** (Figure 4) has an IC_{50} = 0.53 µM against intracellular amastigotes of *L. chagasi* but was ten times less active against intracellular amastigotes of *L. amazonensis* (IC_{50} = 5.13 µM). However, the corresponding ethylenediamine **6** (Figure 4) was active against both intracellular amastigotes of *L. amazonensis* (IC_{50} = 0.94 µM) and *L. chagasi* (IC_{50} = 0.26 µM). Several *N*-alkyl substituted propylenediamines were synthesized and directly evaluated on hamster infected by *L. donovani*.[34] Piperidine and morpholine derivatives, **7** and **8** (Figure 4) respectively, displayed poor antileishmanial in vivo activity. Nonetheless, their corresponding guanidine-1,3-biscarbomethoxy derivatives **9** and **10** have different behaviors since **9** was not active and **10** led to 80% reduction of amastigotes count in the hamster spleen on day 7 after treatment.

[32] Vannier-Santos, M. A.; Menezes, D.; Oliveira, M. F.; de Mello, F. G. *Microbiol. Read. Engl.* **2008**, *154*, 3104–3111.

[33] da Costa, C. F.; Coimbra, E. S.; Braga, F. G.; dos Reis, R. C. N.; da Silva, A. D.; de Almeida, M. V. *Biomed. Pharmacother.* **2009**, *63*, 40–42.

[34] Kumar, V. V.; Singh, S. K.; Sharma, (Late) S.; Bhaduri, A. P.; Gupta, S.; Zaidi, A.; Tiwari, S.; Katiyar, J. C. *Bioorg. Med. Chem. Lett.* **1997**, *7*, 675–680.

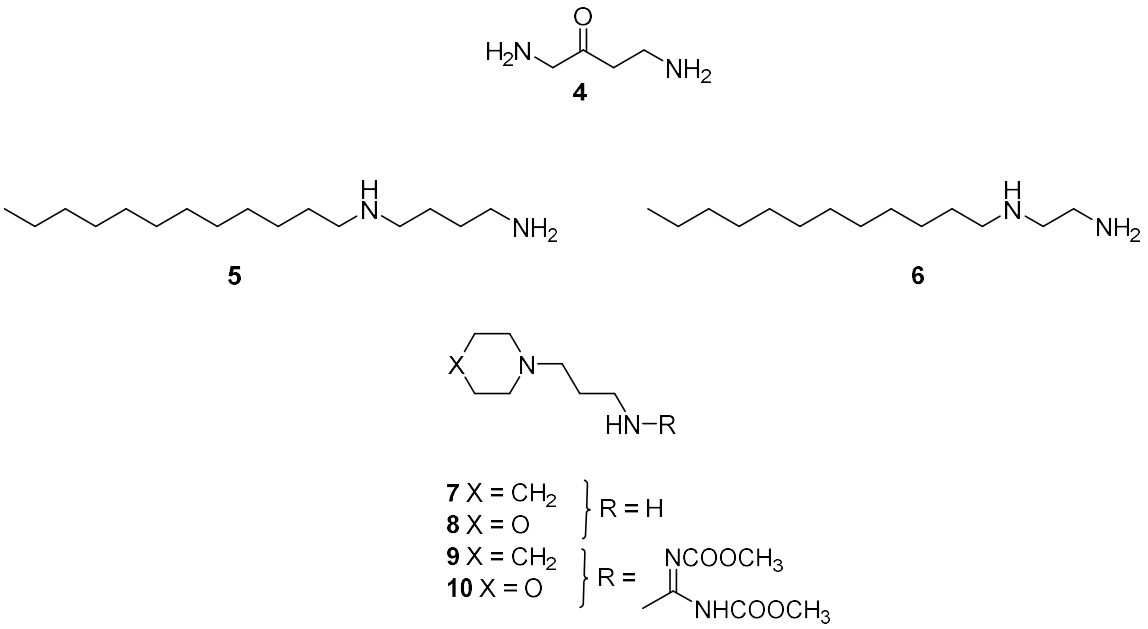

Figure 4: Alkyl-diamine derivatives.

In another study, various diamine monoprotected with *tert*-butyloxycarbonyl (Boc) have been tested in vitro on *Leishmania amazonensis*.[35] Various lengths of carbon chain from 2 carbons to 12 carbons were envisioned. Globally, analogs bearing a longer chain showed higher activity but these derivatives exhibited high cytotoxicity against human hepatoma cells. Once again, the 12-carbon analog, the 1,12-diaminodecane **11** (Figure 5) displayed the best activity with an IC_{50} of 3.78 µM whereas the Boc-protected putrescine **12** was devoid of activity on this strain and also on *T. brucei* and *L. donovani* axenic amastigotes as recently observed in our laboratory.[36] In the latter study, a mono *N*-acylated putrescine, the methoxy acetyl putrescine was inactive on both parasites. Several others mono *N*-acylated diamines were also prepared and tested for antiproliferative activity against *L. amazonensis* and *L. chagasi* (Figure 5).[37] The authors added lipophilic tails to diamines in order to build interaction with the lipidic membrane of the

[35] Pinheiro, A. C.; Rocha, M. N.; Nogueira, P. M.; Nogueira, T. C. M.; Jasmim, L. F.; de Souza, M. V. N.; Soares, R. P. *Diagn. Microbiol. Infect. Dis.* **2011**, *71*, 273–278.

[36] Jagu, E.; Djilali, R.; Pomel, S.; Ramiandrasoa, F.; Pethe, S.; Labruère, R.; Loiseau, P. M.; Blonski, C. *Bioorg. Med. Chem. Lett.* **2015**, *25*, 207–209.

[37] Coimbra, E. S.; Almeida, C. G.; Júnior, W. V.; Dos Reis, R. C. N.; De Almeida, A. C. F.; Forezi, L. S. M.; De Almeida, M. V.; Le Hyaric, M. *ScientificWorldJournal* **2008**, *8*, 752–756.

parasites and therefore facilitate the uptake. Unfortunately, the putrescine linked to the dodecyl chain through an amide bond **13** was not soluble and therefore not tested. Nonetheless, its 10-carbon homologue **14** was barely active (IC_{50} around 10-20 µM) against both strains. These amide analogs were then coupled to linear glucuronic acid in order to increase the solubility of the previous derivatives. A series of ten compounds was then prepared, including ethanamine and putrescine derivatives. All the gluconamides along with the 10- and 12-carbon putrescine analogs, **15** and **16** do not show any activity (Figure 5). In the same study, 7-, 9-, 11- and 13-carbon diamines were linked to a ribonic acid via an amide bond and to either an ethyl or propyl chain to their other amine function. These ribonamides were globally more active than the gluconamides, in particular, the 1,2-diamioethane **17** had an IC_{50} of 2.49 µM against *L. chagasi* in vitro.

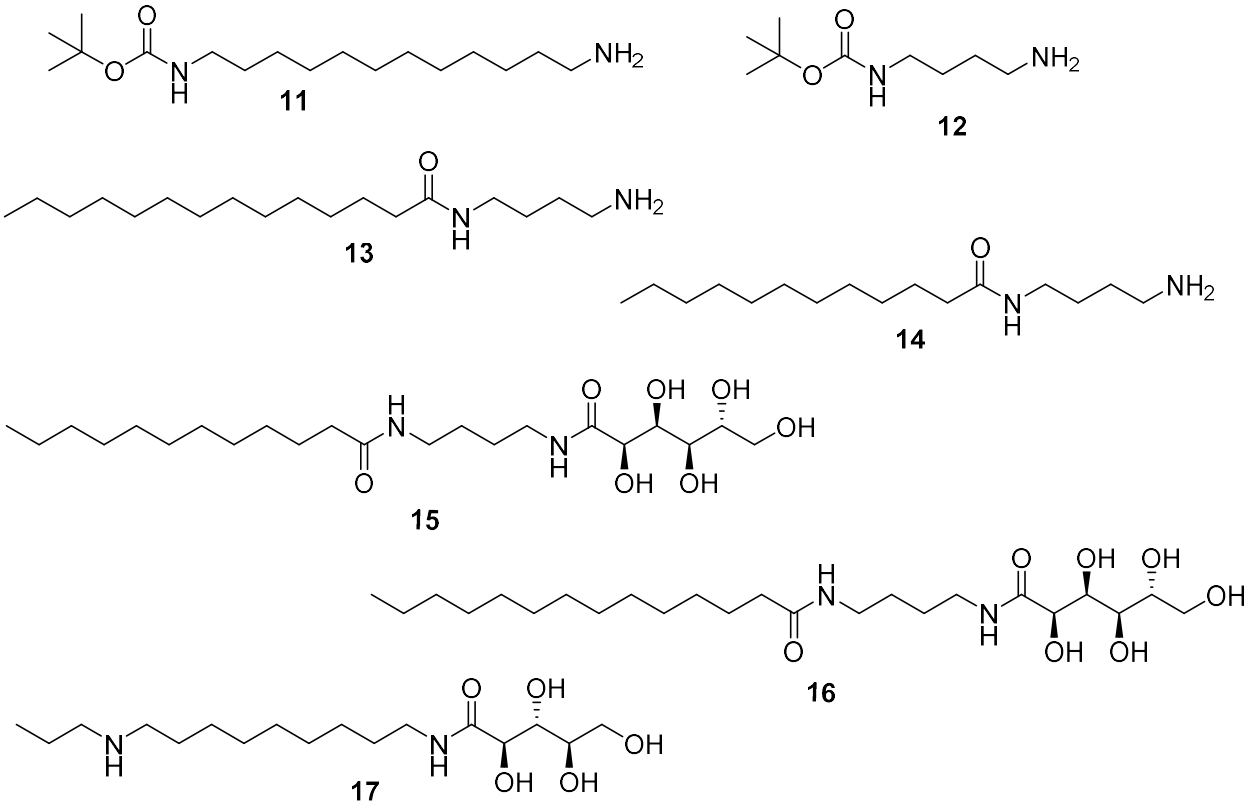

Figure 5: Acyl-diamine derivatives.

Several diamines disubstituted by an alkyl chain on the same nitrogen were also studied such as the *N*,*N*-dibutyl-1,3-propane diamine **18** (Figure 6).[38] This compound had moderate activity on *L. donovani* promastigotes with an IC_{50} of 4.66 µM. Ethylenediamine analogs of this class ramified with a linear tetradecyl chain were tested on promastigote forms of *L. amazonensis*, *L. braziliensis* and *L. donovani*.[39] In this series, the diethyl **19** and the diester **20** (Figure 6) were the most active compounds against the three strains with 80 to 90% of lysis at 10 µg/mL.

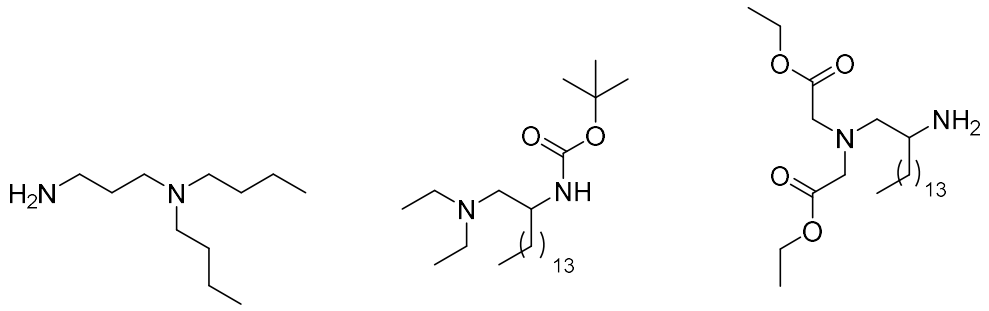

18 19 20

Figure 6: Dialkyl-diamine derivatives.

2. *Aryl- and aroyl-diamines analogs*

Monoaryl-diamines

In the aforementioned study of da Costa et al.[33], two analogs of putrescine, each linked to one pyridyl moiety were synthesized. The ethylenediamine **21** and the propylenediamine **22** (Figure 7) were both inactive in vitro against *L. amazonensis* and *L. chagasi* promastigote forms. In our laboratory, we designed a series of polyamine coupled to one hydroxybenzotriazole ring.[40] Indeed, compound bearing this scaffold displays diverse pharmacological activities often associated with good water solubility and bioavailability as well as limited toxicity. Putrescine **24** was slightly active against *T. b. gambiense* (IC_{50} = 9.5 µM) while its propylenediamine

[38] Labadie, G. R.; Choi, S.-R.; Avery, M. A. *Bioorg. Med. Chem. Lett.* **2004**, *14*, 615–619.

[39] del Olmo, E.; Alves, M.; López, J. L.; Inchaustti, A.; Yaluff, G.; Rojas de Arias, A.; San Feliciano, A. *Bioorg. Med. Chem. Lett.* **2002**, *12*, 659–662.

[40] Jagu, E.; Pomel, S.; Diez-Martinez, A.; Ramiandrasoa, F.; Krauth-Siegel, R. L.; Pethe, S.; Blonski, C.; Labruère, R.; Loiseau, P. M. *Bioorg. Med. Chem.* Accepted.

counterpart **23** was inactive against the same strain. Both diamines **23** and **24** were not able to affect intramacrophage amastigotes of *L. donovani* (Figure 7).

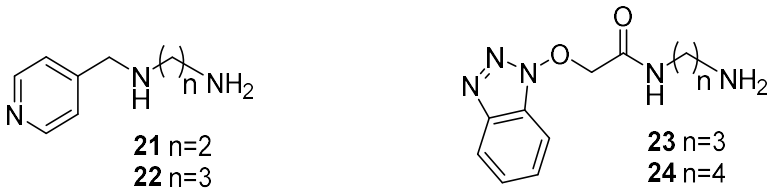

Figure 7: Pyridyl- and hydroxybenzotriazole-diamine derivatives.

A solid-phase approach permitted to synthesize several compounds conjugating quinones and polyamines.[41] Naphthoquinones and anthraquinones have a wide spectrum of anticancer activity, they covalently bind to and intercalate into DNA, inhibit DNA replication and RNA transcription, act as DNA topoisomerase II poisons, produce oxidative stress, and induce DNA breakage and chromosomal aberrations. Moreover, polyaminoquinones have already showed anticancer activity.[42] Lizzi et al.[41] selected 2-phenoxy-anthraquinone (Figure 8) and 2-phenoxy-naphthoquinone in their study. In vitro activity of these compounds was evaluated on various trypanosomes: *T. b. rhodesiense, T. cruzi, L. donovani* promastigotes and axenic amastigotes. Putrescine-anthraquinone conjugate **25** was active against *T. b. rhodesiense* (IC_{50} = 0.35 µM) and *L. donovani* (IC_{50} = 2.82 µM) but was not as efficient against *T. cruzi* (IC_{50} = 18.60 µM) and moreover was cytotoxic at 5.60 µM against rat myoblast L6. The corresponding 5-carbon analog **26**, i.e. the cadaverine-anthraquinone conjugate displayed the same activity as **25** on all of the tested strain except that its activity against *T. b. rhodesiense* was five times better (IC_{50} = 0.07 µM). Therefore, the selectivity index between this parasite and mammalian cells was relatively high (SI = 72). This compound has been evaluated on TryR from *T. cruzi* and happens to be inhibitor of this enzyme with a K_i value of 3.4 µM and was shown to accumulate into the mitochondria of *Leishmania*.

[41] Lizzi, F.; Veronesi, G.; Belluti, F.; Bergamini, C.; López-Sánchez, A.; Kaiser, M.; Brun, R.; Krauth-Siegel, R. L.; Hall, D. G.; Rivas, L.; Bolognesi, M. L. *J. Med. Chem.* **2012**, *55*, 10490–10500.

[42] Bolognesi, M. L.; Calonghi, N.; Mangano, C.; Masotti, L.; Melchiorre, C. *J. Med. Chem.* **2008**, *51*, 5463–5467.

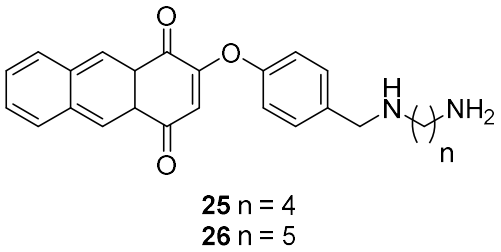

25 n = 4
26 n = 5

Figure 8: Anthraquinone-diamine derivatives with micromolar activity on *T. b. rhodesiense*.

A screening of LOPAC1280 library against TryR of *T. brucei*[43] highlighted the capacity of some tricyclic neuroleptic drug to inhibit the enzyme. One of them, clomipramine (Figure 9) has an IC_{50} = 3.80 µM on TryR of *T. brucei*, and is active against trypanosomes in vivo. Clomipramine **27** has several possible effects on different mechanisms in trypanosomes; it displays an anti-calmonium activity in addition to inhibit TryR. Because of the psychotropic activity of clomipramine, the authors chose to replace the tricyclic ring of clomipramine with the dibenzosuberyl group and the latter group was linked to different polyamines.[44] *N*,*N*-dimethyl-1,2-diaminoethane derivatives **28** and the corresponding diaminopropane derivatives **29** (Figure 9) have shown IC_{50} around 1-2 µM against two strains of *T. b. brucei*. The authors proved that these two diamines were not inhibitors of the TryR from *T. cruzi*.

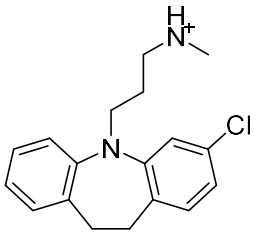

Clomipramine **27**

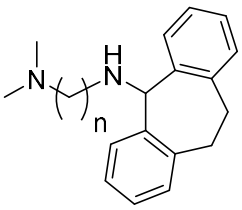

28 n=2
29 n=3

Figure 9: Clomipramine and dibenzosuberyl-diamine derivatives.

[43] Richardson, J. L.; Nett, I. R. E.; Jones, D. C.; Abdille, M. H.; Gilbert, I. H.; Fairlamb, A. H. *ChemMedChem* **2009**, *4*, 1333–1340.

[44] O'Sullivan, M. C.; Durham, T. B.; Valdes, H. E.; Dauer, K. L.; Karney, N. J.; Forrestel, A. C.; Bacchi, C. J.; Baker, J. F. *Bioorg. Med. Chem.* **2015**, *23*, 996–1010.

Bisaryl-diamines

Naphthalimido derivatives have been mostly studied for their antitumoral activity but this scaffold displays some problem of solubility. In order to increase the aqueous solubility, bisnaphthalimidopropyl have been conjugated to polyamine and tested in vitro against *Leishmania infantum*.[45,46] In these studies, four diamines were linked to naphtalimido group through a propyl spacer. The bisnaphtalimido-putrescine derivative **30** (Figure 10) had an IC_{50} of 1-2 µM against *L. infantum* (promastigotes and amastigotes) after 5 days of incubation and was also highly cytotoxic against several cancer cell lines.[47] The authors chose to insert longer alkyl chains in order to avoid the π-π stacking between the two naphthalimido rings and then to improve the aqueous solubility of the derivatives. The 9-carbon diamine homologue **31** (Figure 10) displayed a better activity against the parasite with an IC_{50} of 0.78 µM after only 72 hours of incubation but **31** was also very cytotoxic. The 10-carbon analog of **30** was synthesized but not tested against *L. infantum*.

Acridine-based drugs are well-known to prevent the development of blood-stage malaria parasites[48] but these derivatives were also shown active against trypanosomatids.[49,50] Acridine and its derivatives bind to DNA through intercalation between consecutive nucleotides in the DNA strand. The mode of binding of acridine molecules involves intercalation of the tricyclic ring between adjacent base pairs in the DNA duplex. The acridine moieties are held in place by Van der Waals forces supplemented by stronger ionic bonds to the phosphate ions of the DNA backbone.[51] A series of polyamines bisacridine conjugates has been synthesized and evaluated on several protozoan strains in vitro and cytotoxicity toward different mammalian cells was

[45] Oliveira, J.; Ralton, L.; Tavares, J.; Codeiro-da-Silva, A.; Bestwick, C. S.; McPherson, A.; Thoo Lin, P. K. *Bioorg. Med. Chem.* **2007**, *15*, 541–545.
[46] Tavares, J.; Ouaissi, A.; Lin, P. K. T.; Tomás, A.; Cordeiro-da-Silva, A. *Int. J. Parasitol.* **2005**, *35*, 637–646.
[47] Lin, P. K.; Pavlov, V. A. *Bioorg. Med. Chem. Lett.* **2000**, *10*, 1609–1612.
[48] Hwang, J. Y.; Kawasuji, T.; Lowes, D. J.; Clark, J. A.; Connelly, M. C.; Zhu, F.; Guiguemde, W. A.; Sigal, M. S.; Wilson, E. B.; DeRisi, J. L.; Guy, R. K. *J. Med. Chem.* **2011**, *54*, 7084–7093.
[49] W, O.; C, S.; J, B.; Jp, G.; R, B. *Trop. Med. Parasitol. Off. Organ Dtsch. Tropenmedizinische Ges. Dtsch. Ges. Tech. Zusammenarbeit GTZ* **1995**, *46*, 49–53.
[50] Bonse, S.; Santelli-Rouvier, C.; Barbe, J.; Krauth-Siegel, R. L. *J. Med. Chem.* **1999**, *42*, 5448–5454.
[51] Moloney, G. P.; Kelly, D. P.; Mack, P. *Molecules* **2001**, *6*, 230–243.

assayed as well.[52] The 8-carbon diamines **32** and **33** (Figure 10), respectively bearing either two acridines or two aza-acridine, were the most potent diamino-analogs. Indeed, **32** and **33** were effective at 0.009-0.031 µM against *T. brucei* and moreover **33** was almost not cytotoxic and displayed a selectivity index of 860 between parasite and HL-60 leukemia cells. Both diamines were not active against amastigote forms of *T. cruzi* and *L. major*. However, **32** was more active against *L. donovani* promastigote (99% of parasite death at 10 µM) than **33** (42% of parasite death at 10 µM).

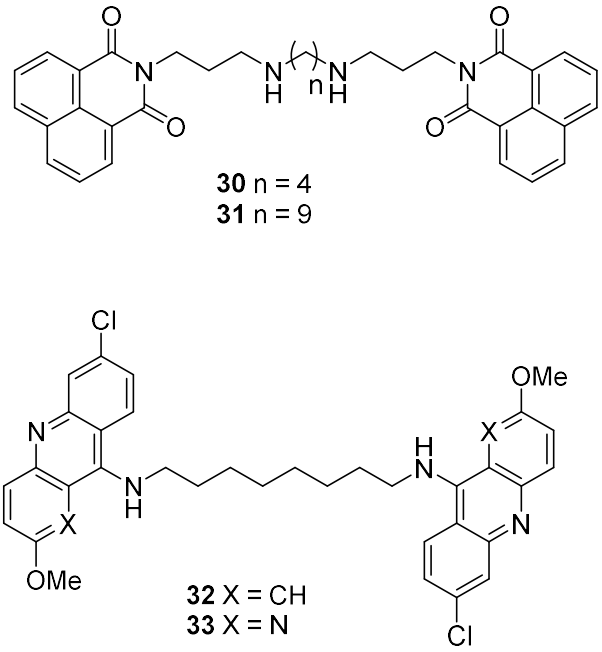

Figure 10: Bisnaphthalimido- and bisacridine-diamines.

In 1985, a bisaryl-diamine was tested on *Crithidia fasciculata* which is not a pathogen Kinetoplastid for human, this organism was thus used as model. N^1,N^6-bis(dihydroxybenzoyl)-1,6-diaminohexane **bisC6DHB 34** (Figure 11) have been identified as an iron-superoxide dismutase (SOD) inhibitor with 80% inhibition at 100 µM.[53] SOD catalyses the conversion of

[52] Caffrey, C. R.; Steverding, D.; Swenerton, R. K.; Kelly, B.; Walshe, D.; Debnath, A.; Zhou, Y.-M.; Doyle, P. S.; Fafarman, A. T.; Zorn, J. A.; Land, K. M.; Beauchene, J.; Schreiber, K.; Moll, H.; Ponte-Sucre, A.; Schirmeister, T.; Saravanamuthu, A.; Fairlamb, A. H.; Cohen, F. E.; McKerrow, J. H.; Weisman, J. L.; May, B. C. H. *Antimicrob. Agents Chemother.* **2007**, *51*, 2164–2172.

[53] Meshnick, S. R.; Kitchener, K. R.; Le Trang, N. *Biochem. Pharmacol.* **1985**, *34*, 3147–3152.

superoxide anions ($O_2^{\cdot -}$) to hydrogen peroxide (H_2O_2). Structurally, crithidial and leishmanial superoxide dismutase is different from the mammalian SOD. The parasite SODs are iron-containing whereas mammalians are either copper, zinc, or manganese-containing enzymes.[54] The iron chelator **34** was demonstrated as a selective and irreversible inhibitor of the parasitic SOD but was not tested in vitro nor in vivo against whole parasites. Twenty years later, a similar structure incorporating the putrescine moiety was assayed in vitro against *T. b. rhodesiense*, *T. cruzi* and *L. donovani* axenic amastigote. Putrescine derivatives **35** (Figure 11) was devoid of activity against *T. cruzi* and *L. donovani* but was fairly active on *T. b. rhodesiense* (IC_{50} = 3.30 µM) and was not cytotoxic against myoblast L6 (IC_{50} = 130 µM).

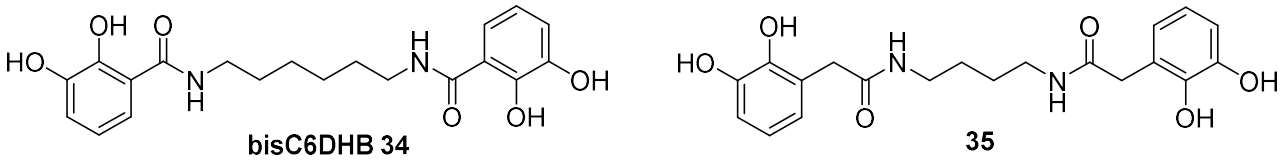

Figure 11: Dihydroxybenzoyl-diamine derivatives.

Recently, Caminos et al.[55] prepared twenty-five symmetric *N*,*N*'-benzyl substituted diamines (Figure 12). The length of the linear chain varied from 3 to 10 carbons and the benzyl moieties were mostly substituted by methoxy and benzyloxy groups. The putrescine bearing 4-benzyloxybenzyl moieties **36** (Figure 12) was the most potent analog in vitro with submicromolar activity against *T. cruzi* epimastigote and nanomolar activity against *T. brucei* and *L. donovani* promastigotes. This compound was cytotoxic against Vero kidney cells (IC_{50} = 5.83 µM) but presented a remarkable effect on *T. cruzi* (IC_{50} = 0.76 µM), the latter parasite being particularly difficult to impair. Globally, the authors observed that a longer central chain provided low antikinetoplastid activity. A vast library of substituted diamines has been achieved by solid support chemistry.[38] A total of 78 compounds have been synthesized and tested against *Leishmania donovani* promastigotes. Diamines used in this study were 1,3-propanediamine or putrescine derivatives substituted at only one extremity of the diamine, which led to unsymmetrical compounds. Essentially the same two dibenzyl moieties were bounded to the

[54] Trant, N. L.; Meshnick, S. R.; Kitchener, K.; Eaton, J. W.; Cerami, A. *J. Biol. Chem.* **1983**, *258*, 125–130.
[55] Caminos, A. P.; Panozzo-Zenere, E. A.; Wilkinson, S. R.; Tekwani, B. L.; Labadie, G. R. *Bioorg. Med. Chem. Lett.* **2012**, *22*, 1712–1715.

diamines but some analogs present two different benzyl groups bore by the same nitrogen. Interestingly, putrescine derivative **37** was 50 times less active than its positional isomer **36** (Figure 12). Increasing the size of the substituent decreased the IC_{50}, showing clearly that the activity was relative to the volume. Thus, the authors focused on the synthesis of 4-benzyloxy derivatives with various substitutions such as aryl, alkyl or halogen. Diamines **38, 39**, **40**, and **41** (Figure 12) were the most active compounds against *L. donovani* with IC_{50} value below 1 µM. It is also remarkable that the 4-carbon diamines, the putrescine analogs, were generally more active than their propylenediamines counterparts.

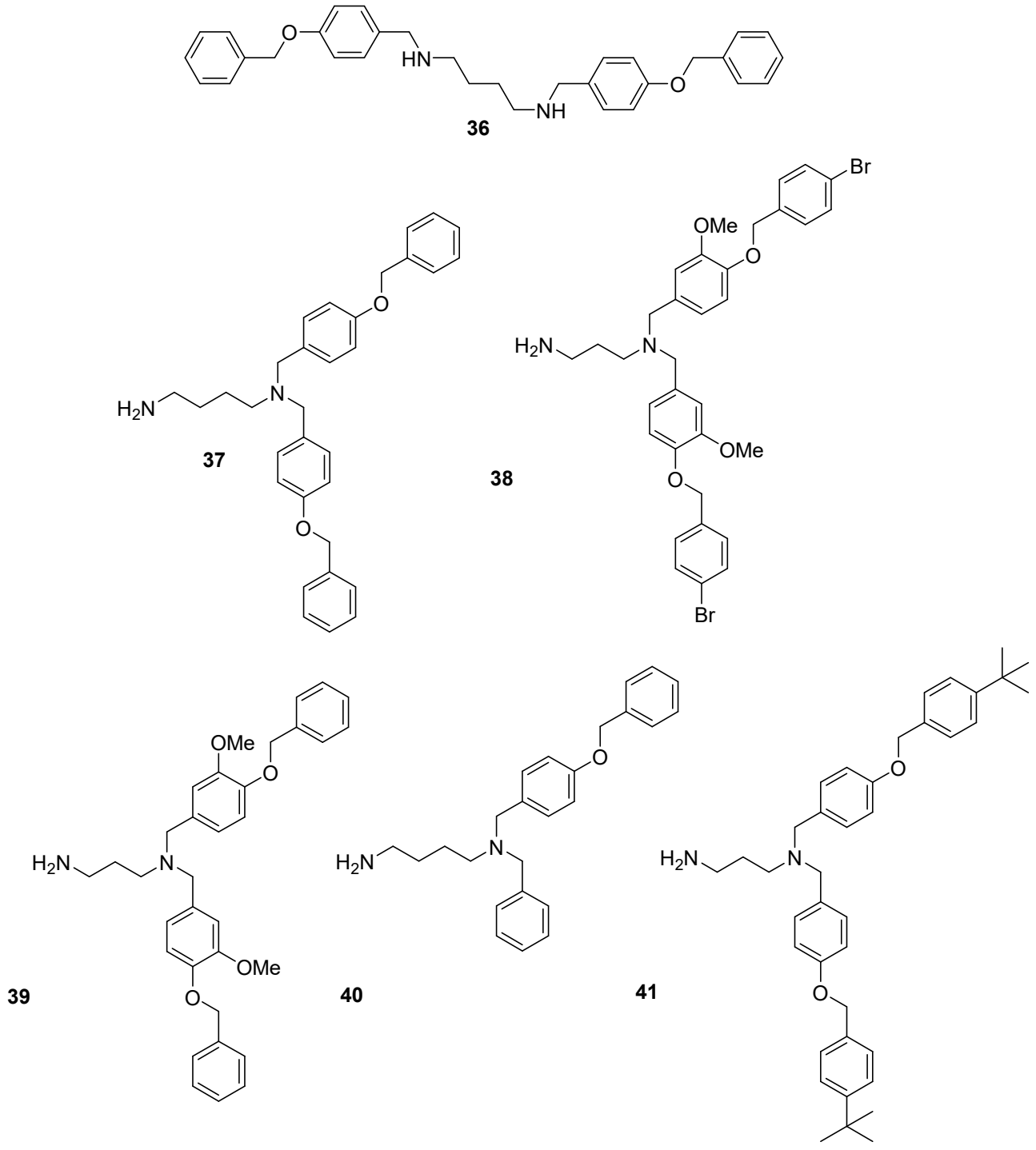

Figure 12: Bisbenzyl-diamines with antikinetoplastid activity at the micromolar range.

III. Spermidine and triamine derivatives

Such as putrescine, spermidine occupies a key position in the polyamine biosynthetic pathway and in this part we will find numerous spermidine analogs developed as antikinetoplastids. Many were identified as inhibitor of trypanothione reductase which is a specific enzyme present in Trypanosomatids. There may be natural or unnatural triamine analogs. For example, norspermidine also called caldine, is a symmetric triamine with a 3-carbon chain found in some organisms.

1. Trypanothione analogs

Kinetoplastids have a unique thiol-based redox metabolism, depending on trypanothione as their principal thiol (Figure 13), in contrast with their human host which utilizes GSH. A major function of the trypanosomatid redox system is to overcome the oxidative stress induced by the host defense mechanisms. The hydroperoxides produce oxidation of the dithiol form of trypanothione ($T(SH)_2$) into the disulfide form (TS_2). This is followed by regeneration of the dithiol by trypanothione reductase (TryR), an NADPH-dependent flavoenzyme.[56] TryR has been genetically validated as a drug target in *T. b. brucei*.[57] Therefore, this enzyme is a prime target for drug design and a large number of TryR inhibitors have been described.[58]

[56] Krauth-Siegel, R. L.; Comini, M. A. *Biochim. Biophys. Acta* **2008**, *1780*, 1236–1248.

[57] Krieger, S.; Schwarz, W.; Ariyanayagam, M. R.; Fairlamb, A. H.; Krauth-Siegel, R. L.; Clayton, C. *Mol. Microbiol.* **2000**, *35*, 542–552.

[58] Krauth-Siegel, R. L.; Bauer, H.; Schirmer, R. H. *Angew. Chem. Int. Ed.* **2005**, *44*, 690–715.

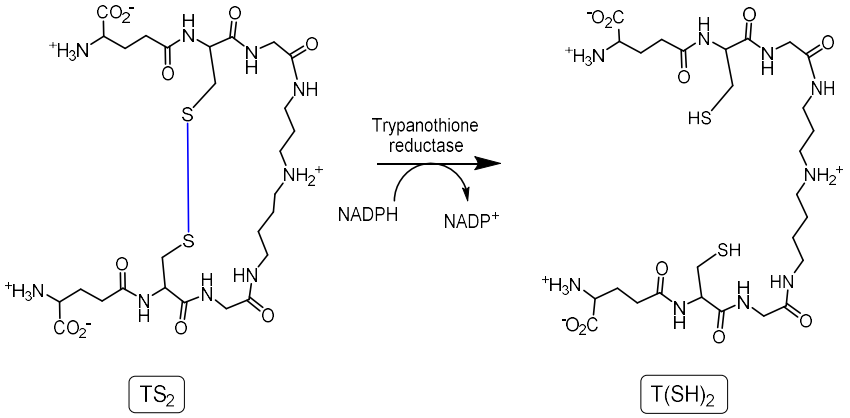

Figure 13: Reaction carried out by trypanothione reductase. Stuctures of the oxidized and the reduced forms of trypanothione.

Trypanothione is biosynthesized by the parasite with spermidine and two molecules of glutathione. One strategy for inhibiting TryR is to use analog structure of trypanothione. A range of substrate analog inhibitors of TryR have been synthesized (Figure 14).[59,60,61] The γ-glutamyl groups have been replaced by either hydrophobic aromatic moieties like Cbz (carbobenzyl) and Fmoc (fluorenylmethyloxycarbonyl) or linear diamine moieties. Furthermore, the disulfide bridge of the macrocyclic analogs **43-49** was substituted by a pair of methylene (**43-47**) or methylene dibromide **48** and an ester bond **49** (Figure 15).

[59] Garrard, E. A.; Borman, E. C.; Cook, B. N.; Pike, E. J.; Alberg, D. G. *Org. Lett.* **2000**, *2*, 3639–3642.

[60] Czechowicz, J. A.; Wilhelm, A. K.; Spalding, M. D.; Larson, A. M.; Engel, L. K.; Alberg, D. G. *J. Org. Chem.* **2007**, *72*, 3689–3693.

[61] Duyzend, M. H.; Clark, C. T.; Simmons, S. L.; Johnson, W. B.; Larson, A. M.; Leconte, A. M.; Wills, A. W.; Ginder-Vogel, M.; Wilhelm, A. K.; Czechowicz, J. A.; Alberg, D. G. *J. Enzyme Inhib. Med. Chem.* **2012**, *27*, 784–794.

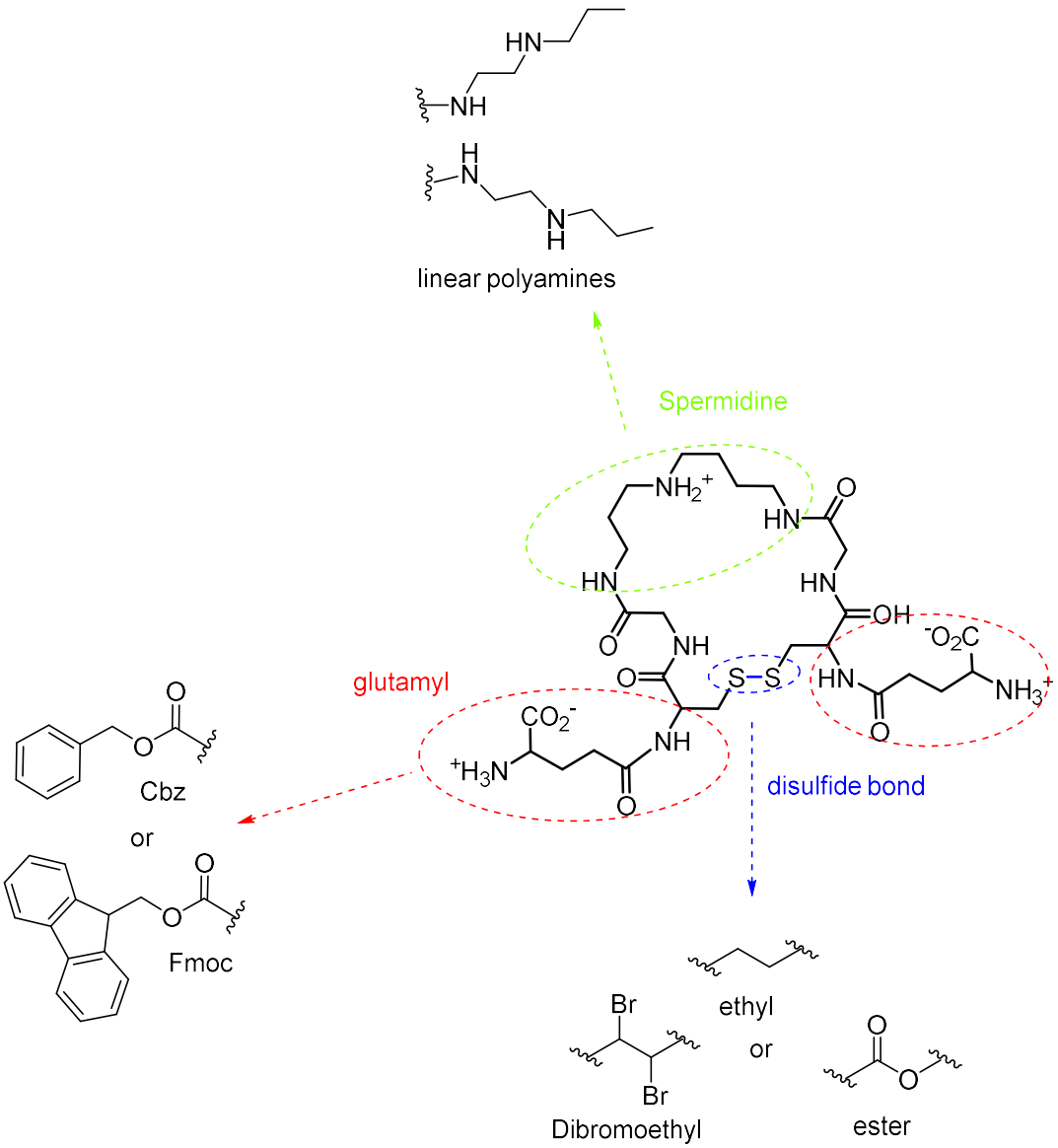

Figure 14: Modifications carried out on trypanothione for the design of substrate analogs.

The best inhibitor of this series, analog **46** (Figure 15), displaying a Fmoc group and an ethylene bridge showed an inhibition of *T. cruzi* TryR with a K_i = 2 µM. This study also showed that TryR binds to compounds with hydrophobic group and accepts a Cbz group in lieu of γ-glutamyl. Dibromide **48** and ester **49** (Figure 15) were noted to bind with low affinity and to be competitive inhibitors of TryR. The binding site of TryR appears to accommodate quite large substituents, in particular near the catalytic cysteine residues since the bulky dibromide analog **48** (Figure 15) is a good inhibitor of TryR (Ki = 15.9 µM).

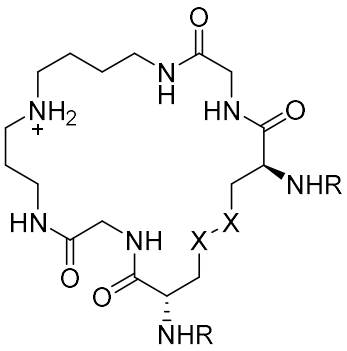

42 R= glutamyl, X= S (trypanothione disulfide)
43 R= glutamyl, X= CH_2 (dethiotrypanothione)
44 R= Cbz, X= CH_2
45 R= Fmoc, X= CH_2

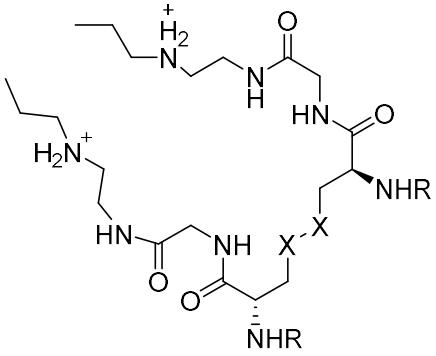

46 R= Fmoc, X= CH_2
47 R= Cbz, X= CH_2
48 R= Cbz, X= CH_2Br

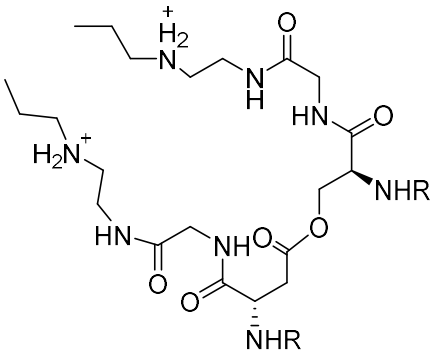

49 R= Cbz

Figure 15: Trypanothione analogs.

A range of polyamine-peptide conjugates has been investigated with solid phase chemistry in order to both establish structure-activity relationships as inhibitors of trypanothione reductase and try to propose an enzymatic mechanism. Based on spermidine-arginine derivatives **50** (Figure 16) displaying a Ki of 0.1 µM,[62] two compounds with structural similarity to TS_2 have been synthesized on solid-phase chemistry.[63] Spermidine and norspermidine have been modified with two residues at their extremities, a tryptophane and an arginine bearing Pmc (2,2,5,7,8-pentamethylchromane-6-sulfonamide) group were added (Figure 16). Substitutions

[62] Smith, H. K.; Bradley, M. *J. Comb. Chem.* **1999**, *1*, 326–332.
[63] Dixon, M. J.; Maurer, R. I.; Biggi, C.; Oyarzabal, J.; Essex, J. W.; Bradley, M. *Bioorg. Med. Chem.* **2005**, *13*, 4513–4526.

have been done on one or both primary amine of the polyamine in order to compare the biological effect. TryR inhibition was not increased compare to the lead compound **50** but **51** and **52** were however active with a Ki of 0.22 and 0.16 µM respectively and showed a behavior of non-competitive inhibitors. Allosteric mechanism, involving binding at the NADPH active site distinct from the disulfide substrate active site and the dimer interface region, was highlighted. Despite of their good inhibition activities, none of the trypanothione analogs were either tested as antikinetoplastids in vitro or in vivo.

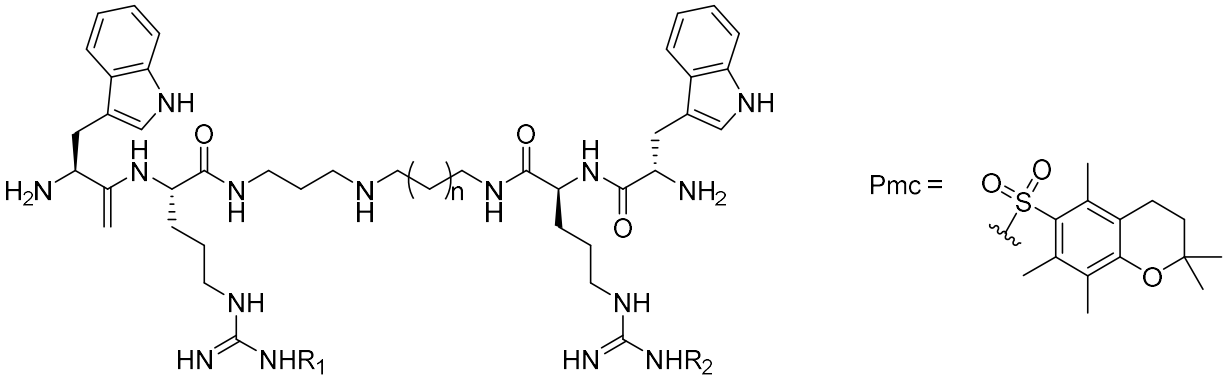

50 n=2, R_1=H, R_2=Pmc/n=2, R_1=Pmc, R_2=H
51 n=1, R_1=H, R_2=Pmc
52 n=1, R_1=R_2=Pmc

Figure 16: Trypanothione analogs.

2. *Acyl- and Alkyl-triamine analogs*

Polyamine-coenzyme A conjugates and truncated coenzyme A derivatives have been demonstrated as potent anticancer compounds with an inhibition of human histone acetyl transferase (HAT).[64] Recently, parasitic lysine acetyl transferase has been validated as a therapeutic target for Kinetoplastids.[65] Consequently, in our laboratory, we proposed to test the truncated coenzyme A derivatives against *T. brucei gambiense* and *L. donovani* axenic amastigotes and intramacrophages forms.[40] Among all the spermidine derivatives compounds

[64] Bandyopadhyay, K.; Banères, J.-L.; Martin, A.; Blonski, C.; Parello, J.; Gjerset, R. A. *Cell Cycle Georget. Tex* **2009**, *8*, 2779–2788.
[65] Alonso, V. L.; Serra, E. C. *J. Biomed. Biotechnol.* **2012**, *2012*.

tested, **53**, a thioamide conjugate (Figure 17), displayed the best activity (IC_{50} = 5.75 µM) against *T. brucei* whereas this *N*-acylated derivative was not active against *L. donovani*. In contrast, the best compound against *L. donovani* was a simple methoxy conjugate **54** (Figure 17) with an IC_{50} of 5.47 µM and this compound was not active against *T. brucei*. Moreover, the substitution on the terminal nitrogen N^1 or N^3 lead to completely different activity. Indeed, the opposite counterpart of **54**, compound **55** (Figure 17) which is substituted by the same function on the N^1 of the spermidine, displayed an IC_{50} of 50 µM against L. donovani and was slightly active against T. brucei. Partially cyclic spermidine derivatives **56**, **57** and **58** (Figure 17) were evaluated against *T. brucei* in vitro and were completely devoid of activity.[66] Analogs of 1,3-diaminopropane where one of the nitrogen atoms is involved in a heterocyclic ring system and the other in an amidine group were evaluated in vivo against *L. donovani*.[34] The authors named these compounds diaminopropane derivatives but we considered these compounds as rigidified triamine derivatives. The best compound of this series was a piperazine linked to a biscarboxymethoxy guanidine function **59** (Figure 17). These derivatives were tested in vivo on hamsters infected by *L. donovani*. Spleen biopsy and count of parasites were carried out. The dose was 50 mg/kg during 5 days intraperitoneal and oral route. **59** exhibited good in vivo effect, with 85% reduction of amastigotes after 7 days. The corresponding free amine **60** was not active whereas its cyano analog **61** (Figure 17) was quite efficient (80% inhibition). Considering that some diamidines with antileishmanial potential have shown inhibition of arginine transport,[67] the author hypothesized that compounds having molecular scaffold where primary amine is incorporated with biscarbomethoxy guanidine **59** could be arginine transport inhibitors.

[66] Zou, Y.; Wu, Z.; Sirisoma, N.; Woster, P. M.; Casero Jr., R. A.; Weiss, L. M.; Rattendi, D.; Lane, S.; Bacchi, C. J. *Bioorg. Med. Chem. Lett.* **2001**, *11*, 1613–1617.

[67] Kandpal, M.; Tekwani, B. L.; Chauhan, P. M.; Bhaduri, A. P. *Life Sci.* **1996**, *59*, PL75-80.

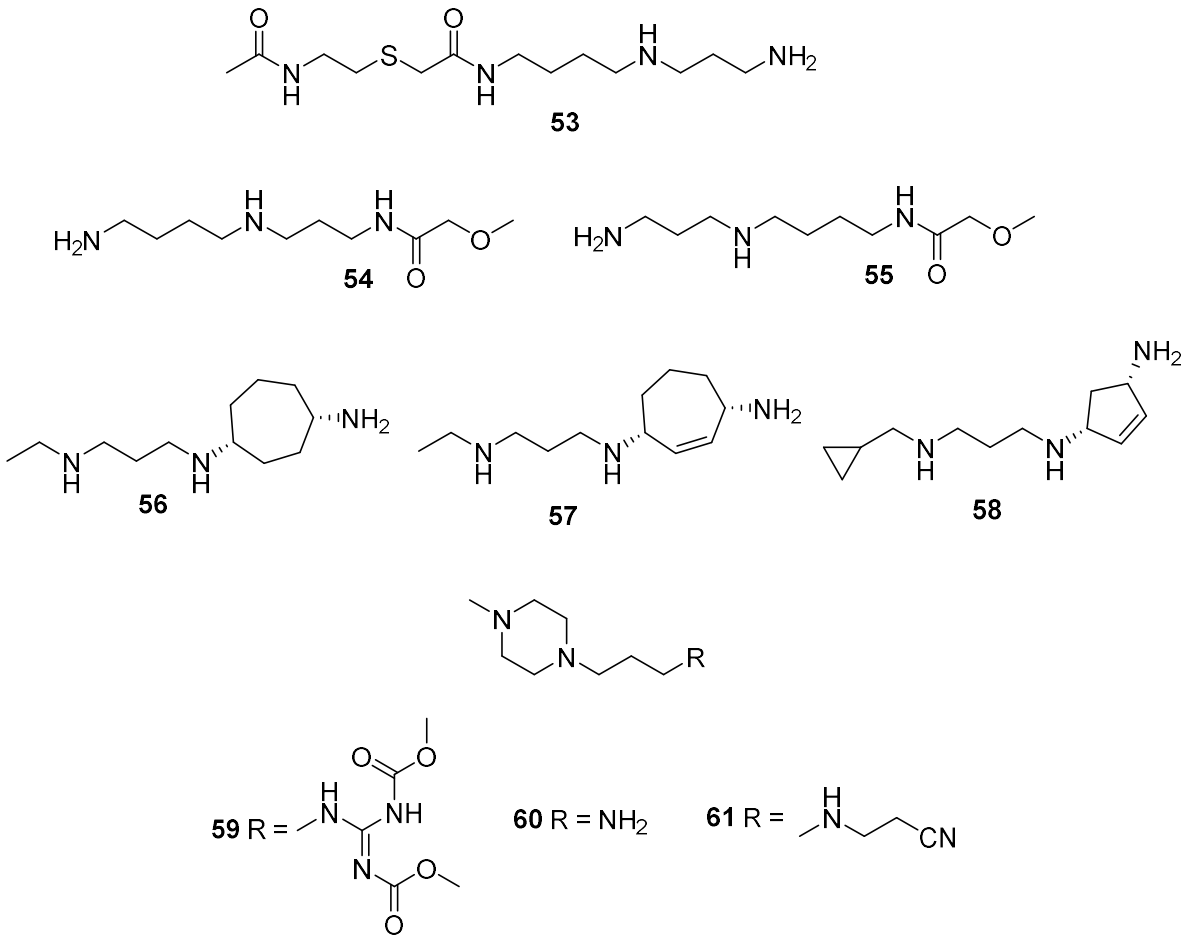

Figure 17: Acyl- and alky-triamine derivatives.

3. *Aryl- and aroyl- triamine analogs*

Monoaryl-triamines

Among the polyamine-quinone derivatives synthesized by Lizzi et al.,[41] the two triamine derivatives: spermidine-2-phenoxy-anthraquinone **62** and spermidine-2-phenoxy-naphthoquinone **63** (Figure 18), displayed good activities against *T. b. rhodesiense* with IC_{50} values of 0.23 µM and 0.72 µM respectively. The selectivity indexes of these compounds are around 12-27 which is weak for potent antikinetoplastids. Moreover, these spermidine analogs were not active against *T. cruzi* and moderatly effective on *L. donovani* axenic amastigotes (IC_{50} of 3.13 and 7.17 µM). Other spermidine derivatives isolated from the New Zealand ascidian

Didemnum sp. have been studied as antiparasitic compounds (**64**, **65**: Figure 18).[68,69] However, these natural products were only mildly active (IC_{50} >40 µM) against *T. b. rhodesiense*, *T. cruzi* and *L. donovani*. The activity of **didemnidine A 64** and **B 65** was slightly increased when the primary amine was protected by a *tert*-butoxycarbonyl group.

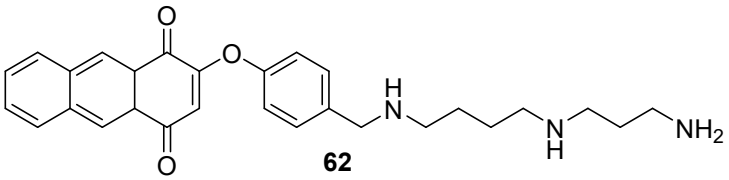

62

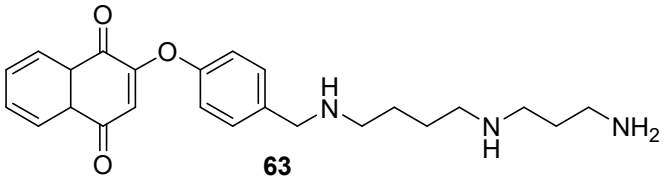

63

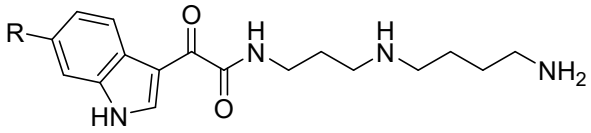

Didemnidine A 64, R= H
Didemnidine B 65, R= Br

Figure 18: Quinone-spermidine derivatives and Didemnidine structures.

Some spermidine derivatives, with a structure close to **bisC6DHB 34** and **35** (Figure 11)[70], have been evaluated on TryR isolated from *Crithidia fasciculata*. Indeed, the study explored variation of the polyamine chain and a monosubstitution by aromatic nucleus. Compounds **66**, **68**, **69** were spermidine monosubstituted by different aryl groups and compound **67** is a derivative

[68] Finlayson, R.; Pearce, A. N.; Page, M. J.; Kaiser, M.; Bourguet-Kondracki, M.-L.; Harper, J. L.; Webb, V. L.; Copp, B. R. *J. Nat. Prod.* **2011**, *74*, 888–892.

[69] Wang, J.; Kaiser, M.; Copp, B. R. *Mar. Drugs* **2014**, *12*, 3138–3160.

[70] Liew, L. P. P.; Kaiser, M.; Copp, B. R. *Bioorg. Med. Chem. Lett.* **2013**, *23*, 452–454.

with rigidified spermidine structure (Figure 19). All these conjugates were not inhibitors of TryR and have not been tested against Kinetoplastids.[71]

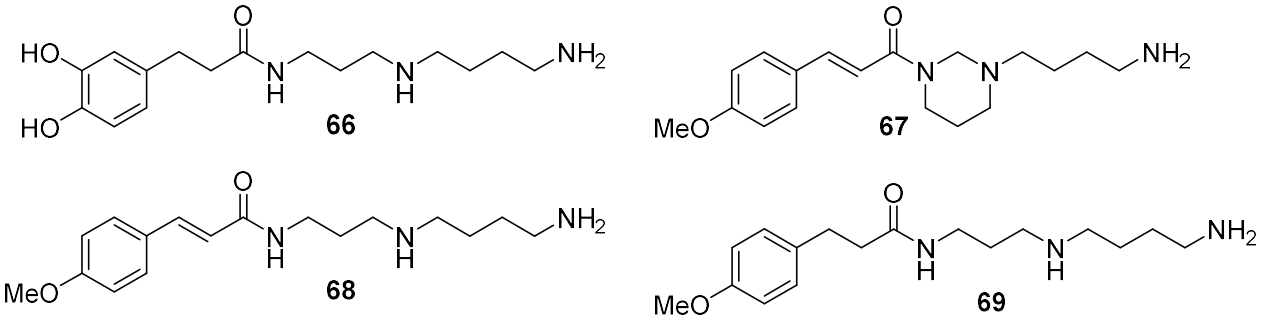

Figure 19: Spermidine monosubstituted with an aryl moiety.

In our recent study, we synthesized spermidine-hydroxybenzotriazole compounds substituted on the three different nitrogen atoms of the polyamine. In the synthetic pathway, we used a Boc protection strategy to afford the final free amine compounds.[40] These compounds have been evaluated against the trypomastigote forms of *T. b. gambiense* and amastigote forms of *L. donovani* axenic and intramacrophage forms. The N^3-substituted spermidine **70** (Figure 20) was active only against *T. b. gambiense* with an IC_{50} of 1.2 µM and a good selectivity index = 85. The spermidine substituted in the central nitrogen **71**, was equally active against *T. b. gambiense* trypomastigotes and *L. donovani* intramacrophage amastigote form with an IC_{50} around 3 µM. Again, the compounds exhibiting the highest antikinetoplastid activity were the Boc protected derivatives. The central nitrogen of spermidine has been also substituted by a benzyloxycarbonyl (Cbz) group **72** and a naphtyl moiety **73** by O'Sullivan et al. (Figure 20).[72] These compounds were assayed as inhibitors of *T. cruzi* TryR and have a Ki > 100 µM. Their in vitro and in vivo trypanocidal effects were not evaluated in this paper.

[71] Ponasik, J. A.; Strickland, C.; Faerman, C.; Savvides, S.; Karplus, P. A.; Ganem, B. *Biochem. J.* **1995**, *311*, 371–375.

[72] O'Sullivan, M. C.; Zhou, Q. *Bioorg. Med. Chem. Lett.* **1995**, *5*, 1957–1960.

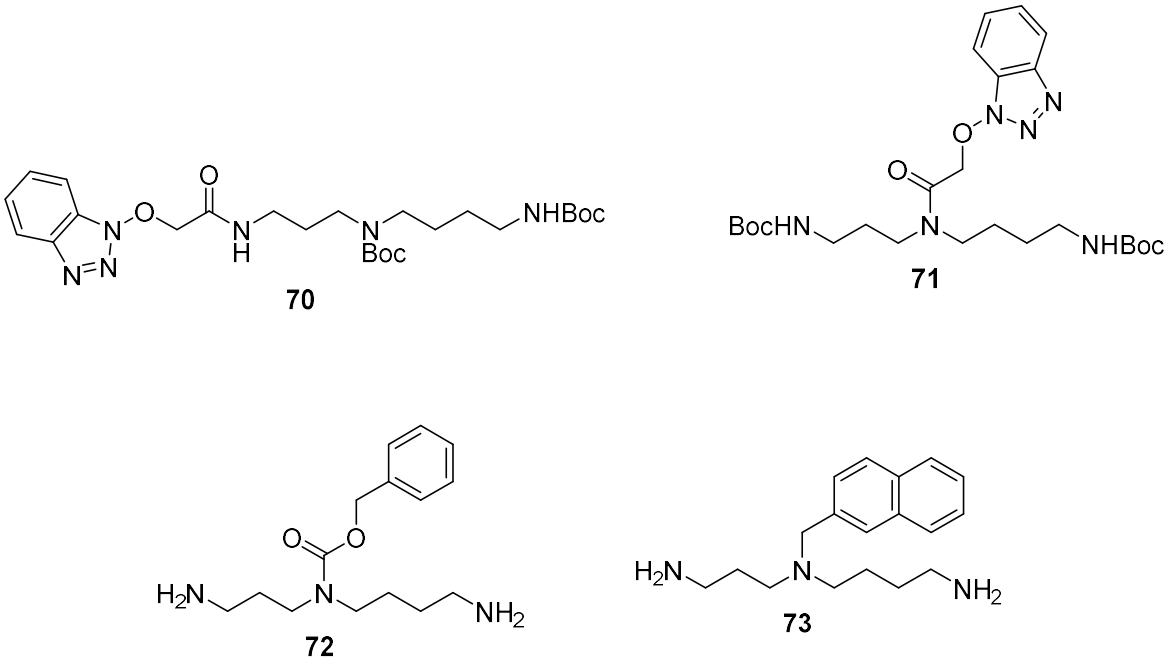

Figure 20: Hydroxybenzotriazole-, benzyloxycarbonyl- and naphtyl-spermidine derivatives.

In 1993, Carter and Fairlamb have characterized a unique adenosine transporter in *T. brucei*.[73] They described few structures which could be uptaken by this transporter and the melamine scaffold was identified as a potent structure. Few years later, Tye et al.[74] chose to couple this motif to natural polyamines in order to specifically target this parasite for delivery of active compound. The N^2-spermidine-melamine conjugate **74** (Figure 21) was shown as a poor competitor of adenosine for its transporter and was also not active against *T. b. brucei* in vitro. Different triamine-dibenzosuberyl derivatives have been evaluated for their trypanocidal activities.[44] Compounds **75**, **76** and **77** (Figure 21) are triamines substituted on the central nitrogen atom by a dibenzosuberyl group. Variations are in the length of the 2-carbon chain between the central nitrogen and primary amines. Compound **75** and **76** are symmetric triamines with 2- and 3-carbon chain respectively whereas **77** is an unsymmetric spermidine derivative. **75** displayed an IC_{50} of 2.8 µM against a drug sensitive strain of *T. b. brucei* and was not found as competitive inhibitors of TryR and **76** displayed a K_i value of 7.6 µM on TryR but has not been tested in vitro on parasite. The most interesting compound of this serie is **77**, with an

[73] Carter, N. S.; Fairlamb, A. H. *Nature* **1993**, *361*, 173–176.

[74] Tye, C. K.; Kasinathan, G.; Barrett, M. P.; Brun, R.; Doyle, V. E.; Fairlamb, A. H.; Weaver, R.; Gilbert, I. H. *Bioorg. Med. Chem. Lett.* **1998**, *8*, 811–816.

IC_{50} of 0.62 µM on *T. brucei* and a K_i value of 4 µM on TryR. The in vivo trypanocidal activity of this compound has been evaluated on mice infected with *T. b. brucei*. Intraperitonal doses were tested once per day in a range of 1.0 to 25 mg/kg on three consecutive days. Unfortunately, no increase in survival time was observed when comparing treated mice the controls.

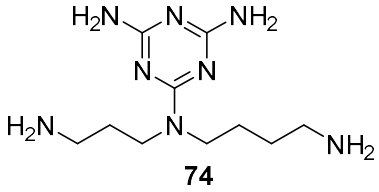

74

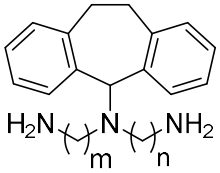

75 m = n = 2
76 m = n = 3
77 m = 3, n = 4

Figure 21: Melamine- and dibenzosuberyl-triamine derivatives.

Bisaryl-triamines

Among the compounds reported by O'Sullivan et al.[72,75], the N^1,N^8-bis(2-naphtylmethyl)-spermidine **78** (Figure 22) showed competitive inhibition of TryR with K_i values of 9.5 µM and displayed IC_{50} values ranging from 0.19 to 0.63 µM against different strains of *T. brucei*. The corresponding benzyl **79** and benzoyl **80** derivatives (Figure 22) were however not inhibitor of TryR. Compound **78** has been evaluated in vivo on infected mice with *T. b. brucei* using the same method as above. In addition, a continuous delivery of **78** (1 µL/h) using a pump during three days has been tested. Nonetheless, **78** did not increase the lifetime of mice infected with *T. b. brucei*. The spermidine bisphenyl acetamide **81** was moderately active against *T. b. rhodesiense* (IC_{50} = 5.9 µM) and completely inactive against *T. cruzi* and *L. donovani* amastigotes. The homologue **82** (Figure 22) with a shorter chain had a similar profile. The closely related bisphenyl structure **83** (Figure 22) bearing a rigidified triamine chain was evaluated on *T. cruzi* TryR and was a poor inhibitor.[71]

[75] O'Sullivan, M. C.; Zhou, Q.; Li, Z.; Durham, T. B.; Rattendi, D.; Lane, S.; Bacchi, C. J. *Bioorg. Med. Chem.* **1997**, *5*, 2145–2155.

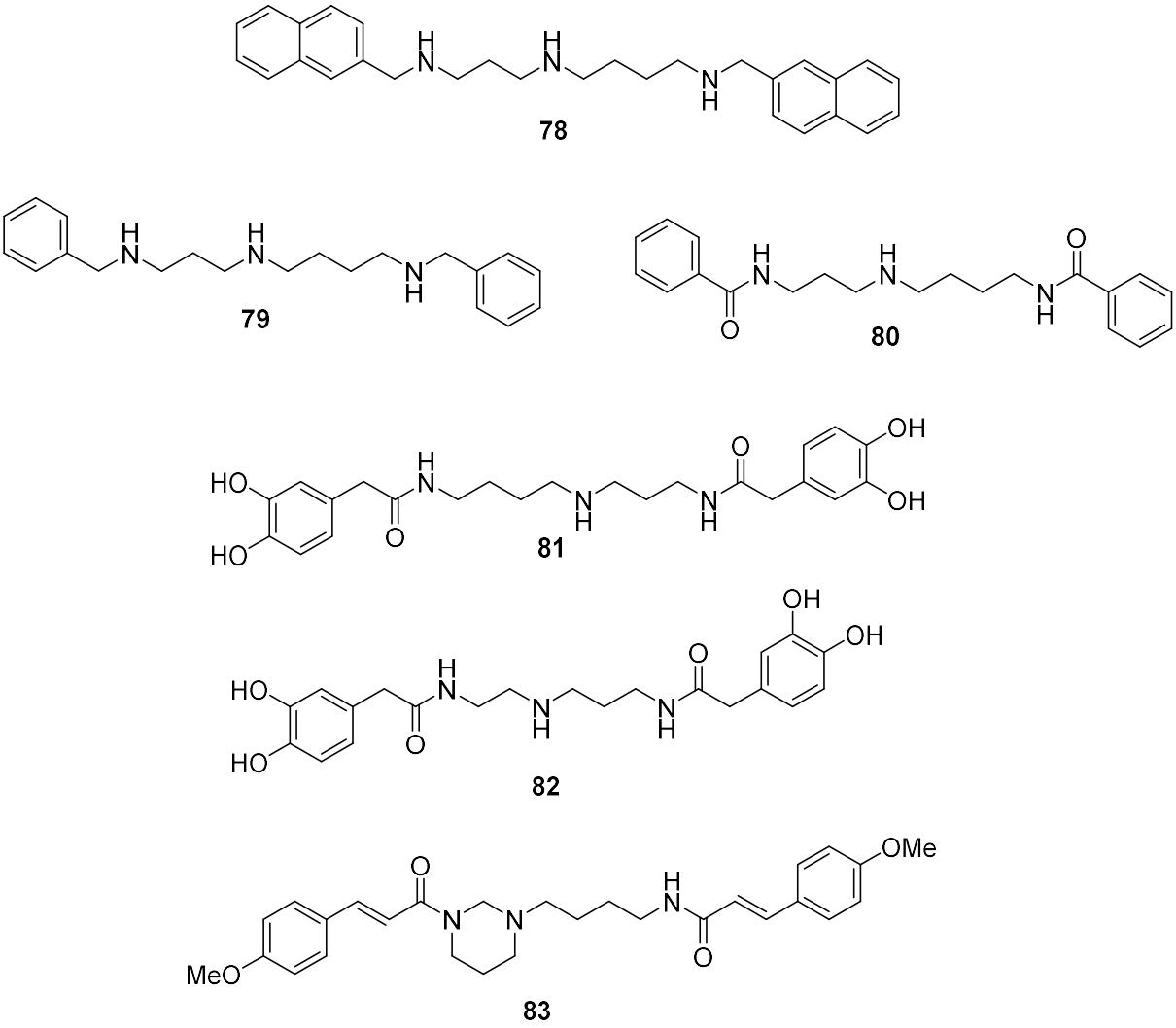

Figure 22: Bisaryl-triamine derivatives.

Furthermore, the bisquinoline-spermidine **84** (Figure 23) showed a particularly high inhibition of TryR with a Ki of 0.85 µM but was not tested directly on Kinetoplastids.[76] In the same study, bisindole-spermidine **85** showed 95% inhibition of TryR at 10 µM and the norspermidine counterpart **86** was also as active on this enzyme. Another bisindole-norspermidine **87** (Figure 23) bearing a maleimide ring had no inhibitory activity on TryR (IC_{50} > 57 µM).[77]

[76] Chitkul, B.; Bradley, M. *Bioorg. Med. Chem. Lett.* **2000**, *10*, 2367–2369.

[77] Salmon, L.; Landry, V.; Melnyk, O.; Maes, L.; Sergheraert, C.; Davioud-Charvet, E. *Chem. Pharm. Bull. (Tokyo)* **1998**, *46*, 707–710.

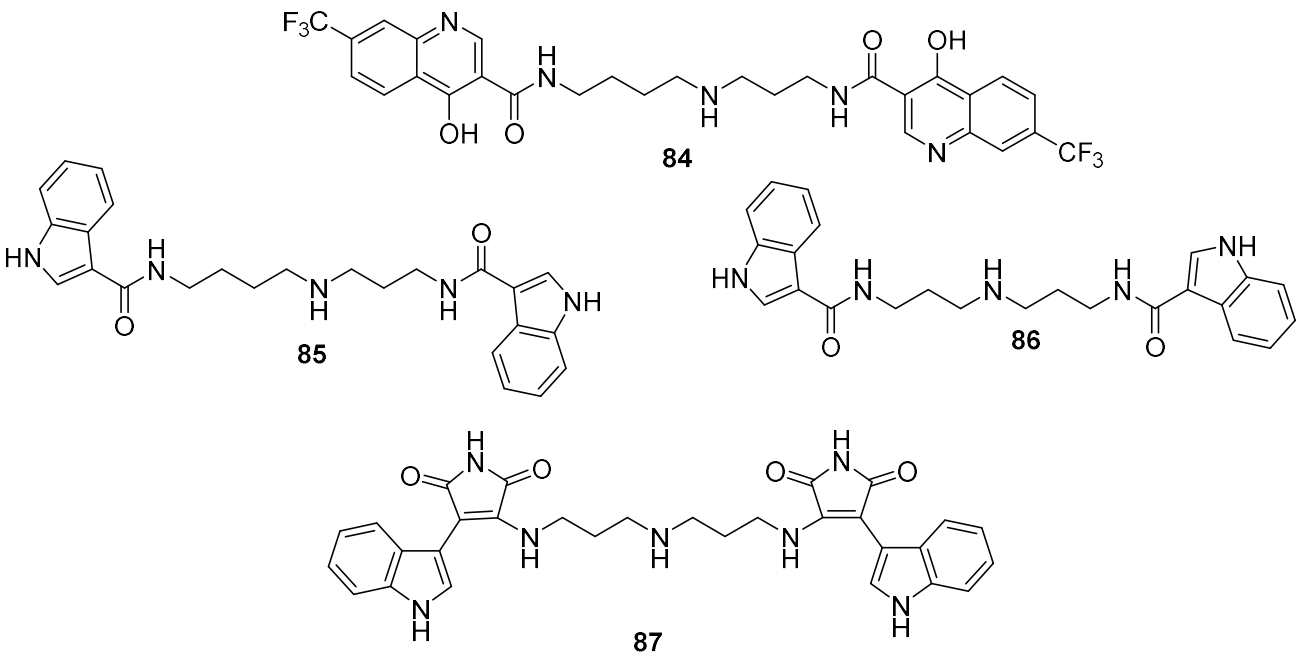

Figure 23: Bisquinoleine- and bisindole-derivatives.

Oliveira[45] and Tavares,[46] who have designed naphthalimidopropyl-putrescine, evaluated also spermidine and triamine derivatives. The bisnaphthalimido-spermidine **88** (Figure 24) was active against *L. infantum* promastigotes with IC_{50} value of 0.47 µM but was also as active on mammalian cancer cell Caco-2. The corresponding norspermidine **89** displayed a similar activity both on *L. infantum* and Caco-2 cells (IC_{50} = 1.54 µM). However, the shorter chain analog **90** was active against the Kinetoplastid strain *L. infantum* (IC_{50} = 0.74 µM) and, interestingly, was not cytotoxic (Figure 24).

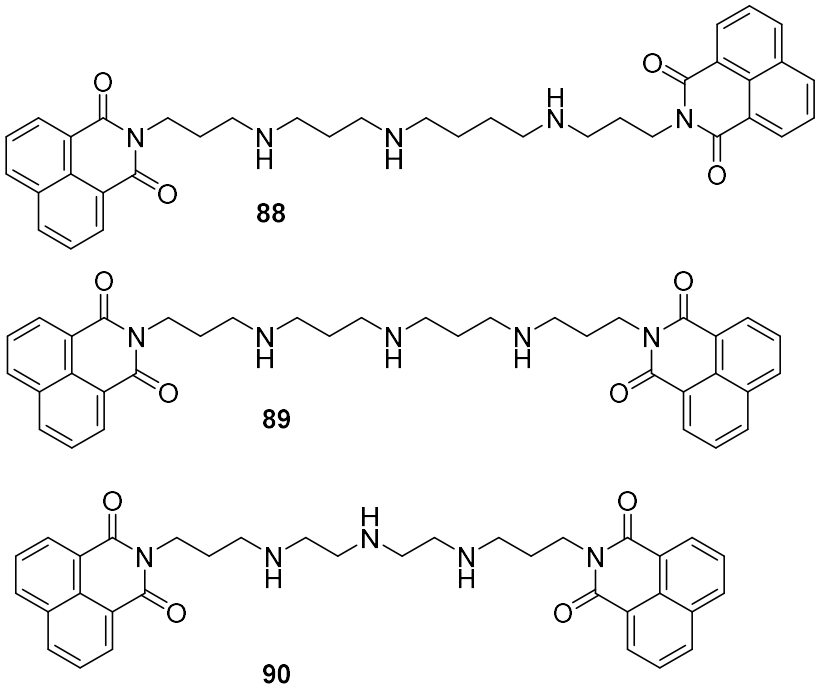

Figure 24: Bisnaphthalimido-triamine with antileishmanial activity on *L. infantum*.

A series of bisacridine-triamine conjugates has been synthesized including spermidine derivatives.[52] Among the spermidines, **91** and **92** (Figure 25) displayed an IC_{50} in the low-nanomolar range toward *T. brucei*. A longer chain on the central nitrogen of spermidine analogs was detrimental for the activity on *T. brucei*. These two spermidine analogs displayed potent in vitro activity against both *L. donovani* promastigotes (>90% of parasite death at 10 µM) and on *L. major* (IC_{50} around 1 µM). Moreover, **91** and **92** had reasonable selectivity index (>200). A norspermidine derivative **93** (Figure 25) methylated on the central nitrogen was the most interesting triamine of this study regarding the activity toward *T. brucei*. Indeed, its IC_{50} against the latter parasite was around 0.001 µM associated with a cytotoxicity on HL-60 cells around 1 µM leading to a high selectivity index (>100). However, a cytotoxicity at 1 µM could be a limitation for further development of this compound.

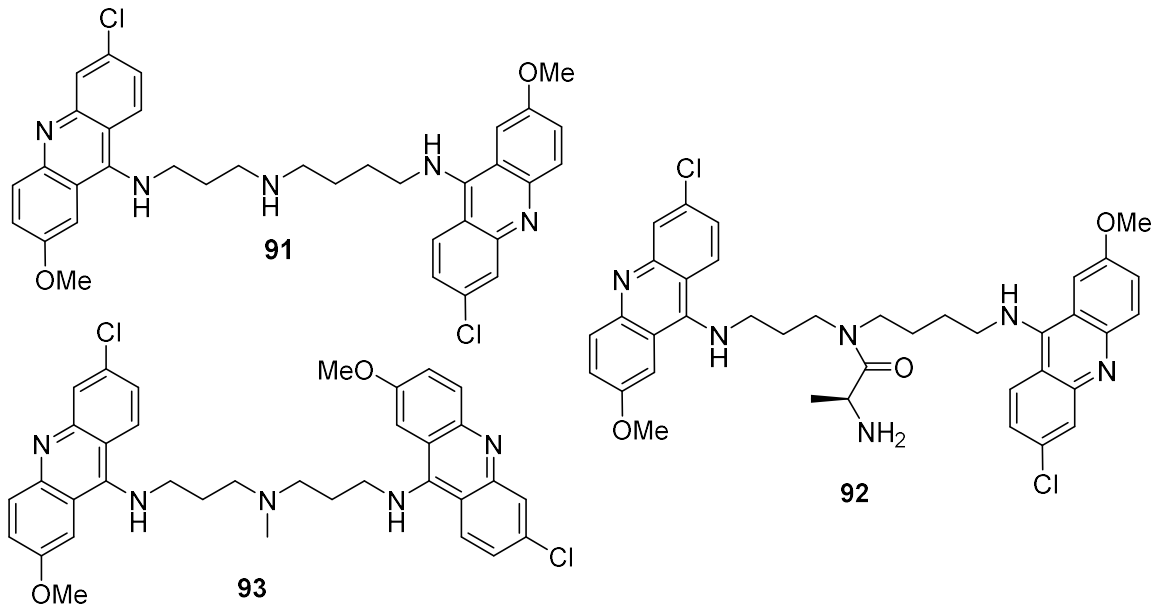

Figure 25: Bisacridine-triamine derivatives active at the nanomolar range against *T. brucei*.

IV. Spermine, tetramine and longer polyaminated derivatives

Spermine is the most representative tetramine in the literature due of its natural abundance. In drug design, numerous modulations could be envisioned on the length of the carbon chains to influence the biological activity. The chemists who work on polyamine chain modulation have adopted a way to number the different chains in order to easily visualize the structure. Thus, spermine incorporates four nitrogen atoms bounded by a 3-carbon chain, plus a 4-carbon and again a 3-carbon chain, is named a 3-4-3 tetramine. In this part, this codification will be used to describe the different natural or unnatural tetramines.

1. Alkyl- and acyl-tetramine analogs

Among *N*-acylated spermine derivative synthesized in our laboratory,[36] the spermine coupled with a thiobiamide moiety **94** (Figure 26) was the most active compound against *T. brucei* but was devoid of activity against *L. donovani*. This structure was shown as inhibitor of the histone acetyltransferase in cancer cells.[64] Even if this enzyme is validated as a therapeutic target for Kinetoplastid, the parasitic target of this compound was not identified. In addition, the (γ-

glutamimyl)spermine **95** (Figure 26), a bisaminoacid terminally functionalized spermine was synthesized and tested on TryR[71] but was a very weak inhibitor of this enzyme.

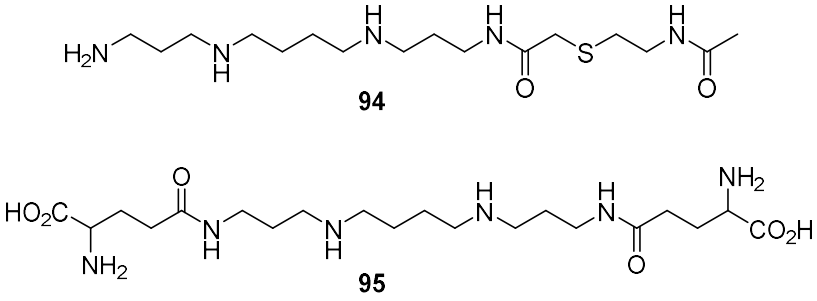

Figure 26: Acyl-spermine derivatives.

Studies involving bisalkyl-polyamines were proceeded to understand the influence of charge, length and flexibility of the polyamine backbone structure on biological activity. Spermine analogs with 3-3-3- (norspermine) or 3-7-3-carbon skeletons were synthesized and tested on *T. b. brucei* and *T. b. rhodesiense.*[78,66] Symmetrical or unsymmetrical derivatives were substituted with different alkyl groups. These compounds have been known for their antitumor activity, their ability to superinduce the spermidine/spermine N^1-acetyltransferase (SSAT), and downregulate ODC and AdoMetDC. Symmetric or unsymmetric norspermine **96-99** were devoid of trypanocidal activity (Figure 27).

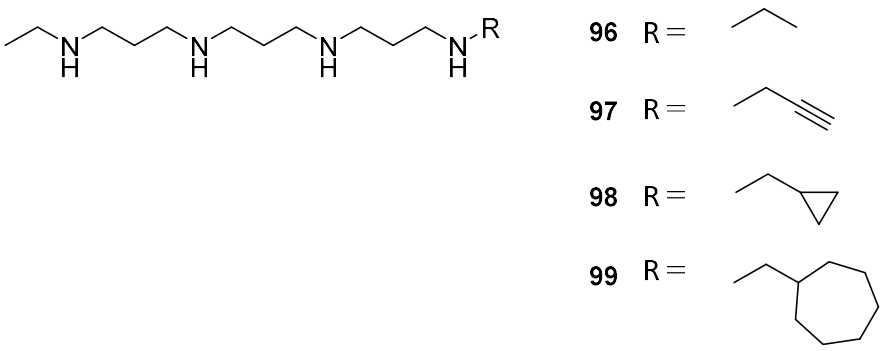

Figure 27: Alkyl-ethylnorspermine derivatives.

The symmetric bismethylbutane-polyamine **100** (Figure 28), a 3-7-3 tetramine had an IC_{50} below 0.04 µM against *T. b. brucei* and was also efficient against arsenical resistant strain of *T. b. rhodesiense* (IC_{50} = 0.16 µM).[66] The corresponding 3-7-3 tetramine **101** (Figure 28) substituted

[78] Bellevue, F. H.; Boahbedason, M.; Wu, R.; Woster, P. M.; Casero, R. A.; Rattendi, D.; Lane, S.; Bacchi, C. J. *Bioorg. Med. Chem. Lett.* **1996**, *6*, 2765–2770.

symmetrically by two cycloheptyl was also quite active against the four strains tested with IC_{50} values around 1 µM.[78] Unsymmetric 3-7-3 alkyl tetramines tested in these study displayed less important trypanocidal activity. A constrained analog **102** (Figure 28), bearing a cycle into the central chain, was trypanocidal against the four strains of *T. b. brucei* (Lab 110 EATRO a pentamidine and melarsen-sensitive strain, *T. b. rhodesiense* K243 and K269 two melarsen-resistant clinically isolated strains and K243 As-10-3, a melarsen and pentamidine resistant clone of clinical isolate).[66] The rigidified tetramine **103** (Figure 28) was noted as poor in vivo agent on mice infected by *L.donovani*.[34] Substituted polyaminoguanidines and polyaminobiguanides have also been prepared and evaluated as potent inhibitors of TryR.[79] The authors hypothesized that polyamine analogs substituted by guanidine parts will lead to different degrees of protonation at physiological pH through changes in pKa values. This could lead to better interactions with various targets. Indeed, a guanidine has a pKa value in the range of 13.0 and 13.5 compared to a secondary amine (pKa~11). Furthermore, biguanide group was found in potent TryR inhibitior such as biguanide chlorhexidine.[80] The derivatives have been synthesized and evaluated on TryR and GR (glutathione reductase), and against *T. b. brucei* in vitro. The best analog of the series was the 3-7-3 backbone compound **104** (IC_{50} = 0.18 µM) bearing the remarkable cycloheptyl moiety (Figure 28).

[79] Bi, X.; Lopez, C.; Bacchi, C. J.; Rattendi, D.; Woster, P. M. *Bioorg. Med. Chem. Lett.* **2006**, *16*, 3229–3232.

[80] Meiering, S.; Inhoff, O.; Mies, J.; Vincek, A.; Garcia, G.; Kramer, B.; Dormeyer, M.; Krauth-Siegel, R. L. *J. Med. Chem.* **2005**, *48*, 4793–4802.

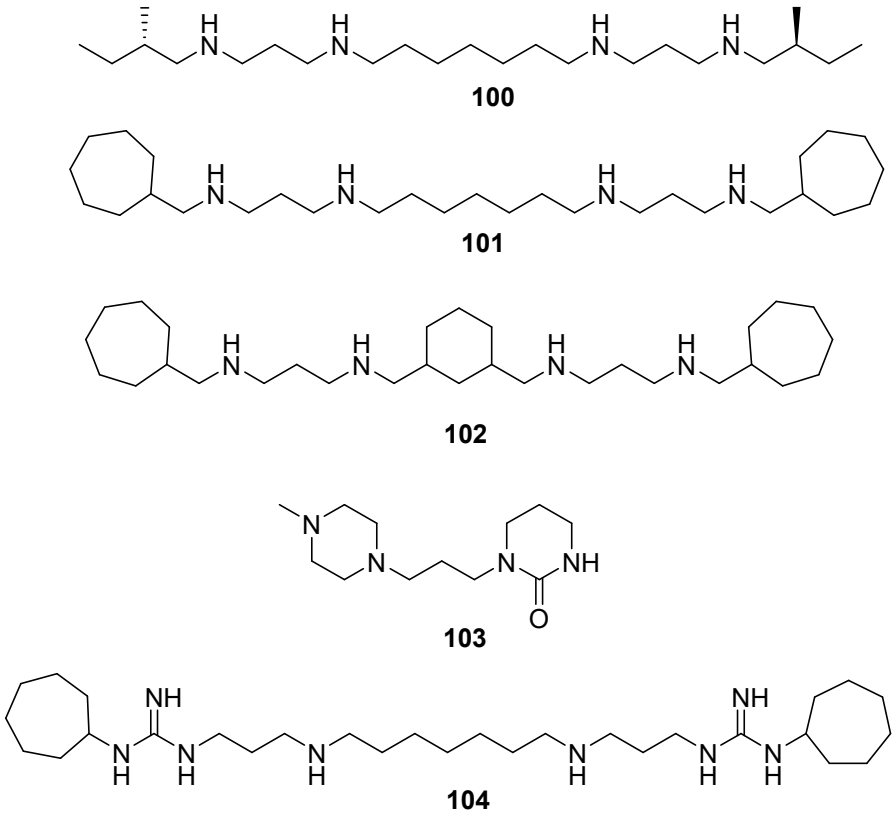

Figure 28: Alkyl-tetramine derivatives.

The 1,3,5-thiadiazinane-2-thione (THTT) is a chemical group known for antimicrobial activity[81] and in the design of prodrug due to its high lipid solubility and its facile hydrolysis by enzymes. Some alkyl linked bis(THTT) derivatives have been found active against *T. b. rhodesiense*.[82,83] Thus, a series of novel bis(1,3,5-thiadiazinane-2-thione)-polyamines has been synthesized and evaluated on three Kinetoplastid strains.[84] Among the diacid-tetramine synthesized, **105** (Figure 29) was the most potent compound against *L. donovani* (IC_{50} = 6.74 µM) and *T. brucei* (IC_{50} = 0.36 µM) associated to a low cytotoxicity against KB cells (IC_{50} = 16.09 µM).

[81] Ilhan, E.; Capan, G.; Ergenç, N.; Uzun, M.; Kiraz, M.; Kaya, D. *Farm. Soc. Chim. Ital. 1989* **1995**, *50*, 787–790.

[82] Coro, J.; Pérez, R.; Rodríguez, H.; Suárez, M.; Vega, C.; Rolón, M.; Montero, D.; Nogal, J. J.; Gómez-Barrio, A. *Bioorg. Med. Chem.* **2005**, *13*, 3413–3421.

[83] Coro, J.; Atherton, R.; Little, S.; Wharton, H.; Yardley, V.; Alvarez Jr., A.; Súarez, M.; Pérez, R.; Rodríguez, H. *Bioorg. Med. Chem. Lett.* **2006**, *16*, 1312–1315.

[84] Coro, J.; Little, S.; Yardley, V.; Suárez, M.; Rodríguez, H.; Martín, N.; Perez-Pineiro, R. *Arch. Pharm. (Weinheim)* **2008**, *341*, 708–713.

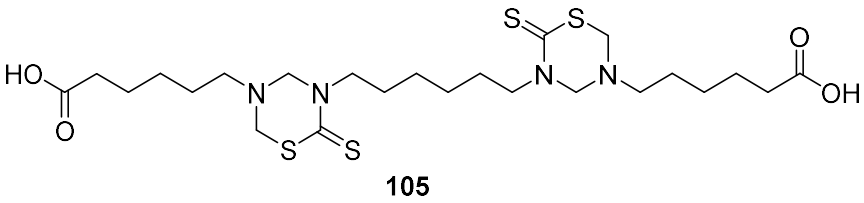

105

Figure 29: Polyaminated 1,3,5-thiazadine-2-thione (THTT) with antikinetoplastid activity.

2. *Aryl-tetramine analogs*

Monoaryl-tetramines

Natural products are a potential source of new and structurally various antikinetoplastid compounds. Some natural products have been found as inhibitor of TryR, such as is the anti-hypertensive agent **kukoamine A 117** [N^1,N^{12}-bis(dihydrocaffeoyl)-spermine] (Figure 33), a novel spermine alkaloid.[71] This molecule is a spermine derivative with catechols at the extremities and inhibits TryR of *Crithidia fasciculata* with a Ki value of 1.8 µM. Kukoamine A analog **106** (Figure 30)**,** a spermine terminally linked to only one cathecol moiety, was tested on TryR since the original kukoamine A was a strong inhibitor of this enzyme. Unfortunately, **106** was a weak inhibitor of TryR (Ki = 85 µM).[71] In the aforementioned study regarding benzotriazole conjugates, we prepared the *N*-acyl benzotriazole-spermine **107** (Figure 30) which was not a good trypanocidal agent (IC_{50} > 10 µM against *T. brucei* and *L. donovani*).[40] The substitution of spermine by phenoxy-anthraquinone **108** or a phenoxy-naphtaquinone **109** fairly improved the activity of the conjugates against the same Kinetoplastids.[41] Once again, the lipophilic Boc-protected benzotriazole-spermine conjugate exerted a better activity than its free amine counterpart.

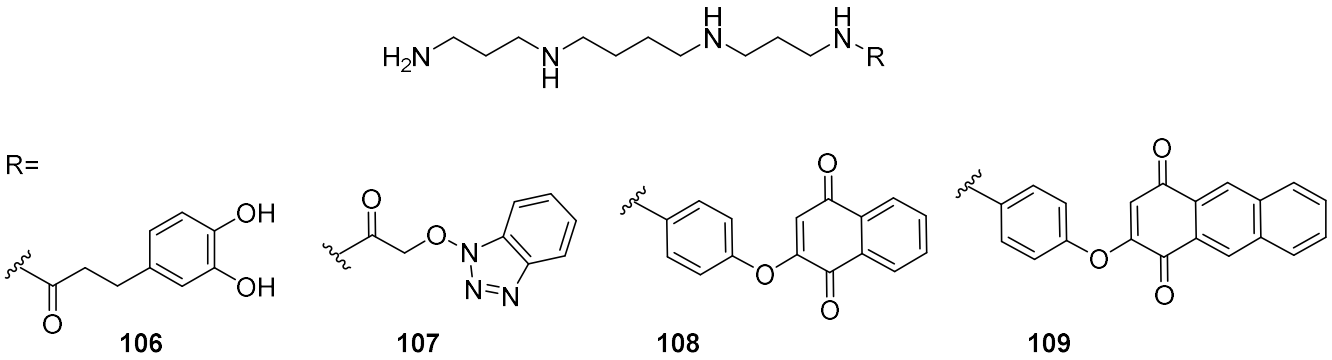

Figure 30: Monoaryl-tetramine derivatives.

Melamine-tetramine conjugates have been also synthesized over three types of compounds.[74] The monosubstitution of the melamine ring on one of the central nitrogen of spermine lead to compound **110** (Figure 31). Terminally substituted 3-7-3 tetramine affords compound **111** and the spermine positional isomer **112** was envisioned as well (Figure 31). A melamine-pentamine conjugates **113** incorporating a spermine structure was additionally prepared (Figure 31). None of these melamine derivatives were able to impair *T. b. brucei* in vitro.

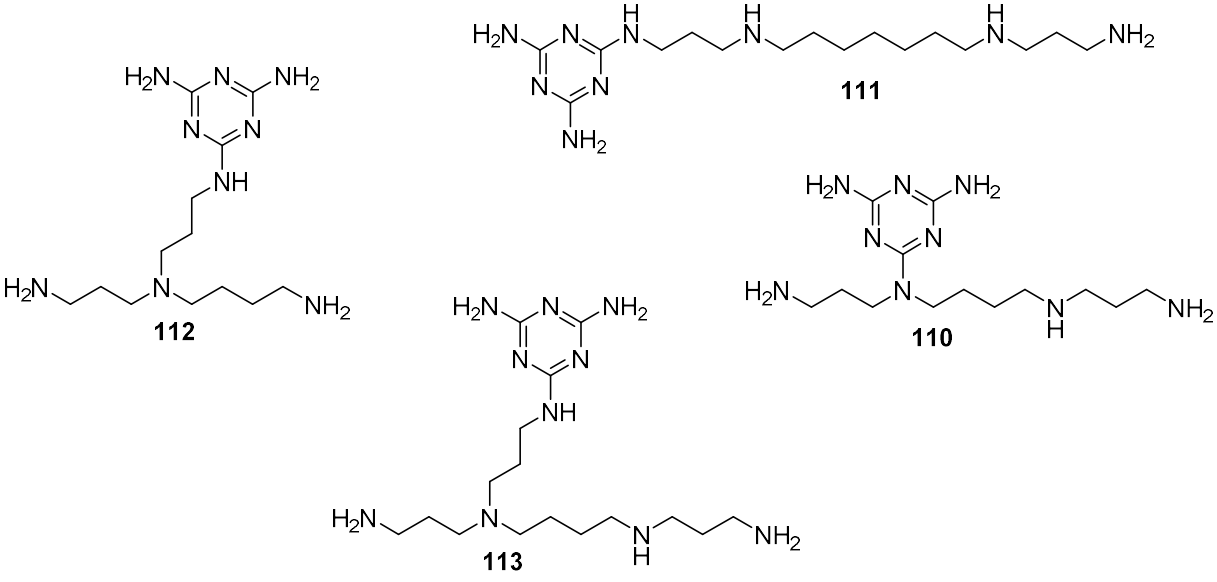

Figure 31: Melamine-tetramine derivatives.

Another positional isomer of spermine, **114** (Figure 32), a diphenyl sulfide moiety bounded to a tetramine, was evaluated on TryR and displayed good activity with an IC_{50} of 1 µM. Monobenzyl-pentamine incorporating the THTT ring showed interesting trypanocidal activities.[84] In this

series, the most potent compound was the diacid **115** (Figure 32) which was active against *T. cruzi* with an IC_{50} of 3.64 µM. However, all the active compounds of this series were cytotoxic.

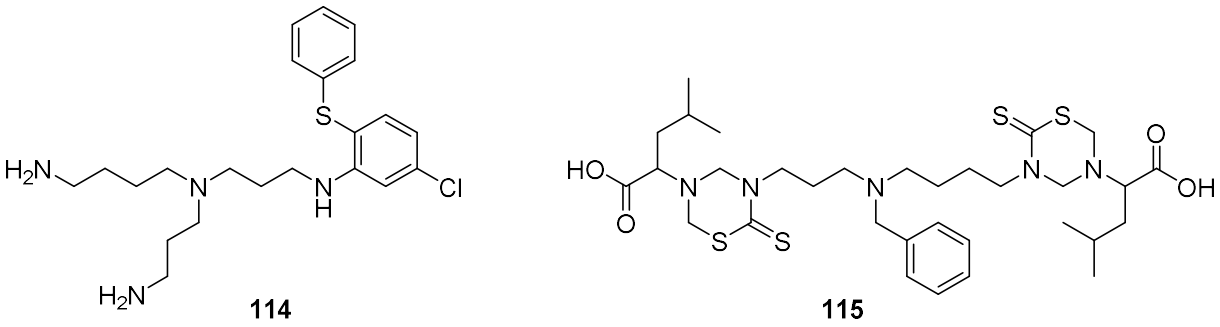

Figure 32: Aryl-tetramine and -pentamine derivatives.

Bisaryl-tetramines

Addition of a second melamine ring at the other extremity of the 3-7-3 tetramine backbone did not increase the activity.[74] An elongated polyamine analog **116** (Figure 33) which has six nitrogen atoms with a 3-3-7-3-3 structure also displayed a low activity against *T. brucei* in vitro (IC_{50} = 24 µM).

Many modifications have been tried on **kukoamine A 117** as described earlier.[70] In spite of the various structural modifications, no increase of the activity has been noted and **kukoamine A 117** stayed the best TryR inhibitor of this series. The authors assumed that polyamine backbone is sufficiently long and flexible allowing cathechol to interact with TryR, and inhibition is decreased in absence of one or both catechol rings. To our knowledge, **kukoamine A 117** has not been tested on trypanosomes in vitro nor in vivo. 1,14-sperminedihomovanillamide (**orthidine F 118**), is another natural product with a structure close to **kukoamine A 117** (Figure 33).[70] Analogs of **orthidine F 118** were mostly derivatives with a hydroxyl or methoxy group at different positions of the benzyl moieties. Analogs with a shorter central chain, i.e 3-2-3 tetramines were also considered in this study. **Orthidine F 118** and analogs have been studied on different parasitic strains and showed strong anti-plasmodium activities (submicromolar IC_{50}), but did not display interesting activity on trypanosomes and leishmania.

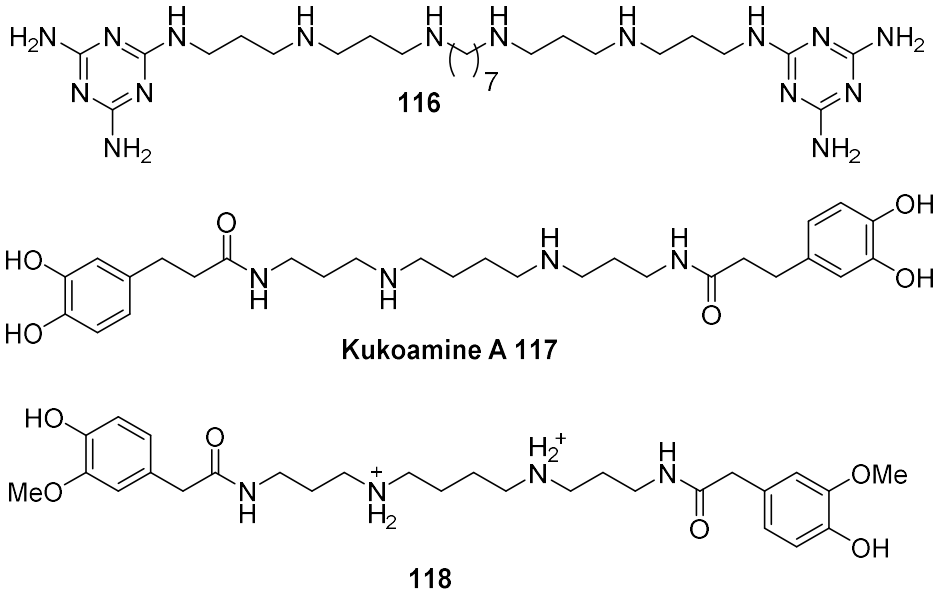

Figure 33: Bisaryl-polyamine derivatives.

In regard to these results obtained on these natural products, the **didemnidine A 64** and **B 65** mentioned above (Figure 18) were considered for structural modifications. Wang et al.[69] chose to synthesize bisindolyl-tetramines as didemnidine analogs. Spermine has been substituted at its extremities, the central chain was extended (3-8-3 and 3-12-3 tetramines) and finally, variation of aromatic substitutents was done with methoxy groups or halogen. After this optimization, the best compound **119** (Figure 34) showed an IC_{50} = 0.18 µM against *T. b. rhodesiense* instead of 44 µM for didemnide B. Unfortunately, it is also the more cytotoxic compound. Another bisbromoindole-spermine derivative **120** (Figure 34) was synthesized and evaluated on TryR. A particularly low Ki value of 0.076 µM was observed for this compound, with 98% of inhibition at 10 µM.[76] Curiously, this compound has not been tested in vitro against any Kinetoplastid. In the same study, a spermine conjugated with two quinoline moieties **121** (Figure 34) was also shown as a strong TryR inhibitor (Ki = 0.75 µM).

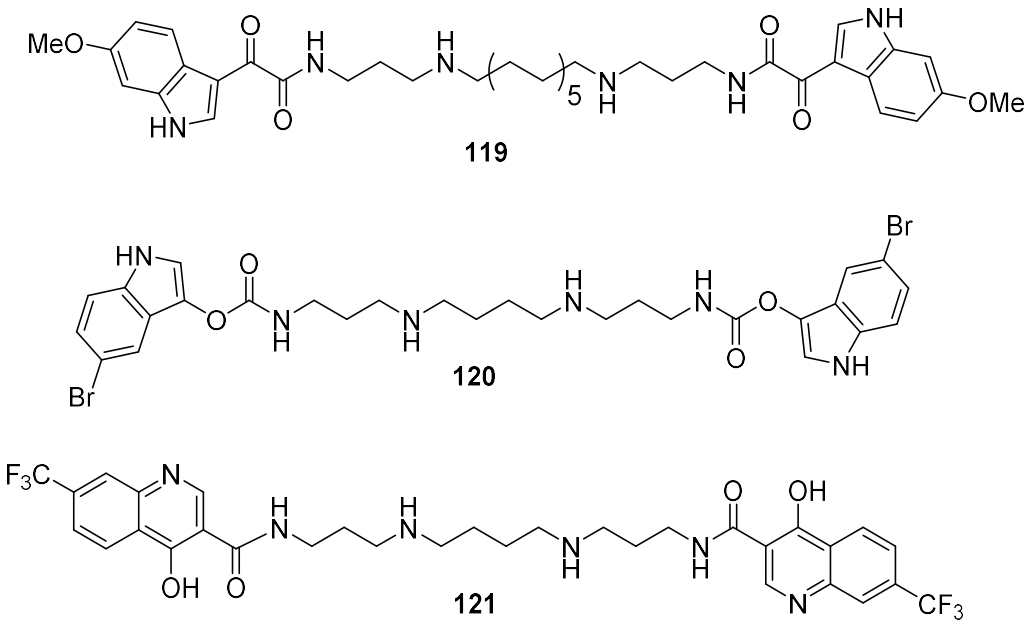

Figure 34: Bisindole- and bisquinoline-tetramine derivatives.

Among the bisacridines analogs,[52] few tetramine (3-3-3; 3-5-4 and 2-3-2) have been synthesized and the 2-3-2 analog **122** (Figure 35) was the most potent tetramine. It displayed good activity in vitro against *T. brucei* (IC_{50} around 0.001 µM) and against *L. donovani* promastigote with 99% lethality at 10 µM. **122** was also active on *L. major* intramacrophage amastigotes at 1 µM. Remarkably, the rigidified piperazinyl tetramine **123** (Figure 35) was clearly less active against the leishmanial strains. Bisnaphthalimidipropyl-spermine derivative **124** (Figure 35) was the least interesting polyamine in comparison with putrescine and spermidine analogs described earlier. Indeed, this **124** displayed IC_{50} of 7.56 and 12.28 µM against *L. infantum* promastigotes and axenic amastigotes respectively.[46]

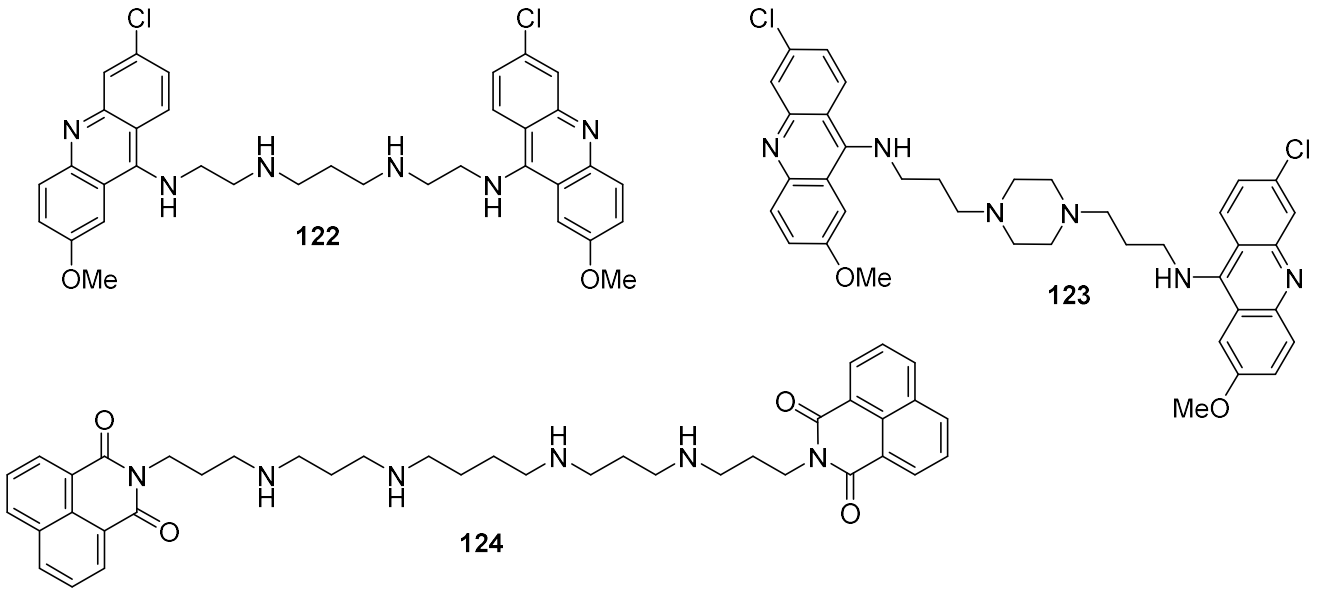

Figure 35: Bisacridine- and bisnaphthalimido-tetramine derivatives.

Historically, the first polyamine analogs described as antikinetoplastid agents were *N,N'*-bisbenzyl derivatives from Marion Merrell Dow Research Institute in Cincinnati. Initially, bisbenzyl-polyamines were identified as potent antimalarial,[85] and inhibited proliferation of HeLa cells.[86] At the beginning of the 90s, the 3-7-3 tertamine **MDL27695** (**126)** (Figure 36) was demonstrated effective against *L. donovani*. This compound has been assayed in vitro and in vivo on mice infected by visceral leishmaniasis. The results showed that **MDL27695 (126)** eliminate 77 to 100% of parasite in vitro at 1 µM.[87] In vivo, male BALB/c mice were infected by *L. donovani* and 15 mg per kg (three times per days) was found to be the highest dose tolerated by the mice and 10 day-treatment lead to 99.9% parasite suppression. It was demonstrated that *N,N'*-bisbenzyl-polyamine analogs were converted by polyamine oxidase (PAO) into their free polyamine counterparts. However, parasite suppression by **MDL27695 (126)** was equivalent

[85] Bitonti, A. J.; Dumont, J. A.; Bush, T. L.; Edwards, M. L.; Stemerick, D. M.; McCann, P. P.; Sjoerdsma, A. *Proc. Natl. Acad. Sci. U. S. A.* **1989**, *86*, 651–655.

[86] Edwards, M. L.; Snyder, R. D.; Stemerick, D. M. *J. Med. Chem.* **1991**, *34*, 2414–2420.

[87] Baumann, R. J.; Hanson, W. L.; McCann, P. P.; Sjoerdsma, A.; Bitonti, A. J. *Antimicrob. Agents Chemother.* **1990**, *34*, 722–727.

with or without coadministration of a known PAO inactivator,[88] indicating that parasite suppression was due to **MDL27695 (126)** itself and not its metabolite. Thus, a toxicological evaluation in rats suggested a reasonable therapeutic index. A similar study has been done with treatment by bisbenzyl-polyamine analog on golden hamster infected with *L. donovani*.[89] Results showed that polyamine levels in the liver and spleen were decreased after treatment with **MDL27695 (126)**. This compound has been tested on *T. cruzi* and was able to reduce the infectivity of the parasite in vitro at a concentration below 1 µM.[90] This compound was also tested against four strains of *T. brucei* in vitro and was moderately active (IC_{50} around 10-15 µM). In this study, another bisbenzyl-polyamine analog called **MDL27699 (129)** has shown a similar effect on *T. cruzi*. Two *N*,*N*'-thiophene-substitued polyamine analogs (**MDL28302 (130)**, **MDL29431 (131)**) (Figure 36) have also been tested in vitro on *T. cruzi*.[91] In these conjugates, 3-6-3 tetramines were alternatively bounded to the α- or β-positions of a thiophene nucleus. **MDL28302 (130)** and **MDL29431 (131)** (Figure 36) inhibited host cell invasion and intracellular multiplication. However, the inhibitory effect of either *N*,*N*'-thiophene substituted derivatives were reversible. Likewise, *N*,*N*'-thiophene-substitued polyamine analogs are converted into free polyamine by PAO but in this case inhibition of parasitic infectivity by these compounds was not demonstrated when treated with the specific PAO inhibitor. This result suggested that conversion of the *N*,*N*'-thiophene-substituted analogs to the corresponding free polyamine plays a key role for their inhibitory activity. All these bisaryl-polyamine analogs were able to inhibit *T. cruzi* penetration as well as its replication within a mammalian host cell. The influence of length of the central carbon chain has been studied and three other bisbenzyl-polyamine analogs have been tested in vitro for their antileishmanial activity.[92] The length of the chain of these analogs (**MDL27693** (**125)**, **MDL27700 (127)** and **MDL27994 (128)**) (Figure 36) ranged from 6 to 12 carbons. In vitro assay have shown that the activity increased with the length of this carbon chain. **MDL27994 (128)** which bears a 12-carbon central chain displayed an IC_{50} of 4 µM against *L. donovani* promastigotes whereas **MDL27695 (126)** had an IC_{50} of 18 µM in the

[88] Seiler, N.; Duranton, B.; Raul, F. *Prog. Drug Res. Fortschritte Arzneimittelforschung Prog. Rech. Pharm.* **2002**, *59*, 1–40.

[89] Mukhopadhyay, R.; Madhubala, R. *Pharmacol. Res.* **1993**, *28*, 359–365.

[90] Majumder, S.; Kierszenbaum, F. *Antimicrob. Agents Chemother.* **1993**, *37*, 2235–2238.

[91] Majumder, S.; Kierszenbaum, F. *Mol. Biochem. Parasitol.* **1993**, *60*, 231–239.

[92] Mukhopadhyay, R.; Madhubala, R. *Exp. Parasitol.* **1995**, *81*, 39–46.

same conditions. *L. donovani* promastigotes were treated with DFMO and then incubated in the presence of the bisbenzyl-polyamine analogs at subinhibitory concentrations. **MDL27693 (125)**, **MDL27695 (126)** and **MDL27700 (127)** rescued the cells completely from DFMO toxicity, whereas **MDL27994 (128)** failed. This observation suggests that the analogs could substitute for intracellular function of putrescine and/or spermidine. The experiments of thermal denaturation of leishmanial DNA indicated that all the analogs bind directly to DNA. These polyamine analogs additionally inhibited ODC and AdoMetDC activity but exogenous polyamine did not reverse the growth inhibition. The authors suggested that bisbenzyl-polyamine analogs block the intracellular binding of the natural polyamines or displace intracellular polyamine from their binding sites. The mechanism of inhibition of leishmanial growth by polyamine analogs could rely on the inhibition of macromolecular polyamine synthesis leading to cell death. The repression of polyamine biosynthesis by analog may be another event resulting in slowing the growth of the parasite, although it may not be a major toxic event. Furthermore, these compounds induce a decrease of intracellular polyamine level which could significate that bisbenzyl analogs interact with polyamine transporter of *L. donovani*. More recently, analogs of **MDL27695 (126)** were tested against *T. brucei* in vitro and the bisphenyl **132** (Figure 36) was active with IC_{50} below 1 µM.[66]

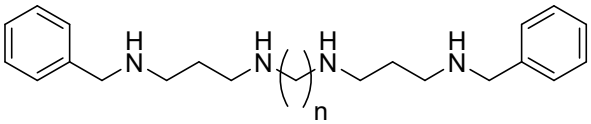

MDL27693 (125) n=6
MDL27695 (126) n=7
MDL27700 (127) n=10
MDL27994 (128) n=12

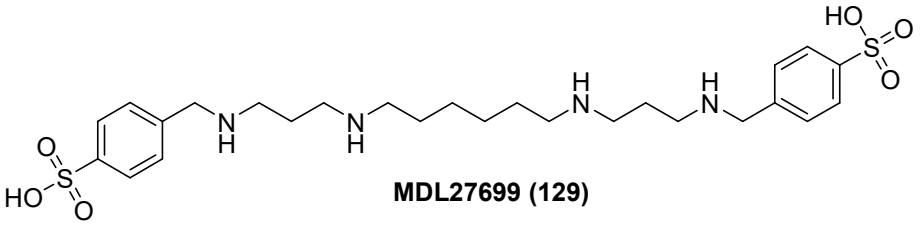

MDL27699 (129)

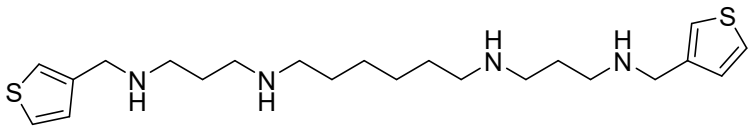

MDL28302 (130)

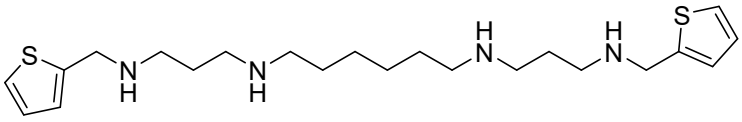

MDL29431 (131)

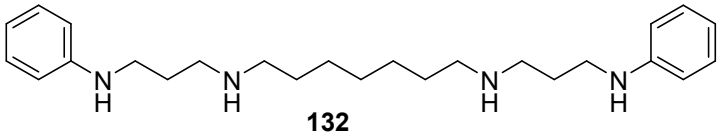

132

Figure 36: Derivatives from Marion Merrell Dow Research Institute and bisphenyl analog 132.

In the aforementioned polyaminoguanidines and polyaminobiguanides,[79] the most effective compound against *T. brucei* in vitro was a phenyl derivative **133** (IC_{50} = 0.09 µM) (Figure 37) which has a structure close to **126** with biguanides in lieu of secondary amines. Interestingly, the most effective compound in this series did not correspond to the most potent inhibitor of TryR. The spermine analog of **126**, i.e a 3-4-3 tetramine *N*-terminally substituted by benzyl moieties **135** (Figure 37), was synthesized. This compound and the corresponding benzoyl derivative **134** (Figure 37) were only tested on TryR and were not inhibitor of this enzyme (Ki > 100 µM).[75] In the same study,[72] O'Sullivan described spermine substituted in their two central nitrogen atoms by aryl groups. **136** (Figure 37), the benzyl isomer of **135** was a better inhibitor of TryR (Ki = 19

µM). Nonetheless, bisnaphtylpropyl-spermine **137** and bisphenylpropyl-spermine **138** (Figure 37) were good inhibitors of TryR (Ki = 3-5 µM) and were active in vitro against the four tested strains of *T. brucei* in vitro (IC_{50} = 0.5–0.9 µM). These two latter compounds were further tested on mice infected with *T. brucei* but were devoid of activity.

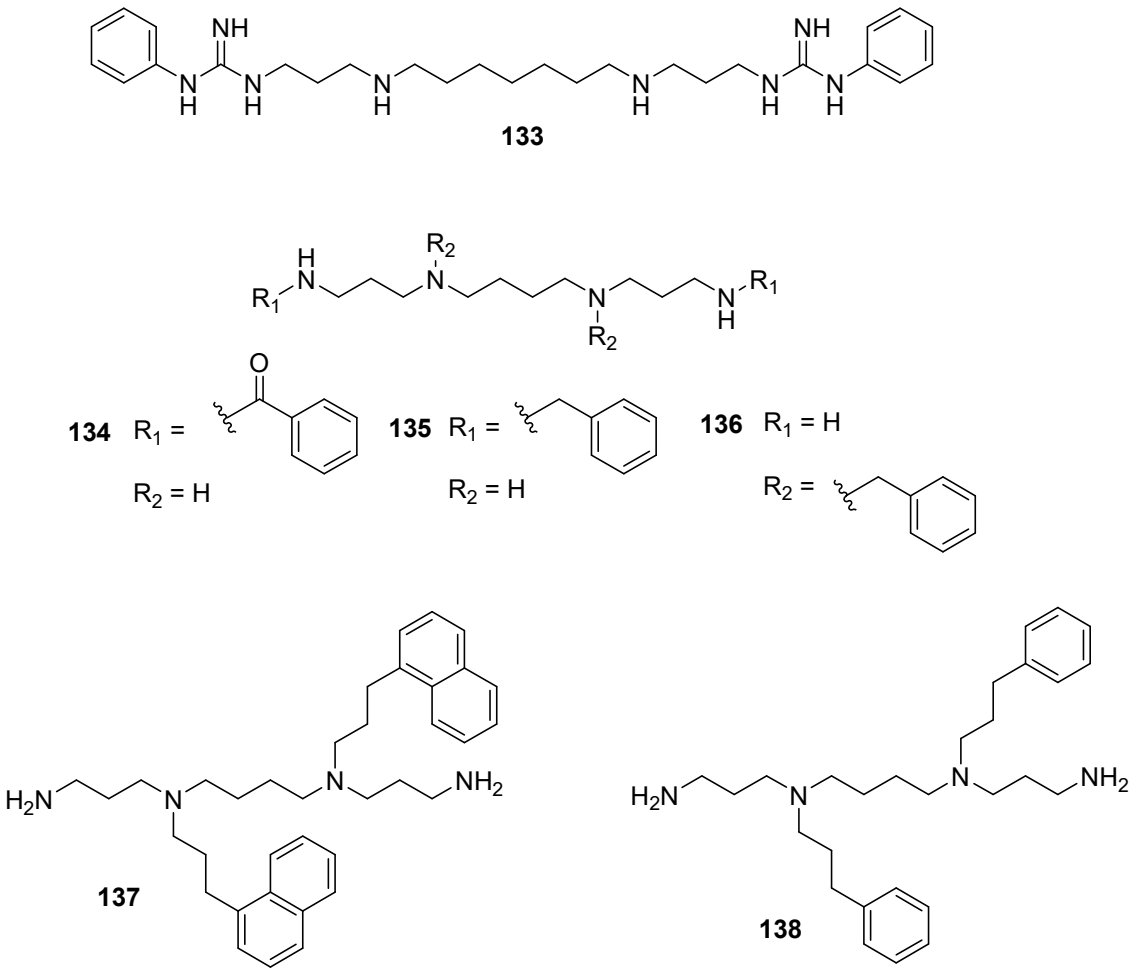

Figure 37: Bisaryl-tetramine derivatives.

O'Sullivan et al. who prepared dibenzosuberyl-spermidine derivatives, have also synthesized a spermine conjugate with this dibenzosuberyl moiety (Figure 38).[44] The spermine has been disubstituted by the dibenzosuberyl group on the central nitrogen atom and led to compound **139** (Figure 38). This dibenzosuberyl-spermine showed a better activity on TryR (Ki = 0.25 µM) than clomipramine and its trypanocidal activity was 2.55 µM (IC_{50}). Unfortunately, as Spd-DBS,

spermine derivative **139** did not show interesting in vivo activity against *T. b. brucei*. Bonnet et al.[93] have proceeded to a docking study using computer method for prediction of the activity of some considered compounds. It has been proved that the binding site in TryR is larger than in GR and has a good affinity for hydrophobic group. This molecular modeling indicated that the hydrophobic pocket in the active site of TryR could accommodate a bulky aromatic entity and in fact, it was found a higher activity of bis-derivatives than for mono-derivatives. In view of the above observations, bisamino diphenylsulfides have been prepared and few modifications have been realized in order to establish structure-activity relationships. TryR inhibition has been better for amine than for amide linker between polyamine and aromatic groups, the distance between these two groups seems to be optimal for biological activities with a 4-carbon chain. The variations of the heteroatom in the aromatic rings did not have any effect on TryR activity. Moreover, the nature of the substituents on the rings could modify the activity. Thereby, the replacement of the chloride by a methoxy group or suppression of the acetyl group led to a decreased activity. The best TryR inhibitor of the series was **140** (Figure 38) with a Ki value of 0.4 µM.

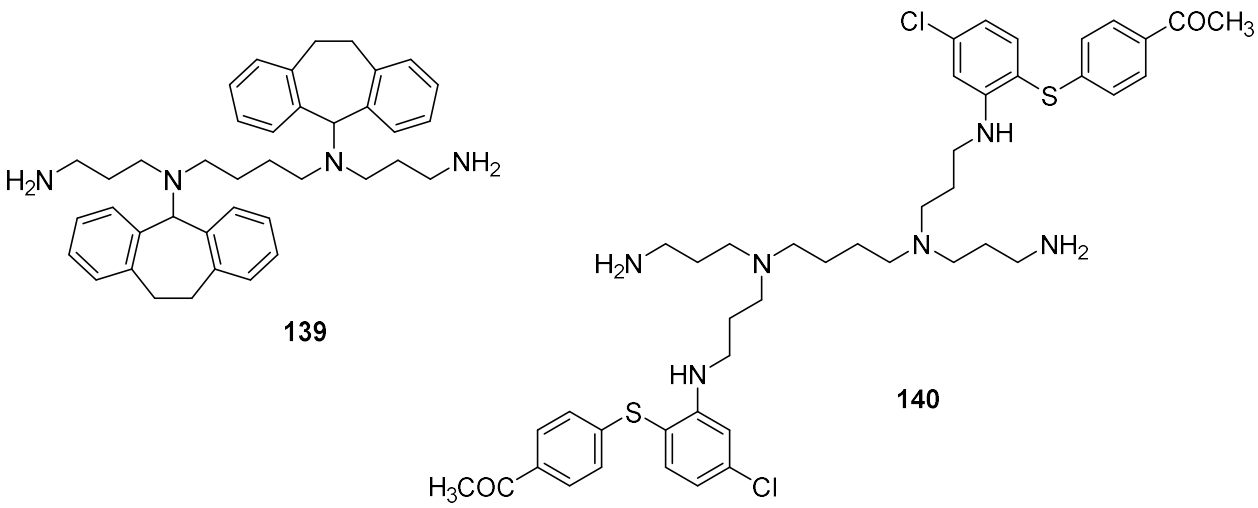

Figure 38: Bisdibenzosuberyl- and bisaminodiphenylsulfide-polyamine.

[93] Bonnet, B.; Soullez, D.; Davioud-Charvet, E.; Landry, V.; Horvath, D.; Sergheraert, C. *Bioorg. Med. Chem.* **1997**, *5*, 1249–1256.

V. Macrocyclic polyamines

Azamacrocycles have been identified as SOD inhibitor of *T. cruzi*,[94] *Leishmania infantum* and *Leishmania braziliensis.*[95] Structures are macrocycles containing triamine skeletons. These aza-scorpiands could bind iron superoxide dismutase by their side chain as observed by ^{1}H NMR and by the catabolites from the parasites after treatment. A trypanocidal activity was found in the three life stages of *T. cruzi* (epimastigote, amastigote and trypomastigote forms) with interesting selectivity index in comparison with Vero cells (host cell). Indeed, **141** (Figure 39) shows a better trypanocidal activity against *T. cruzi* than the reference compound benznidazole and a selectivity index fifty times higher. Moreover, its specificity has been demonstrated since the active compound inhibited Fe-SOD with value near to 100% at 12.5 µM and did not inhibit the human SOD. The best compound **141** has been tested in vivo on mice infected by *T. cruzi.* Infected animals were treated with 1 mg per kg per day during five days via the intraperitoneal route. Then, the number of blood trypomastigote forms of *T. cruzi* were counted every two 2 days from 5 to 60 days post-infection. After 60 days post-infection and treatment with **141**, the parasitemia level was considerably decreased. Moreover, parasitemia did not reappear after cycles of immosupression which could be considered as a cure. This compound is currently in preclinical development. In vitro assays have been done on promastigote, axenic amastigote and intramacrophage forms of *L. infantum* and *L. braziliensis* but no in vivo experiment have been described. Results showed that all the compounds were more active and less toxic than meglumine antimoniate (Glucantime®). **142** (Figure 39) displayed an IC_{50} of 6.30 µM against *L. infantum* intramacrophage amastigote, and **141** an IC_{50} of 10.4 µM against *L. braziliensis* intramacrophage amastigote. Furthermore, compounds inhibited also the leishmanial Fe-SOD activity. **142** showed a complete inhibition at 5 µM and 12.5 µM concentrations for *L. infantum* and *L. braziliensis,* respectively.

[94] Olmo, F.; Marín, C.; Clares, M. P.; Blasco, S.; Albelda, M. T.; Soriano, C.; Gutiérrez-Sánchez, R.; Arrebola-Vargas, F.; García-España, E.; Sánchez-Moreno, M. *Eur. J. Med. Chem.* **2013**, *70*, 189–198.

[95] Marín, C.; Clares, M. P.; Ramírez-Macías, I.; Blasco, S.; Olmo, F.; Soriano, C.; Verdejo, B.; Rosales, M. J.; Gomez-Herrera, D.; García-España, E.; Sánchez-Moreno, M. *Eur. J. Med. Chem.* **2013**, *62*, 466–477.

Recently, the same team published tetradentate polyamines as efficient metallodrugs against *T. cruzi*.[96] Mn-based polyamine and polyamine complexes were studied in vitro and in vivo. The macrocycle 1,4,7-tris(2-pyridylmethyl)-1,4,7-triazacyclononane, compound **143** (Figure 39), showed an in vitro IC_{50} around 7 µM for each form of *T. cruzi* with a better selectivity index than the reference compound benznidazole in each case, and it is consequently the best compound of this series. Other in vitro assay with infection of Vero cells by metacyclic forms of *T. cruzi* proved that **143** was able to reduce infection by 81%. In view of these good results, compound **143** has been chosen for further investigation with infected mice in acute and chronic phases. At the dose of 15 mg/kg body mass, compound **143** showed a partially curative effect (reduction by 33%). Moreover, **143** is inhibitor of the Fe-SOD of the parasite with an IC_{50} value of 18 µM.

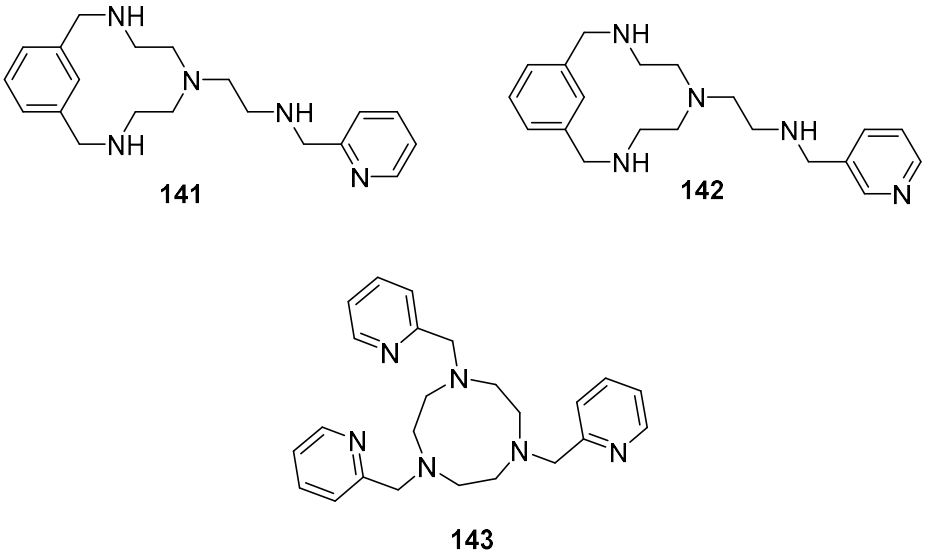

Figure 39: Macrocyclic polyamines developed as antikinetoplastid agents.

Lunarine **145** (Figure 40) is a macrocyclic spermidine extracted from the plant *Lunaria biennis*. Originally, this natural molecule was thought to inhibit TryR due to its spermidine part and its size approximatively equivalent to trypanothione. Lunarine was found as a potential active

[96] Olmo, F.; Costas, M.; Marín, C.; Rosales, M. J.; Martín-Escolano, R.; Cussó, O.; Gutierrez-Sánchez, R.; Ribas, X.; Sánchez-Moreno, M. *J. Chemother.* **2016**, *0*, 1–11.

compound by a virtual screening on TryR and showed a competitive time-dependent behavior.[97] This natural macrocycle displayed a modest K_i of 144 µM on TryR and Hamilton et al.[98,99] carried out structural modification in order to increase the inhibition activity. An advanced study has been done for compounds which showed a good inhibitory activity in order to understand inhibition mechanism. Modifications of the tricyclic nucleus appeared to have a detrimental effect on the enzymatic inhibition and compounds without polyamine did not have enzymatic activity. The trypanocidal activities of the lunarine derivatives were evaluated against *T. brucei* trypomastigotes and showed no activity at concentration below 100 µM except the racemic (±)-lunarine that displayed an IC_{50} of 65 µM.

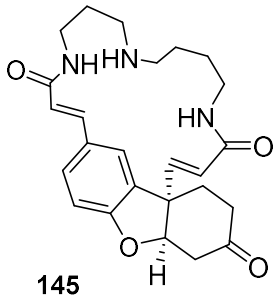

145

Figure 40: Lunarine 145 as inhibitor of trypanothione reductase.

VI. Aryl-bispolyamine derivatives

Polyamines linked to monoindolylmaleimides have been also described as inhibitors of trypanothione reductase from *T. cruzi*.[100] Again, modulations were based on linear or rigidified polyamine chain with piperazine derivative. The best compound of this series was compound

[97] Bond, C. S.; Zhang, Y.; Berriman, M.; Cunningham, M. L.; Fairlamb, A. H.; Hunter, W. N. *Structure* **1999**, *7*, 81–89.

[98] Hamilton, C. J.; Saravanamuthu, A.; Fairlamb, A. H.; Eggleston, I. M. *Bioorg. Med. Chem.* **2003**, *11*, 3683–3693.

[99] Hamilton, C. J.; Saravanamuthu, A.; Poupat, C.; Fairlamb, A. H.; Eggleston, I. M. *Bioorg. Med. Chem.* **2006**, *14*, 2266–2278.

[100] Salmon, L.; Landry, V.; Melnyk, O.; Maes, L.; Sergheraert, C.; Davioud-Charvet, E. *Chem. Pharm. Bull. (Tokyo)* **1998**, *46*, 707–710.

146 (Figure 41), which displayed an IC_{50} of 5.4 µM on TryR from *T. cruzi*. The corresponding conjugate with only one branched polyamine was not a good inhibitor. The authors mentioned that adding cationic charges can be beneficial for tight binding inside the active site of TryR. However, these molecules have been tested in vitro against *T. cruzi*, *T. brucei* and *L. infantum* and all of them were inactive.

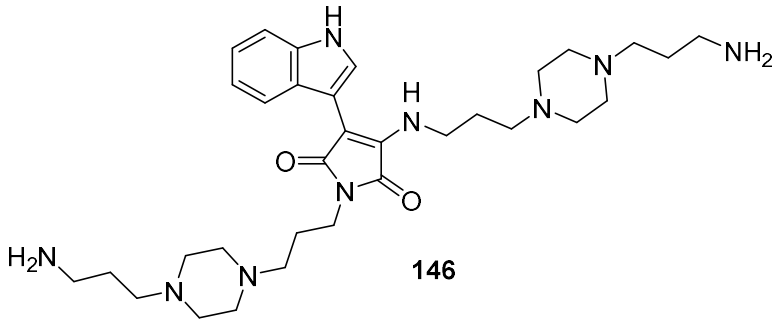

Figure 41: Monoindolmaleimides-bistetramine.

In the aforementioned study regarding lunarine derivatives, the majority of the analogs were either constructed with the tricyclic moiety of lunarine or a benzofurane nucleus linked to two identical polyamines.[98] Each central aryl moieties was linked to two spermidines **147**, two *N*,*N*-dimethylputrescines **148** and two triamines-containing piperazine cycle **149** (Figure 42). All these bispolyamine derivatives were not inhibitor of TryR and were not active against *T. b. rhodesiense* in vitro.

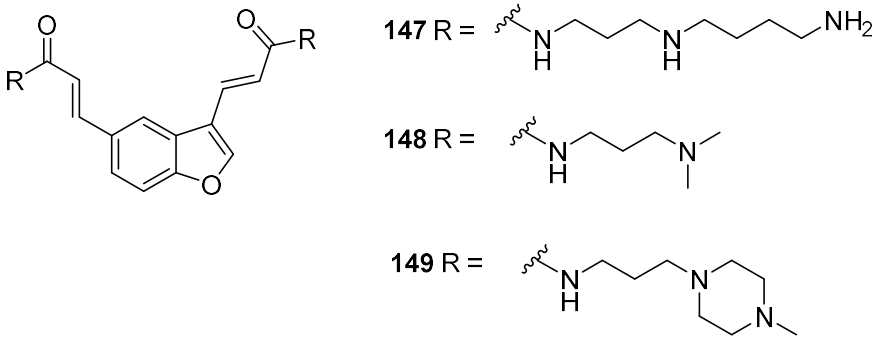

Figure 42: Lunarine derivatives.

VII. Conclusion

This chapter reports on five major chemical polyamine entities with various derivatives. The literature mentions trypanothione reductase as the most encountered target. Most of the published studies drew conclusions only based on in vitro testing against Kinetoplastids. Therefore, the identification of novel polyamines mostly relies on structure-in vitro activity relationships in the major Kinetoplastids (i. e. *T. b. brucei, T. cruzi,* and *Leishmania sp*.).

Main lessons from structure-activity relationship (SAR)

Effect of polyamines on trypanothione reductase

For the majority of these reported polyamine derivatives, the target is unkown. However, when known, it is very often TryR. Indeed, trypanothione reductase seems to be the most studied and the most relevant target for polyamine derivatives, in particular for compounds bearing an aryl hydrophobic part. The best inhibitor on TryR was the substrate analog **52** (Figure 43) with a Ki of 0.16 µM.

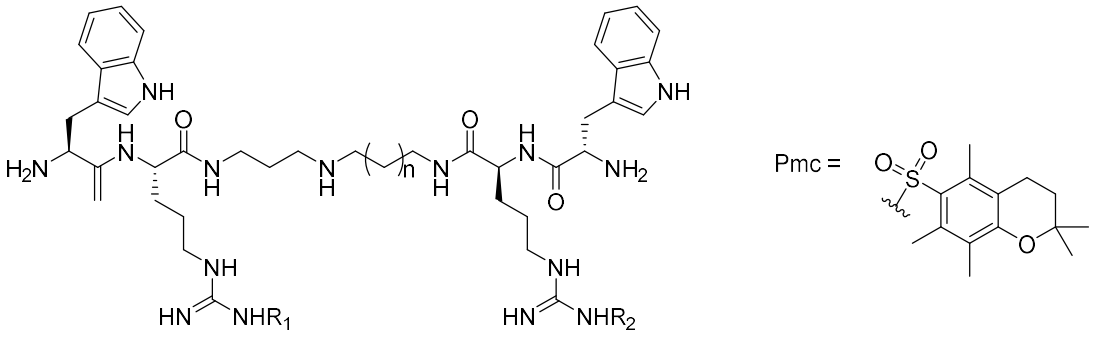

52 n=1, R_1=R_2=Pmc

Figure 43: Structure of the most efficient polyamine-based TryR inhibitor.

Effect of polyamine chains

The length of the diamine chain appears to play a role as important as the function coupled to it. Thus, a better activity was obtained with long carbon chains (around 12 carbons). However, the more the chain is long and the less it is water soluble. Generally, the putrescine chains seem more active than shorter chains with 2 or 3 carbons. Modifications of the spermidine chain do

not appear as critical for the biological activity. Only slight modifications have been performed on this polyamine as assayed with norspermidine. However, we can note different behavior when spermidine is conjugated on one side or the other, suggesting that targeted enzyme recognized preferentially one side of this polyamine. Elongation of the spermine chain by a 3-7-3 carbon chain has been often made and seems to be a quite good skeleton for antikinetoplastid activity. Some molecules bearing a double polyamine chain have been designed and evaluated but no activity has been observed.

Effect of substituents on the polyamine

Concerning the conjugated group attached to the polyamine, no acyl derivatives displayed sufficiently interesting activity. Labile groups attached to the amine functions, such as Boc generally increased the activity. This could be due to higher lipophilicity of the compound allowing better diffusion through the kinetoplastid membrane. Alkyl-polyamine derivatives were more effective for the tetramine derivatives than for diamine or triamine ones. Among them, bisalkyl symmetric derivatives seemed to be more efficient than unsymmetric compounds. In particular, the biscycloheptyl motif was shown to lead to higher activity. For the aryl and aroyl derivatives, we have distinguished the mono- and the di-substituted polyamine. Some mono-substituted diamine and triamine displayed antikinetoplastid activity with a good selectivity index as quinone-anthraquinone and hydroxybenzotriazole-spermine derivatives. Remarkably, mono-aryl/aroyl-tetramine derivatives were not active or are cytotoxic. However, a lot of disubstituted polyamines have been synthesized and many of them display interesting activities. Most efficient motifs seem to be benzyl, benzyloxybenzyl, naphthyl and acridinyl groups. Among the diamine, bisacridine derivatives showed nanomolar activity against *T. brucei* and bisbenzyloxy derivatives below 1 µM against *L. donovani*. In this category of bisaryl, the most efficient compound was **126** (Figure 36) which displayed activity against different Kinetoplastids in vivo.

In vivo evaluation

A number of compounds have been evaluated in vivo on different kinetoplastid organisms. O'Sullivan et al. have evaluated their best compound on mice infected by *T. b. brucei*.[75] Unfortunately, the in vivo trypanocidal activities were not as good as expected. Even with a

continuous delivery, these polyamine derivatives may be rapidly excreted or metabolized. Indeed, compounds bearing amino group could be substrate of some mammalian enzymes as amine oxidases or polyamine acetyltransferases which led to no retention of compound in the mammalian organism. In order to avoid this potential rapid excretion, amino group could be substituted by a methyl or another alkyl group in order to decrease the hydrophilic character of these compounds. For example, compound **59** is a cyclic spermidine which has been methylated and evaluated on hamster infected with *L. donovani*. This compound displayed an antileishmanial activity through intraperitoneal and oral routes. However, it has been demonstrated that this compound was also toxic for macrophages. In contrast, compound **141** (Figure 44) have been evaluated in vivo and appear to be able to cure animals infected with *T. cruzi*. This is a very promising compound for development of new antiparasitic drug, and it is currently in preclinical trial. Furthermore, the bisbenzyl-polyamine analog **MDL27695** (**126)** (Figure 44) have also display a good antileishmanial activity (on *L. donovani*) with 97% suppression of parasites at a dose of 15 mg per kg per day during 10 days. However, this compound has not been further studied.

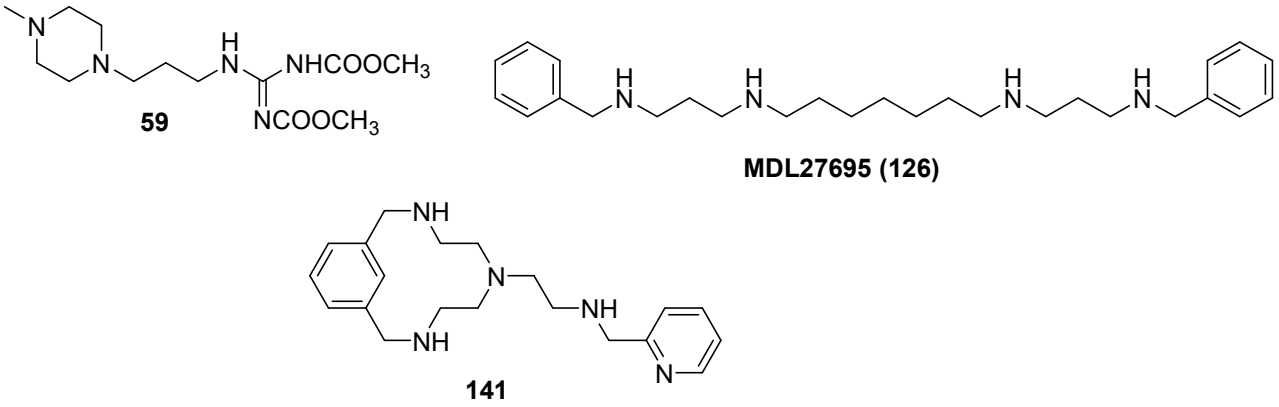

Figure 44

Structure/function studies involving the substituted polyamine analogs have revealed that considerable structural diversity is allowed among active analogs, and that small changes in chemical structure can lead to significant, and in some case, dramatic, changes in biological activity. The results and comparison between compounds must be interpreted carfully due to the metabolic differences of the organism studied and the different methods used.

Perspectives

Despite the difficulty to identify clear-cut structure-activity relationships, the significant in vivo activity of bisbenzyl-polyamine analogs is the proof that targeting polyamine metabolism is a promising way of research for antikinetoplastid drugs. Unfortunately, the present literature is poor of in vivo antikinetoplastid activity and pharmacokinetics data in these series. Considering the interesting levels of in vitro activity of some polyamines, further studies should include more optimized in vivo protocols combined with analysis of their fate and biodistribution and, the identification of biological targets by using pharmacoproteomics and relative approaches.

Chapter 2: Research project

Origin of the project

This research project is based on the design, chemical synthesis and in vitro antikinetoplastid activity evaluation on two parasites (*Trypanosoma brucei* and *Leishmania donovani)* of new polyamine derivatives targeting parasitic histone acetyltransferase and trypanothione reductase.

In our laboratory, bisubstrate type compounds were developed for their potent antitumor activity, the target of these compounds being the histone acetyltransferase (HAT) of mammalian cells. As HAT was recently validated as a therapeutic target in Kinetoplastids,[65] this enzyme could be used as a therapeutic target of some antikinetoplastid agents. Here, I describe the characterization, and biological function of this enzyme and, its involvement in therapeutic research.

I. Polyamines as histone acetyltransferase inhibitors

1. Chromatin structure

The genomes of eukaryotes are composed of multiple chromosomes, each containing a linear molecule of DNA. Although the numbers and sizes of chromosomes vary considerably between different species, their basic structure is the same in all eukaryotes. All the genomic information is contained in DNA and the total extent length of DNA, for example in Human cell, is nearly two meters. Nonetheless, this DNA must be confined into a nucleus with a diameter of only 5 to 10 µm and thus DNA of eukaryotic cells is rolled up around proteins called histones by strong bindings (Figure 45). The complexes between eukaryotic DNA and histones are called chromatin.

The extent of chromatin condensation varies during the life cycle of the cell. During the interphase (nondividing stage) of cells, most of the chromatin is decondensed and distributed throughout the nucleus. During this period of the cell cycle, genes are transcribed into RNA and the DNA is also replicated in preparation for cell division. Most of the euchromatin, corresponding to weakly condensed DNA, appears to form 30 nm-fibers in the interphase and is organized into large loops containing approximately 50 to 100 kb of DNA. About 10% of the euchromatin, containing the genes that are actively transcribed, is in a more decondensed state (the 10-nm conformation) that allows transcription. In eukaryotes, chromatin structure is thus intimately linked to the control of gene expression. In contrast to euchromatin, about 10% of interphase chromatin, called heterochromatin, is in a very highly condensed state. Heterochromatin is transcriptionally inactive and contains highly repeated DNA sequences, such as those present in centromeres and telomeres. Decondensed chromatin is necessary for DNA transcription.[101]

2. Histones

The major proteins of chromatin are the histones, small proteins containing a high proportion of basic amino acids (arginine and lysine) that facilitate binding to the negatively charged DNA molecule. There are five major types of histones, called H1, H2A, H2B, H3, and H4, which are very similar among different species of eukaryotes. The basic structural unit of chromatin, the nucleosome, is composed of eight histones around which is wrapped 146 bases pairs of DNA. The packaging of DNA into nucleosomes yields a chromatin fiber. The chromatin is further condensed by coiling into a 30 nm-fiber, containing about six nucleosomes per turn (Figure 45).

[101] Tomita, S.; Abdalla, M. O. A.; Fujiwara, S.; Yamamoto, T.; Iwase, H.; Nakao, M.; Saitoh, N. *Wiley Interdiscip. Rev. RNA* **2016**.

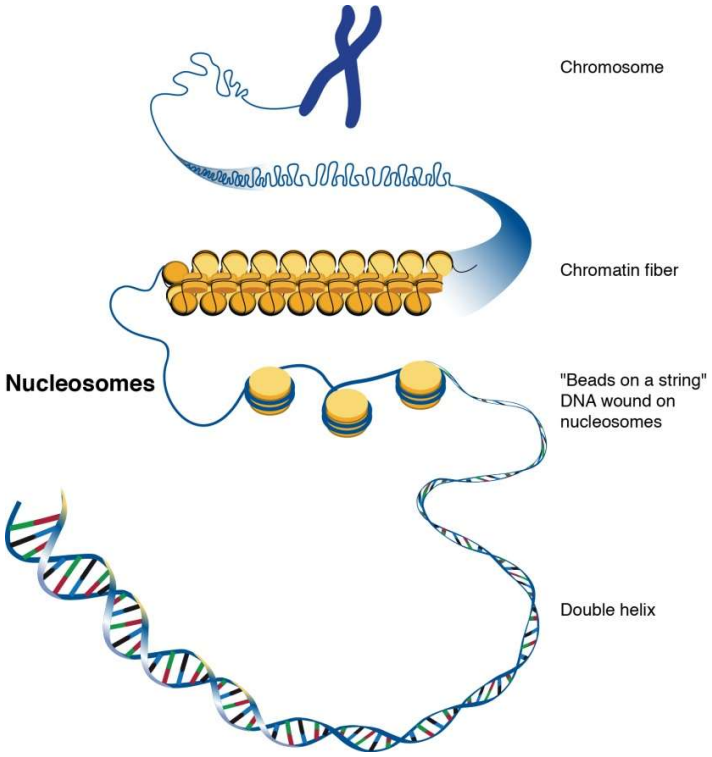

Figure 45: The packaging of DNA into the nucleus. ***(Image from https://unlockinglifescode.org)***

For the accessibility to DNA, some structural change must be operated at the chromatin level and more precisely at the nucleosome scale. For that, the *N*-terminal part of the histone is modified (acetylation, phosphorylation, methylation…) and these modifications influence the affinity of histone protein to DNA.[102] Chromatin modifiers are a large and varied group of enzymes that modulate a wide range of epigenetic functions. The inabilities to bind DNA, adjust chromatin conformation and modify histones allow them to influence gene expression making them powerful targets for epigenomic research and potential therapeutic targets. Among these chromatin modifiers, we focused on histone acetyltransferase.

[102] Kowalski, A.; Pałyga, J. *Biol. Cell* **2016**, n/a-n/a.

3. Histone acetyltransferase (HAT)

Histone acetyltransferases (HATs) are the workhorses of the epigenome. These enzymes have a huge role in epigenetic regulation of gene expression. HATs catalyze the transfer of an acetyl group from acetyl coenzyme A to a *N*-terminal function of lysine residue from histone (Figure 46). These acetylations neutralize the positive charge on histone and induce diminutions of both the affinity between histone and DNA and the interactions between adjacent nucleosomes. This leads to modifications in the architecture of chromatin. Subsequent active transcription allows the access for transcriptional and repair factors.[103] Acetylation is a reversible process and the histone deacetylases (HDAC) catalyze the reverse reaction which is also involved in gene transcription. Indeed, deacetylations are associated to gene repression (Figure 46).

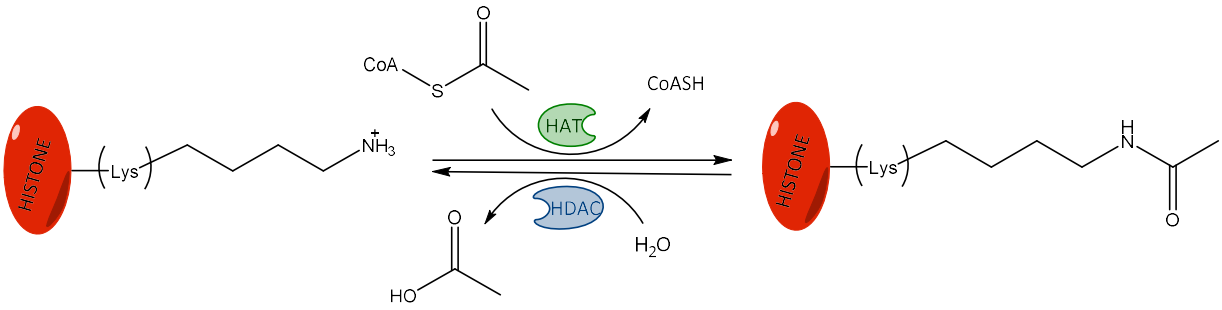

Figure 46: Acetylation and deacetylation of lysine's histone, catalyzed by HAT and HDAC, respectively.

HATs can also acetylate non-histone proteins, such as nuclear receptors and other transcription factors to facilitate gene expression. HATs and HDACs are classified into many families that are often conserved from yeast to human. Some reviews have focused on the various HAT families and their roles in chromatin function, transcription regulation or cell fate.[104,105]

[103] Grunstein, M. *Nature* **1997**, *389*, 349–352.

[104] Legube, G.; Trouche, D. *EMBO Rep.* **2003**, *4*, 944–947.

[105] Marmorstein, R.; Roth, S. Y. *Curr. Opin. Genet. Dev.* **2001**, *11*, 155–161.

4. Human HAT bisubstrate inhibitors

In 1982, Cullis and Wolfenden have designed inhibitors of the acetylation reaction.[106] These inhibitors conjugate spermidine to Coenzyme A (CoA) via an amide bond. These molecules which were called bisubstrate or bivalent inhibitors consist in two conjugated fragments, each targeting a different binding site of the enzyme (Figure 47). This kind of inhibitor has been developed for HAT.[107]

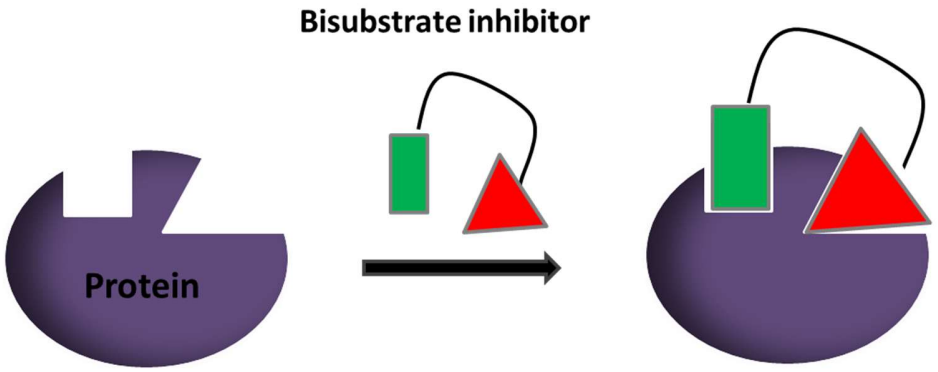

Figure 47: Principle of bisubtrate inhibitor.

Here, the two different substrate parts are firstly the lysine of the histone and secondly acetylcoenzyme A. Thus, regarding the inhibitor from Cullis et al.[106], the polyamine part mimics the *N*-terminal part of the lysine from histones. An inhibition greater than 50% of histone acetyltransferase has been obtained with these compounds at a concentration of 16 nM. The synthesis of these molecules has been performed through a non regioselective pathway and led to a mixture of compounds (Figure 48).

[106] Cullis, P. M.; Wolfenden, R.; Cousens, L. S.; Alberts, B. M. *J. Biol. Chem.* **1982**, *257*, 12165–12169.
[107] Wapenaar, H.; Dekker, F. J. *Clin. Epigenetics* **2016**, *8*, 59.

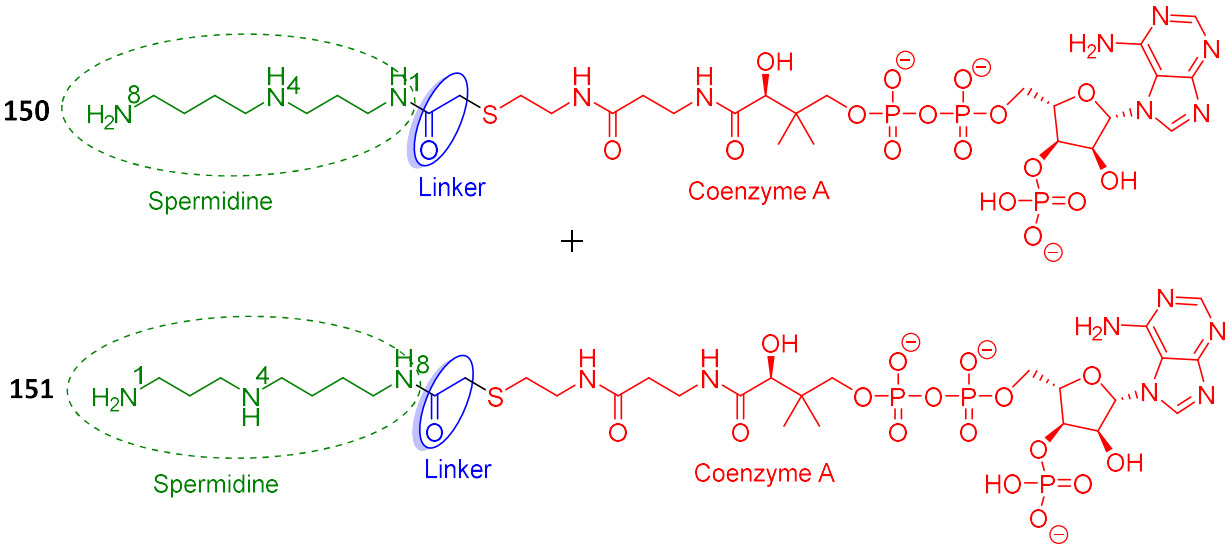

Figure 48: Spermidine-CoA 1a and 1b by Cullis et al.[106]

In the 90s, Roblot et al. [108] have developed a regioselective synthesis and have obtained **150** and **151** separately. For that, the authors developed a synthesis of selected spermidine protected by Boc (*tert*-butyloxycarbonyl) protecting group. This method will be more detailed in the next chapter. Then, the synthesis pathway used a bromoacetyl reactive intermediate **152** (Figure 49) from the substitution of the protected polyamine with the bromoacetic acid. In addition, they have synthesized **153** and **154** which is a compound with a truncated coenzyme A part. This was done in order to verify if the biological activities of these compounds require the entire coenzyme A.

[108] Roblot, G.; Wylde, R.; Martin, A.; Parello, J. *Tetrahedron* **1993**, *49*, 6381–6398.

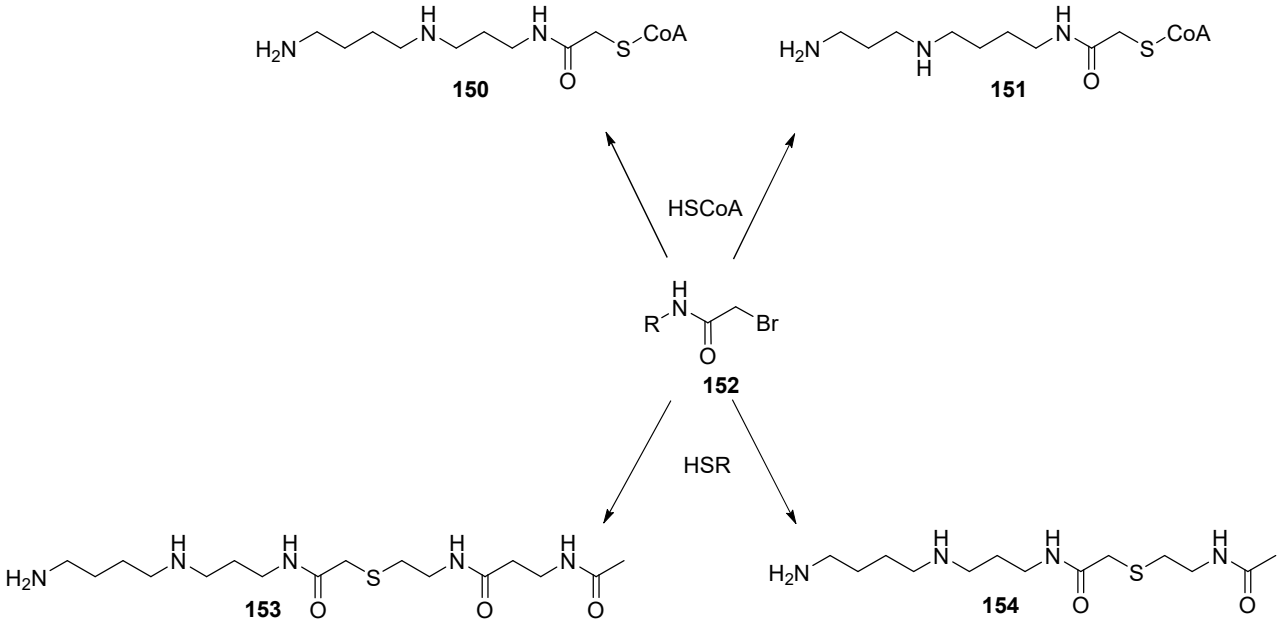

Figure 49: Synthesis by Roblot et al.[108] with a bromoacetyl intermediate.

Cellular effects of these compounds have been examined and it has been found that **150** acts on whole cells to inhibit histone acetylation, DNA synthesis and DNA repair. Moreover, **150** has a synergic effect with other well-known chemotherapeutic agents or UV-C irradiation to induce cancer cell killing.[109] The truncated analog **153** displayed enhanced cellular effects. It was assumed that the absence of negative charge carried by the CoA moiety could improve the cellular uptake. Normal cell lines are slightly or not damaged by these compounds. Authors suggest that **150** and **153** could be preferentially internalized into tumor cells through the polyamine transporter. Nonetheless, this hypothesis has not been verified. In 2011, other analogs have been synthesized and evaluated in vitro on the isolated p300 histone acetyltransferase. In this study, modulation of the polyamine part has been carried out. Coenzyme A moiety has been substituted with different diamines having chain length from 3 to

[109] Bandyopadhyay, K.; Banères, J.-L.; Martin, A.; Blonski, C.; Parello, J.; Gjerset, R. A. *Cell Cycle Georget. Tex* **2009**, *8*, 2779–2788.

5 carbons, piperazine or benzyl group.[110] The most efficient compound of the series was the one bearing the longest chain and with Boc protecting group on terminal amine.

5. Applications to the search of antikinetoplastid agents

Genome sequencing has revealed that four HATs are encoded by genomes of *Leishmania major* and *Trypanosoma cruzi* and three by the one of *Trypanosoma brucei*.[111] These parasites have many unique features in their biphasic life cycle such as concerted replication of nuclear genome and kinetoplastid DNA in a single copy in the mitochondria, polycistronic message formation and nearly complete dependence on the post-transcriptional mechanism for differential gene expression.[112] Among HATs that have been identified and characterized, TbHAT1 and TbHAT2 (from *T. brucei*) and LdHAT1 (from *L. donovani*) have been demonstrated as being essential for cellular growth.[113,114] Accordingly, HAT clearly represents a new validated therapeutic target for drug development against Kinetoplastids. Furthermore, polyamine

[110] Kwie, F. H. A.; Briet, M.; Soupaya, D.; Hoffmann, P.; Maturano, M.; Rodriguez, F.; Blonski, C.; Lherbet, C.; Baudoin-Dehoux, C. *Chem. Biol. Drug Des.* **2011**, *77*, 86–92.

[111] Ivens, A. C.; Peacock, C. S.; Worthey, E. A.; Murphy, L.; Aggarwal, G.; Berriman, M.; Sisk, E.; Rajandream, M.-A.; Adlem, E.; Aert, R.; Anupama, A.; Apostolou, Z.; Attipoe, P.; Bason, N.; Bauser, C.; Beck, A.; Beverley, S. M.; Bianchettin, G.; Borzym, K.; Bothe, G.; Bruschi, C. V.; Collins, M.; Cadag, E.; Ciarloni, L.; Clayton, C.; Coulson, R. M. R.; Cronin, A.; Cruz, A. K.; Davies, R. M.; Gaudenzi, J. D.; Dobson, D. E.; Duesterhoeft, A.; Fazelina, G.; Fosker, N.; Frasch, A. C.; Fraser, A.; Fuchs, M.; Gabel, C.; Goble, A.; Goffeau, A.; Harris, D.; Hertz-Fowler, C.; Hilbert, H.; Horn, D.; Huang, Y.; Klages, S.; Knights, A.; Kube, M.; Larke, N.; Litvin, L.; Lord, A.; Louie, T.; Marra, M.; Masuy, D.; Matthews, K.; Michaeli, S.; Mottram, J. C.; Müller-Auer, S.; Munden, H.; Nelson, S.; Norbertczak, H.; Oliver, K.; O'Neil, S.; Pentony, M.; Pohl, T. M.; Price, C.; Purnelle, B.; Quail, M. A.; Rabbinowitsch, E.; Reinhardt, R.; Rieger, M.; Rinta, J.; Robben, J.; Robertson, L.; Ruiz, J. C.; Rutter, S.; Saunders, D.; Schäfer, M.; Schein, J.; Schwartz, D. C.; Seeger, K.; Seyler, A.; Sharp, S.; Shin, H.; Sivam, D.; Squares, R.; Squares, S.; Tosato, V.; Vogt, C.; Volckaert, G.; Wambutt, R.; Warren, T.; Wedler, H.; Woodward, J.; Zhou, S.; Zimmermann, W.; Smith, D. F.; Blackwell, J. M.; Stuart, K. D.; Barrell, B.; Myler, P. J. *Science* **2005**, *309*, 436–442.

[112] Hammarton, T. C.; Mottram, J. C.; Doerig, C. *Prog. Cell Cycle Res.* **2003**, *5*, 91–101.

[113] Kawahara, T.; Siegel, T. N.; Ingram, A. K.; Alsford, S.; Cross, G. A. M.; Horn, D. *Mol. Microbiol.* **2008**, *69*, 1054–1068.

[114] Maity, A. K.; Saha, P. *FEMS Microbiol. Lett.* **2012**, *336*, 57–63.

transporters have been described as overexpressed into certain Kinetoplastids as it will be discussed afterward.

II. Thesis project

Objectives:

- The evaluation of previously synthesized bisubstrate inhibitors on in vitro kinetoplastid models in order to get a molecular skeleton for further rational chemical synthesis.
- The design, chemical synthesis and characterization of three chemical series.
- The biological in vitro evaluation against parasite cultures.
- Evaluation of the synthesized polyamines on putative targets (HAT and TryR).
- Development of new fluorescent assay for the polyamine transport.

In this part, I will therefore present the different series of polyamines that we opted to synthesize. The different assays for the biological evaluation will be then summarized. Lastly, the interest for a new transport assay will be introduced.

1. Synthesis

In this project, we designed three series of polyamine. The first series of compounds consist in the "Acyl" polyamines and contains the aforementioned bisubstrate inhibitors of HAT and new conjugates derived from the existing ones. A second part is dedicated to aryl-polyamine molecules and is divided into two series: hydoxybenzotriazole- (HOBt) and bisbenzyl-polyamines.

1.1. Acyl

For the acyl series, we prepared conjugated molecules containing three parts (Figure 50):

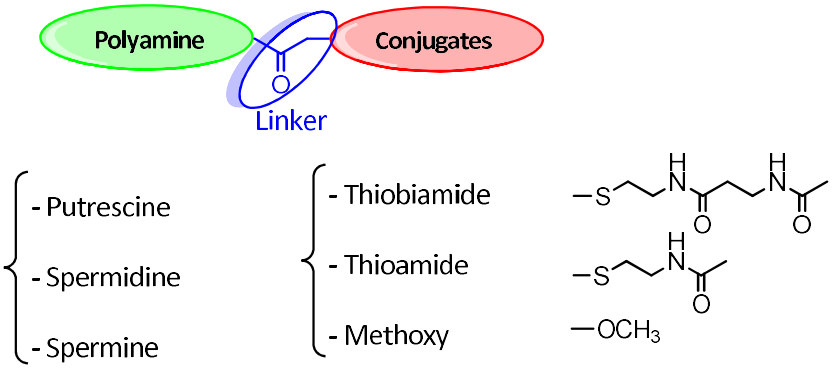

Figure 50: Schematic representation of designed molecules.

- A polyamine part which consists in one of the three most prevalent polyamines in nature namely putrescine, spermidine or spermine.
- A 2-carbon linker that seems to be the most efficient. Indeed, it was shown that a longer spacer could decrease the biological activity.[115]
- A moiety consisting of either a truncated coenzyme A or a very small conjugates such as a methoxy group.

1.2. Aryl

In a second time, we were interested in aryl-conjugates. Indeed, numerous active polyamine derivatives against Kinetoplastids display a hydrophobic part such as an aryl or heteroaryl group. Moreover, it has been demonstrated that the presence of a hydrophobic part is often required for efficient inhibition of TryR and this enzyme tolerates a large spectrum of aryl structure.

a. HOBt

Among the hetero-aryl nucleus, benzotriazole group is one of the most recently developed for drug design.[116] Hence, we developed a series of hydroxybenzotriazole conjugates with different polyamine groups (Figure 51).

[115] Sagar, V.; Zheng, W.; Thompson, P. R.; Cole, P. A. *Bioorg. Med. Chem.* **2004**, *12*, 3383–3390.
[116] Ren, Y. *Med. Chem.* **2014**, *4*.

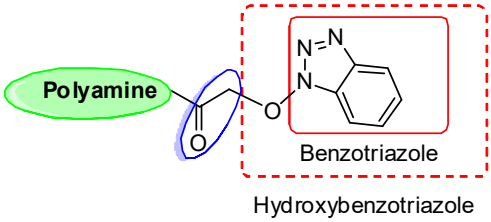

Figure 51: Schematic structure of the hydroxybenzotriazole derivatives.

b. Benzyl

In the first chapter, we reviewed the polyamine derivatives classified depending on the nature of the polyamine, i. e. putrescine, spermidine or spermine. Many spermidine derivatives were found biologically active. Therefore, we chose to develop a spermidine series that is conjugated on the N^3-nitrogen atom which seems to be more efficient in view of preliminary results in our laboratory. On the other hand, one of the most active polyamine described in the literature is a bisbenzyl derivative.[90] Furthermore, it has been shown that dibenzylation on the same nitrogen could enhance the activity.[38] For these reasons, our spermidine series will be disubstituted on the N^3 by different benzyl moieties (Figure 52).

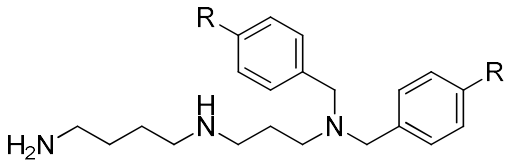

Figure 52: General structure of the bisbenzyl derivatives.

In addition, incorporation of a 4-benzyloxy group onto the benzyl group has been demonstrated to enhance the activity. Thus, we chose to operate modifications of the benzyl by addition of a benzyloxy group. Other modifications on the aryl substituent and on the polyamine chain were performed in order to establish structure-activity relationship for this series.

2. Biological evaluation of the polyamine derivatives

In this part, I present the different biological models to evaluate our compound as antikinetoplastid agents. *Trypanosoma brucei gambiense* and *Leishmanial donovani donovani*, are considered for the assessment of in vitro antikinetoplastids activity. Furthermore, as mentioned earlier, two enzymes, HAT and TryR were envisioned as target of our polyamines.

2.1. In vitro antikinetoplastids activity

All the synthesized compounds have been evaluated in the laboratory of Antiparasitic Chemotherapy in the Faculté de Pharmacie Université Paris-Sud in Châtenay-Malabry which is partner of this project. For that, we chose two species of Kinetoplastids; *Trypanosoma brucei gambiense* and *Leishmania donovani donovani*.

- *Trypanosoma brucei gambiense*

Among Trypanosomatids, *Trypanosoma brucei gambiense* is responsible for the West African sleeping sickness which is fatal in the absence of treatment. This parasite is often tested since the culture in vitro is straightforward and since many reports contain data on this Kinetoplastid, it is useful for comparison purpose. After treatment with different concentrations of inhibitor, cell viability of *T. b. gambiense* is measured through resazurin reduction assay in 96-well microplates as described in the experimental part.[117] Viable trypanosomes with active metabolism can reduce resazurin into the resorufin product which is pink and fluorescent. Then, fluorescence is measured in a microplate reader. The decrease of fluorescence indicates a parasite growth inhibition.

[117] Riss, T. L.; Moravec, R. A.; Niles, A. L.; Duellman, S.; Benink, H. A.; Worzella, T. J.; Minor, L. In *Assay Guidance Manual*; Sittampalam, G. S.; Coussens, N. P.; Nelson, H.; Arkin, M.; Auld, D.; Austin, C.; Bejcek, B.; Glicksman, M.; Inglese, J.; Iversen, P. W.; Li, Z.; McGee, J.; McManus, O.; Minor, L.; Napper, A.; Peltier, J. M.; Riss, T.; Trask, O. J.; Weidner, J., Eds.; Eli Lilly & Company and the National Center for Advancing Translational Sciences: Bethesda (MD), **2004**.

- *Leishmania donovani*

Leishmania donovani is responsible for visceral leishmaniasis, the most severe form of leishmaniasis. In the insect vector, *L. donovani* displays a promastigote form. In human the metacyclic promastigotes transform into amastigotes and divide. For this study, we chose to evaluate our compounds on the amastigote forms (axenic and intramacrophage forms) which are found in human host. Promastigotes are grown and transformation to amastigote was induced by using suitable culture conditions.[118] In vitro evaluation on axenic amastigotes and intramacrophages amastigotes were performed using SYBR green reagent. SYBR green specifically binds double-stranded DNA by intercalating between base pairs, and fluoresces only when bound to DNA. Indeed, parasite growth was determined by quantification of DNA. Fluorescence was measured and compared to those from the range obtained with different parasite densities.

2.2. Enzyme

a. Histone acetyltransferase

In order to promote LdHAT1 in *Leishmania donovani* as a therapeutic target, we chose to produce and purify this enzyme. Then, the synthesized compounds would be tested in vitro on the purified enzyme in order to evaluate their potential inhibitory activity. A Master 2 student was hired in order to complete this part of the project.

- Enzyme purification

The plasmid pET 21b+ / LdHAT1, kindly provided from Professor P. Saha laboratory, was used to express and produce His6-tagged LdHAT1 in *E. coli*. Following protein extraction, His6-LdHAT1 was purified using nickel affinity chromatography.

[118] Cheikh-Ali, Z.; Caron, J.; Cojean, S.; Bories, C.; Couvreur, P.; Loiseau, P. M.; Desmaële, D.; Poupon, E.; Champy, P. *ChemMedChem* **2015**, *10*, 411–418.

- **Enzyme activity**

Different methods are available for measurement of HAT activity: spectrophotometric, fluorescence or radiolabeled methods. The last one is very sensitive but requires specific organization and authorization.

For the current project, we decided to adapt the method used in our laboratory on mammalian HAT. It is a spectrophotometric method which consists in a UV-visible colorimetric titration described by Thompson et al.[119] Thiol function of coenzyme A reacts with DTNB (Ellman's reagent) to give 2-nitro-5-thiobenzoate (NTB), which absorbs at 405 nm (Figure 53). Series of dosages have been done to establish the activity of the HAT. Thus, during the enzymatic reaction, the released CoASH should react with DTNB and the formation of NTB is followed to determine the enzymatic activity.

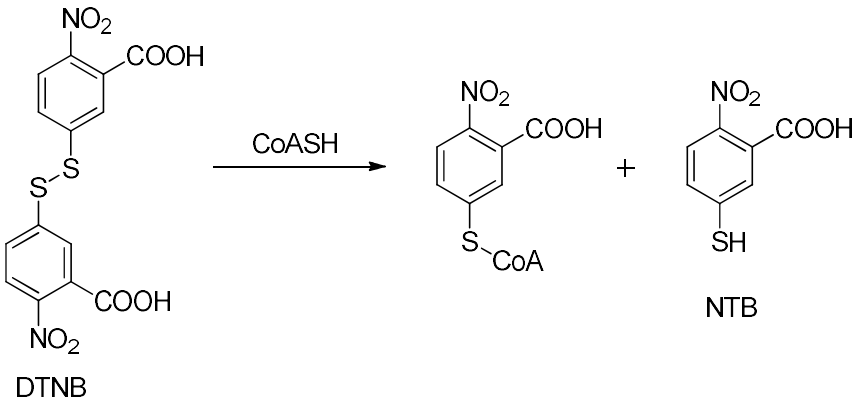

Figure 53: Reaction of DTNB with CoASH produced by HAT activity.

Alternatively, fluorescent assay is described by Trievel et al.[120] Coenzyme A generated in the HAT assay reacts with the sulfhydryl-sensitive dye 7-diethylamino-3-(4'-maleimidylphenyl)-4-methylcoumarin (CPM), yielding to an adduct which fluoresces strongly at 469 nm (Figure 54).

[119] Thompson, P. R.; Wang, D.; Wang, L.; Fulco, M.; Pediconi, N.; Zhang, D.; An, W.; Ge, Q.; Roeder, R. G.; Wong, J.; Levrero, M.; Sartorelli, V.; Cotter, R. J.; Cole, P. A. *Nat. Struct. Mol. Biol.* **2004**, *11*, 308–315.
[120] Trievel, R. C.; Li, F. Y.; Marmorstein, R. *Anal. Biochem.* **2000**, *287*, 319–328.

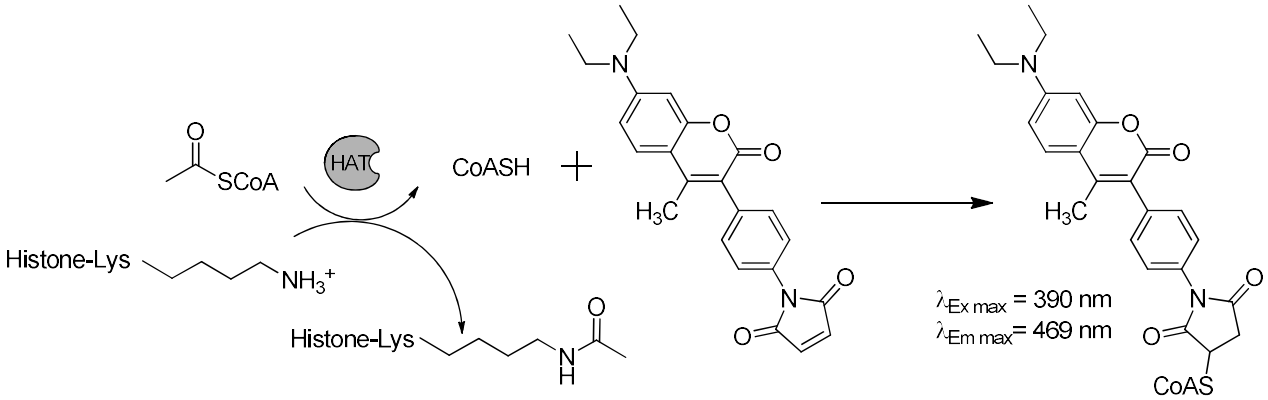

Figure 54: Fluorescent assay for the detection of CoASH produced by HAT activity.

Unfortunately, it was not possible to produce enough material and to devise a protocol for the determination of LdHAT1 activity during this internship.

b. Trypanothione reductase

As it was discussed in the first chapter, a wide range of polyamine derivatives target TryR. For this reason, we decided to screen our compounds against this enzyme which is a possible target. During this thesis, I had the opportunity to spend two weeks in the laboratory of Professor Luise Krauth-Siegel in Heidelberg (Germany). Thanks to the high expertise and technical method of Krauth-Siegel's laboratory, I was able to set up enzymatic evaluation on TryR and therefore evaluate our synthetic compounds. This enzyme catalyses the reduction reaction of the disulfide group of the trypanothione disulfide which is essential for the defense against oxidative stress (Figure 55). TryR was obtained from *Trypanosoma brucei* as described in the experimental part and TryR was assayed spectrophotometrically following the trypanothione-dependent oxidation of NADPH at 340 nm.

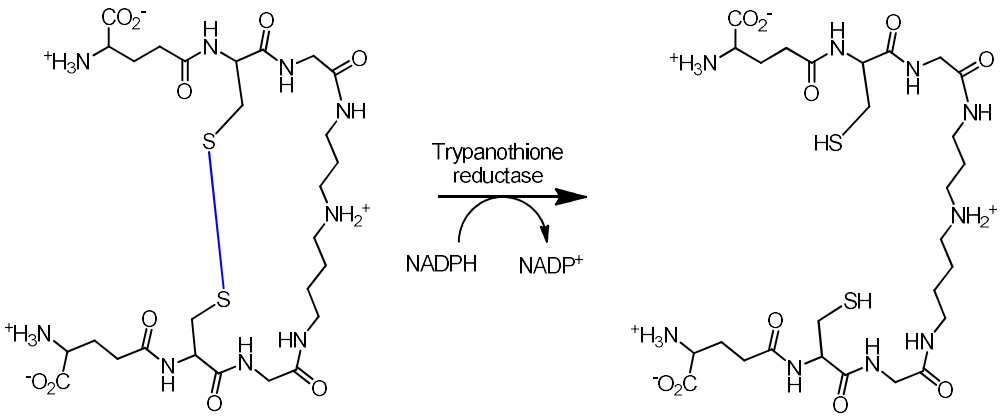

Figure 55: Reaction carried out by trypanothione reductase. Stuctures of the oxidized and the reduced forms of trypanothione.

3. Polyamine transport evaluation on competent parasite

All the polyamine derivatives described earlier are potentially uptaken into cells by polyamine transporters which are overexpressed in parasite.[121,122] In order to evidence this polyamine cargo, the usual method is based on competition with radiolabeled spermidine. However, this method has a number of disadvantages like cost, specific material requirements and habilitation. In contrast, utilization of fluorescent probes could be easier to set up. Thus, we chose to develop a competitive binding assay using fluorescent probes (Figure 56). We used this fluorescent assay to evidence the potential of our compounds to use polyamine transporters.

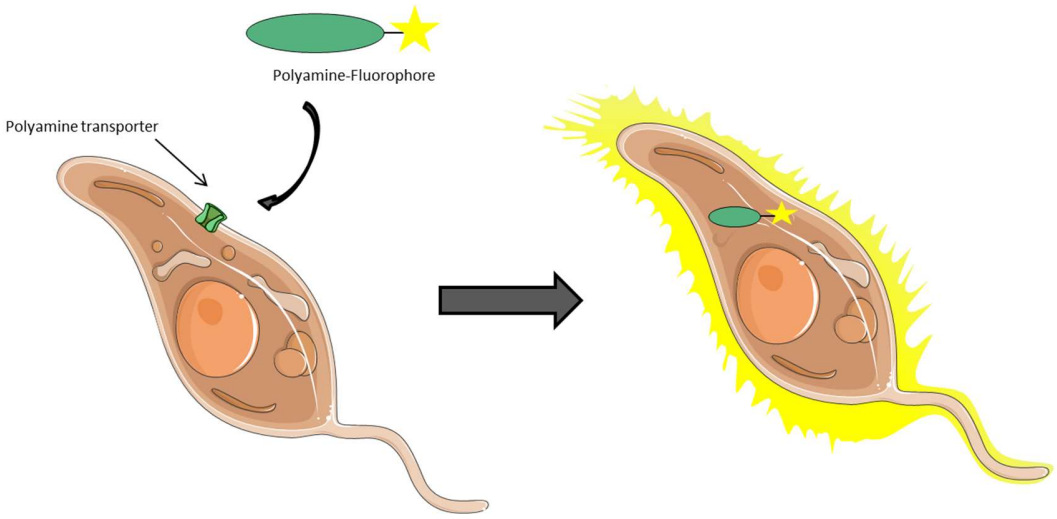

Figure 56: Fluorescent assay principle.

[121] Bacchi, C. J.; Nathan, H. C.; Hutner, S. H.; McCann, P. P.; Sjoerdsma, A. *Science* **1980**, *210*, 332–334.
[122] Thibault, B.; Clement, E.; Zorza, G.; Meignan, S.; Delord, J.-P.; Couderc, B.; Bailly, C.; Narducci, F.; Vandenberghe, I.; Kruczynski, A.; Guilbaud, N.; Ferré, P.; Annereau, J.-P. *Cancer Lett.* **2016**, *370*, 10–18.

Chapter 3: Acyl-polyamine derivatives

Our team previously reported the potent anticancer activity of polyamine-coenzyme A conjugates as bisubstrate inhibitors of human histone acetyl transferase (HAT).[109] Furthermore, parasitic histone acetyl transferase has been validated as a therapeutic target for Kinetoplastids.[65,114] Taking into consideration the similarities regarding the polyamine dependence of both cancer cells and Kinetoplastids, we became interested in testing our polyaminated compounds against these parasites. Among the previously prepared polyamines, the most potent antitrypanosomal agent was the polyamine derivative **153** where the coenzyme A was partially truncated (Figure 57).

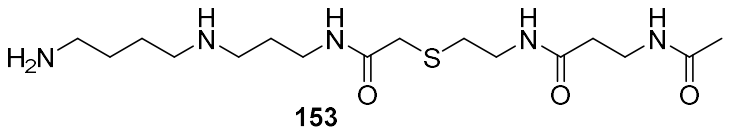

153

Figure 57: Structure of the hit molecule 153 against Kinetoplastid.

Even though the parasitic target of **153** is not clearly identified, the originality of this structure and the relevant pharmacological activity led us to prepare new derivatives with molecule **153** as the hit compound. In this series, we chose to synthesize *N*-acylated conjugates of three commonly found polyamines: putrescine, spermidine, and spermine. Three groups of polyamine derivatives containing different acylated moieties were synthesized (Figure 58): (i) the thiobiamide conjugates by analogy with the hit molecule **153**; (ii) thioamide; (iii) or only a methoxy group to evaluate the importance of a simple amide group. Since spermidine is an unsymmetric polyamine, we synthesized the N^1-, N^2- and N^3-spermidine conjugates to evaluate such modification on the biological activity.

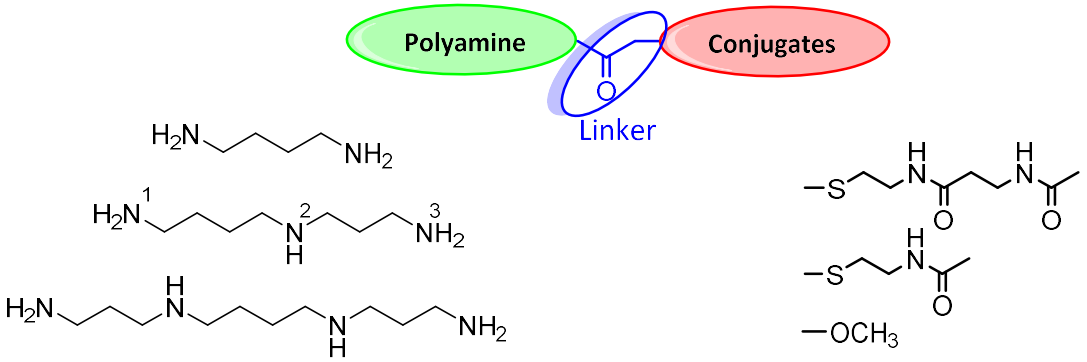

Figure 58: General structurse of Acylconjugates.

I. Retrosynthesis

In this chapter, the synthetic pathway (Figure 59) is inspired by Roblot et al. The final free amine would be obtained as hydrochloride salt from the corresponding Boc-protected derivatives. The Boc-protected molecules should be prepared from the coupling of a nucleophile moiety to a reactive bromo intermediate. The latter intermediate would be synthesized through amide bond formation between bromoacetyl bromide and protected polyamine. The protection of the different polyamine would be carried out using the classical Boc group.

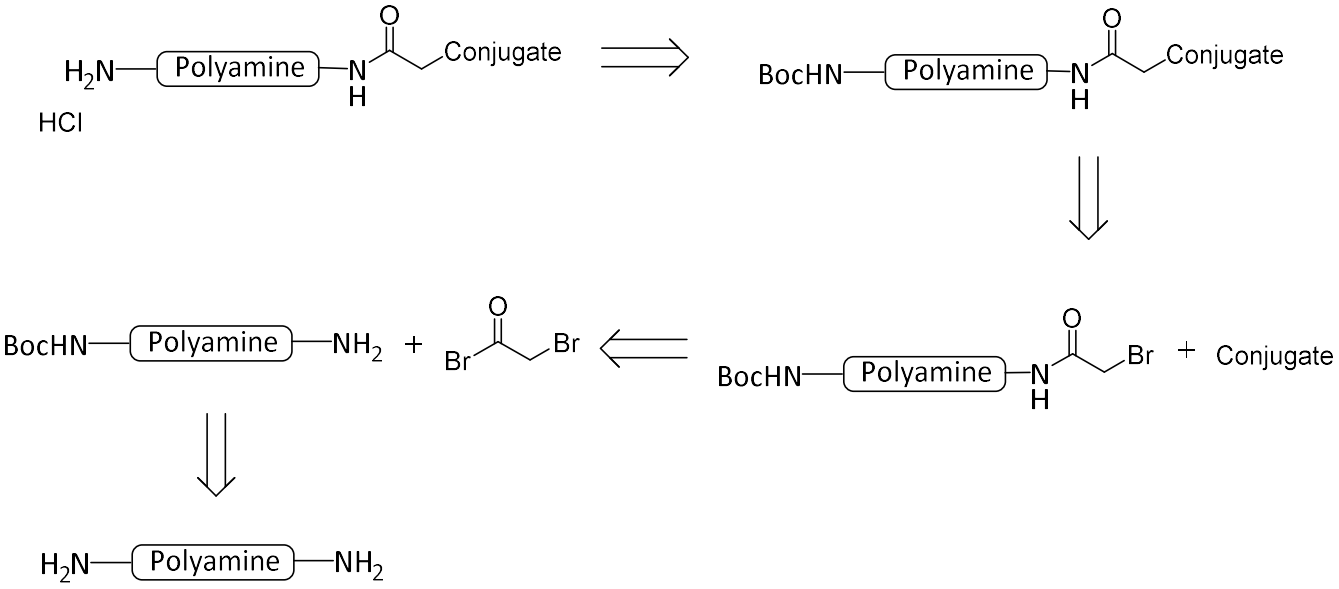

Figure 59: Retrosynthetic pathway envisionned for the *N*-acylated conjugates.

II. Polyamines protections

2.1. Putrescine

The *tert*-butyloxycarbonyl (Boc) group is a well-known protecting group for amine function. The reagent di-tert-butyl dicarbonate (Boc_2O) easily reacts to give protected amine. Putrescine is a diamine and its monoprotection is more challenging than the simple reaction scheme might indicate. Boc-anhydride reagent cannot differentiate between the two identical amino moieties in the substrate. The result is a crude mixture of unprotected, monoprotected and diprotected diamines. To prevent this, we utilized a large excess of diamine (5 eq) in comparison to Boc reagent. Solution of Boc_2O in dichloromethane was added dropwise to a solution of diamine. The commercial diamine is not recycled since it is not expensive. Without purification, the monoprotected putrescine **155a** is obtained in a good yield of 90% (Figure 60).

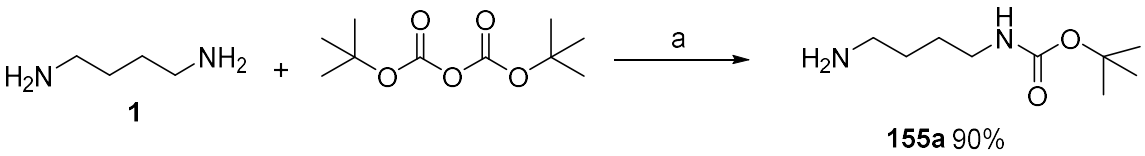

Figure 60: Monoprotection of putrescine. *Reagent and condition*: (a) Boc_2O, DCM, 0°C to rt, overnight.

2.2. Spermidine

Spermidine **2** is an unsymmetrical linear polyamine. It is thus necessary to establish a synthetic strategy involving selective protection of spermidine. Two different synthetic pathways were devised depending on which nitrogen atom will be protected or not (Figure 61). 1,4-diaminobutane (putrescine) is monoprotected as described below and then react by Michael addition with acrylonitrile to afford the nitrile compound **156**. The second Boc group was introduced by treatment of **156** with Boc_2O. Nitrile was reduced in the corresponding amine by hydrogenation using Raney nickel as catalyst to give the N^1-N^2-diBoc-spermidine **155b** (Figure 61A).

In contrast, to obtain the N^3-N^2-diBoc-spermidine, the starting material was 1,3-diaminopropane **158** which has been monoprotected by a Boc group according to the same method used for putrescine. In this case, the carbon chain was extended by nucleophilic substitution with 4-chlorobutanenitrile. Similarly, the resulting secondary amine of **160** was protected and the nitrile group was hydrogenated to afford the selectively protected spermidine **155c** (Figure 61B).

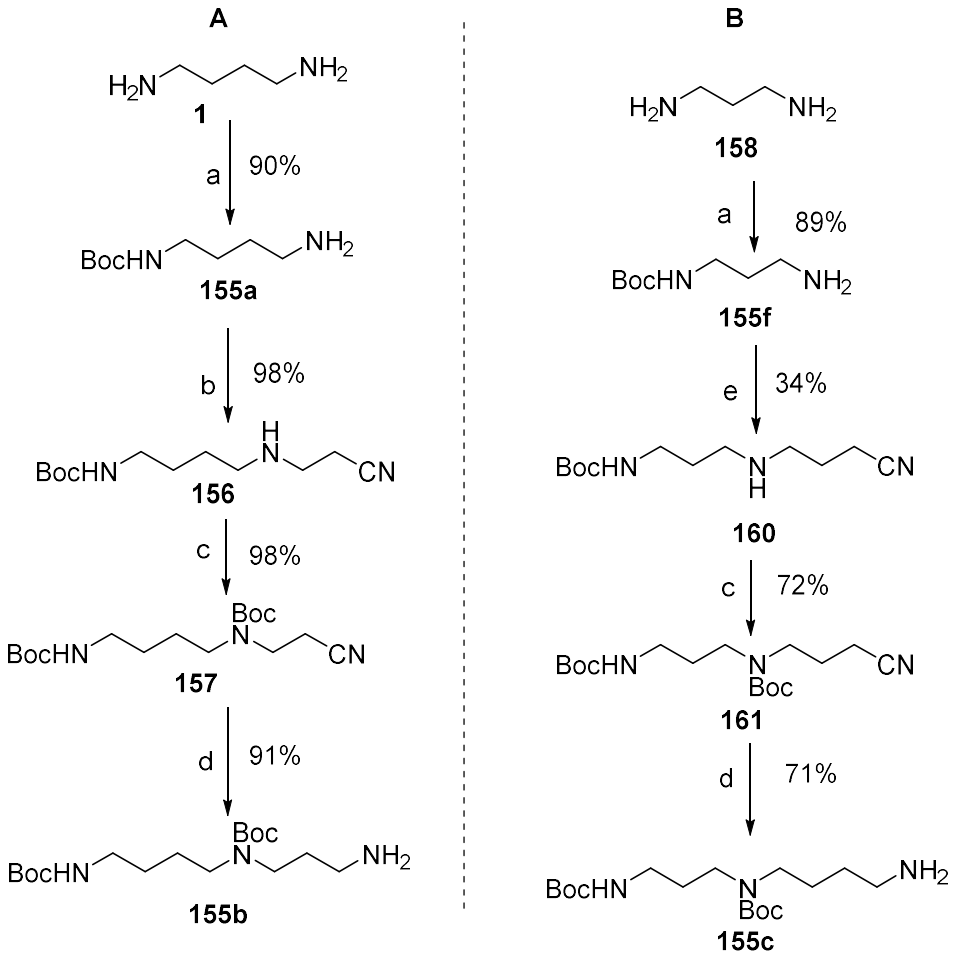

Figure 61: Synthesis of the two spermidines with selective protection. *Reagents and conditions*: (a) Boc_2O, DCM, 0°C to rt, overnight; (b) CH_2CHCN, MeOH, rt, overnight; (c) Boc_2O, DCM, rt, 1h; (d) H_2/Ni Raney, EtOH, rt, 1h; (e) Na_2CO_3, $Cl(CH_2)_3CN$, reflux, 6h.

We then focused on selective protection which allows coupling on the central nitrogen without affecting the terminal amine. To this end, we followed the method of Chadwick et al.[123] which utilized 2 equivalents of 2-(*tert*-butoxycarbonyloxyimino)-2-phenylacetonitrile (BOC-ON). Compound **155d** was purified by recrystallization into diisopropylether and was obtained in acceptable yield of 40% (Figure 62).

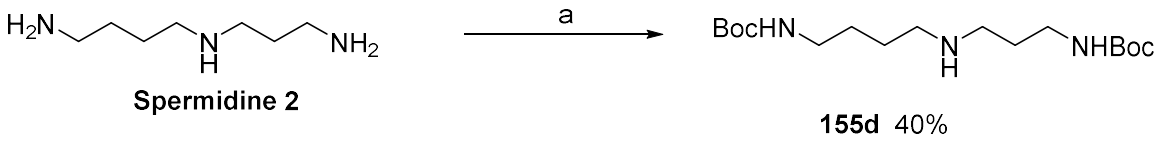

Spermidine 2

155d 40%

Figure 62: Protection of both terminal amine of spermidine. *Reagents and conditions*: (a) BOC-ON, THF, rt, overnight.

155b, **155c**, and **155d** were synthesized in large amounts in global yield of 78, 15 and 40% respectively.

2.3. Spermine

Unlike spermidine, spermine is a symmetrical polyamine which makes the selective protection a little easier. In fact, Blagbrough et al.[124,125] developed a desymmetrization protocol for spermine to avoid repetitive steps, laborious chromatographic purifications and low yield (Figure 63). First, the method consists in selective protection on one of the primary amine of spermine **3** with a trifluoroacetyl moiety. The ratio of primary amine toward the protecting reagent, ethyl trifluoroacetate is critical in order to afford mono-trifluoroacetamide. In one pot, the resulting free amines were protected with Boc to give the fully protected spermine. Then, selective deprotection of the trifluoroacetamide was performed by increasing the pH to 11 with concentrated aqueous ammionac. After purification by flash chromatography, triBocSpermine **155e** was obtained on gram-scale in 50% yield.

[123] Chadwick, J.; Jones, M.; Mercer, A. E.; Stocks, P. A.; Ward, S. A.; Park, B. K.; O'Neill, P. M. *Bioorg. Med. Chem.* **2010**, *18*, 2586–2597.

[124] Geall, A. J.; Blagbrough, I. S. *Tetrahedron* **2000**, *56*, 2449–2460.

[125] Blagbrough, I. S.; Geall, A. J. *Tetrahedron Lett.* **1998**, *39*, 439–442.

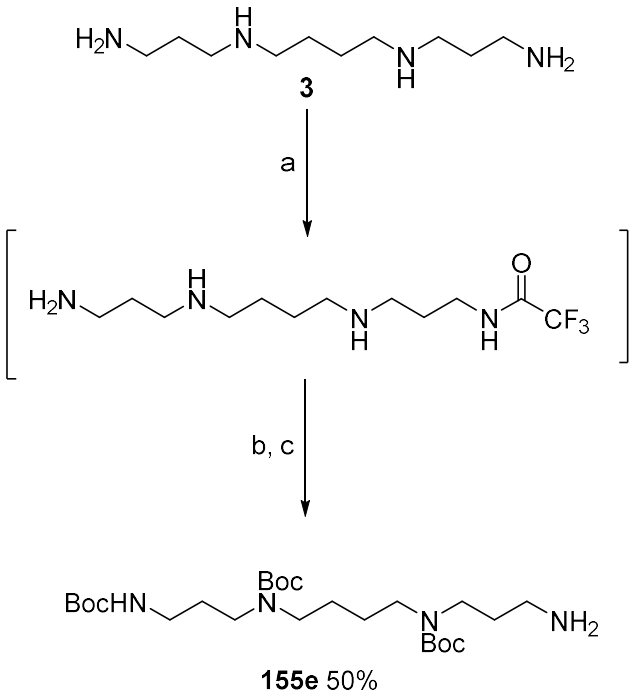

Figure 63: Synthesis of TriBocSpermine by Blagbrough et al.[125] *Reagents and conditions*: (a) CF_3COOEt (1 eq), MeOH, -78°C, 1h; (b) Boc_2O (4 eq), MeOH, 25°C, 15h; (c) aq. MeOH, NH_3, 25°C, 15h.

Few years after, les laboratoires Pierre Fabre published similar method without chromatographic purification.[126] We adopted this second method (Figure 64). Briefly, the first step was run into dichloromethane instead of methanol and the second step was performed in the presence of triethylamine base in tetrahydrofurane. Trifluoroacetyl protecting group was removed by cesium carbonate in a mixture of solvent (methanol/water). After solvent evaporation, residue is treated with diisopryl ether and an acidic aqueous solution (0.5 N HCl). The TriBocSpermine **155e** was decanted from a 3-layer system. After drying, the purity of the compound did not necessitate further purification.

[126] Guminski, Y.; Grousseaud, M.; Cugnasse, S.; Brel, V.; Annereau, J.-P.; Vispé, S.; Guilbaud, N.; Barret, J.-M.; Bailly, C.; Imbert, T. *Bioorg. Med. Chem. Lett.* **2009**, *19*, 2474–2477.

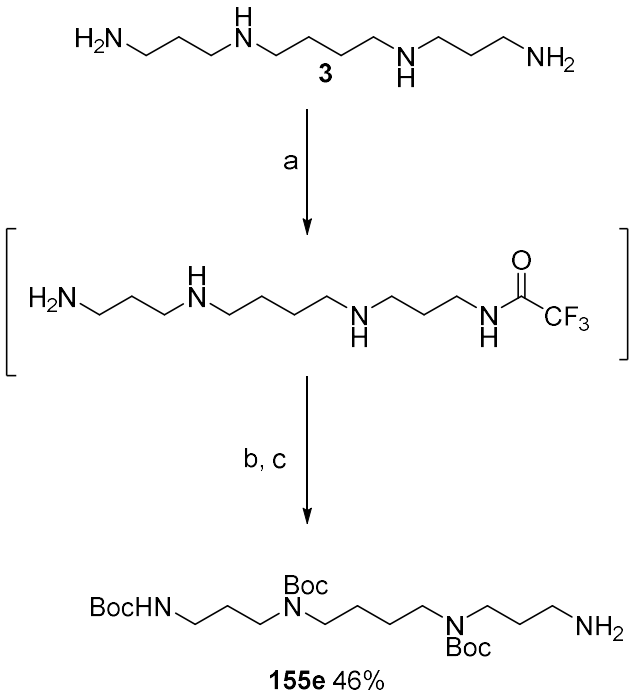

Figure 64: Synthesis of TriBocSpermine by Guminski et al.[126] *Reagents and conditions*: (a) CF_3COOEt (1 eq), DCM, 0°C, 1h; (b) Boc_2O (4 eq), NEt_3, THF, rt, 3h; (c) Cs_2CO_3, MeOH/H_2O 8:2, rt, 15h.

All these selectively protected polyamines will be used as initial building blocks for the synthesis of all the conjugates in the next chapters.

III. Synthesis of *N*-Acylated conjugates

3.1. Thiobiamide and thioamide conjugates

Regarding these analogs, the coupling step of the carboxymethyl spacer initially performed by Roblot et al.[108] with bromoacetic acid and coupling agent (BOP and HOBt) was changed. In fact, this method was not effective or led to very low yield in our case. After optimization, the best condition for incorporation of the bromoacetyl function was the use of high concentration of bromoacetyl bromide in dichloromethane (yield from 74 to 80%).

Spermidines conjugated to a truncated CoA analog **166**, **153** and **168** were synthesized from their Boc-protected counterparts **165**, **164** and **167** respectively in a two-step procedure: coupling with bromoacetyl bromide as described above and subsequent nucleophilic

substitution involving the required thiol derivatives 3-acetamido-*N*-(2-mercaptoethyl)propanamide or *N*-acetyl-cysteamine (Figure 65).

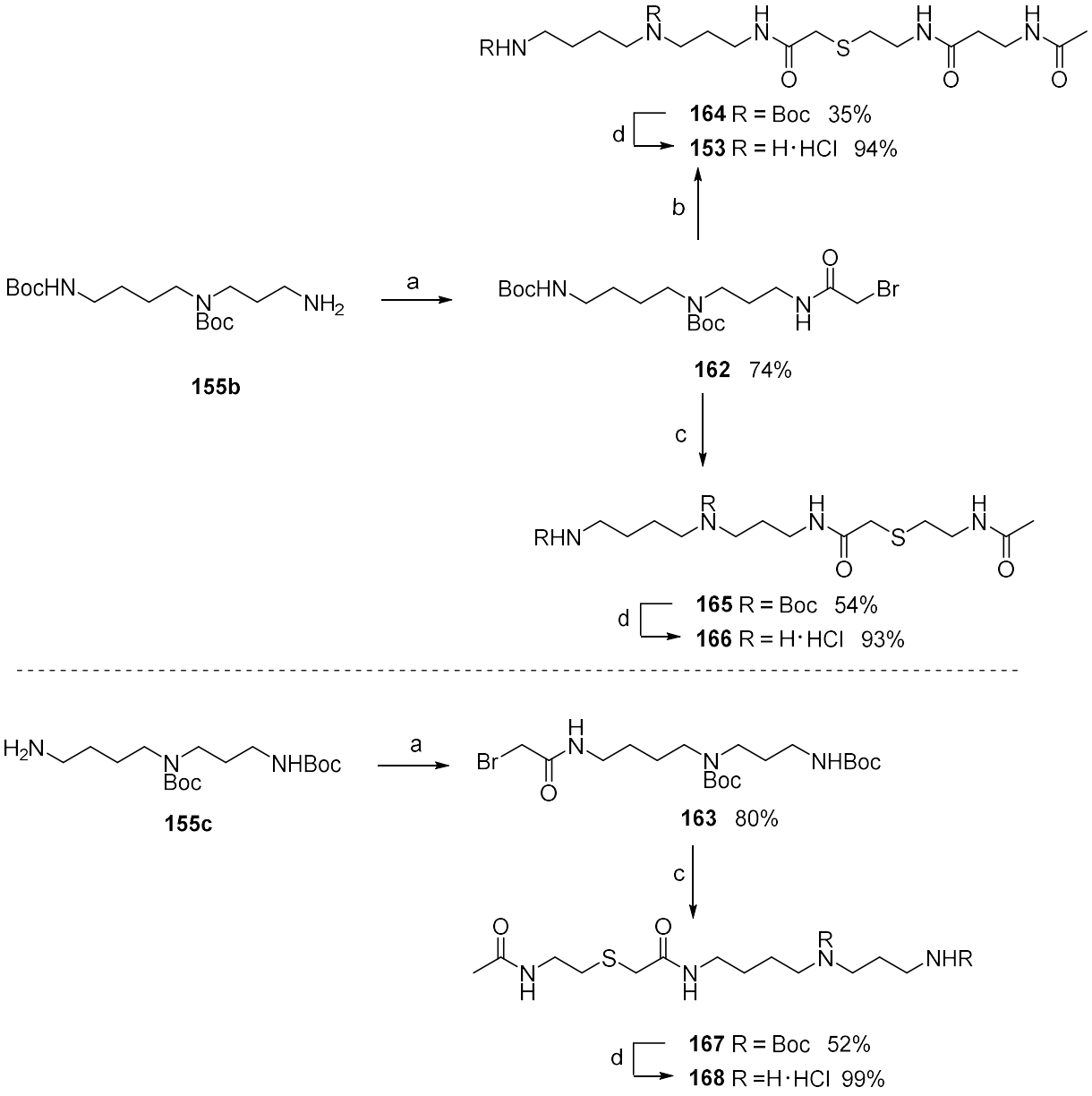

Figure 65: Spermidine thiobiamide and thioamide derivatives synthesis. *Reagents and conditions*: (a) $BrCH_2COBr$, DCM, -10°C to rt, 3h; (b) 3-acetamido-*N*-(2-mercaptoethyl)propanamid, triethyl ammonium bicarbonate buffer 1M, MeOH, rt, overnight; (c) *N*-acetylcysteamine, NEt_3, DCM, rt, overnight; (d) HCl/dioxane 4M, rt, 1h.

The *N*-acylated spermines **170** and **172** were prepared through a four-step protocol using a similar process as that used for the preparation of **153**, **166** and **168**. TriBoc spermine **155e** was prepared in the same conditions as previously described. TriBocSpermine **155e** was then bromoacetylated and the resulting bromo derivative was reacted with the thiol of 3-acetamido-*N*-(2-mercaptoethyl)propanamide or *N*-acetylcysteamine, respectively, to give the final hydrochloride salts **170** and **172** in 13% and 28% overall yields after deprotection (Figure 66).

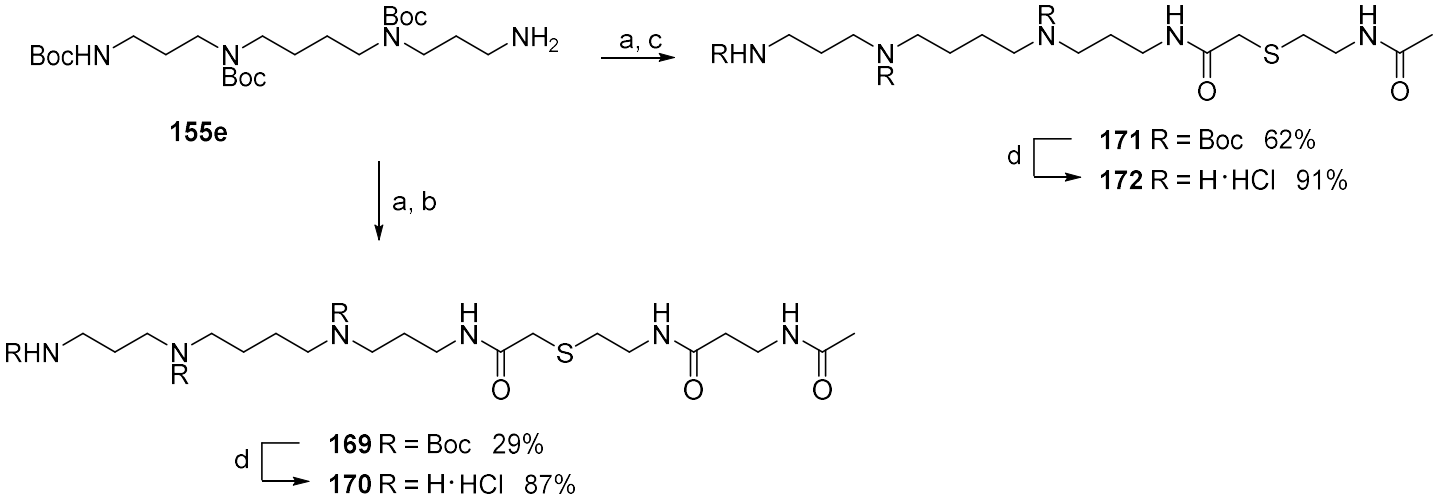

Figure 66: Synthesis of spermine derivatives. *Reagents and conditions*: (a) $BrCH_2COBr$, DCM, -10°C to rt, 3h; (b) 3-acetamido-*N*-(2-mercaptoethyl)propanamide, triethyl ammonium bicarbonate buffer 1M, MeOH, rt, overnight; (c) *N*-acetylcysteamine, NEt_3, DCM, rt, overnight; (d) HCl/dioxane 4M, rt, 1h.

3.2. Methoxylated conjugates

All the methoxy derivatives have been synthesized by a general procedure of coupling using methoxyacetic acid in presence of *N,N'*-Dicyclohexylcarbodiimide (DCC). *N*-acylated putrescine **179** was prepared from the protected putrescine **155a**. Removal of Boc protecting group was carried out in standard conditions with hydrochloric acid providing **180** as the hydrochloride salt. Regarding the spermidine derivatives **174**, **176** and **178**, the three amine groups were independantly mono-*N*-acylated using the appropriate Boc-protected spermidines reported earlier (Figure 67).

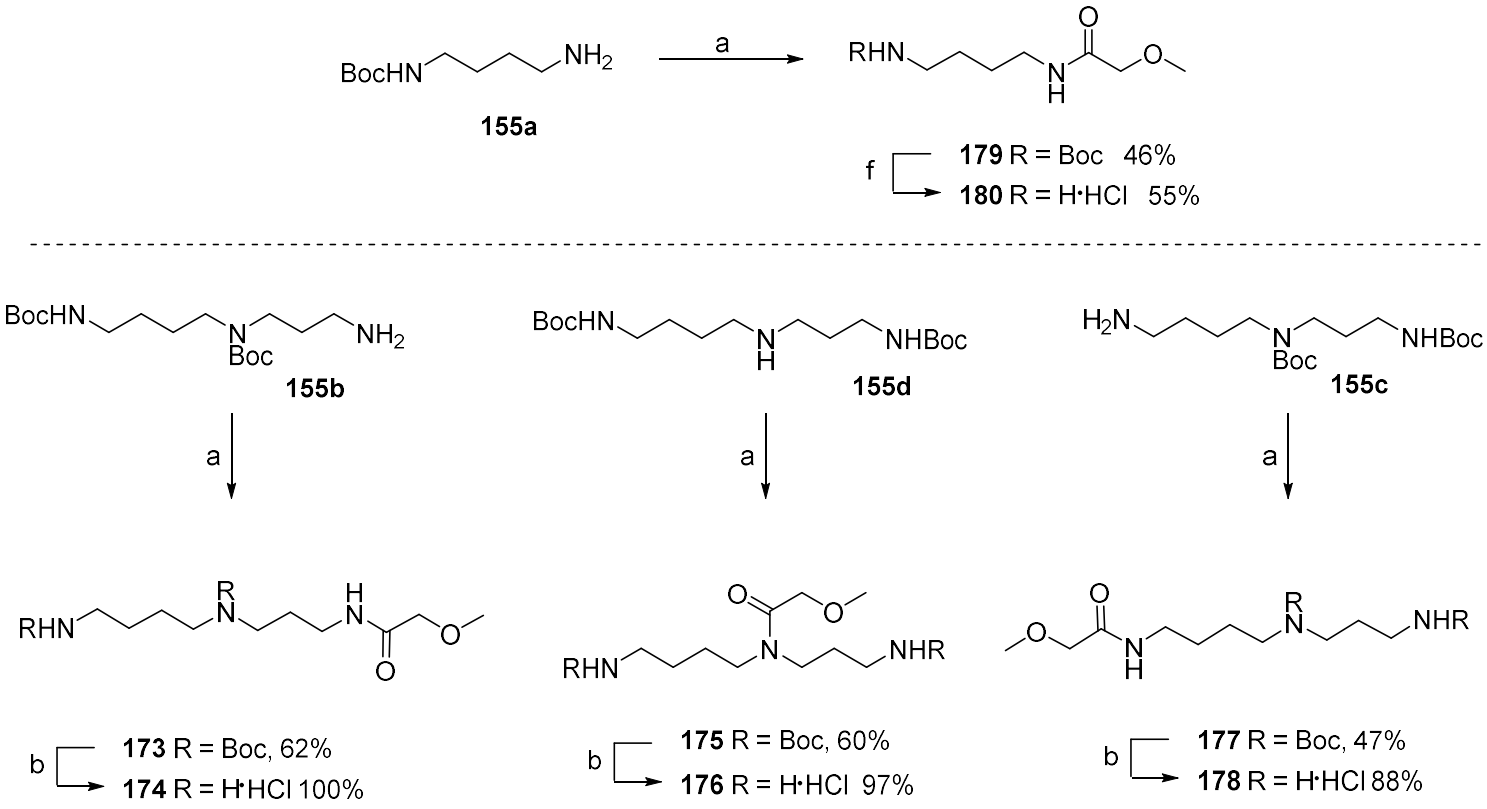

Figure 67: Synthesis of methoxy derivatives. *Reagents and conditions*: (a) $CH_3OCH_2CO_2H$, DCC, DCM, rt, overnight; (b) HCl/dioxane 4M, rt, 1h.

IV. Biological evaluation

The compounds were tested in vitro against *Trypanosoma brucei gambiense* trypomastigotes and *Leishmania donovani* axenic amastigotes to evaluate the antikinetoplastid activity.[127] Pentamidine and miltefosine were included in the assays as positive controls for *T. brucei* and *L. donovani*, respectively. In this evaluation, the activity was expressed in IC_{50} (concentration inhibiting the parasite growth by 50%). In vitro evaluation on *Leishmania donovani* intramacrophage amastigotes was also carried out to evaluate the potential uptake of the

[127] Audisio, D.; Messaoudi, S.; Cojean, S.; Peyrat, J.-F.; Brion, J.-D.; Bories, C.; Huteau, F.; Loiseau, P. M.; Alami, M. *Eur. J. Med. Chem.* **2012**, *52*, 44.

compounds at 100 µM in RAW 264.7 cells. This macrophage cell line was used as a host model of *L. donovani* amastigote and provided qualitative information about the cytotoxic effect of the compounds at 100 µM on mammalian cells. None of the compounds displayed activity on *Leishmania donovani* intramacrophage amastigotes and from this assay, we also observed no macrophage cell death. Therefore, we can expect that our compounds are not cytotoxic up to 100 µM.

Whereas putrescine analogs (compounds **155a**, **179** and **180**) were not active in vitro both on *T. b. gambiense* trypomastigotes and *L. donovani* axenic amastigotes, some spermidine and spermine derivatives exhibited activities on both parasites (Table 1). However, the biological activity was more marked against African trypanosomes (7 active compounds) than against Leishmania (3 active compounds).

Table 1: In vitro activity of acyl derivatives.

SI: Selectivity index calculated from cytotoxicity/IC_{50}; SI_{Tb}: relative to IC_{50} on *T. b. gambiense*; SI_{Ld}: relative to IC_{50} on *L. donovani* axenic amastigotes.

Compounds	*T. b. g.* IC_{50} (µM) ± SD	SI_{Tb}[a]	*L. d.* LV9 axenic amastigotes IC_{50} (µM) ± SD	SI_{Ld}[b]
153 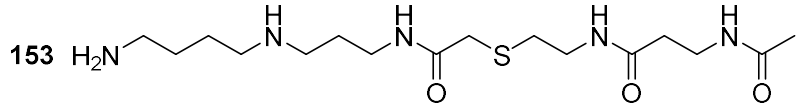	11.5±8.0	8	>100	-
155a 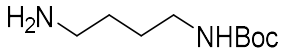	>100	-	>100	-
155b 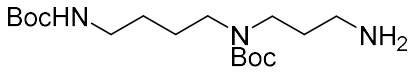	11.6 ±1.9	8	>100	-
155d 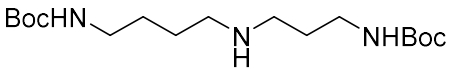	>100	-	>100	-
179 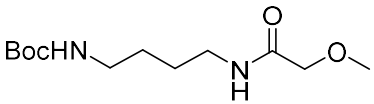	>100	-	>100	-
180 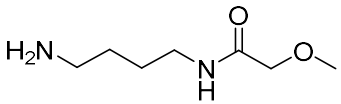	>100	-	>100	-

Compounds	*T. b. g.* IC_{50} (µM) ± SD	SI_{Tb}[a]	*L. d.* LV9 axenic amastigotes IC_{50} (µM) ± SD	SI_{Ld}[b]
173 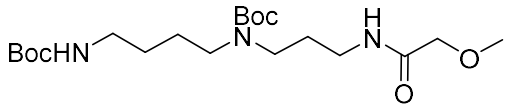	>100	-	>100	-
174 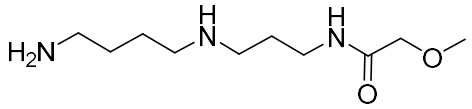	>100	-	5.5±0.9	18
177 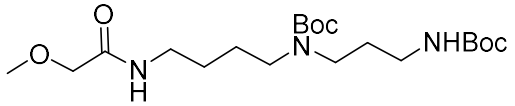	>100	-	>100	-
178 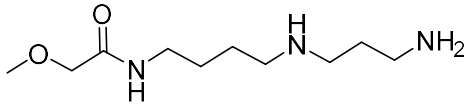	15.6±7.3	6	50±25	2
175 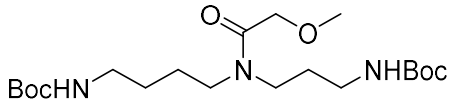	>100	-	>100	-
176 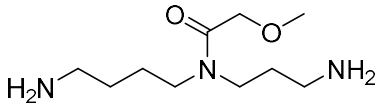	>100	-	>100	-
166 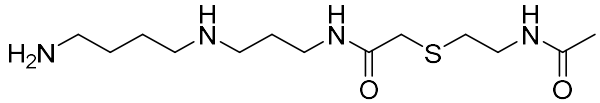	14.7±4.0	7	70.8±31.4	1.5

Compounds	*T. b. g.* IC_{50} (µM) ± SD	SI_{Tb}[a]	*L. d.* LV9 axenic amastigotes IC_{50} (µM) ± SD	SI_{Ld}[b]
168 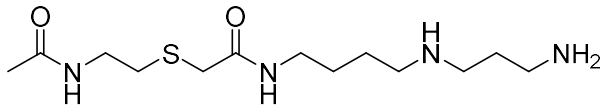	5.7±2.3	17	>100	-
170 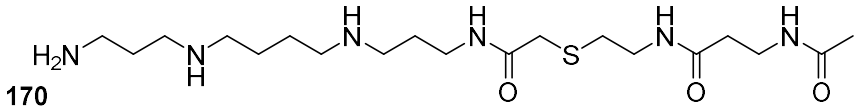	2.9±2.0	34	>100	-
172 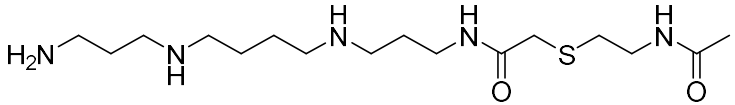	1.9±1.3	52	>100	-
Miltefosine	/	-	1.9 ±0.6	8
Pentamidine	0.010±0.0	7500	/	-

The most interesting antitrypanosomal activity was obtained with compounds **153** (hit compound), **155b**, **178**, **166**, **168**, **170** and **172** with the most active compounds having IC_{50} values in a range from 1 to 6 µM (**168**, **170** and **172**). Regarding spermine and spermidine conjugated with either thioamide or thiobiamide moieties, the antitrypanosomal activity is increased by a factor of 4–7 in favor of the spermine derivatives (**170** and **172** compared to **153** and **166**). The Selectivity Index of compound **172**, as the ratio between toxicity on macrophages/antiparasitic activity, was higher than 52. However, these compounds were barely or not active against *L. donovani*.

Among the spermidine derivatives, three compounds **153**, **155b** and **168** were specifically active on *T. b. gambiense* and another one **174** exhibited specific antileishmanial activity. The Selectivity Index of compound **174** and **168** were higher than **153** and **155b**. Spermidine analogs **178** and **166** were the sole compounds able to moderately act on both the parasites. Finally, methoxy group seemed not to significantly influence the antiparasitic activity and specificity toward one parasite whereas thioamide and thiobiamide substituents conferred predominant antitrypanosomal activity.

Secondly, the internalized compounds could interact with the polyamine metabolism of the parasites. Evaluation on *Tb*TryR was at hand and every *N*-acylated polyamine have been tested for a potential inhibition of TryR. No inhibitions of TryR have been observed for these compounds.

V. Conclusion

The biological results highlighted the antiparasitic specificity monitored within a small chemical series, opening the way for further hypothesis as a function of the level of interaction of the compounds with the biological targets.[36] Firstly, histone acetyl transferase (HAT) could be the target to be inhibited by the compounds. Unfortunately, enzymatic assays on this enzyme have not been conducted so far because of timing constraints. However, as soon as the enzyme will

be obtained, compounds should be evaluated against this target. In addition, no compound was able to inhibit the *Tb*TryR suggesting a limited effect on the parasite polyamine metabolism.

Chapter 4: Aryl-polyamine derivatives

In line with our program toward the development of polyamine-based antikinetoplastid agents as well as published data, we decided to couple polyamines to aryl moieties found in several antikinetoplastid agents. Indeed, as described in the chapter 1, many natural or synthetic polyamine derivatives have been studied for their antiparasitic ability and most of them were found as disruptors of the trypanothione metabolism. Antikinetoplastid activity was mainly observed with conjugates bearing a hydrophobic moiety, particularly an aryl group, directly linked to the polyamine. In this study, we chose to either add one heteroaryl (benzotriazole nucleus) or two aryls (various bisbenzyl).

I. Hydroxybenzotriazole conjugates

1. Strategy

The benzotriazole scaffold was chosen since it is widely used by medicinal chemists for the development of drug candidates.[116] This heterocycle was originally incorporated as a bioisosteric replacement of imidazole nucleus or the corresponding benzene-fused compound, benzimidazole, a common pharmacophore clinically used in anthelminthic drugs.[128] The benzotriazole scaffold is able to bind various targets via non-covalent interactions such as hydrogen bonds or van der Waals interactions and π stacking. Compounds bearing this scaffold display diverse pharmacological activities often associated with good water solubility and bioavailability as well as limited toxicity. Among pharmacologically active benzotriazoles, the particular 1-hydroxybenzotriazole motif (Figure 68) was found having antibacterial,[129] antitubercular,[130] antiviral[131] and antiproliferative activities.[132] In these compounds, either ether

[128] Martin, R. J. *Vet. J. Lond. Engl. 1997* **1997**, *154*, 11–34.

[129] Huczyński, A.; Janczak, J.; Antoszczak, M.; Stefańska, J.; Brzezinski, B. *J. Mol. Struct.* **2012**, *1022*, 197–203.

[130] Augustynowicz-Kopeć, E.; Zwolska, Z.; Orzeszko, A.; Kazimierczuk, Z. *Acta Pol. Pharm.* **2008**, *65*, 435–439.

or ester bonds link various molecular scaffolds to 1-hydroxybenzotriazole through its hydroxyl group.

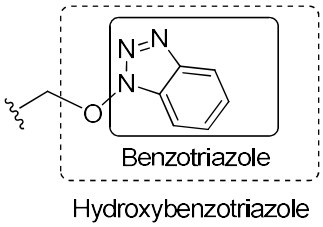

Figure 68: 1-hydroxybenzotriazole motif.

For example, in the latter class of anticancer agents, benzotriazole-substituted trimethoxybenzoate **181** (Figure 69) exhibited strong antiproliferative activity (IC_{50} = 1.7 µg/mL). Furthermore, this compound has been demonstrated as histone deacetylase (HDAC) inhibitor (IC_{50} = 9.4 µg/mL). Benzotriazole moiety was also found in antikinetoplastid agents.[133] Indeed, the *N*-benzenesulfonyl benzotriazole **182** (Figure 69) displayed in vitro activity against epimastigotes of *T. cruzi* with an IC_{50} of 21.56 µg/mL.

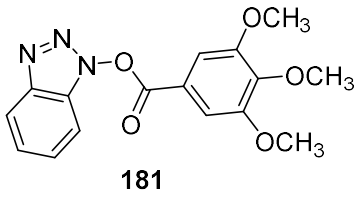

181

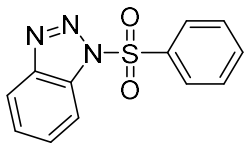

182

Figure 69: 1-hydroxybenzotriazole and benzotriazole derivatives as anticancer and antikinetoplastid agents.

In our case, hydroxybenzotriazole group was considered as a privileged scaffold since it can be readily incorporated starting from the commercially available peptide coupling reagent 1-hydroxybenzotriazole. Four polyamines of biological interest – 1,3-propanediamine **158**, putrescine **1**, spermidine **2**, and spermine **3** – were coupled to the benzotriazole moiety through an amide bond (Figure 70). Only one hydroxybenzotriazole group was inserted in each case.

---

[131] Verschueren, K. H. G.; Pumpor, K.; Anemüller, S.; Chen, S.; Mesters, J. R.; Hilgenfeld, R. *Chem. Biol.* **2008**, *15*, 597–606.

[132] Fu, J.; Yang, Y.; Zhang, X.-W.; Mao, W.-J.; Zhang, Z.-M.; Zhu, H.-L. *Bioorg. Med. Chem.* **2010**, *18*, 8457–8462.

[133] Becerra, M. C.; Guiñazú, N.; Hergert, L. Y.; Pellegrini, A.; Mazzieri, M. R.; Gea, S.; Albesa, I. *Exp. Parasitol.* **2012**, *131*, 57–62.

Spermine **3** was linked to the benzotriazole exclusively via its primary amine group. Regarding the unsymmetric polyamine, spermidine **2**, N^1-, N^2- and N^3-spermidine conjugates were prepared through the linkage of either the primary or secondary amines. The latter compounds were designed to study the biological importance of the benzotriazole position on the spermidine.

Polyamine derivatives were synthesized from previously reported *tert*-butyloxycarbamate (Boc) protected polyamines (**155a-e**). Many carbamates have been designed as prodrugs[134] as they have chemical stability and capability to permeate cell membranes.[135] Also, some carbamates have been found to be more active than the corresponding free amines (i.e. the antileishmanial activity).[35] Literature data on the metabolic hydrolysis of therapeutic carbamates showed that those derived from aliphatic amines had longer life-span[136] than the corresponding free amines, maybe due to an increase of the bioavailability into the organism. In addition, we targeted *T. b. gambiense* and *Leishmania donovani*, two species that do not express polyamine transporters.[23,137,138,139] For all these reasons, we evaluated the Boc protecting intermediates, as well as the final free amine derivatives. The Boc derivatives, as more lipophilic compounds, could cross more easily the parasite plasma membrane.

2. Synthesis

As with the previous *N*-acyl series, hydroxybenzotriazole (HOBt) derivatives have been prepared from polyamine protected selectively by Boc group (**155a-e**). Firstly, compounds were prepared by the same methodology as earlier using bromo acetylbromide in order to synthetize a bromoacetyl intermediate. This molecule is reacted with HOBt to afford compounds **165a-d** (Figure 70).

---

[134] Testa, B.; Mayer, J. M. In *Hydrolysis in Drug and Prodrug Metabolism*; Verlag Helvetica Chimica Acta, **2003**; pp. 419–534.

[135] Ghosh, A. K.; Brindisi, M. *J. Med. Chem.* **2015**, *58*, 2895–2940.

[136] Vacondio, F.; Silva, C.; Mor, M.; Testa, B. *Drug Metab. Rev.* **2010**, *42*, 551–589.

[137] Le Quesne, S. A.; Fairlamb, A. H. *Biochem. J.* **1996**, *316 (Pt 2)*, 481–486.

[138] Basselin, M.; Coombs, G. H.; Barrett, M. P. *Mol. Biochem. Parasitol.* **2000**, *109*, 37–46.

[139] Xiao, Y.; McCloskey, D. E.; Phillips, M. A. *Eukaryot. Cell* **2009**, *8*, 747–755.

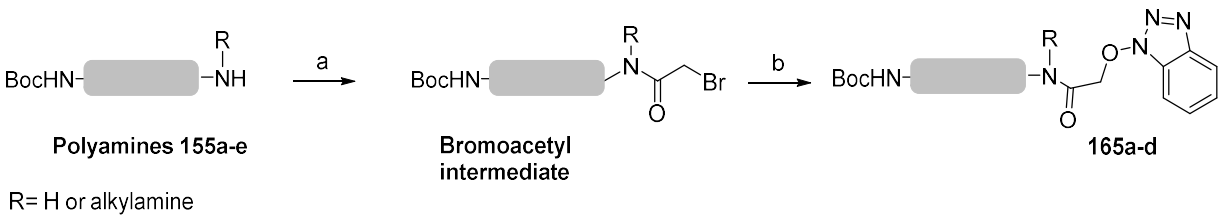

Figure 70: Synthesis pathway using bromoacetyl intermediate. *Reagents and conditions*: (a) Bromoacetyl bromide, DCM, 0°C to rt, 3h; (b) HOBt, NEt_3, DCM, rt, overnight.

However, we developed a more convergent route, using a common precursor hydroxbenzotriazole acetic acid **164** which could react directly with protected polyamine (Figure 71).

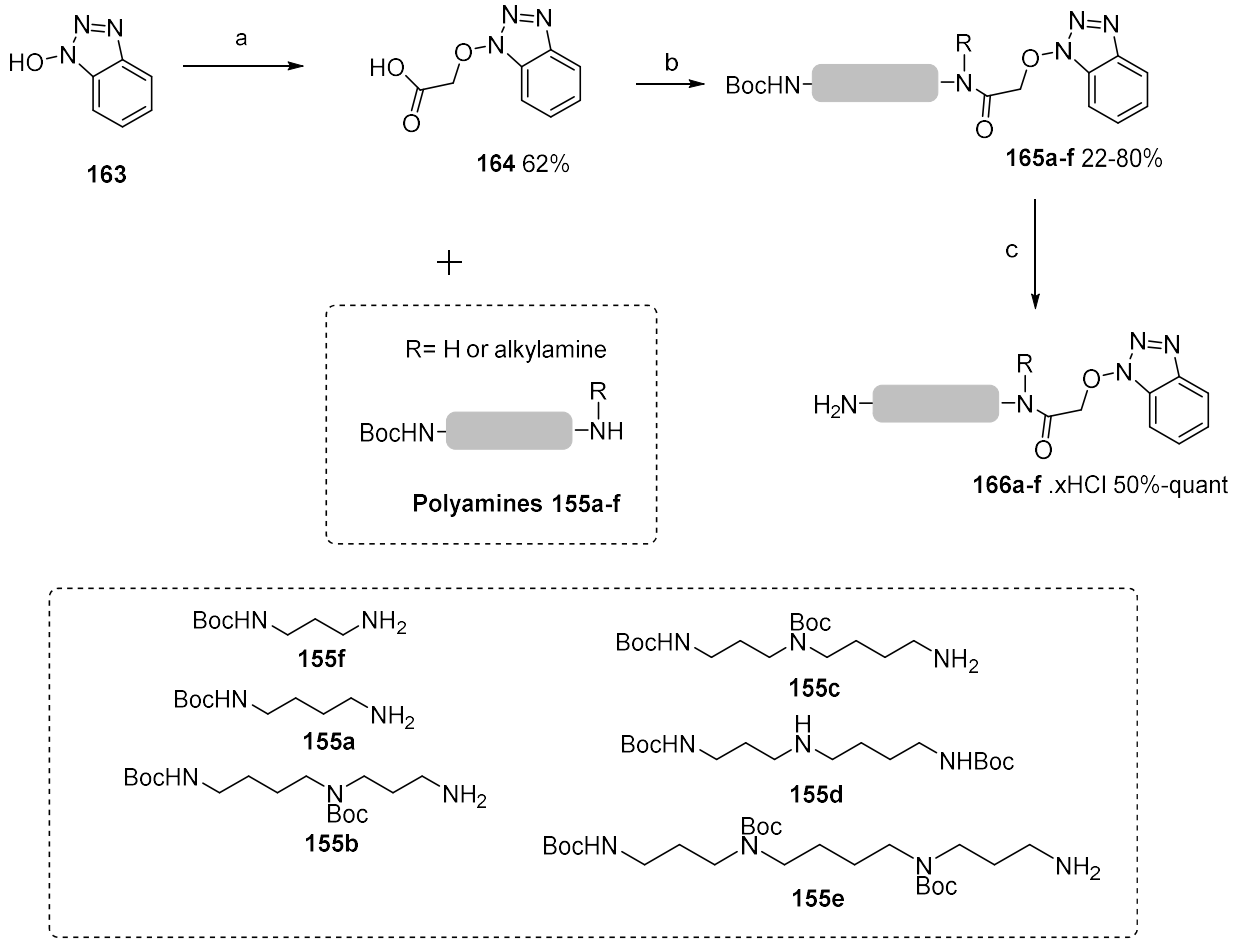

Figure 71: Synthesis of benzotriazoles conjugates. *Reagents and conditions*: (a) $ClCH_2COOH$, NaOH, EtOH, 40 °C, 16 h; (b) BOP, NEt_3, DCM/DMF, rt, 16 h; (c) HCl/Dioxane 4M, rt, 16 h.

The carboxylic acid **164** was prepared in 62% by the alkylation of 1-hydroxybenzotriazole **163** with chloroacetic acid in alkaline medium using the method published by Boido et al.[140] In order to react the benzotriazole scaffold at desired positions of the polyamines, selective *N*-Boc protection of other functional amino groups was made. The various *N*-Boc protected polyamines **155a-f** were synthesized according to previously reported procedures.[108,125] Amide bond formation between *N*-Boc polyamines **155a-f** and carboxylic acid **164** yielded the protected intermediates **165a-f** in 22-80%. Removal of the Boc group was carried out in a 4M

[140] Boido, A.; Vazzana, I.; Mattioli, F.; Sparatore, F. *Farmaco* **2003**, *58*, 33.

hydrochloric solution in dioxane, to afford hydrochloride salts of the polyamine-hydroxybenzotriazole conjugates **166a-f** (Figure 71).

3. Biological evaluation

Thirteen compounds were tested in vitro against both *T. b. gambiense* (strain FéoITMAP/1893) trypomastigotes and *Leishmania donovani* (MHOM/ET/67/HU3, also called LV9) axenic and intramacrophage amastigotes. Pentamidine and miltefosine were included in the assay as reference drugs for *T. b. gambiense* and *L. donovani*, respectively. The cytotoxic effect of the compounds on RAW 264.7 mammalian cells was evaluated in order to determine the selectivity index (SI) toward parasitic cells. The results are depicted in Table 2.

Table 2: Antikinetplastid activities and cytotoxicity of benzotriazole conjugates.

[a] ClogP: Calculated logP with Virtual Computational Chemistry Laboratory, *http://www.vcclab.org, 2005.*[141]

[b] 50% growth inhibitory concentration

[c] SI: Selectivity Index calculated from cytotoxicity/IC_{50} ; SI_{Tb}: relative to IC_{50} on *T. b. gambiense*; SI_{aa}: relative to IC_{50} on *L. donovani* axenic amastigotes; SI_{ia}: relative to *L. donovani* intramacrophage amastigotes

ND: not determined

Compounds	ClogP[a]	*T. b. g.* IC_{50} (µM) ± SD	SI_{Tb}[c]	*L. d.* LV9 axenic amastigotes IC_{50} (µM) ± SD	SI_{aa}[c]	*L. d.* LV9 intramacrophage amastigotes IC_{50} ±SD (µM)[b]	SI_{ia}[c]	Cytotoxicity on macrophages CC_{50} ± SD (µM)[b]
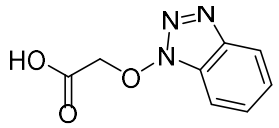 **164**	0.8	> 100	-	> 100	-	> 100	-	> 100
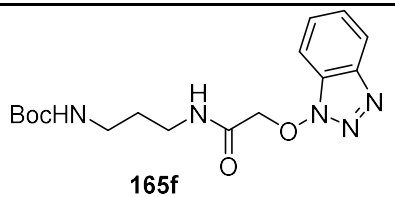 **165f**	1.5	28.8 ± 8.3	3	> 100	-	56.7 ± 1.9	2	> 100

[141] Tetko, I. V.; Gasteiger, J.; Todeschini, R.; Mauri, A.; Livingstone, D.; Ertl, P.; Palyulin, V. A.; Radchenko, E. V.; Zefirov, N. S.; Makarenko, A. S.; Tanchuk, V. Y.; Prokopenko, V. V. *J. Comput. Aided Mol. Des.* **2005**, *19*, 453–463.

Compounds	ClogP[a]	*T. b. g.* IC_{50} (µM) ± SD	SI_{Tb}[c]	*L. d.* LV9 axenic amastigotes IC_{50} (µM) ± SD	SI_{aa}[c]	*L. d.* LV9 intramacrophage amastigotes IC_{50} ±SD (µM)[b]	SI_{ia}[c]	Cytotoxicity on macrophages CC_{50} ± SD (µM)[b]
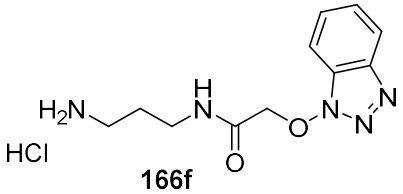 **166f**	0.2	> 100	-	> 100	-	29.5 ± 2.1	3	> 100
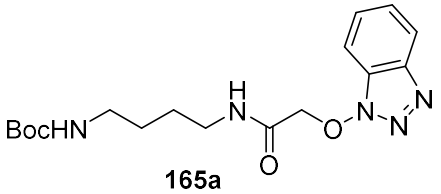 **165a**	1.6	> 100	-	> 100	-	>100	-	> 100
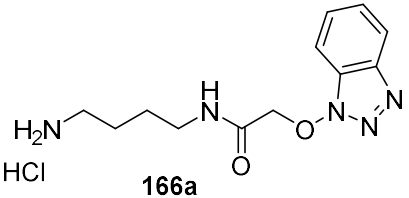 **166a**	0.3	9.5 ± 6.9	11	> 100	-	>100	-	> 100
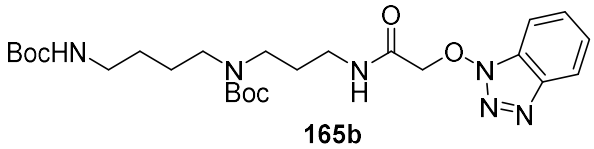 **165b**	1.8	**1.2 ± 0.2**	**85**	60.5 ± 10.5	1.6	67.8 ± 15.2	1	>100
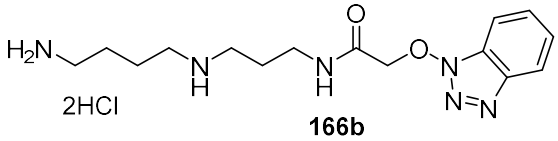 **166b**	0.3	72.0 ±12.2	1	>100	1.5	>100	-	>100

Compounds	ClogP[a]	*T. b. g.* IC_{50} (µM) ± SD	SI_{Tb}[c]	*L. d.* LV9 axenic amastigotes IC_{50} (µM) ± SD	SI_{aa}[c]	*L. d.* LV9 intramacrophage amastigotes IC_{50} ±SD (µM)[b]	SI_{ia}[c]	Cytotoxicity on macrophages CC_{50} ± SD (µM)[b]
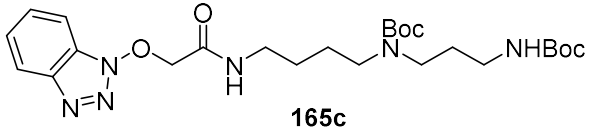 **165c**	1.8	**2.0 ± 0.5**	**50**	>100	-	41.4 ± 4.9	2	>100
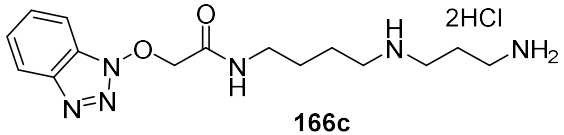 **166c**	0.3	38.7± 4.4	3	>100	9	>100	-	>100
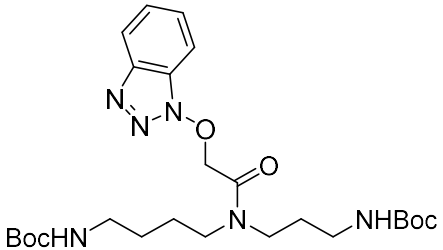 **165d**	2.8	3.2 ± 0.3	4	11.5 ± 1.8	1	3.1 ± 0.6	4	12.5 ± 1.4
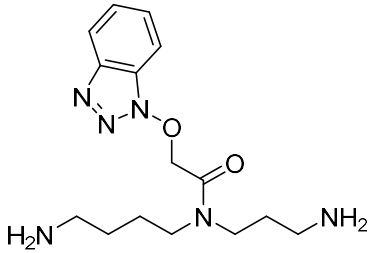 **166d**	0.1	25.3 ± 5.3	4	>100	-	23.4 ± 2.0	4	>100

Compounds	ClogP[a]	*T. b. g.* IC_{50} (µM) ± SD	SI_{Tb}[c]	*L. d.* LV9 axenic amastigotes IC_{50} (µM) ± SD	SI_{aa}[c]	*L. d.* LV9 intramacrophage amastigotes IC_{50} ±SD (µM)[b]	SI_{ia}[c]	Cytotoxicity on macrophages CC_{50} ± SD (µM)[b]
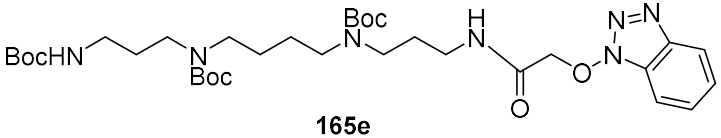 **165e**	3.8	**3.5 ± 0.5**	**10**	27.0 ± 0.9	1.4	34.7 ± 5.7	1	37.4 ± 1.0
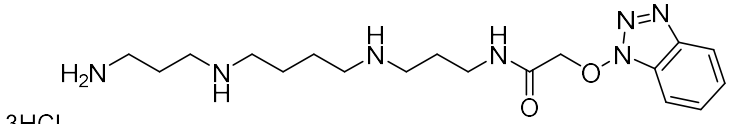 **166e**	0.3	13.8 ± 4.1	7	10.9 ± 1.6	9	38.6 ± 12.2	3	>100
Miltefosine	-	ND	-	1.9 ± 0.6	8.3	1.5 ± 0.3	10	15.8 ± 0.9
Pentamidine	-	0.010 ± 0.002	7500	ND	-	ND	-	75 ± 0.5

Firstly, spermidine has been described in the literature as possibly activating trypanosome multiplication in one *T. b. gambiense* strain (Wellcome strain) whereas this effect was not significantly observed in *T. b. brucei* ILtat 1.4 strain.[142] In our study, we observed that the IC_{50} of spermidine was about 3 µM on our *T. b. gambiense* Féo strain. These apparent contradictory results could be ascribed to the trypanosome polymorphism leading to a large variability of drug susceptibility in this parasite genus, as it is observed for the clinically used drug, eflornitine.

Secondly, we verified that the common nucleus, (benzotriazolyl)oxyacetic acid **164**, was not active against the tested parasites. This compound was also not cytotoxic and this was the case for most of the tested polyamines. The conjugates bearing a diamine moiety either Boc-protected or not (**165a-e** and **166a-e**) lacked any significant biological activity.

Four compounds exhibited IC_{50} values below 5 µM against *T. b. gambiense*. The most active compounds with IC_{50} less than 2 µM proved to be Boc-protected spermidine derivatives conjugated with the benzotriazole at one of their primary amines (**165b** and **165c**). Interestingly, compound **165c** was specifically trypanocidal as it did not exert any in vitro antileishmanial activity. This specificity was also found although slightly less pronounced for compound **165b**. Their free counterparts, compounds **166b** and **166c** led to a dramatic decrease of the in vitro trypanocidal activity. In particular, compound **166b** was sixty times less active than compound **165b** (Boc-protected). This is also valid, although to a lesser extent, in the case of the spermidine derivatives branched at the central nitrogen (**165d** and **166d**). The lipophilic Boc-protected conjugates (in agreement with predictive ClogP values shown in Table 2) exerted a better activity against *T. b. gambiense* than the corresponding conjugates with free amines. In contrast to **165d** which is slightly cytotoxic (12.5 ± 1.4 µM), the spermidine derivatives linked to the benzotriazole via their primary amines (**165b** and **165c**) have very interesting in vitro trypanocidal activity with an SI higher than 50.

The same trend was observed with the spermine conjugates (**165e** and **166e**) but the differences between Boc- and non-protected derivatives were only weak.

[142] Nishimura, K.; Yanase, T.; Araki, N.; Ohnishi, Y.; Kozaki, S.; Shima, K.; Asakura, M.; Samosomsuk, W.; Yamasaki, S. *J. Parasitol.* **2006**, *92*, 211–217.

Regarding *L. donovani* axenic amastigotes, the two most active compounds, **165d** (Boc-protected) and **166e** (without Boc), exhibited IC_{50} of about 10 µM. The presence of Boc did not enhance the in vitro antileishmanial activity since **165e** is three times less active than the unprotected spermine **166e**. It should be noted that all active compounds against *L. donovani* were also among the most active ones against *T. b. gambiense*.

Only compound **165d** was active on intramacrophage amastigotes of *L. donovani* with an IC_{50} value of 3 µM and a SI of 4. Interestingly, the compound displayed a higher activity on intramacrophage amastigotes of *L. donovani* than on the axenic amastigotes. This enhanced activity could be due to physiological modifications of the parasite once inside the macrophage.

As opposed to trypanocidal activity, no clear-cut relationships could be established between the antileishmanial activity and the lipophilicity of the compounds. Among the different targets in Kinetoplastid affected by polyamine derivatives, TryR is the most frequently identified.[41,75] Functional TryR is essential to combat oxidative stress in these parasites. This NADPH-dependent flavoenzyme reduces trypanothione disulfide (TS_2) and displays structural and functional similarities to glutathione reductase (GSR), the closest related enzyme in mammalian cells. However, TryR and human GSR have mutually exclusive substrate specificities.[143] Based on its preference for positively charged ligands,[144,145] we decided to study our compounds as putative inhibitors of recombinant *T. brucei* TryR.

[143] Lueder, D. V.; Phillips, M. A. *J. Biol. Chem.* **1996**, *271*, 17485–17490.

[144] Stoll, V. S.; Simpson, S. J.; Krauth-Siegel, R. L.; Walsh, C. T.; Pai, E. F. *Biochemistry (Mosc.)* **1997**, *36*, 6437–6447.

[145] Sullivan, F. X.; Sobolov, S. B.; Bradley, M.; Walsh, C. T. *Biochemistry (Mosc.)* **1991**, *30*, 2761–2767.7.

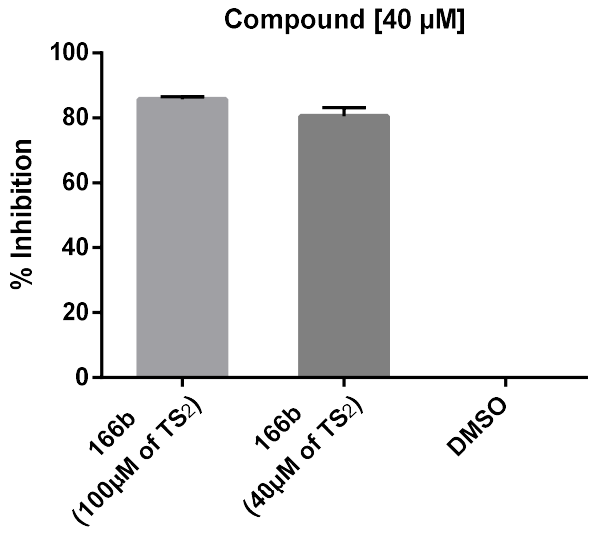

Figure 72: Inhibition of *Tb*TryR by 166b. The activity was measured following the NADPH consumption at 340 nm as described in the Experimental Section. The assays contained a fixed concentration of 100 or 40 µM of TS_2 and 40 µM of inhibitor. The controls contained the same amount of DMSO used to dissolve the compounds. 4c displayed the same degree of inhibition at both substrate concentrations.

All compounds were subjected to TryR assays using a fixed concentration of 40 µM in assay buffer containing 5% DMSO. The activity was measured in the presence of 40 and 100 µM TS_2, respectively, and the percentage of inhibition was calculated. Only one compound showed a noticeable activity at 40 µM (Figure 72). The spermidine derivative **166b** inhibited the TryR to 80% under these conditions. The finding that the degree of inhibition was independent of the substrate concentration indicated that the compounds did not act as pure competitive ligands.

In light of the interesting preliminary activity of this spermidine derivative, we determined the inhibitor constant and type of inhibition. The Lineweaver-Burk plot showed that **166b** behaves as mixed-type inhibitors, with calculated Ki- and Ki'-values of 6.7 µM and 16.8 µM, respectively (Figure 73).

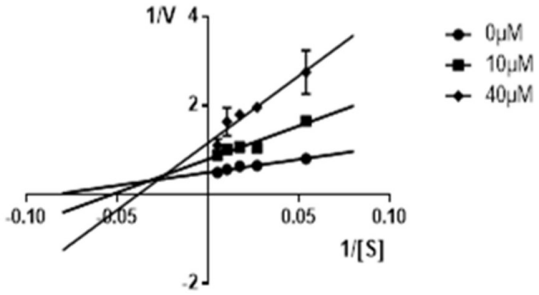

Figure 73: Lineweaver-Burk plot of compound 166b. The assays contained 0, 10, and 40 µM of inhibitor, respectively, and the TS_2 concentration was varied. The data are the mean of three determinations ± standard deviations.

This type of inhibition was already observed on TryR.[71] Moreover, inhibitors with such a good Ki value also display strong trypanocidal activity in vitro and surprisingly, **166b** was not active against *T. b. gambiense*. Interestingly, the Boc-protected counterpart of this polyamine, **165b**, exhibited high activity against *T. b. gambiense* but was not an inhibitor of TryR. As described above, the trypanocidal activity correlated with the lipophilicity of the polyamine. Thus, we may hypothesize that the more lipophilic Boc-protected polyamine (**165b**) diffuses via hydrophobic interaction through the membrane of the parasite and once inside the cell, the Boc moieties would be removed to provide the free polyamine **166b**.

Even though less active towards the parasite, the spermidine **166c** and the spermine **166e** followed a comparable trend, in line with a prodrug-like effect supposed for **165b** to **166b**. Indeed, the polyamines **166c** and **166e** were not trypanocidal whereas their Boc-protected equivalent (**165c** and **165e**) displayed significant activity against *T. b. gambiense*. Since **166c** and **166e** are not inhibitors of TryR, we assume that these deprotected polyamines would target different enzymes of the parasite. Similarly, the increased activity of **165d** on intramacrophage amastigotes compared to axenic *L. donovani* could be due to structural modifications of this polyamine such as Boc removal by macrophage metabolism.

4. Conclusion

We have designed and synthesized an original series of polyamine-hydroxybenzotriazole conjugates. Only **166b** showed real TryR inhibition activity meaning that this enzyme is not the main target of our derivatives series. In vitro evaluation against two parasites, *T. b. gambiense*

and *L. donovani* allowed identification of two polyamine derivatives as potential antikinetoplastid agents. Compound **165b** appeared as the most active derivative against *T. b. gambiense* with an IC_{50} value of 1 µM and without any cytotoxicity up to 100 µM. Another compound of this series, **165d**, exhibited an IC_{50} value of 3 µM towards intramacrophage amastigotes of *L. donovani* which are particularly difficult to target. We will further investigate these two compounds through microsomal stability and then study the in vivo antikinetoplastid activity on experimental African trypanosomiasis (for **165b**) and leishmaniasis mice models (for **165d**).

II. Benzyl conjugates

1. Strategy

The bisbenzyl-polyamines described in the first chapter were outstanding inhibitors of TryR often associated with a good in vitro activity against both *L. donovani* and *T. cruzi*.[90,146] Furthermore, these compounds displayed a high selectivity index.

With these previous reports and the observation that aryl-polyamines derivatives show activities against parasitic diseases, we decided to explore the synthesis of spermidine derivatives as potent antileishmaniasis and antitrypanosomiasis compounds. A library of various tertiary amines was prepared. Indeed, in our previous results, spermidine analogs exhibited the most interesting antikinetoplastids activity, in particular, derivatives bearing aromatic substituent on the N^3-nitrogen atom. Thus, spermidine was disubstituted on the N^3-nitrogen by different aryl groups. Some bisbenzyl derivatives were inspired from existing literature. Indeed, thiophene,[91] benzyloxybenzyl, diphenyl[38] and naphthalene[72] have also been identified as efficient substitutents for trypanocidal activity. Therefore, we elaborated some spermidine derivatives bearing these scaffolds (Figure 74).

[146] Baumann, R. J.; Hanson, W. L.; McCann, P. P.; Sjoerdsma, A.; Bitonti, A. J. *Antimicrob. Agents Chemother.* **1990**, *34*, 722–727.

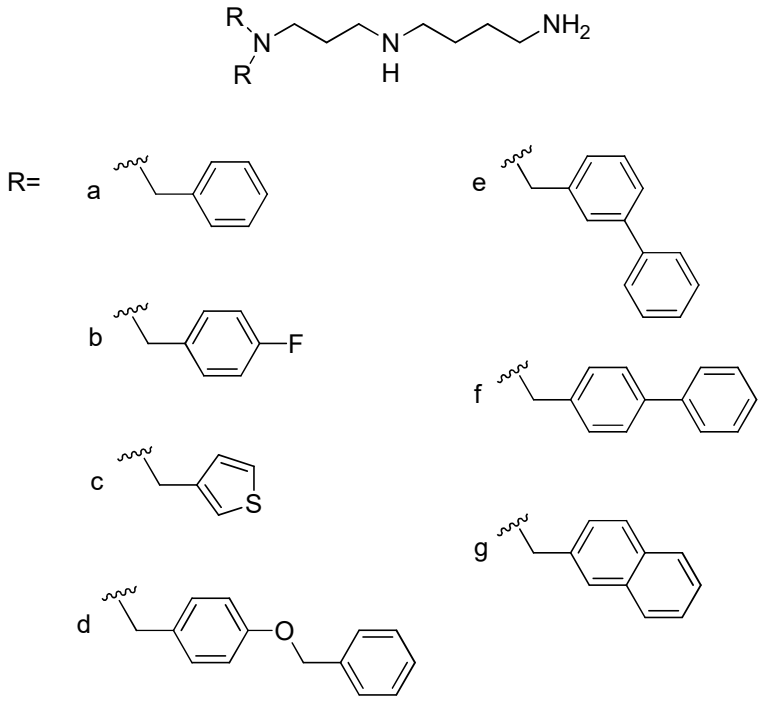

Figure 74: General structure of benzyl and analog derivatives.

Moreover, in order to increase the bioavailability, we made some additional modifications of these derivatives: i) we chose to introduce fluorine atom on the para position of the phenyl ring which is well known to avoid rapid metabolization;[147] ii) In second intention, it has been decided to prepare some polyamine derivatives bearing a rigidified polyamine chain since constraint structures generate better bioavailability.[148] It has been shown that polyamine derivatives bearing substituent in α-position of the amine were not hydroxylated by the spermine oxidase in organism.[149,150] Thus, these modifications increase the metabolic stability of derivatives. Consequently, we introduced a cyclohexyl ring on the polyamine skeleton (Figure 75) in order to combine rigidifications of the structure and prevent fast degradation of the compound.

[147] Bazzini, P.; Wermuth, C. G. In *The Practice of Medicinal Chemistry (Third Edition)*; Academic Press: New York, **2008**; pp. 429–463.

[148] Mann, A. In *The Practice of Medicinal Chemistry (Third Edition)*; Academic Press: New York, **2008**; pp. 363–379.

[149] Lakanen, J. R.; Coward, J. K.; Pegg, A. E. *J. Med. Chem.* **1992**, *35*, 724–734.

[150] Järvinen, A.; Grigorenko, N.; Khomutov, A. R.; Hyvönen, M. T.; Uimari, A.; Vepsäläinen, J.; Sinervirta, R.; Keinänen, T. A.; Vujcic, S.; Alhonen, L.; Porter, C. W.; Jänne, J. *J. Biol. Chem.* **2005**, *280*, 6595–6601.

Furthermore, we will be able to compare the linear and the cyclic polyamine structure toward the biological effect.

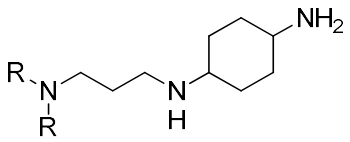

Figure 75: General structure of the rigidified polyamine derivatives.

2. Synthesis

Diaryl derivatives **172a-g** were synthesized in four steps, starting from commercially available benzyl chloride or benzyl bromide **168a-g** (Figure 76). Firstly, preparation of *N*-diaryl-aminoalcohol **169a-g** was carried out using 3-aminopropanol **167** and benzyl halides **168a-g** in presence of potassium carbonate in different solvent according to the benzyl halides **168a-g** solubility (Acetone, DCM or DMF, see experimental section). The hydroxyl group was mesylated to provide activated compounds **170a-g**. Nucleophilic replacement of mesylate with monoprotected diaminobutane in the presence of Hünig's base provided **171a-g** in 12-41% yield on two steps. Disubstitution was occasionnally observed during this reaction and afforded byproducts **173a** and **173b**. These compounds were isolated and included in the study for biological evaluation.

The Boc protecting group was removed by treatment with HCl solution in dioxane at a concentration of 4M. Thus, the final compounds **172a-g, 174a** and **174b** were obtained as hydrochloride salt.

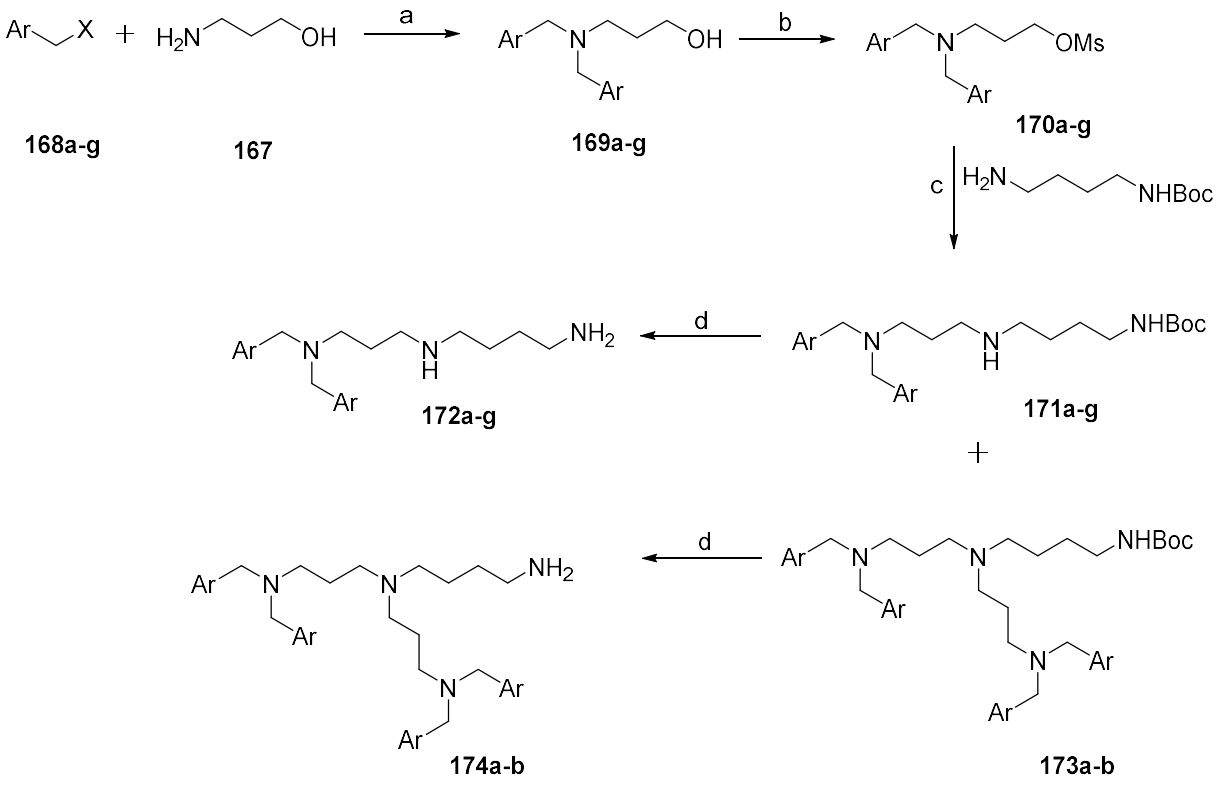

Figure 76: Synthesis of diaryl derivatives. *Reagents and conditions*: (a) K_2CO_3, Acetone or DCM or DMF, rt, 12-16 h; (b) CH_3SO_2Cl, DIEA, DMAP, DCM, 0 °C to rt, 16h; (c) DIEA, ACN, reflux, 16h; (d) HCl/Dioxane 4M, rt, 16 h.

In an attempt to confer a degree of structural rigidity, analog of **172a** and **172b** featuring restricted rotation in the central polyamine chain were designed. This was accomplished by incorporating a *trans*-cyclohexane ring into the polyamine skeleton (Figure 77). Thus, *trans*-1,4-diaminocyclohexane **175** was monosubstituted by a Boc protecting group according to aforementioned method. MonoBoc-diaminohexane **176** was then coupled to two different mesylated intermediates **170a** and **170b** to give N^1-(3-(diarylamino)propyl)cyclohexane-1,4-diamine **177a** and **177b**. During this substitution reaction with the fluorinated mesylate **170b**, a second product was observed. This latter compound is derived from disubstitution of the mesylate **170b** conducting to a tertiary amine **179b**. Likewise, this byproduct was isolated, then deprotected to compound **180b** and included in the biological assay. **177a** and **177b** were also deprotected to afford the final compounds **178a** and **178b**.

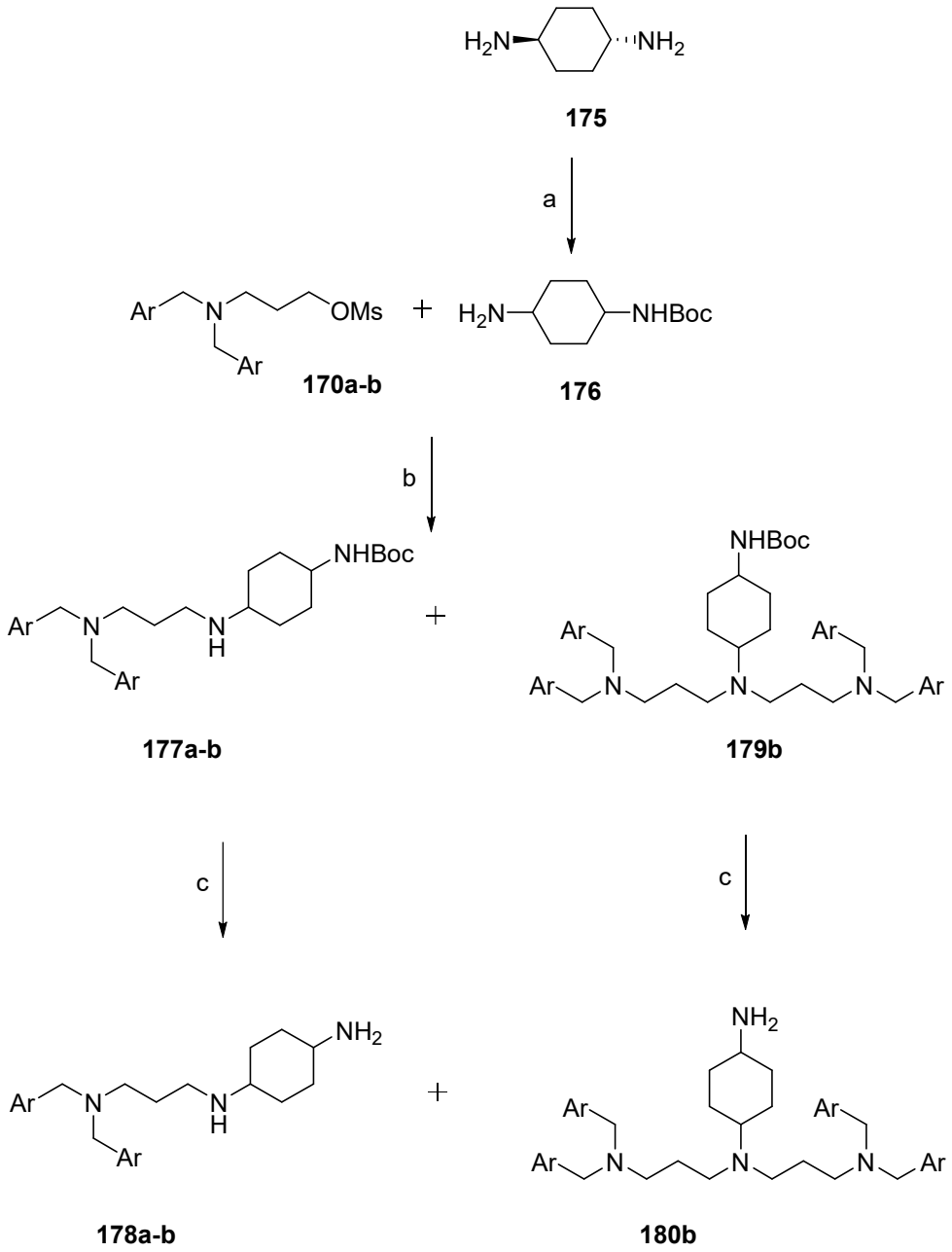

Figure 77: Synthesis of ((diaryl)aminopropyl)cyclohexanediamine. *Reagents and conditions*: (a) Boc_2O, DCM, 0 °C to rt, 16 h; (b) DIEA, ACN, reflux, 16h; (c) HCl/Dioxane 4M, rt, 16 h.

3. Biological evaluation

Boc-protected and -deprotected molecules have been evaluated in vitro against both *T. b. gambiense* trypomastigotes and *Leishmania donovani* axenic and intramacrophage amastigotes. The results of the in vitro screening are shown in Table 3.

Regarding the difference of activity between the Boc protected and the free amine compounds, it is difficult to infer a general trend that either increase or not the activity. In most cases, the protecting group did not influence the biological effect, except for the couples Boc-protected polyamine/free polyamine: **171a**/**172a**, **173b**/**174b** and **171f**/**172f** on *T. b. gambiense*.

Against *T. b. gambiense*, ten compounds of this series have displayed an IC_{50} below 1 µM. However, two of them have shown cytotoxicity on non-infected macrophages below 3 µM (**174a** and **174b**) and five below 5 µM (**172f**, **171g**, **172g**, **177b** and **178b**). The two most interesting compounds against this parasite were **171a** and **173a** which displayed IC_{50} of 0.6 and 0.3 µM respectively. Both have a cytotoxicity effect around 12 µM which lead to selectivity index of 22 and 35 respectively. The naphthalene **172g** appeared also to be a potential trypanocidal agent due to its good activity (IC_{50} = 0.4 µM) and selectivity index of 11.

Concerning the activity against *Leishmania donovani*, we observed that the vast majority of compounds displayed similar or better activity on intramacrophage than on axenic amastigotes. **173a** also remarkable since it displayed IC_{50} of 2.5 µM against *L. donovani* axenic amastigotes and, interestingly, an IC_{50} of 1.5 µM against the intramagrophage ones. **174b** which is the fluorinated deprotected analog of **173a**, was equally active against axenic amastigote and slightly less active on intramacrophage, but this compound had a strong cytotoxicity on macrophage (IC_{50} = 1.5 µM). Thiophene **171c**, **172c** and benzyloxybenzyl **171d**, **172d** derivatives did not shown any activity against *L. donovani*. Remarkably, we observed that the 3-ethyl-1,1'-biphenyl **172e** derivative was not leishmanicidal whereas the 4-ethyl-1,1'-biphenyl **172f** had a moderate activity against both axenic and intramacrophage amastigotes (IC_{50} of 3.9 and 7.1 µM).

When compound **172a** is compared with the rigidified analog **178a**, an improvement of the antikinetoplastid activity could be noted as well as an enhancement of the cytotoxic effect.

However, the fluorobenzyl derivative **178b**, rigidified with the cyclohexane diamine displayed an IC_{50} of 0.4 µM against *T. b. gambiense* and a selectivity index of 12.

Table 3: Antikinetoplastid activities and cytotoxicity of benzyl conjugates.

[a] SI: Selectivity Index calculated from cytotoxicity CC_{50}/IC_{50} ; SI_{Tb}: relative to IC_{50} on *T. b. gambiense*; SI_{aa}: relative to IC_{50} on *L. donovani* axenic amastigotes; SI_{ia}: relative to *L. donovani* intramacrophage amastigotes

[b] 50% growth inhibitory concentration

ND: not determined

Compounds	*T. b. g.* IC_{50} (µM) ± SD	SI_{Tb}[a]	*L. d.* LV9 axenic amastigotes IC_{50} (µM) ± SD	SI_{aa}[a]	*L. d.* LV9 intramacrophage amastigotes IC_{50} ±SD (µM)[b]	SI_{ia}[a]	Cytotoxicity on macrophages CC_{50} ± SD (µM)[b]
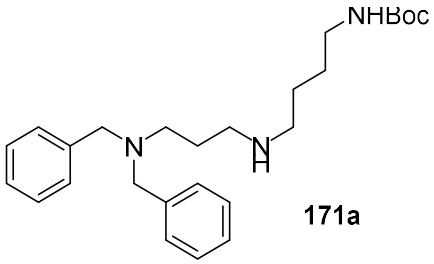 **171a**	**0.6 ± 0.1**	**22**	14.6 ± 3.6	1	3.4 ± 1.2	4	12.5
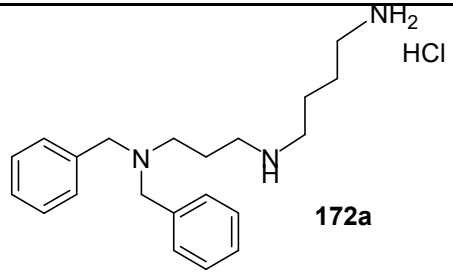 **172a**	8.8 ± 2.2	2	> 100	-	27.4 ± 2.7	1	17.7 ± 0.6

Compounds	*T. b. g.* IC_{50} (µM) ± SD	SI_{Tb}[a]	*L. d.* LV9 axenic amastigotes IC_{50} (µM) ± SD	SI_{aa}[a]	*L. d.* LV9 intramacrophage amastigotes IC_{50} ±SD (µM)[b]	SI_{ia}[a]	Cytotoxicity on macrophages CC_{50} ± SD (µM)[b]
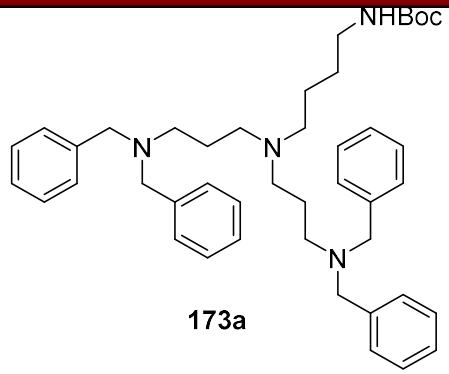 173a	**0.3 ± 0.1**	**35**	2.5 ± 0.7	3	**1.5 ± 0.2**	**8**	12.5
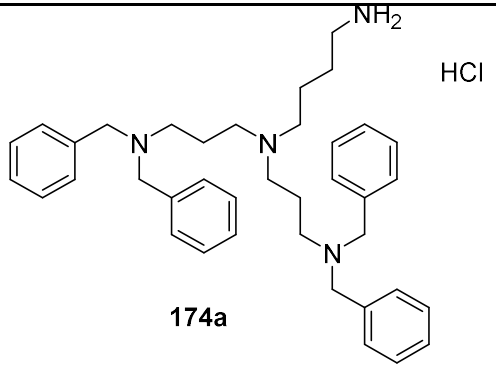 174a	0.9 ± 0.2	1	57.3 ± 4.1	-	22.4 ± 5.8	-	1.2 ± 0.2

Compounds	*T. b. g.* IC_{50} (µM) ± SD	SI_{Tb}[a]	*L. d.* LV9 axenic amastigotes IC_{50} (µM) ± SD	SI_{aa}[a]	*L. d.* LV9 intramacrophage amastigotes IC_{50} ±SD (µM)[b]	SI_{ia}[a]	Cytotoxicity on macrophages CC_{50} ± SD (µM)[b]
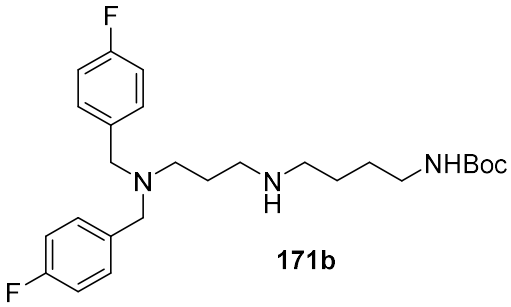 **171b**	2.0 ± 0.2	4	14.7 ± 0.5	-	14.5 ± 0.9	-	8.7 ± 0.2
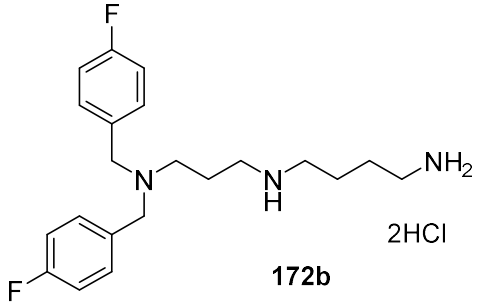 **172b**	3.5 ± 0.5	9	70.3 ± 2.3	-	35.8 ± 4.2	1	33.1 ± 0.2
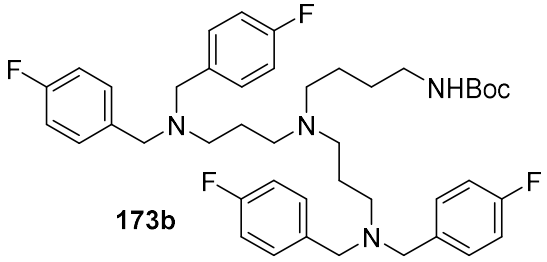 **173b**	1.9 ± 0.2	6	6.6 ± 0.1	2	16.6 ± 4.2	-	12.0 ± 3.2

Compounds	*T. b. g.* IC_{50} (µM) ± SD	SI_{Tb}[a]	*L. d.* LV9 axenic amastigotes IC_{50} (µM) ± SD	SI_{aa}[a]	*L. d.* LV9 intramacrophage amastigotes IC_{50} ±SD (µM)[b]	SI_{ia}[a]	Cytotoxicity on macrophages CC_{50} ± SD (µM)[b]
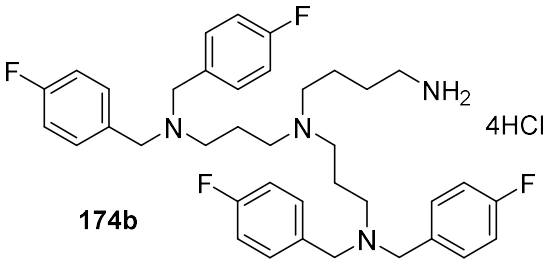 **174b**	**0.1 ± 0.0**	**15**	2.0 ± 0.8	1	6.5 ± 1.6	-	1.5 ± 0.3
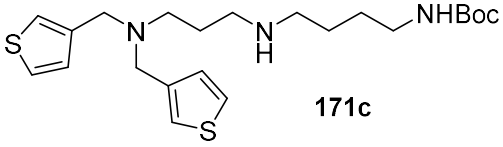 **171c**	**1.5 ± 0.1**	**11**	25.3 ± 0.5	1	21.1 ± 1.0	1	16.4 ± 0.2
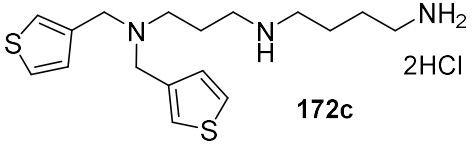 **172c**	6.1 ± 0.9	8	>100	-	59.1 ± 3.3	1	52.8 ± 1.1
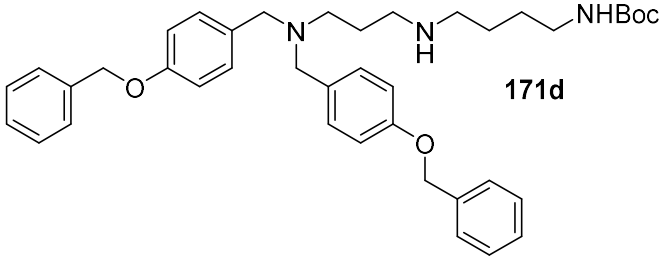 **171d**	4.7 ± 0.2	7	26.4 ± 1.6	1	42.0 ± 6.2	1	33.3 ± 2.8

Compounds	*T. b. g.* IC_{50} (µM) ± SD	SI_{Tb}[a]	*L. d.* LV9 axenic amastigotes IC_{50} (µM) ± SD	SI_{aa}[a]	*L. d.* LV9 intramacrophage amastigotes IC_{50} ±SD (µM)[b]	SI_{ia}[a]	Cytotoxicity on macrophages CC_{50} ± SD (µM)[b]
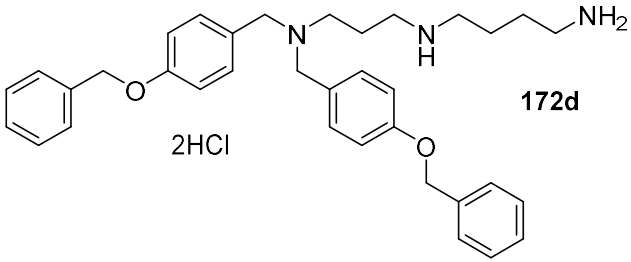 **172d** 2HCl	35.5 ± 0.5	3	72.2 ± 8.5	1	>100	1	>100
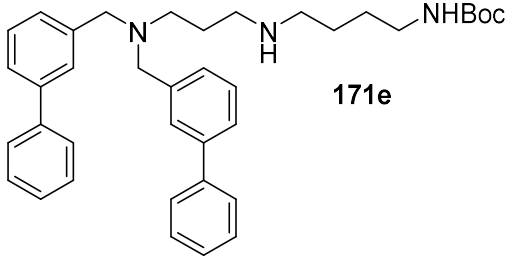 **171e**	33.9 ± 0.6	3	79.5 ± 5.5	-	>100	-	> 100
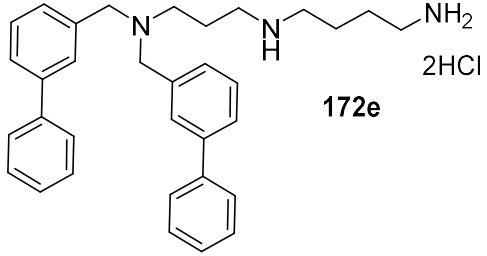 **172e** 2HCl	8.7 ± 0.6	3	35.7 ± 1.3	1	27.8 ± 5.4	1	30.3 ± 3.0
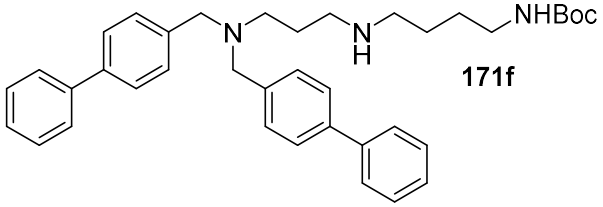 **171f**	14.4 ± 2.2	7	38.5 ± 4.6	2	41.7 ± 1.	2	> 100

Compounds	*T. b. g.* IC_{50} (µM) ± SD	SI_{Tb}[a]	*L. d.* LV9 axenic amastigotes IC_{50} (µM) ± SD	SI_{aa}[a]	*L. d.* LV9 intramacrophage amastigotes IC_{50} ±SD (µM)[b]	SI_{ia}[a]	Cytotoxicity on macrophages CC_{50} ± SD (µM)[b]
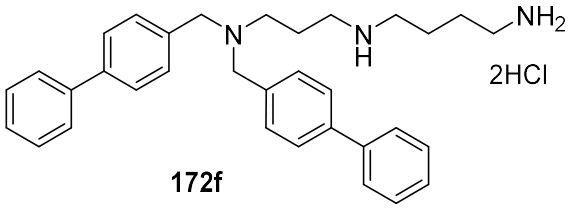 **172f**	**0.2 ± 0.0**	**21**	3.9 ± 0.1	1	7.1 ± 1.4	1	4.2 ± 0.0
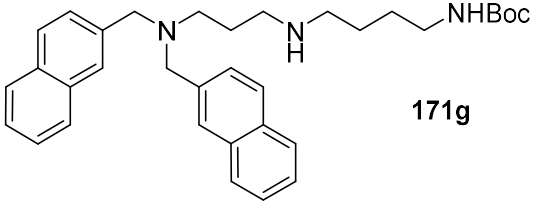 **171g**	0.8 ± 0.0	5	3.8 ± 0.1	1	6.1 ± 2.9	1	4.3 ± 0.1
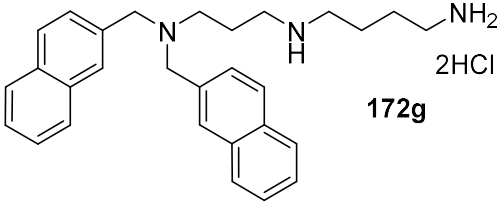 **172g**	**0.4 ± 0.0**	**11**	5.0 ± 0.4	1	8.7 ± 0.3	1	4.9 ± 1.1
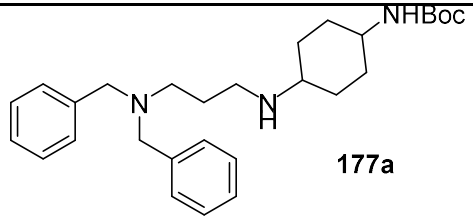 **177a**	0.7 ± 0.1	7	14.2 ± 2.1	-	5.4 ± 1.8	1	5.1 ± 1.4

Compounds	*T. b. g.* IC_{50} (µM) ± SD	SI_{Tb}[a]	*L. d.* LV9 axenic amastigotes IC_{50} (µM) ± SD	SI_{aa}[a]	*L. d.* LV9 intramacrophage amastigotes IC_{50} ±SD (µM)[b]	SI_{ia}[a]	Cytotoxicity on macrophages CC_{50} ± SD (µM)[b]
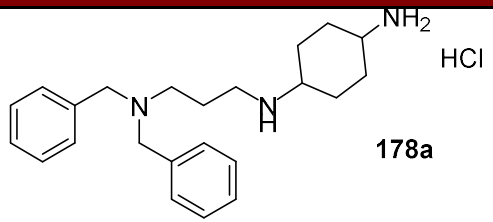 **178a**	2.1 ± 0.0	4	>100	-	6.6 ± 1.2	1	7.6 ± 2.2
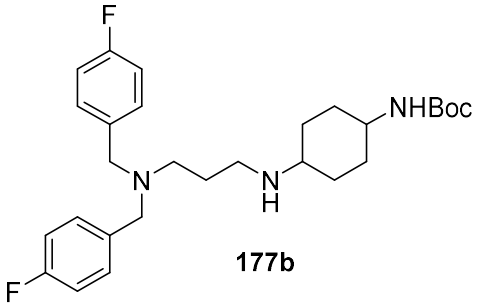 **177b**	0.5 ± 0.0	8	6.8 ± 0.2	1	6.8 ± 0.4	1	4.2 ± 0.0
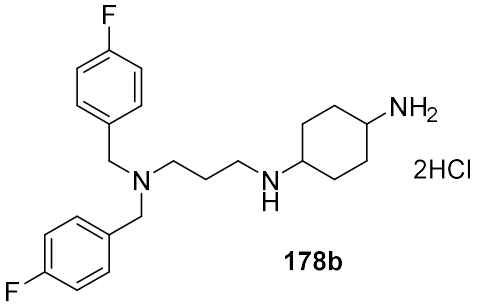 **178b**	**0.4 ± 0.0**	**12**	44.4 ± 2.0	-	12.4 ± 3.5	-	4.4 ± 0.0

Compounds	*T. b. g.* IC_{50} (µM) ± SD	SI_{Tb}[a]	*L. d.* LV9 axenic amastigotes IC_{50} (µM) ± SD	SI_{aa}[a]	*L. d.* LV9 intramacrophage amastigotes IC_{50} ±SD (µM)[b]	SI_{ia}[a]	Cytotoxicity on macrophages CC_{50} ± SD (µM)[b]
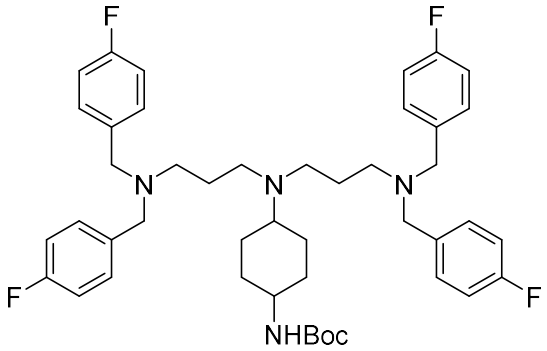 **179i**	**4.2 ± 0.2**	**24**	10.2 ± 0.3	10	17.2 ± 6.6	6	>100
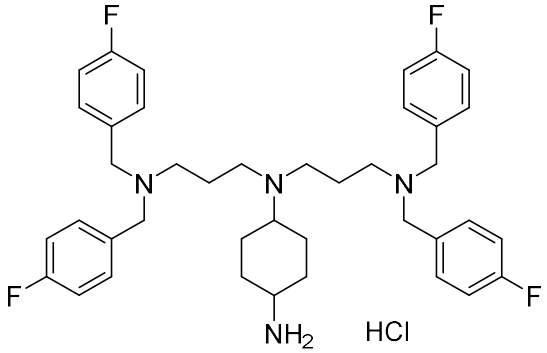 **180i**	10.4 ± 1.2	-	15.7 ± 1.3	-	4.2 ± 1.6	1	4.5 ± 1.0
Miltefosine	ND	-	1.9 ± 0.6	8.3	1.5 ± 0.3	10	15.8 ± 0.9
Pentamidine	0.01 ± 0.002	7500	ND		ND		75 ± 0.5

As mentioned earlier, TryR is an attractive drug target for polyamines since large number of different TryR inhibitors reported so far were polyamine derivatives bearing an aryl hydrophobic part.

Among the active compounds, seven of them have been evaluated on TryR from *T. b*. in Heidelberg. A first screening at a fixed concentration of inhibitor at 40 µM in assay buffer containing 5% DMSO has been carried out on these compounds. The activity was measured in the presence of 40 and 100 µM TS_2, respectively, and the percentage of inhibition was calculated. The results of assay using 40 µM TS_2 were depicted in the Figure 78.

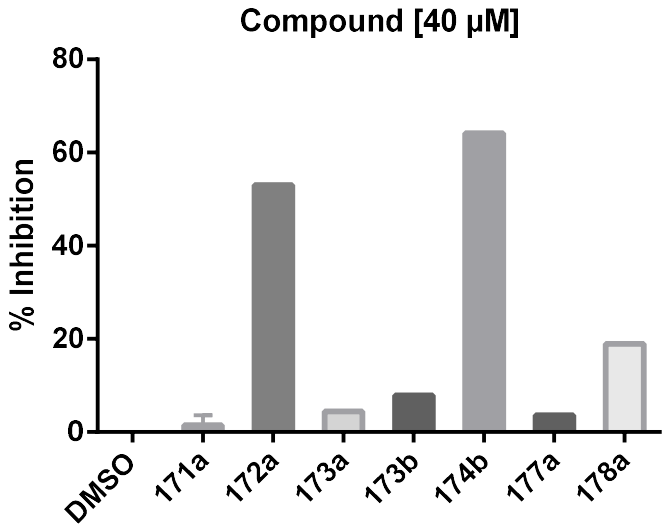

Figure 78: Inhibition of *Tb*TryR. The activity was measured following the NADPH consumption at 340 nm as described in the Experimental Section. The assays contained a fixed concentration of 100 or 40 µM of TS_2 and 40 µM of inhibitor. The controls contained the same amount of DMSO used to dissolve the compounds.

Two compounds displayed an activity higher than 50% inhibition at 40 µM (**172a** and **174b**). However, compound **174b** seems to present substrate dependent inhibition. Indeed, **174b** showed more than 60% of inhibition at a TS_2 concentration of 40 µM, and around 30% of inhibition when substrate concentration is reaching 100 µM. In contrast, percentage of inhibition for compound **172a** was independent of the substrate concentration which means that this derivative acts as pure competitive ligand.

In view of this preliminary result for this spermidine derivative, we determined the inhibitory constant and the type of inhibition (Figure 79).

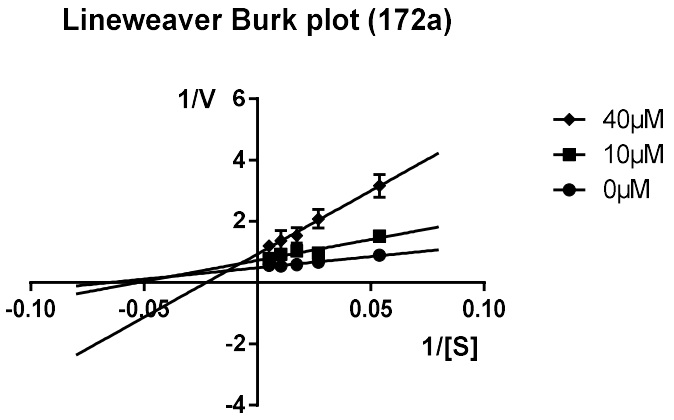

Figure 79: Lineweaver-Burk plot of compound 172a. The assays contained 0, 10, and 40 µM of inhibitor, respectively, and the TS_2 concentration was varied. The data are the mean of three determinations ± standard deviations.

The Lineweaver-Burk plot showed that **172a** behaves as mixed-type inhibitors, with calculated Ki- and Ki'-value of 7.5 µM and 20 µM, respectively (Figure 79). With this assay, we have identified a target of this compound which displays an IC_{50} of 8.8 µM against *T. b. gambiense*.

4. Conclusion and perspectives

Twenty four new polyamines derivatives have been synthesized and evaluated in vitro against *T. b. gambiense* and *L. donovani*. Many of them displayed a good trypanocidal activity on *T. b. gambiense*. In spite of a high level of toxicity against non-infected macrophages, some derivatives were promising for the development of new antikinetoplastid compounds, in particular, compound **173a** which displayed an activity against *T. brucei* at 0.3 µM and selectivity index of 35. Additionnal experiment will be realized for evaluation of the eighteen remaining compounds on TryR. Considering that some compounds showed an antikinetoplastid activity without inhibitory effect on TryR, further studies are required to determine the mechanism of action, and the target of these compounds. Regarding the activity against *L. donovani*, we highlighted new structures which were efficient against the intramacrophage form of the parasite. However, the major disadvantage found in the literature for this kind of derivatives is a weak in vivo activity. Many authors suggested that lack of trypanocidal activity on infected animal is probably due to either rapid excretion of polyamine derivatives or fast metabolism in

mammalian host. In our study, we tried to increase the bioavailability with structural modifications. Further investigation should be carried out with in vivo assay on mice infected by *T. brucei* for compounds which have been optimized for a better bioavailability. Compound **178b** which has a fluorine atom on the benzyl group and for which the polyamine chain have been rigidified, displayed an in vitro trypanocidal activity at 0.4 µM. Thus, this molecule have been structurally optimized and considering its in vitro activity, **178b** will be evaluated in vivo on the *Trypanosma brucei*/Swiss mice model.

Chapter 5: Fluorescent probes for polyamines transporters.

During their life cycle, Kinetoplastids are exposed to different biological environments in the insect or in the mammalian host. These different environments have dissimilar composition of nutrients and, parasites need a strong capacity to acclimate for good metabolic activity. Kinetoplastids need these nutrients for survival and growth, the replacement of biosynthetic pathways by transport systems is a good deal since the need of energy is lower during a nutrient import than during its biosynthesis. Polyamines are essential compounds for parasite life as it is reported in the chapters before, thus using transporter as a source of polyamine is a positive strategy for parasite. Membrane transporters can uptake polyamine from the extracellular environment. These uptake systems are well described in bacteria and yeast but are poorly characterized at the molecular level for mammalian and protozoan parasites. However, biochemical functionality of the transporter have been studied in some protozoans.

I. Polyamine transporter in mammalian cells

Intracellular concentrations of the natural polyamine putrescine, spermidine and spermine are regulated by a polyamine transport system. Mutant cell lines lacking the ability to uptake polyamines from the extracellular medium are still capable of releasing polyamines. This indicates that uptake and release are function of two different transport systems. Polyamine internalization and efflux are both energy-dependent and saturable processes that can suggest the existence of carrier-mediated mechanism.[151] In term of mammalian polyamine transport, two models have been proposed by Belting and Poulin groups, respectively (Figure 80).

[151] Seiler, N.; Delcros, J. G.; Moulinoux, J. P. *Int. J. Biochem. Cell Biol.* **1996**, *28*, 843–861.

Belting's model involves a multi-step endocytic process.[152] In this system, polyamines first bind to high-affinity sites on transmembrane protein. Then membrane is invaginated into vesicles which become endocytosed. Further processing of molecular signaling induces a cleavage between polyamine and the protein liberating the polyamines into the aqueous compartment of the vesicle.

In contrast, Poulin's group suggested that polyamines enter the cell via a simple active transport system and are then sequestered by polyamine sequestering vesicles (PSVs).[153] In this system, the vesicles are pre-existing into the cytosol and can release polyamine (Figure 80).

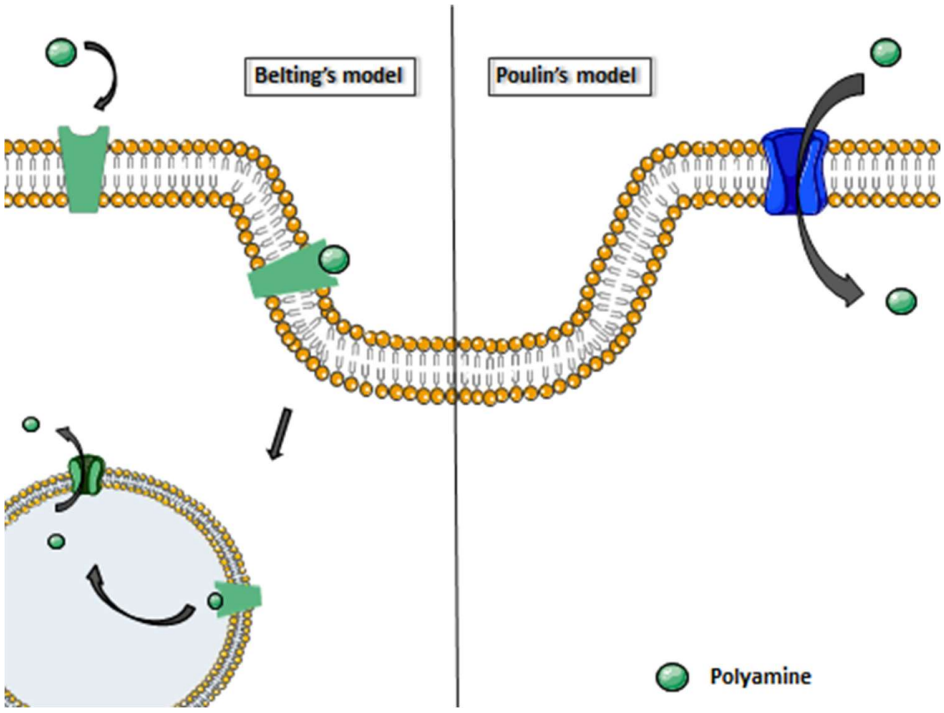

Figure 80: Two models for the import of polyamines into mammalian cells.

Belting and Poulin models may not be mutually exclusive and may work cooperatively or as a dual import system. Whatever the mechanism, the process is blocked when normal intracellular

[152] Belting, M.; Mani, K.; Jönsson, M.; Cheng, F.; Sandgren, S.; Jonsson, S.; Ding, K.; Delcros, J.-G.; Fransson, L.-Å. *J. Biol. Chem.* **2003**, *278*, 47181–47189.

[153] Soulet, D.; Gagnon, B.; Rivest, S.; Audette, M.; Poulin, R. *J. Biol. Chem.* **2004**, *279*, 49355–49366.

level of polyamine is attained. Thus, polyamine homeostasis is accomplished by balancing polyamine biosynthesis, transport and polyamine degradation. It was demonstrated that this sensitive feedback is controlled by a small regulatory protein called AZ (antizyme).[154] When intracellular level of polyamine increases, activation of AZ will limit polyamine import into the cell by an unknown mechanism so far. Degradation and consumption of polyamines by the cell could play a role in regulating transport activity as well. Consumption refers to metabolic alteration of the polyamine structure inducing a decrease of the available polyamine pools. These modifications include acetylation of polyamines by spermidine/spermine acetyl transferase (SSAT) which is a cytosolic enzyme.[155] Acetylated derivatives are better substrates for excretion than the polyamines themselves.

II. Polyamine transporter in parasites

Trypanosoma cruzi lacks arginine and ornithine decarboxylase, the two first enzymes in polyamine biosynthesis, and is therefore incapable of biosynthesis de novo. Therefore, it is dependent on the uptake of putrescine from the host.[156] Identification and functional characterization of two polyamine transporters in *T. cruzi* have been described. These transporters were high-affinity transporters that recognized both putrescine and cadaverine but not spermidine and spermine. The parasite can obtain putrescine from the human host but not cadaverine. A source of cadaverine for *T. cruzi* could be the actinomycetes residing in the gut of the vector.[157] The diamine transporters possess the ability to cover the entire cell surface and thus increase the putrescine uptake when putrescine becomes scarce. This suggest the existence of one or more cellular signaling mechanism that sense putrescine availability. Due to its transporter and signaling system, *T. cruzi* overcomes its inability to synthesize polyamine de novo. Furthermore, *T. cruzi* also has the capacity to transport exogenous spermidine by

[154] Mitchell, J. L. A.; Simkus, C. L.; Thane, T. K.; Tokarz, P.; Bonar, M. M.; Frydman, B.; Valasinas, A. L.; Reddy, V. K.; Marton, L. J. *Biochem. J.* **2004**, *384*, 271–279.

[155] Pegg, A. E. *Biochem. J.* **1986**, *234*, 249–262.

[156] Persson, K.; Aslund, L.; Grahn, B.; Hanke, J.; Heby, O. *Biochem. J.* **1998**, *333 (Pt 3)*, 527–537.

[157] Hamana, K.; Matsuzaki, S. *FEMS Microbiol. Lett.* **1987**, *41*, 211–215.

transporter identified and called TcPAT12,[158] and there is indirect evidence that the parasite could be capable of uptaking extracellular spermine.[159] Recently, the polyamine transporter TcPAT12 was overexpressed in *T. cruzi* epimastigotes. It was shown that the regulation of the polyamine transport induces significant parasite growth when different concentration of polyamines is used.[160] *Trypanosoma brucei*, on the opposite, displays very low putrescine uptake and no evidence of any polyamine transporter has been found in the genome. For this reason, an inhibition of ODC could be very critical for *T. brucei* survival, and makes it a sensible strain to DFMO effect.

Leishmania infantum promastigote form was the first for which a description of polyamine transports system has been done.[161] This transport system for putrescine has been identified and characterized by measuring the uptake of radioactively labelled putrescine into the parasite. These results have been confirmed in *Leishmania donovani* promastigotes in which a second polyamine transporter has been described for spermidine.[162] The influx of spermidine was seven times more effective than putrescine but affinity of both spermidine and putrescine transporters were the same for the respective polyamines. Therefore, transporters showed differences when a competition is made with diamines and polyamine which means that uptake of putrescine and spermidine is supported by two distinct transport systems. The transport of putrescine and spermidine is also described into *Leishmania mexicana* on promastigotes and amastigotes form.[138] In the same study, the transport was found temperature- and pH-dependent. Results from kinetic analyses confirm that putrescine and spermidine use different transporters. Total understanding and molecular characterization of polyamine transporters in

[158] Carrillo, C.; Canepa, G. E.; Algranati, I. D.; Pereira, C. A. *Biochem. Biophys. Res. Commun.* **2006**, *344*, 936–940.

[159] Ariyanayagam, M. R.; Fairlamb, A. H. *Mol. Biochem. Parasitol.* **1997**, *84*, 111–121.

[160] Reigada, C.; Sayé, M.; Vera, E. V.; Balcazar, D.; Fraccaroli, L.; Carrillo, C.; Miranda, M. R.; Pereira, C. A. *J. Membr. Biol.* **2016**.

[161] Balaña-Fouce, R.; Ordóñez, D.; Alunda, J. M. *Mol. Biochem. Parasitol.* **1989**, *35*, 43–50.

[162] Kandpal, M.; Tekwani, B. L. *Life Sci.* **1997**, *60*, 1793–1801.

Kinetoplastids is far from being achieved. A gene has been identified and cloned, *Lm*POT1 that encodes a polyamine transporter from *Leishmania major*.[163]

III. Polyamine transport system as drug target

Antitumoral agents

Nearly all of anticancer drugs in clinical use or trial are limited by systemic host toxicity, in spite of their potent cell killing activity in vitro. This high level of toxicity is due to their non-specific actions. An attractive alternative would be to exploit the already well-known activity of identified anticancer drugs by attaching them to a molecule which is transported into cancer cells via a selective transport system. One possibility for this approach is the polyamine transport system. In fact, tumor cells present high polyamine transport activity in comparison to normal cells.[164] It was proven that the polyamine transport system tolerates structural modifications which allow uptake of polyamine-conjugates.[165] Cullis et al. have synthesized a wide range of polyamines conjugated with various cytotoxic agents including chlorambucil.[166] Most of the chlorambucil-polyamine derivatives displayed an IC_{50} better than chlorambucil itself. Determination of the polyamine analog incorporation was measured by inhibition of uptake of ^{14}C-labelled spermidine. All the polyamine conjugates were competitive inhibitors of spermidine uptake with K_i values between 0.02 and 80 µM. F14512 is a spermine combined with epipodophyllotoxin which is a known inhibitor of topoisomerases II. This potent antitumor agent is the most successful polyamine conjugate and is currently developed in clinical trial (Figure 81).[167]

[163] Hasne, M.-P.; Ullman, B. *J. Biol. Chem.* **2005**, *280*, 15188–15194.
[164] Wallace, H. M.; Keir, H. M. *Biochem. J.* **1982**, *202*, 785–790.
[165] Phanstiel, O.; Kaur, N.; Delcros, J.-G. *Amino Acids* **2007**, *33*, 305–313.
[166] Cullis, P. M.; Green, R. E.; Merson-Davies, L.; Travis, N. *Chem. Biol.* **1999**, *6*, 717–729.
[167] Kruczynski, A.; Pillon, A.; Créancier, L.; Vandenberghe, I.; Gomes, B.; Brel, V.; Fournier, E.; Annereau, J.-P.; Currie, E.; Guminski, Y.; Bonnet, D.; Bailly, C.; Guilbaud, N. *Leukemia* **2013**, *27*, 2139–2148.

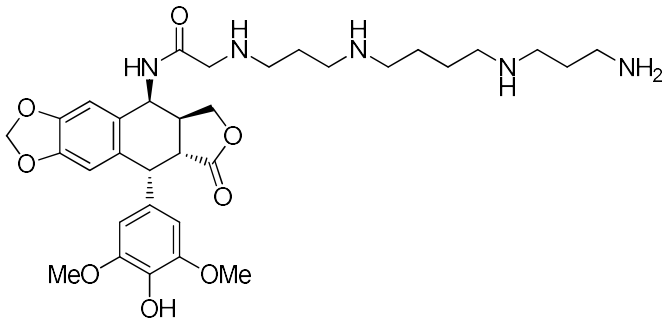

Figure 81: Chemical structure of F14512, a spermine-epipodophyllotoxin conjugate.

Antikinetoplastid agents

The inhibition of polyamine biosynthetic pathway by DFMO is often compromised since most of the protozoan can import them from the extracellular medium. This disadvantage could be exploited by targeting the polyamine uptake mechanism to either block the polyamine uptake or use the transport as a drug targeting system. Such an approach may be particularly effective in the case of *T. cruzi* which is polyamine auxotroph. Furthermore, this could be applied for other protozoan since their polyamine transport system has been demonstrated more active than human polyamine transport system.[121] Because of the necessity for the parasite to use profusely the polyamines, this transporter could be distorted for active drug targeting strategy for search of antikinetoplastid compounds. The purpose is to capitalize on the efficient polyamine transport systems to target specifically the Kinetoplastids (leishmania/Trypanosome) and facilitate the internalization of pharmacologically active compounds covalently linked to the polyamines. The literature is still scarce for this type of strategy against Kinetoplastids. As mentioned in chapter 1, it was hypothesized that bisbenzyl-polyamines from Marion Merrell Dow Research institute could bind to the polyamine transporter of *L. donovani* promastigote and lead to an intracellular depletion of putrescine and spermidine.[92] Furthermore, Lizzi et al.[41] envisioned that these polyamine-quinone conjugates could be transported via a similar mechanism in *T. cruzi*.

As summarize earlier, polyamine transport system can be distorted to deliver drugs. However, it is important to prove that polyamine-analogs were incorporated via polyamine transport system. The most widely used method for measuring polyamine transport is the radioisotopic

method that measures the radioactivity uptake with radiolabeled polyamines. Despite the fact that this method is very accurate and explicit, some disadvantages are also present. This method is expensive, time consuming, and need an appropriate laboratory with authorized worker. To avoid these disadvantages, we were interested in devising a fluorescent assay. To our knowledge, such method has not been reported so far in Kinetoplastid and it would allow the accurate determination of the affinity of structurally diverse polyamines for the polyamine transport system. Furthermore, the fluorescent polyamine probes synthesized in order to study the polyamine transporter in mammalian cells could be useful also in Kinetoplastids.

IV. Fluorescent assays

Fluorescent probes for cancer cell

In parallel of chlorambucil analogs, Cullis et al.[166] have synthesized polyamine conjugated with the fluorescent chromophore MANT (*N*-Methylanthraniloyl), **181** and **182**, in order to localize the modified polyamine (Figure 82). Flow cytometry studies have shown that spermidine-MANT derivative was rapidly uptaken in Chinese hamster ovary cell line (CHO) with a plateau within several hours. With PTS-deficient mutant (CHO-MG), the authors demonstrated that non specific uptake was very slow. Moreover, observation using conventional fluorescence microscopy provided clear evidence that the polyamine-fluorophore has been internalized. To sum up, this study delivers few evidence of internalization of polyamine analogs, including fluorescent probes, by the polyamine transport system in mammalian cells.

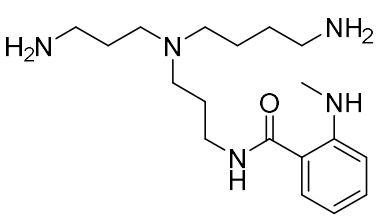

181

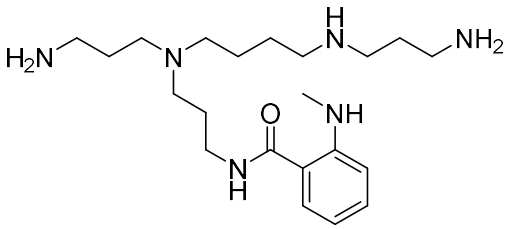

182

Figure 82: Spermidine- and spermine-MANT conjugates synthesized by Cullis et al.[166]

Furthermore, a fluorescence-based assay was published to identify the activity of the polyamine transport system in tumor cells.[126] The author synthesized a series of spermine conjugate to different fluorophores. Phenylxanthenes, rhodamine, lissamine, benzofuranes such as 4-nitro-benzol[1,2,5]oxadiazole (NBD) and bodipy. Potential fluorescent probes were chosen in function of their optimal wavelength of excitation/emission, quantum yield, selectivity for PTS-positive cells and minimum bleaching upon light irradiation. All the synthesized fluorescent probes were evaluated for spectral properties, their cellular incorporation were also tested for a competition assays against F14512 (spermine-epipodophyllotoxin derivative Figure 81).[168] In addition, comparison of the probes internalization between CHO cells and its PTS-deficient mutant (CHO-MG) was used in order to attest specific incorporation of fluorescent probes by polyamine transporter. Bodipy derivatives as **183** (Figure 83) were good candidates due to a high and stable signal but did not display PTS selectivity. The best fluorescent polyamine probes were N^1-spermine-nitrobenzoxadiazole **184** and N^1-methylspermine-nitrobenzoxadiazole **185** (Figure 83) which displayed high fluorescence intensity, strong competition with F14512 and marked differential uptake in CHO and CHO-MG cells.

[168] Barret, J.-M.; Kruczynski, A.; Vispé, S.; Annereau, J.-P.; Brel, V.; Guminski, Y.; Delcros, J.-G.; Lansiaux, A.; Guilbaud, N.; Imbert, T.; Bailly, C. *Cancer Res.* **2008**, *68*, 9845–9853.

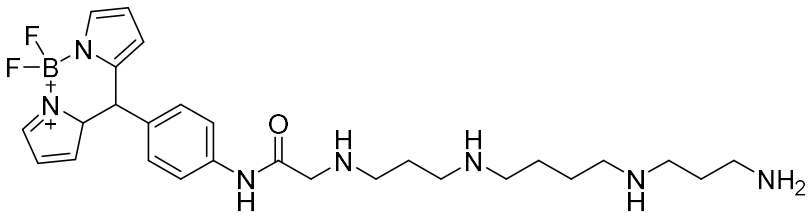

Spermine-bodipy **183**

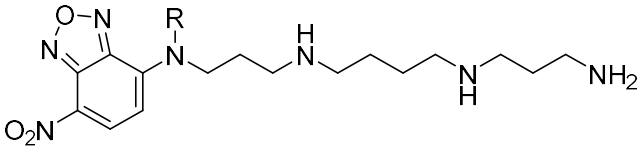

184 R = H, sperminenitrobenzoxadiazole
185 R = CH_3, methylsperminenitrobenzoxadiazole

Figure 83: Polyamine probes by Guminski et al.[166]

Fluorescent probes for Kinetoplastids

Based on the latter study, we hypothesized that reported "polyamine-fluorophore" conjugates would be also efficient in trypanosomes. We directly used the most relevant probes from the work published by "les laboratoires Pierre Fabre"[126]. I was granted a COST CM1307 Short Term Scientific Mission in April 2015 to start working on that project at the Institute of Infection, Immunity and Inflammation at University of Glasgow UK, under the supervision of Professor Michael Barret. The purpose was to examine the behavior of the polyamine fluorescent probes with Kinetoplastids and determine whether incorporation into parasites is achieved through polyamine transport.

Synthesis of polyamine-NBD probes

Five probes were envisioned for the study of the kinetoplastid polyamine transport system. The retrosynthetic pathway was the same as "les laboratoire Pierre Fabre" designed earlier and is presented on Figure 84. Putrescine and spermine derivatives have already been synthesized by Guminski et al.[126] In addition, we chose to prepare two spermidine probes attached to the two

different terminal amines. Each probe was obtained from the nucleophilic aromatic substitution of amines on chloro-nitrobenzoxadiazole (NBD chloride).

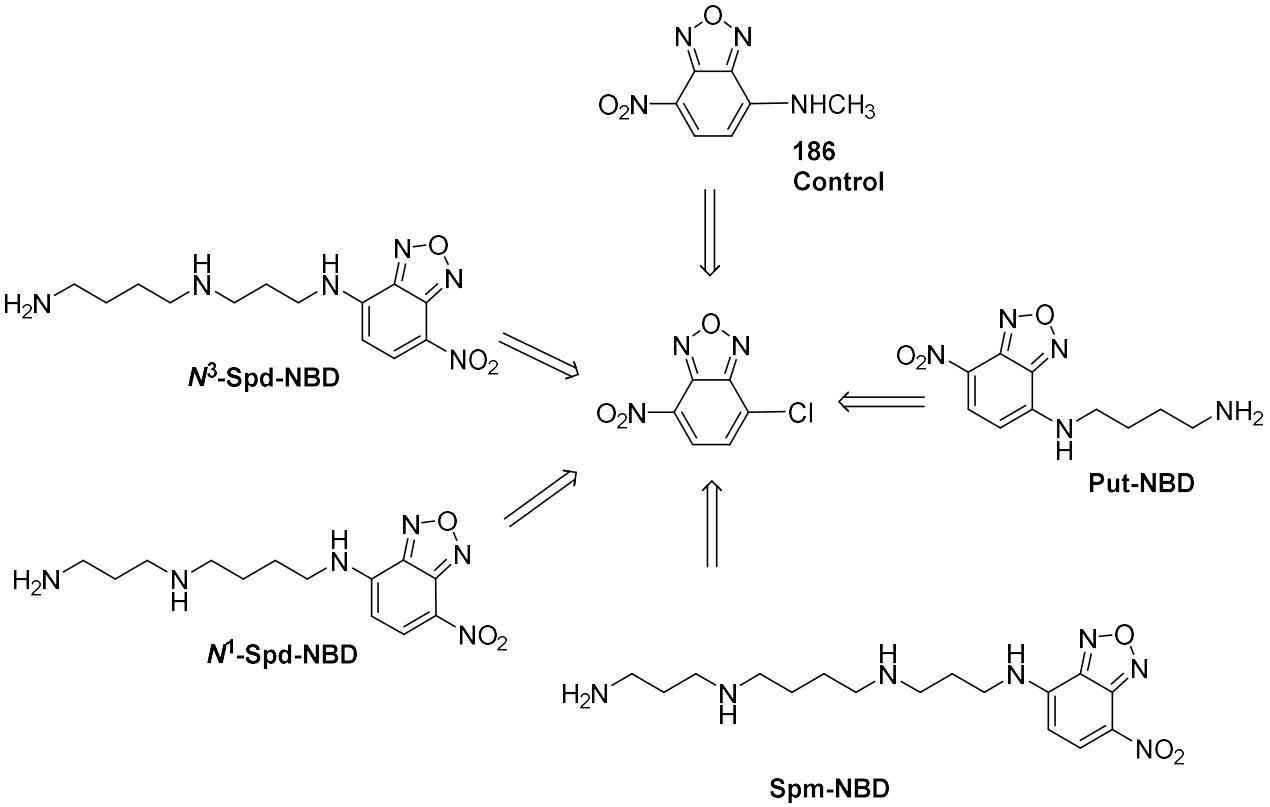

Figure 84: Retrosynthesis of five polyamine probes.

186 fluorophore control with no polyamine moiety was obtained from methylamine and chloro-NBD in methanol with a yield of 61%. All the polyamine probes were prepared according to protocols described by Guminski et al.[126] Mono-protected putrescine **155a** was reacted with chloro NBD to give an intermediate Boc-putrescine-NBD in 50% yield after recrystallization from diisopropyl ether. Boc-protected spermidine/spermine and chloro-NBD have been coupled according to a general procedure by reacting primary amine with chloro-NBD in presence of cesium carbonate in acetonitrile to give protected intermediate compounds in yield ranging from 21 to 80%. Spermidine and spermine intermediates **187b**, **187c** and **187e** were purified on flash column chromatography on silica gel. All these intermediates were deprotected in the same conditions, i.e. stirring overnight in a HCl solution 4M in dioxane to afford **put-NBD (188a)** as a putrescine derivative, **Spm-NBD (188e)** as a spermine derivative and, ***N*^{1}-Spd-NBD (188c)** and ***N*^{3}-Spd-NBD (188b)** as spermidine derivatives linked to different nitrogen atom of this

unsymmetrical polyamine. On these two steps, the global yields were good, except for **188e** (21%) and **188a** (25%). All the compounds have been used directly without any synthesis optimization (Figure 85).

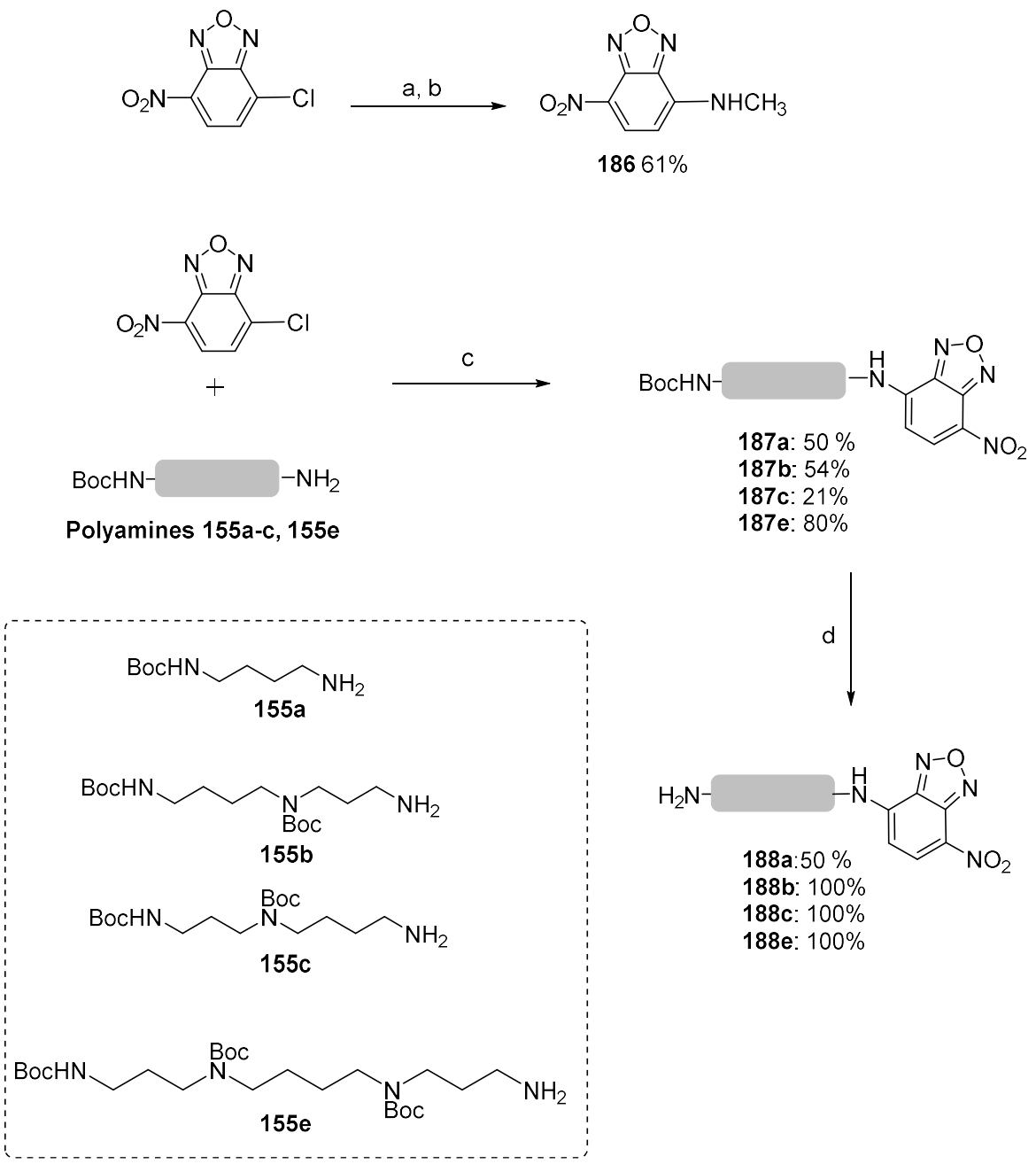

Figure 85: Synthesis of polyamine-NBD derivatives. *Reagents and conditions:* (a) NH_2CH_3, MeOH, reflux, 2h; (b) $NaHCO_3$; (c) Cs_2CO_3, Acetonitrile, reflux, 2h; (d) HCl/Dioxane 4M, rt, Overnight.

Biological evaluation of polyamine-NBD probes

1. Cytotoxicity

All the synthesized polyamine probes have been evaluated for their in vitro activity against *T. brucei*. No toxicity that could have induced the unfeasibility of the study has been observed for these compounds (Table 4).

Table 4: Biological activity of polyamine probes against *Trypanosoma brucei gambiense*.

Compounds	**186**	**put-NBD(188a)**	***N*^{1}-Spd-NBD (188b)**	***N*^{3}-Spd-NBD (188c)**	**Spm-NBD (188e)**
IC_{50} (µM) ±SD	>100	>100	>100	>100	96.96 ± 15.51

2. Fluorescent experiments

During my internship in Glasgow, I worked on few kinds of organisms (*Leishmania mexicana* promastigote form, *L. mexicana* amastigote axenic form and *Trypanosoma brucei brucei* bloodstream form).

Firstly, the different probes were incubated with parasites and we observed whether fluorescence can be seen into the cell. The incubation was done at probes concentration of 100 µM from 1h to 20h. Fluorescence into the parasite was measured and the results were described in the tables as "-" in the case where no fluorescence could be observed, "+" when fluorescence observation is weak, "++" when only some parasite display fluorescence inside and "+++" when a clear and strong fluorescence is observed. In addition, the experiments have been performed with fixed cells. In these conditions, cells are dead and have lost the ability to internalized molecule by a dynamic biological process. Thus, with this method we can observe if uptake is carried out by an active transporter.

- *Leishmania mexicana* promastigote form

Results of incubation performed with *Leishmania mexicana* promastigotes are presented in table 5. The two spermidine-NBD derivatives did not produce any fluorescence even after twenty hours of incubation. **Spm-NBD** displayed fluorescence after 2 hours and only in some parasites. Consequently, these polyamine probes seem to be not uptaken by the parasite. However, fluorescence was observed when parasites were incubated with the putrescine derivative. Based on its structure, **186** should not be uptaken by the polyamine transporter of parasite. However, high fluorescence was observed in its presence (Fig. 86). This suggests that the probe with no polyamine part is either internalized by another transport system or by passive diffusion. The fixed cells were not fluorescent suggesting that the internalization of probes was made via an active transport system.

Table 5: Fluorescence observation on *L. mexicana* promastigote form with polyamine probes. (-): no fluorescence; (+): weak fluorescence; (++): some parasites are fluorescents; (+++): strong fluorescence.

Compounds (100 µM)	**Incubation times *L. mexicana* promastigote**				**Fixed cells (10 µM)**
	1h	2h	3h	20h	
N^3-Spd-NBD	-	-	-	-	-
N^1-Spd-NBD	-	-	-	-	-
Spm-NBD	-	++	++	++	-
Put-NBD	+++	+++	+++	+++	-
186	+++	+++	+++	+++	-

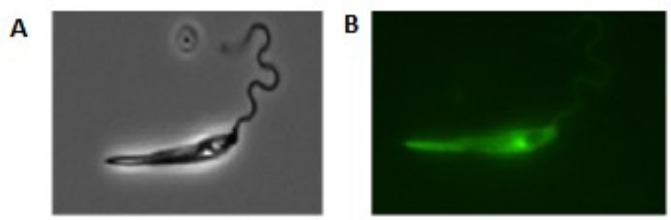

Figure 86: *L. mexicana* promastigote after 1 h incubation with 186. A) Brightlight B) FITC filter.

- *Leishmania mexicana* amastigote axenic form

One and two hours of incubation with axenic amastigote have been performed (Table 6). With ***N*^{3}-Spd-NBD** and **Spm-NBD**, slight fluorescence was noted, and an effect could be observed with ***N*^{1}-Spd-NBD** only after 2h. The results on amastigote display a completely different behavior with polyamine probes but **186** is still going into the parasite. At this stage, *L. mexicana* no longer uses a transporter to uptake **186** since fixed cells are also fluorescent. This difference observed between promastigote and amastigote forms could be explained by the structural modifications of the parasitic membrane at these two stages. **Put-NBD** seemed to be more promising but only some of the parasites display fluorescence.

Table 6: Fluorescence observation on *Leishmania mexicana* amastigote axenic form with polyamine probes. (-): no fluorescence; (+): weak fluorescence; (++): some parasites are fluorescents; (+++): strong fluorescence.

Compounds (100 µM)	**Incubation times *L. mexicana* amastigote**				**Fixed cells (10 µM)**
	1h	2h	3h	20h	
***N*^{3}-Spd-NBD**	++	++	nd	nd	+++
***N*^{1}-Spd-NBD**	-	++	nd	nd	+++
Spm-NBD	++	++	nd	nd	+
Put-NBD	++	++	nd	nd	+++
186	+++	+++	nd	nd	+++

- *Trypanosoma brucei brucei* bloodstream form

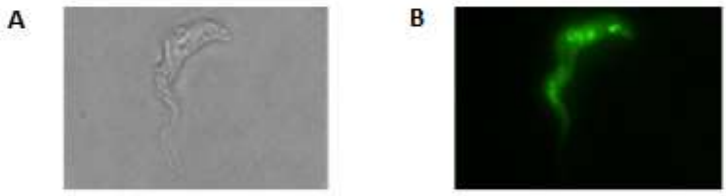

Figure 87: Microscopy picture after 1h incubation with Put-NBD. A) Brightlight B) FITC filter.

T. b. brucei was used as control strains since this organism do not express the polyamine transporter (Table 7).[163] Polyamines probes seemed to be uptaken by the cell (Figure 87) and negative control **186** is less fluorescent than that obtained in the previous cases. As we can see on the Figure 7, fluorescence is localized in a small part of the parasite. We can assume that probes have been uptaken by endocytosis. To evaluate this hypothesis, an inhibitor of endocytosis (chloroquine or leupeptin) was added at the same concentration (namely 100µM) 1h before probes addition. Microscopic observation did not allow us to see any differences with or without these inhibitors. It was noted that incubation at a concentration of 100 µM was cytotoxic after twenty hours with almost all the probes.

Table 7: Fluorescence observation on *Trypanosoma brucei brucei* bloodstream form with polyamine probes. (-): no fluorescence; (+): weak fluorescence; (++): some parasites are fluorescents; (+++): strong fluorescence.

Compounds (100 µM)	**Incubation times *T. b. brucei***				**Fixed cells (10 µM)**
	1h	2h	3h	20h	
***N*^{3}-Spd-NBD**	+++	nd	+++	+++	+++
***N*^{1}-Spd-NBD**	+++	nd	+++	nd	+++
Spm-NBD	++	nd	+++	nd	+++
Put-NBD	+++	nd	+++	nd	+++
186	++	nd	++	nd	+++

- Macrophages THP-1.

Experiment was also performed with THP-1 macrophages, which is a human cell line used for infection by *L. mexicana* amastigote (Table 8). Every tested fluorescence probes were able to penetrate the non-infected macrophage (Figure 88).

Table 8: Fluorescence observation on macrophages THP-1 with polyamine probes. (-): no fluorescence; (+): weak fluorescence; (++): some cells are fluorescents; (+++): strong fluorescence.

Compounds (100 µM)	Incubation times macrophage THP-1				Fixed cells (10 µM)
	1h	2h	3h	20h	
***N*^{3}-Spd-NBD**	+++	+++	+++	+++	+++
***N*^{1}-Spd-NBD**	+++	+++	+++	+++	+++
Spm-NBD	+++	+++	+++	+++	+++
Put-NBD	+++	+++	+++	+++	+++
186	+++	+++	+++	+++	+++

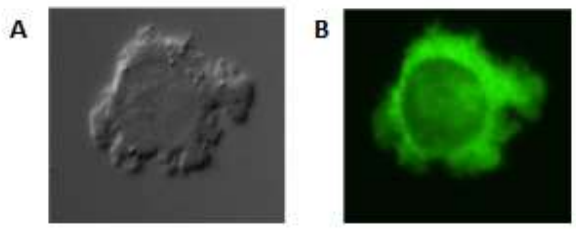

Figure 88: THP-1 macrophage after 1 h incubation with *N*^{3}-Spd-NBD. A) Brightlight B) FITC filter.

V. Transport Assays

Despite these results, we then verified that the probes were uptaken using the polyamine transport system by competition with natural polyamines. Large excess of natural polyamine (10mM of putrescine, spermidine or spermine) has been added before the incubation with the probes. Unfortunately, no difference in fluorescence was observed. We therefore concluded that these polyamine derivatives do not use the polyamine transport system for getting into the cell.

Amino acid transport

Amino acids play a vital role in the life cycle of parasite, some serving as alternative carbon sources and energy reserves.[169] Arginine is an essential amino acid for Leishmania, and therefore its metabolism and homeostasis depends on supply from external pools. This amino acid has the function to funnel carbon atoms into the polyamine biosynthetic pathway. A specific transporter, LdAAP3, from *Leishmania donovani* has been characterized.[170] In view of the structure of **put-NBD**, it was conceivable that this molecule could be recognized and uptaken by this arginine transporter. Therefore, competition experiments with **put-NBD** which seems to be the most efficient among the probes, have been done not only with arginine but also with the 20 others natural amino acids. Experiments were performed with *L. mexicana* promastigotes. The results did not show difference of fluorescence when the parasite were incubated with 10 mM of arginine. In contrast, among amino acids, three have decreased or stopped the fluorescence. Indeed, aspartic acid and cysteine blocked the polyamine probes uptake and glutamic acid decreased strongly the fluorescence. It can be assumed that the probes use aspartate transport to get into the cell. To prove this hypothesis, transport assays using radiolabeled aspartate have been done.

The aspartate transport in the parasite *Leishmania mexicana* promastigote has been studied with [^{3}H]-aspartic acid. With a PhD student in Glasgow, I learned and participated to the

[169] Opperdoes, F. R.; Coombs, G. H. *Trends Parasitol.* **2007**, *23*, 149–158.

[170] Shaked-Mishan, P.; Suter-Grotemeyer, M.; Yoel-Almagor, T.; Holland, N.; Zilberstein, D.; Rentsch, D. *Mol. Microbiol.* **2006**, *60*, 30–38.

radiolabeled experiments. Parasites were washed in a special assay buffer and then incubated with a solution of [^{3}H]-aspartic acid at a determined concentration. The reaction was stopped by centrifugation and, separation between cells and the non-incorporated [^{3}H] aspartic acid was made across inert oil. The range in which L-aspartate uptake is proportional to the incubation time was first determined (Fig. 89). The maximum velocity Vmax and the apparent Michaelis-Menten constant Km values were 1052 pmol/s per 10^7 cells, and 123 µM respectively.

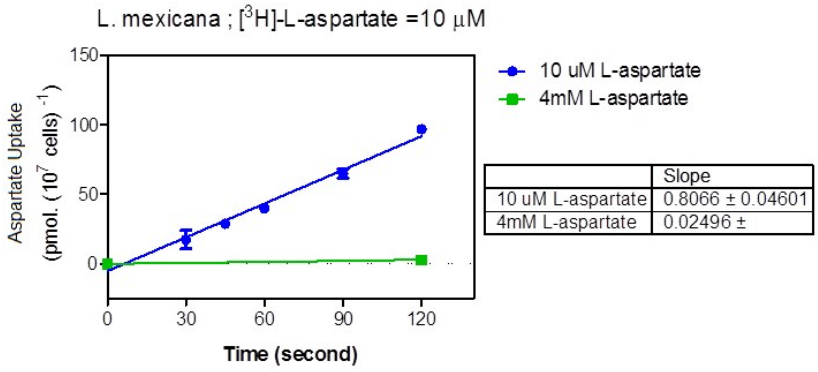

Figure 89: Kinetics of aspartate transport.

The specificity of the transport system in *L. mexicana* promastigote was evaluated by competition analysis using a range of concentration of some other amino acids. Aspartate transport was inhibited by cysteine, but this was not true when arginine or glutamate were used (Figure 90). Thus, we highlighted that cysteine could use the aspartate transporter for internalization into *L. mexicana* promastigote which has not been described so far. Competition analysis with **put-NDB** also showed an inhibition at 2.5 mM, but considering the extreme hill-slope, this is unlikely to be a direct effect on the L-aspartate transporter (Figure 90).

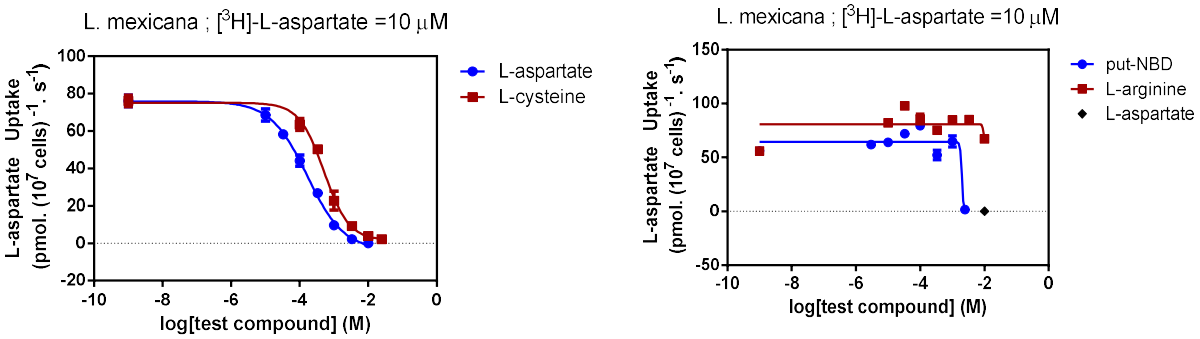

Figure 90: Competition assay of Put-NBD with radiolabeled aspartate.

The studies performed during this short term scientific mission in Glasgow showed that the method using polyamine fluorescent probes for cancer cell to identify polyamine transport system was not applicable in parasite. As a matter of fact, these probes do not seem to use the polyamine transport system in Kinetoplastid. Polyamine derivatives are probably incorporated by another transporter. This transporter may recognize the other moiety of the compound. It could be interesting to identify this transporter. In view of Pierre Fabre work, the mammalian cells use polyamine transporter to uptake these compounds. In mammalian cell, **186** which is essentially the NDB part is not incorporated whereas it showed the best fluorescent activity for parasites. These results showed that the polyamine transport system is different in Kinetoplastid and it may exist another transporter recognizing the NDB part which is not present in mammalian cells.

Spermidine transport

These surprising results were not expected and we chose to verify by another method. Moreover, we assayed another kind of Kinetoplastid, *L. donovani*, which is the strain used for our in vitro activity assays. In order to ensure that the fluorescent probes use the polyamine transporter, we used a radiolabeled competitive assay with [^{3}H]-spermidine. First, I had to get trained during three days in order to obtain the habilitation to work with radiolabeled compounds. Then, this assay has been established using expertise obtained in Glasgow and was performed in the CEA laboratory with the collaboration of Dr. Jean-Christophe CINTRAT. Indeed, the IBITECS laboratory possesses the requirement for achievement of this experiment. The

spermidine transport in *Leishmania donovani* promastigotes has been studied with [^{3}H]-tetrahydrochloride spermidine and competition have been carried out with three NBD-probes (spermidine and spermine) and the control compound methyl-NBD (**186**).

As for the aspartate assay transport, optimization have been done in order to found the concentration of radiolabeled and the needed time of incubation. Experiments were performed at a concentration of 10 µM of [^{3}H]-spermidine and with a reaction time of 10 min. To establish the efficiency of the transporter, [^{3}H]-spermidine transport was measured in the presence of the competitive natural substrate spermidine. In presence of cold spermidine, transport of radiolabeled spermidine was inhibited with an IC_{50} value of 34 µM (Figure 91). This inhibition is a control which permit to know that the measure involved the spermidine transport.

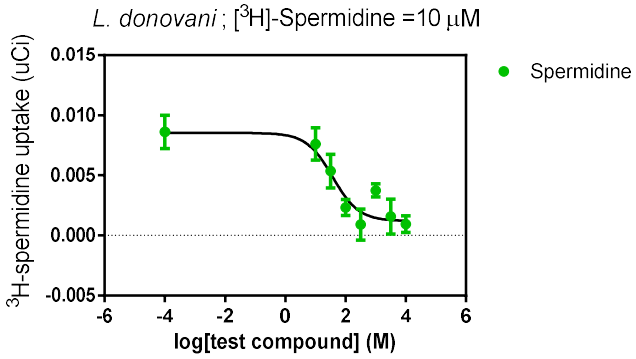

Figure 91: Competition assay with cold spermidine.

A second control consisted in evaluating the inhibition of the fluorophore not coupled to polyamine. **186** did not inhibit the [^{3}H]-spermidine transport, and was clearly not actively uptaken by the spermidine transporter (Figure 92). This result confirm that internalization of **186** do not use polyamine transporter but may use another transport system (at least in *L. mexicana* promastigote).

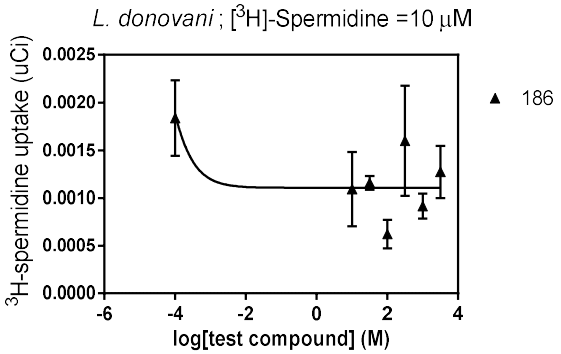

Figure 92: Competition assay with Methyl-NBD (186).

Then, the polyamine probes were evaluated by the same method. Each compound was tested in a range of concentration from 10 mM to 1 µM in triplicate and every experiment has been carried out in a minimum of three times. The results are depicted in figure 93.

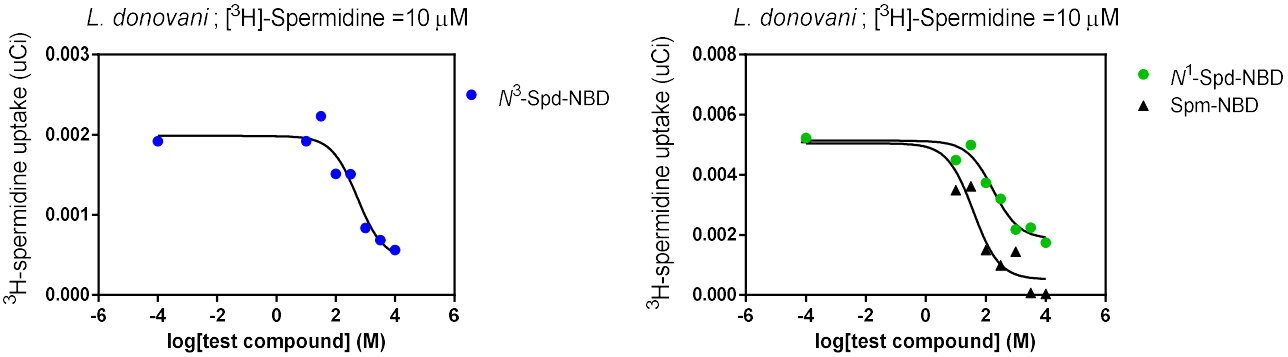

Figure 93: Competition assay with spermidine and spermine probes.

***N*^{3}-Spd-NBD** did compete with the radiolabeled spermidine although a relatively high concentration of the probe was needed (IC_{50} = 475 µM). ***N*^{1}-Spd-NBD** (IC_{50} = 177 µM) and **Spm-NBD** (IC_{50} = 60 µM) probes were however better at competing with radiolabeled spermidine. In particular, the spermine conjugate is competitive enough to be used in a fluorescent assay.

The figure 94 represents a diagram of inhibition capacity of polyamines probes. The ability to the *L. donovani* promastigote to uptake [^{3}H]-spermidine was evaluated in the presence of non-radiolabeled spermidine and in the presence of fluorescent probes each at concentration of

100, 300 or 1000 µM. Results are plotted as a percentage of spermidine uptake obtained without inhibitor (control).

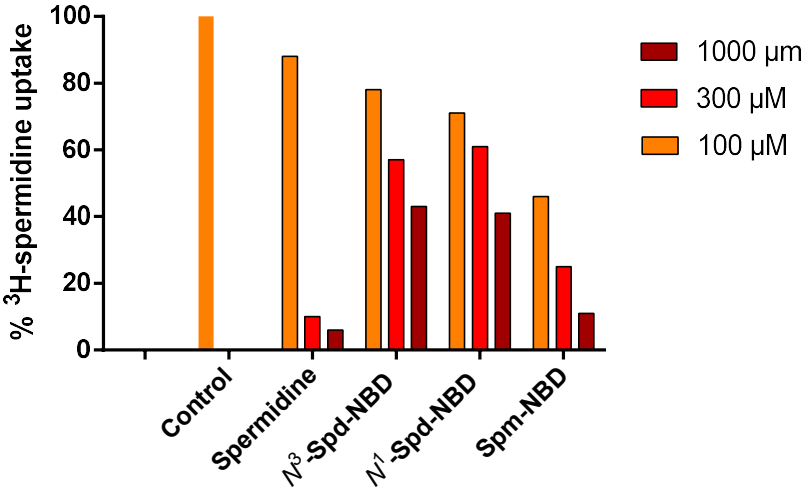

Figure 94: Competition profile of polyamine probes. Control represents the percentage of ^{3}H-spermidine uptake in absence of inhibitor.

These results were not in accordance with the observations made in Glasgow. However, differences could be explained by the use of different strains of Kinetoplastid. Furthermore, the qualitative fluorescence observation that we have done in Glasgow may be not enough sensitive for a real appreciation of competition.

VI. Conclusion and perspective

In this study, we have highlighted the internalization of fluorescent polyamines by a spermidine transporter in *Leishmania donovani* promastigote. It would be now necessary to further develop the competitive binding assay using the best fluorescent probes, i.e. the spermine nitrobenzoxadiazole (**Spm-NBD**; IC_{50} = 60µM).

The probe will be incubated with a high density of *L. donovani* and fluorescence will be measured. The internal fluorescence of parasites will be examined using a confocal microscope at different time interval. From these data we will draw a kinetic curve of the uptake. The next

step will be the comparison of those probes to common polyamines which are natural substrates of the polyamine transporter. Several controls will be carried out (passive diffusion, fluorophore with no polyamine moiety) and a decrease in fluorescence will mean that our probe is competitive to the original substrate and therefore uses the polyamine transporter. Then, we could validate a new fluorescent-based method to identify compounds able to use the polyamine transporter system in Kinetoplastid. This method would be readily implemented in any biochemistry laboratory interested in studying the polyamine transport in Kinetoplastid.

Conclusion & perspectives

The topic of this thesis is at the interface of chemistry and biology and the objectives were to design, synthesize and evaluate new polyamine derivatives as antikinetoplastid agents. Inspired by literature data and previous work from our laboratory, we elaborated new synthetic compounds as potential antikinetoplastids.

A comprehensive bibliographic work on antikietoplastid polyamine analogs was carried out in the first chapter, in order to have a global vision of literature. We took in consideration the literature's observation for designing new potential compounds. Overall, 53 polyamine derivatives were synthesized in order to specifically target Kinetoplastid. Biological evaluation of these compounds included in vitro assay against *T. b. gambiense* and *L. donovani* (amastigote axenic and intramacrophage forms) and enzymatic assays on *Tb*TryR.

The Acyl derivatives were the first series studied. These compounds were based on the previous work in the laboratory about polyamine derivative as bisubstrate inhibitors of human histone acetyltransferase. We assayed these compounds as antiparasitic agents. Even if some of these derivatives displayed biological activities with IC_{50} around 1 µM, we were not able to demonstrate that the target was the parasitic histone acetyltransferase.

Thirteen original hydroxybenzotriazole-polyamine conjugates were synthesized and evaluated and, two appeared as potential antikinetoplastid agents. Indeed, we highlighted a spermidine-hydroxybenzotriazole with an IC_{50} value of 1 µM against *T. b. gambiense* and a selectivity index of 85. In addition, we identified a compound which displayed an antikinetoplastid activity on *L. donovani* intramacrophage form.

In the last designed series, we focused on the design of inhibitors of the TryR enzyme. For that, bisbenzyl-spermidine derivatives were prepared. Many of the 24 compounds synthesized had a IC_{50} values in the micromolar range against the two strains tested. Moreover, we identified that the enzymatic target of these derivatives is TryR. In order to avoid the bioavailability problems

found in literature with in vivo assays, we chose to evaluate an active compound which was structurally optimized for a better bioavailability. This compound will be evaluated in vivo on the *Trypanosoma brucei*/Swiss mice model. Depending of the in vivo results, the pharmacokinetic profile of the molecule could be improved.

In parallel, we started the development of a new fluorescent assay for polyamine transporter. The synthesis of fluorescent polyamine probes were performed in Orsay, the preliminary fluorescent experiment were carried out in Glasgow and radiolabeled assay performed in the CEA of Saclay. These experiments allowed to highlight the potential of these probes on *L. donovani* promastigote. This project is at a substantially advanced stage but further development should be carried out. In addition, experiment on *L. donovani* intramacrophage amastigote could be also envisioned. Indeed, polyamine transport in Kinetoplastids at this stage has not been studied. To this end, particular techniques leading to the differential lysis of the macrophage membrane and not the parasitic ones could be used. Then, the fluorescence into amastigote forms would be measured by the same method used for promastigote forms.

Experimental part

Chemistry

All chemical reagents were of analytical grade, obtained from Acros, Alfa Aesar, or Aldrich, and used without further purification except for hydroxybenzotriazole (HOBt) which was recrystallized from diethyl ether. Solvents were obtained from SDS or VWR-Prolabo. Dichloromethane was dried on molecular sieves and used immediately. Chromatography was performed using silica gel (35-70 µm, Merck). Concentration of solutions was performed under reduced pressure at temperature below 40°C using rotary evaporator. Analytical TLC was performed using Silica Gel 60 F_{254} pre-coated aluminum plates (Merck). Spots were visualized by treatment with ninhydrine revelator followed by heating and/or by absorbance of UV light at 254 nm. NMR spectra were collected on Bruker DRX 250 (^{1}H at 250 MHz and ^{13}C at 75 MHz) or 300 (^{1}H at 300 MHz and ^{13}C at 90 MHz) spectrometer using MestReNova software. Chemical shift are reported in ppm (δ) and coupling constants in Hz (J). ^{1}H NMR spectra were performed in $CDCl_3$, MeOD or D_2O. High-resolution mass spectrometry (HRMS) analyses were performed by electrospray with positive (ESI^+).

I. Protected polyamines.

Compound 155a:

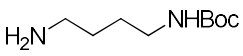

1,4-butanediamine (4,85g, 55mmol, 6 eq.) was dissolved in 50mL of dry DCM. To this solution, Boc_2O (2g, 9,16mmol, 1 eq.) in DCM was added dropwise under argon atmosphere at 0 °C. Mixture was stirring overnight at room temperature. Then, white solid was filtered, washed with DCM. The organic layers were washed with water and brine, dried with $MgSO_4$ and

evaporated to give the compound **155a** as a colorless oil. The product was used without further purification.

Colorless oil, (90%). Rf (Cyclohexane/EtOAc: 5:5) = 0.40.

^{1}H NMR (250 MHz, MeOD): δ = 3.04 (t, *J* = 6,7 Hz, 2H), 2.62 (t, *J* = 6,7 Hz, 2H), 1.47 (t, *J* = 6,7 Hz, 4H), 1.43 (s, 9H) ppm.

^{13}C NMR (75 MHz, MeOD): δ = 156,2, 79,1, 41,9, 40,6, 31,0, 28,6, 27,6 ppm.

IR-TR (cm-1) : 3321 (NH amide, NH2), 2910 (-C-H alcanes), 1642 (C=O amide), 1142 (C-O ester).

Compound 155b and 155c were obtained from the cyano-precursor as described by Roblot et al.[108]:

Compound 155b:

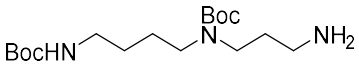

Yellow oil, (91%). R_f (DCM/MeOH: 9:1) = 0.3.

^{1}H NMR (300 MHz, MeOD): δ = 3.18-3.13 (m, 4H), 2.96 (t, *J* = 6.8 Hz, 2H), 2.61 (t, *J* = 7.1 Hz, 2H), 1.68-1.60 (m, 6H), 1.43 (s, 18H) ppm.

HRMS-ESI(+): calcd for $C_{17}H_{36}N_3O_4$: 346.2700, found: 346.2688 $[M+H]^+$.

Compound 155c:

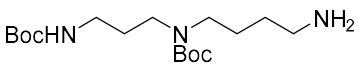

Yellow oil, (71%). R_f (DCM/MeOH: 9:1) = 0.3.

^{1}H NMR (300 MHz, MeOD): δ = 3.08-3.06 (m, 2H), 2.63-2.58 (m, 2H), 2.36-2.26 (m, 4H), 1.56-1.50 (m, 6H), 1.34 (s, 18H) ppm.

HRMS-ESI(+): calcd for $C_{17}H_{36}N_3O_4$: 346.2700, found: 346.2702 $[M+H]^+$.

Compound 155d:

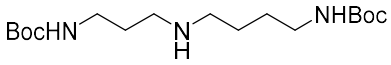

To a strirring solution of spermidine (1 g, 6.88 mmol, 1eq.) in anhydrous THF at 0 °C was added Boc-ON (3.4 g, 13.77 mmol, 2 eq.). After stirring for 4h at 0 °C, the solvent was removed under reduced pressure and the residue was taken up in diethyl ether and washed with saturated aqueous NaOH until the yellow coloration was removed. The organic layers were dried over $MgSO_4$ and concentrated under reduced pressure to give a white solid. Recrystallization from di-isopropyl ether gave **115d** (982 mg, 40%) as a white crystalline solid.

White solid, (40%). R_f (Cyclohexane/EtOAc: 5:5) = 0.40.

^{1}H NMR (300 MHz, MeOD): δ = 5.15 (s, 1H), 4.83 (s, 1H), 3.20 (m, 4H), 2.65 (m, 4H), 1.69 (m, 2H), 1.53 (m, 4H), 1.43 (s, 18H) ppm.

^{13}C NMR (90 MHz, MeOD): δ = 156.1, 78.7, 49.9, 40.3, 30.0, 28.8, 27.8 ppm.

HRMS-ESI(+): calcd for $C_{17}H_{36}N_3O_4$: 346.2700, found: 346.2695 $[M+H]^+$.

Compound 155e:

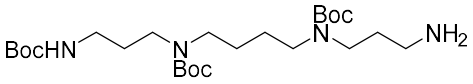

Spermine (1.51 g, 7.5 mmol) was dissolved in DCM at 0°C. Ethyltrifluoroacetate (7.5 mmol) was added dropwise and the mixture was stirred for 1h. After evaporation of the solvent, the crude residue is taken in THF, NEt_3 (3eq.) and Boc_2O (3eq.) were added and the mixture was stirred for 3h. After evaporation, the trifluoroacetyl protecting group was removed with Cs_2CO_3 in MeOH/H_2O: 8:2. The solvents were evaporated and the residue treated with di-isopropylether and aqueous solution HCl (0.5 N).The oily insoluble organic material in both aqueous and organic solvent was decanted from a three-layer system. After drying, the compound was obtained as a pale yellow oil. The product was used without further purification.

Yellow oil. (46%). R_f (DCM/MeOH: 9:1) = 0.5.

^{1}H NMR (300 MHz, $CDCl_3$): δ = 3.28-3.25 (m, 2H), 3.18-3.07 (m, 6H), 3.00-2.96 (m, 2H), 2.81 (t, *J* = 7.3 Hz, 2H), 1.84-1.75 (m, 2H), 1.55-1.52 (m, 2H), 1.38-1.34 (m, 4H), 1.33 (s, 27H) ppm.

^{13}C NMR (90 MHz, $CDCl_3$): δ = 156.0, 99.7, 28.6, 28.21, 25.5 ppm.

HRMS-ESI(+): calcd for $C_{25}H_{51}N_4O_6$: 503.3803, found: 503.3796 $[M+H]^+$.

Compound 155f:

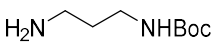

Compound **155f** was obtained using the same procedure as described for compound **155a**.

Colorless oil, (89%). Rf (Cyclohexane/EtOAc: 5/5) = 0.38.

^{1}H NMR (250 MHz, MeOD): δ = 3.20 (q, *J* = 6,3 Hz, 2H), 2.77 (t, *J* = 6,6 Hz, 2H), 1.58 (q, *J* = 6,7 Hz, 2H), 1.45 (s, 9H) ppm.

^{13}C NMR (75 MHz, CD_3OD): δ = 156,2, 79,1, 41,9, 40,6, 31,0, 28,6, 27,6 ppm.

HRMS-ESI(+): calcd for $C_8H_{19}N_2O_2$: 175.1441, found: 175.1449 $[M+H]^+$.

II. Hydroxybenzotriazole compounds.

Synthesis of (benzotriazolyl)oxyacetic acid (164)

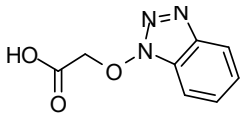

To a solution of hydroxybenzotriazole (5 g, 37 mmol) in ethanol (100 mL), was added 3.48 g of chloroacetic acid (1 eq.) and 3 g of sodium hydroxide (2 eq.). The solution was stirred overnight at 40°C. After evaporation, the residue was dissolved in water and washed with ether. Then the aqueous layer was acidified with 1N HCl and the precipitate was collected and washed with water to give **164**.

White powder, (62%). m.p. 169.5°C (170.5-171.5 °C litt.).

^{1}H NMR (300 MHz, MeOD): δ= 8.01-7.81 (m, 2H), 7.61 (t, *J*= 7.5 Hz, 1H), 7.47 (t, *J*= 7.5 Hz, 1H), 5.28 (s, 2H) ppm.

HRMS-ESI(+): calcd for $C_8H_7N_3O_3$: 194.0417, found: 194.0414 $[M+H]^+$.

General procedure for synthesis of compounds 165a-e:

To a solution of carboxylic acid **164** in DCM/DMF (1:1) was added successively the protected polyamine (0.5 mmol, 1 eq.), BOP reagent (0.5 mmol, 1 eq.) followed by the addition of triethylamine (2 mmol, 4 eq.). The mixture was stirred overnight at room temperature, the solvent was then evaporated under reduced pressure and the residue was taken up with brine and ethyl acetate. The organic phase was separated and washed successively with 5% aq. citric acid, 5% aq. $NaHCO_3$ and water, dried over Na_2SO_4, and evaporated. Purification was carried out by column chromatography (Cyclohexane/Ethyl Acetate).

Compound 165f:

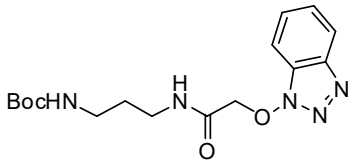

Column chromatography (Cyclohexane/Ethyl Acetate 5:5); Light-colored oil (20%).

^{1}H NMR (300 MHz, $CDCl_3$): δ= 8.00 (d, J= 8.0 Hz, 1H), 7.73 (d, J= 8.0 Hz, 1H), 7.65 (s, 1H), 7.58 (t, J= 7.5 Hz, 1H), 7.43 (t, J= 7.5 Hz, 1H), 5.00 (s, 2H), 3.47 (q, J= 6.3 Hz, 2H), 3.23 (q, J= 6.3 Hz, 2H), 1.78-1.68 (m, 2H), 1.44 (s, 9H) ppm.

^{13}C NMR (90 MHz, $CDCl_3$): δ= 165.9, 156.7, 128.6, 125.2, 120.2, 110.2, 79.8, 77.9, 36.1, 29.9, 24.2 ppm.

HRMS-ESI(+): calcd for $C_{16}H_{23}N_5O_4$: 372.1642, found: 372.1631 $[M+Na]^+$.

Compound 165a

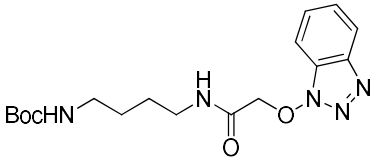

Column chromatography (Cyclohexane/Ethyl Acetate 5:5); Light-colored oil (54%).

^{1}H NMR (300 MHz, $CDCl_3$): δ= 8.00 (d, *J*= 7.5 Hz, 1H), 7.60 (t, *J*= 7.5, 1.5 Hz, 1H), 7.55 (d, *J*= 7.5 Hz, 1H), 7.44 (t, *J*= 7.5, 1.5 Hz, 1H), 4.95 (s, 2H), 3.45 (q, *J*= 7.5, 1.5 Hz, 2H), 3.16 (q, *J*=7.5, 1.5 Hz, 2H), 1.59 (m, 4H), 1.43 (s, 9H) ppm.

^{13}C NMR (90 MHz, $CDCl_3$): δ= 164.9, 157.1, 128.8, 124.3, 121.2, 110.8, 79.7, 79.1, 39.1, 28.4, 26.5 ppm.

HRMS-ESI(+): calcd for $C_{17}H_{25}N_5O_4$: 386.1799, found: 386.1789 $[M+Na]^+$.

Compound 165b:

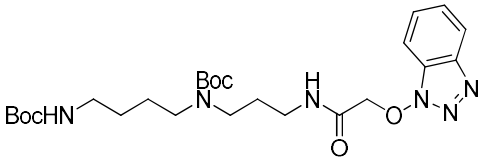

Column chromatography (Cyclohexane/Ethyl Acetate 5:5); Light-colored oil (10%).

^{1}H NMR (300 MHz, $CDCl_3$): δ= 7.98 (d, *J*= 8.0 Hz, 1H), 7.88 (d, *J*= 8.0 Hz, 1H), 7.53 (t, *J*= 7.5 Hz, 1H), 7.38 (t, *J*= 7.5 Hz, 1H), 5.32 (s, 2H), 3.15-2.88 (m, 6H), 1.85-1.82 (m, 2H), 1.48-1.40 (m, 6H), 1.43 (s, 18H) ppm.

^{13}C NMR (90 MHz, $CDCl_3$): δ= 165.2, 153.5, 128.2, 124.7, 119.8, 110.3, 79.3, 78.7, 39.6, 36.9, 28.4, 26.2 ppm.

HRMS-ESI(+): calcd for $C_{25}H_{40}N_6O_6$: 543.2902, found: 543.2880 $[M+Na]^+$.

Compound 165c:

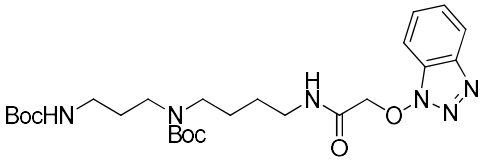

Column chromatography (Cyclohexane/Ethyl Acetate 5:5); Light-colored oil (21%).

^{1}H NMR (300 MHz, $CDCl_3$): δ= 8.00 (d, *J*= 8.0 Hz, 1H), 7.84 (d, *J*= 8.0 Hz, 1H), 7.63 (t, *J*= 7.5 Hz, 1H), 7.48 (t, *J*= 7.5 Hz, 1H), 5.08 (s, 2H), 3.19-3.16 (m, 6H), 3.05-2.99 (m, 2H), 1.69-1.66 (m, 2H), 1.44-1.42 (m, 22H) ppm.

^{13}C NMR (90 MHz, $CDCl_3$): δ= 168.4, 157.4, 128.5, 125.3, 118.9, 109.2, 79.7, 78.7 36.8, 27.3, 25.1 ppm.

HRMS-ESI(+): calcd for $C_{25}H_{40}N_6O_6$: 543.2902, found: 543.2874 $[M+Na]^+$.

Compound 165d:

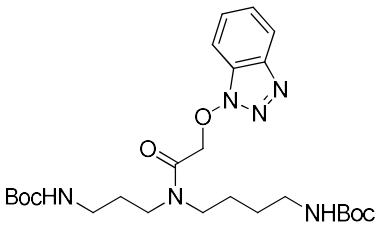

Column chromatography (Cyclohexane/Ethyl Acetate 3:7); Light-colored oil (17%).

^{1}H NMR (300 MHz, $CDCl_3$): δ= 7.94 (d, *J*= 8.0 Hz, 1H), 7.80 (d, *J*= 8.0 Hz, 1H), 7.49 (t, *J*= 7.5 Hz, 1H), 7.34 (t, *J*= 7.5 Hz, 1H), 4.04 (s, 2H), 3.32-3.28 (m, 4H), 3.15-3.07 (m, 4H), 1.68-1.66 (m, 6H), 1.39 (s, 18H) ppm.

^{13}C NMR (90 MHz, $CDCl_3$): δ= 169.4, 156.4, 128.2, 124.8, 119.7, 110.0, 79.6, 78.8, 32.4, 28.1, 27.6, 24.5 ppm.

HRMS-ESI(+): calcd for $C_{25}H_{40}N_6O_6$: 543.2902, found: 543.2925 $[M+Na]^+$.

Compound 165e:

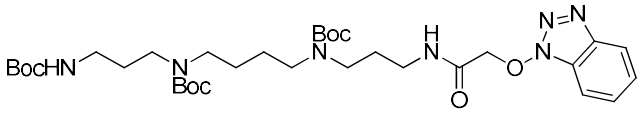

Column chromatography (Cyclohexane/Ethyl Acetate 4:6); Light-colored oil (92%).

^{1}H NMR (300 MHz, $CDCl_3$): δ= 8.02 (d, *J*= 8.0 Hz, 1H), 7.77 (d, *J*= 8.0 Hz, 1H), 7.53 (t, *J*= 7.5 Hz, 1H), 7.40 (t, *J*= 7.5 Hz, 1H), 5.00 (s, 2H), 3.25-3.23 (m, 2H), 3.13-3.10 (m, 8H), 1.89-1.87 (m, 2H), 1.68-1.66 (m, 8H), 1.42 (s, 27H) ppm.

^{13}C NMR (90 MHz, $CDCl_3$): δ= 165.6, 156.6, 156.3, 155.6, 143.6, 128.5, 125.1, 109.2, 79.9, 77.9, 47.0, 44.3, 43.8, 43.4, 37.8, 37.4, 35.7, 29.8, 28.6, 27.8, 26.1, 26.0 ppm.

HRMS-ESI(+): calcd for $C_{33}H_{55}N_7O_8$: 678.4112, found: 678.4078 $[M+H]^+$.

General procedure for synthesis of compounds 166a-e:

Boc-protected polyamines were deprotected using an excess of 4M HCl in dioxane. The mixture was stirred overnight at room temperature and the solvent was removed under reduced pressure to afford the final product as pure hydrochloride salt.

Compound 166f:

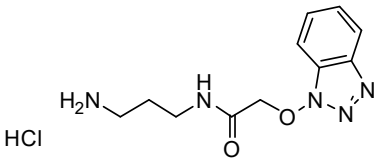

Light-colored solid (quantitative yield).

^{1}H NMR (300 MHz, D_2O): δ= 7.89 (d, *J*= 7.9 Hz, 1H), 7.74 (d, *J*= 7.9 Hz, 1H), 7.57 (t, *J*= 7.5 Hz, 1H), 7.45 (t, *J*= 7.5 Hz, 1H), 5.03 (s, 2H), 3.26-3.24 (m, 2H), 2.88-2.85 (m, 2H), 1.79-1.76 (m, 2H) ppm.

^{13}C NMR (90 MHz, D_2O): δ= 170.3, 131.3, 130.8, 128.3, 127.6, 120.6, 114.3, 110.9, 79.1, 46.8, 37.7, 28.0 ppm.

HRMS-ESI(+): calcd for $C_{11}H_{15}N_5O_2$: 250.1291, found: 249.1294 $[M+H]^+$.

Compound 166a:

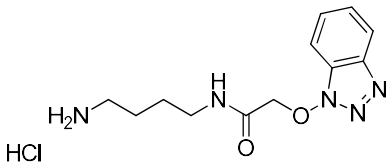

Light-colored solid (72%).

^{1}H NMR (300 MHz, D_2O): δ= 8.00 (d, *J*= 7.5 Hz, 1H), 7.60 (t, *J*= 7.5, 1.5 Hz, 1H), 7.55 (d, *J*= 7.5 Hz, 1H), 7.44 (t, *J*= 7.5, 1.5 Hz, 1H), 4.94 (s, 2H), 3.11-3.07 (m, 2H), 2.79-2.66 (m, 2H), 1.48-1.39 (m, 4H) ppm.

^{13}C NMR (90 MHz, D_2O); δ= 165.5, 126.8, 123.6, 117.5, 109.8, 75.8, 46.6, 37.4, 24.4 ppm.

HRMS-ESI(+): calcd for $C_{12}H_{17}N_5O_2$: 264.1455, found: 264.1445 $[M+H]^+$.

Compound 165b:

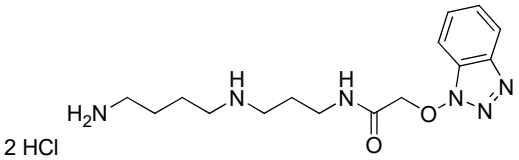

Light-colored solid (50%).

^{1}H NMR (300 MHz, D_2O): δ= 7.82 (d, *J*= 7.9 Hz, 1H), 7.77 (d, *J*= 7.9 Hz, 1H), 7.69 (t, *J*= 7.5 Hz, 1H), 7.58 (t, *J*= 7.5 Hz, 1H), 4.31 (s, 1H), 4.12 (s, 1H), 3.09-3.02 (m, 8H), 2.10-2.01 (m, 2H), 1.76-1.73 (m, 4H) ppm.

^{13}C NMR (90 MHz, D_2O): δ= 172.0, 130.9, 127.4, 113.5, 78.5 39.4, 24.5 ppm.

HRMS-ESI(+): calcd for $C_{15}H_{24}N_6O_2$: 321.2034, found: 321.2031 $[M+H]^+$.

Compound 166c:

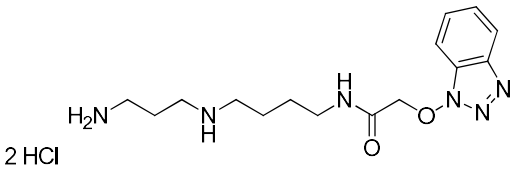

Light-colored solid (quantitative yield).

^{1}H NMR (300 MHz, D_2O): δ= 7.90 (d, *J*= 7.9 Hz, 1H), 7.75 (d, *J*= 7.9 Hz, 1H), 7.66 (t, *J*= 7.5 Hz, 1H), 7.43 (t, *J*= 7.5 Hz, 1H), 5.02 (s, 1H), 4.04 (s, 1H), 3.19-3.06 (m, 2H), 3.04-2.94 (m, 6H), 2.08-2.02 (m, 2H), 1.75-1.50 (m, 4H) ppm.

^{13}C NMR (90 MHz, D_2O): δ= 168.8, 129.9, 127.3, 119.7, 109.9, 78.5, 44.8, 38.8, 24.3 ppm.

HRMS-ESI(+): calcd for $C_{15}H_{24}N_6O_2$: 321.2034, found: 321.2026 $[M+H]^+$.

Compound 166d:

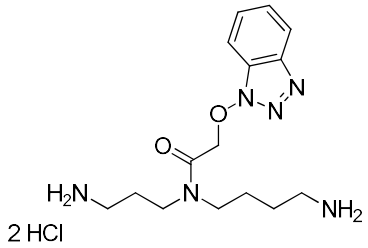

Light-colored solid (quantitative yield).

^{1}H NMR (300 MHz, D_2O): δ= 7.92 (d, *J*= 7.9 Hz, 1H), 7.85 (d, *J*= 7.9 Hz, 1H), 7.57 (t, *J*= 7.5 Hz, 1H), 7.42 (t, *J*= 7.5 Hz, 1H), 4.22 (s, 2H), 3.43-3.49 (m, 4H), 2.98-2.93 (m, 4H), 1.95-1.92 (m, 2H), 1.71-1.60 (m, 4H) ppm.

^{13}C NMR (90 MHz, D_2O): δ= 158.3, 130.9, 127.5, 120,2, 110.2, 78.3, 45.6, 37.2, 24.3 ppm.

HRMS-ESI(+): calcd for $C_{15}H_{24}N_6O_2$: 321.2034, found: 321.2022 $[M+H]^+$.

Compound 166e:

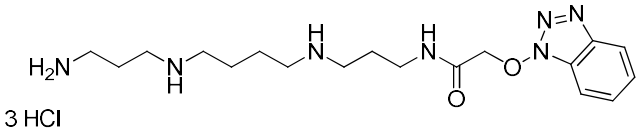

Light-colored oil (quantitative yield).

^{1}H NMR (360 MHz, D_2O): δ= 7.70 (m, 4H), 5.11 (s, 1H), 4.22 (s, 1H), 4.11 (s, 2H), 3.34 (s, 1H), 3.34-3.30 (m, 2H), 3.15-3.05 (m, 4H), 2.08-2.04 (m, 4H), 2.01-1.90 (m, 2H), 1.88-1.75 (m, 8H) ppm.

^{13}C NMR (90 MHz, D_2O): δ= 169.6, 130.2, 127.5, 119.9, 110.3, 78.3, 46.9, 46.8, 44.9, 44.5, 36.5, 36.0, 25.3, 23.7, 22.7 ppm.

HRMS-ESI(+): calcd for $C_{18}H_{31}N_7O_2$: 378.2612, found: 378.2599 $[M+H]^+$.

III. Benzyl compounds.

General procedure for the synthesis of the aminoalcohols 169a-g:

A mixture of the corresponding benzyl chloride/bromide (2.1 eq.), 3-aminopropanol (1.0 eq.) and K_2CO_3 (5.0 eq.) in acetone, dichloromethane or dimethylformamide was stirred at room temperature. After completion of the reaction (12-16 h) monitored by TLC, the reaction mixture was filtered and the filtrate was concentrated under reduced pressure. The residue was purified by silica gel chromatography to afford the corresponding aminoalcohol.

Compound 169a:

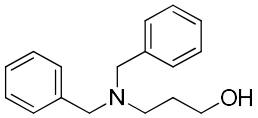

Conditions: Benzylbromide in acetone.

Yellow oil, (70%). R_f (Cyclohexane/EtOAc, 8:2) = 0.26.

^{1}H NMR (300 MHz, MeOD): δ= 7.35-7.21 (m, 10H), 3.56-3.53 (m, 6H), 2.55 (t, J = 6.5 Hz, 2H), 1.76 (m, 2H) ppm.

^{13}C NMR (90 MHz, D_2O): δ= 138.1, 128.9, 128.2, 63.4, 58.3, 52.7, 27.9 ppm.

HRMS-ESI(+): calcd for $C_{17}H_{21}NO$: 255.1623, found: 255.1629 $[M+H]^+$.

Compound 169b:

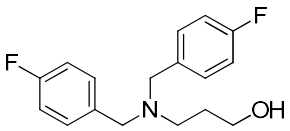

Conditions: 4-Fluorobenzyl chloride in acetone.

Yellow oil (32%). R_f (Cyclohexane/EtOAc, 8:2) = 0.32.

^{1}H NMR (300 MHz, $CDCl_3$): δ= 7.28 (td, J = 6.5, 5.6 Hz, 4H), 7.04 (t, J = 8.7 Hz, 4H), 4.46 (s, 1H), 3.65 (t, J = 6.5 Hz, 2H), 3.54 (s, 4H), 2.64 (t, J = 6.5 Hz, 2H), 1.81-1.74 (m, 2H), 1.62 (s, 1H).

^{13}C NMR (90 MHz, $CDCl_3$): δ= 163.75, 160.49, 133.84, 130.69, 130.59, 115.48, 115.20, 63.77, 57.74, 52.97, 29.70, 28.06 ppm.

HRMS-ESI(+): calcd for $C_{17}H_{20}F_2NO$: 292.1507, found: 292.1516 $[M+H]^+$.

Compound 169c:

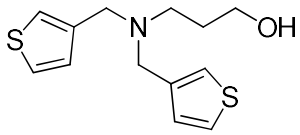

Conditions: 3-(bromomethyl)thiophene in DCM.

White solid. (74%) R_f (Cyclohexane/EtOAc, 1:1) = 0.43.

^{1}H NMR (300 MHz, $CDCl_3$): δ= 7.29 (dd, *J* = 4.9, 3.0 Hz, 2H), 7.14 (dd, *J* = 3.0, 0.8 Hz, 2H), 7.06 (dd, *J* = 4.9, 0.8 Hz, 2H), 5.06 (br s, 1H), 3.70 (d, *J* = 5.2 Hz, 2H), 3.61 (s, 4H), 2.65 (d, *J* = 5.8 Hz, 2H), 1.76 (dt, *J* = 10.8, 5.5 Hz, 2H) ppm.

^{13}C NMR (75 MHz, $CDCl_3$): δ =138.9, 128.3, 126.0, 123.2, 64.2, 53.5, 53.0, 28.0 ppm.

HRMS-ESI(+): calcd for $C_{13}H_{18}NOS_2$: 268.0824, found: 268.0815 $[M+H]^+$.

Compound 169d:

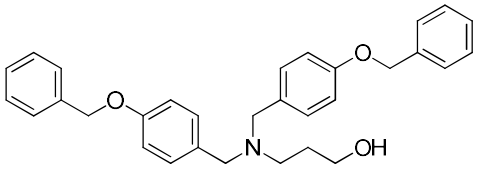

Conditions: 4-benzyloxy(benzyl) chloride in DMF.

White solid. (47%) R_f (Cyclohexane/EtOAc, 1:1) = 0.51.

^{1}H NMR (300 MHz, $CDCl_3$): δ= 7.46-7.38 (m, 10H), 7.27 (d, *J* = 8.6 Hz, 4H), 6.97 (d, *J* = 8.6 Hz, 4H), 5.08 (s, 4H), 3.67 (m, 2H), 3.54 (s, 4H), 2.67 (m, 2H), 1.81 (m, 2H), 1.63 (s, 1H) ppm.

^{13}C NMR (75 MHz, $CDCl_3$): δ = 158.1, 137.0, 130.4, 128.6, 127.9, 127.5, 114.8, 77.5, 77.0, 76.5, 70.0, 57.7, 27.8 ppm.

HRMS-ESI(+): calcd for $C_{31}H_{34}NO_3$: 468.2533, found: 468.2513 $[M+H]^+$.

Compound 169e:

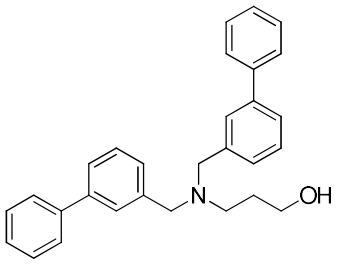

Conditions: 3-phenylbenzyl bromide in DMF.

White solid. (78%) R_f (Cyclohexane/EtOAc, 6:4) = 0.54.

^{1}H NMR (300 MHz, $CDCl_3$): δ= 7.64-7.60 (m, 8H), 7.46-7.38 (m, 10H), 4.70 (s, 1H), 3.72 (s, 4H), 2.76 (m, 2H), 1.85 (m, 2H), 1.61 (m, 2H) ppm.

^{13}C NMR (75 MHz, $CDCl_3$): δ = 144.7, 140.6, 138.9, 130.1, 128.8, 127.9, 128.1, 128.0, 127.5, 125.3, 60.2, 59.4, 53.8, 28.8 ppm.

HRMS-ESI(+): calcd for $C_{29}H_{30}NO$: 408.2322, found: 408.2313 $[M+H]^+$.

Compound 169f:

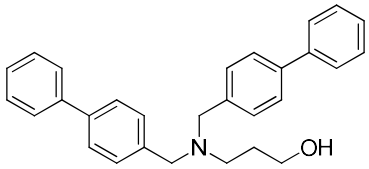

Conditions: 4-phenylbenzyl bromide in DMF.

White solid. (58%) R_f (Cyclohexane/EtOAc, 65:35) = 0.55.

^{1}H NMR (300 MHz, $CDCl_3$): δ= 7.63 - 7.54 (m, 8H), 7.50 - 7.29 (m, 10H), 4.70 (br s, 1H), 3.73 (t, *J* = 5.3 Hz, 2H), 3.67 (s, 4H), 2.72 (t, *J* = 5.7 Hz, 2H), 1.83 (tt, *J* = 5.7, 5.3 Hz, 2H) ppm.

^{13}C NMR (75 MHz, $CDCl_3$): δ = 141.0, 140.3, 137.49, 129.7, 128.9, 127.3, 127.2, 64.1, 58.5, 53.5, 28.2 ppm.

HRMS-ESI(+): calcd for $C_{29}H_{30}NO$: 408.2322, found: 408.2309 $[M+H]^+$.

Compound 169g:

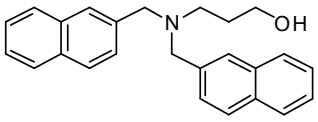

Conditions: 2-(bromomethyl)naphthalene in DCM.

White solid. (86%) R_f (Cyclohexane/EtOAc, 65:35) = 0.46.

^{1}H NMR (300 MHz, $CDCl_3$): δ = 7.91 – 7.75 (m, 8H), 7.56 – 7.46 (m, 6H), 4.68 (br s, 1H), 3.79 (s, 4H), 3.67 (t, *J* = 5.3 Hz, 2H), 2.74 (t, *J* = 5.8 Hz, 2H), 1.83 (tt, *J* = 5.8, 5.3 Hz, 2H) ppm.

^{13}C NMR (75 MHz, $CDCl_3$): δ = 136.0, 133.4, 132.9, 128.4, 128.2, 127.8, 127.2, 126.2, 125.9, 63.9, 59.0, 53.3, 28.3 ppm.

HRMS-ESI(+): calcd for $C_{25}H_{26}NO$: 356.2009, found: 356.2000 $[M+H]^+$.

General procedure for the synthesis of the methanosulfonates 170a-g:

Methanesulfonyl chloride (2.0 eq.) in DCM (0.22 M) was cooled at 0 °C using an ice bath. A mixture of the corresponding aminoalcohol (1.0 eq.), di-isopropylethylamine (5.0 eq.) and DMAP (10 mol%) in DCM (0.44 M) was added dropwise under stirring. The reaction mixture was stirred at low temperature for 5 min and then, at rt for 16 h. Then, the dark red-brown reaction mixture was poured into a mixture of ice-water and DCM and the organic layer was separated. The aqueous phase was extracted with DCM three times. The combined organic layers were washed with water and brine, dried with $MgSO_4$ anhydride and evaporated to give the intermediate mesylate product as pale yellow gummy solid. The product was used without further purification.

Compound 170a:

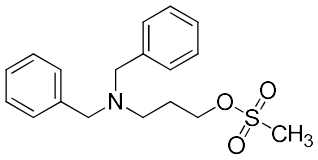

R_f (Cyclohexane/EtOAc, 8:2) = 0.28.

^{1}H NMR (300 MHz, $CDCl_3$): δ = 7.35-7.32 (m, 10H), 4.24 (t, 2H, *J* = 6.5 Hz), 3.55 (s, 4H), 2.82 (s, 3H), 2.55 (t, 2H, *J* = 6.5 Hz), 1.92 (cq, 2H, *J* = 6.5 Hz) ppm.

^{13}C NMR (75 MHz, $CDCl_3$): δ = 138.6, 128.8, 127.4, 126.7, 67.6, 61.0, 52.8, 37.6, 26.7 ppm.

Compound 170b:

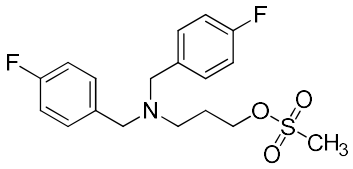

R_f (Cyclohexane/EtOAc, 8:2) = 0.33.

^{1}H NMR (300 MHz, $CDCl_3$): δ = 7.29 (td, J = 6.5, 5.6 Hz, 4H), 7.02 (t, J = 8.7 Hz, 4H), 4.26 (t, *J* = 6.5 Hz, 2H), 3.52 (s, 4H), 2.89 (s, 3H), 2.54 (t, *J* = 6.5 Hz, 2H), 1.91 (cq, *J* = 6.5 Hz, 2H) ppm.

^{13}C NMR (75 MHz, $CDCl_3$): δ = 163.66, 160.41, 130.29, 115.34, 115.06, 67.82, 57.60, 52.54, 49.15, 37.30, 31.53, 26.91 ppm.

HRMS-ESI(+): calcd for $C_{18}H_{22}F_2NO_3S$: 370.1283, found: 370.1312 $[M+H]^+$.

Compound 170c:

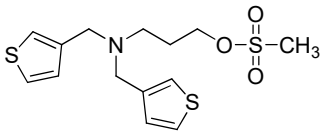

R_f (Cyclohexane/EtOAc, 1:1) = 0.62.

^{1}H NMR (300 MHz, $CDCl_3$): δ = 7.35 - 7.25 (m, 2H), 7.17 - 7.11 (m, 2H), 7.09 - 7.04 (m, 2H), 4.27 (t, *J* = 6.4 Hz, 2H), 3.60 (s, 4H), 2.92 (s, 3H), 2.56 (t, *J* = 6.6 Hz, 2H), 1.91 (p, *J* = 6.6, 6.4 Hz, 2H) ppm.

^{13}C NMR (75 MHz, $CDCl_3$): δ = 140.2, 128.4, 125.8, 122.6, 68.2, 53.3, 49.4, 37.4, 27.3 ppm.

HRMS-ESI(+): calcd for $C_{14}H_{20}NO_3S_3$: 346.0600, found: 346.0582 $[M+H]^+$.

Compound 170d:

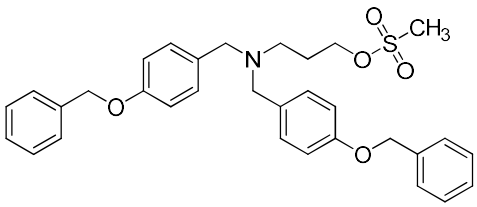

R_f (Cyclohexane/EtOAc, 6:4) = 0.73.

^{1}H NMR (300 MHz, $CDCl_3$): δ = 7.47-7.38 (m, 10H), 7.36-7.23 (m, 4H), 6.96-6.93 (m, 4H), 5.07 (s, 4H), 4.24 (t, *J* = 6.4 Hz, 2H), 3.49 (s, 4H), 2.82 (s, 3H), 2.53 (m, 2H), 1.92-1.90 (m, 2H) ppm.

^{13}C NMR (75 MHz, $CDCl_3$): δ = 158.3, 137.4, 131.2, 129.6, 125.7, 122.6, 69.9, 61.5, 54.0, 38.4, 26.0 ppm.

HRMS-ESI(+): calcd for $C_{32}H_{36}NO_5S$: 546.2236, found: 546.2208 $[M+H]^+$.

Compound 170e:

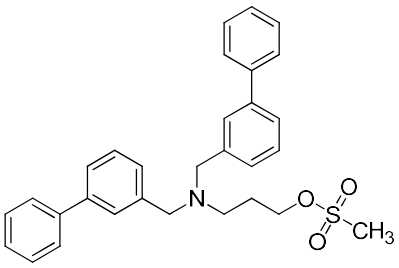

R_f (Cyclohexane/EtOAc, 6:4) = 0.77.

^{1}H NMR (300 MHz, $CDCl_3$): δ= 7.78-7.44 (m, 18H), 4.89 (s, 4H), 4.69-4.66 (m, 2H), 4.28 (m, 2H), 3.67 (s, 3H), 2.67-2.61 (m, 2H) ppm.

^{13}C NMR (75 MHz, $CDCl_3$): δ = 154.8, 141.4, 137.1, 132.3, 129.8, 126.7, 125.0, 124.8, 124.5, 123.9, 64.2, 62.1, 52.0, 37.6, 27.9 ppm.

HRMS-ESI(+): calcd for $C_{30}H_{32}NO_3S$: 486.2091, found: 486.2065 $[M+H]^+$.

Compound 170f:

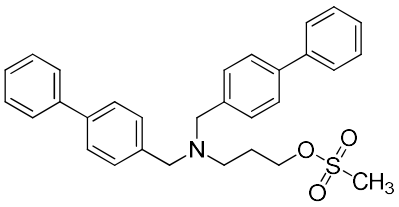

R_f (Cyclohexane/EtOAc, 65:35) = 0.42.

^{1}H NMR (300 MHz, $CDCl_3$): δ = 7.65 - 7.54 (m, 8H), 7.51-7.41 (m, 8H), 7.39-7.30 (m, 2H), 4.30 (t, J = 6.4 Hz), 3.65 (s, 4H), 2.82 (s, 3H), 2.63 (t, J = 6.5 Hz, 2H), 1.97 (tt, J = 6.5, 6.4 Hz, 2H) ppm.

^{13}C NMR (75 MHz, $CDCl_3$): δ = 141.0, 140.1, 138.5, 129.4, 128.9, 127.3, 127.2, 127.1, 68.2, 58.4, 49.5, 37.3, 27.2 ppm.

HRMS-ESI(+): calcd for $C_{30}H_{32}NO_3S$: 486.2097, found: 486.2077 $[M+H]^+$.

Compound 170g:

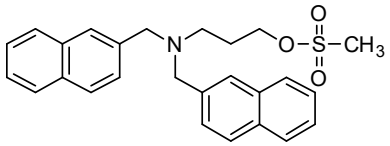

R_f (Cyclohexane/EtOAc, 65:35) = 0.50.

^{1}H NMR (300 MHz, $CDCl_3$): δ = 7.89 - 7.72 (m, 8H), 7.54 (dd, J = 8.5, 1.5 Hz, 2H), 7.50 - 7.44 (m, 4H), 4.24 (t, J = 6.4 Hz, 2H), 3.76 (s, 4H), 2.65 (t, J = 6.6 Hz, 2H), 2.61 (s, 3H), 1.95 (tt, J = 6.6, 6.4 Hz, 2H) ppm.

^{13}C NMR (75 MHz, $CDCl_3$): δ = 137.0, 133.5, 132.9, 128.2, 127.8, 127.7, 127.3, 126.2, 125.8, 68.1, 59.1, 49.5, 37.1, 27.3 ppm.

HRMS-ESI(+): calcd for $C_{26}H_{28}NO_3S$: 434.1784, found: 434.1776 $[M+H]^+$.

General procedure for the synthesis of the *N*HBoc amines 171a-g, 173a, 173b:

To a solution of the corresponding methanosulfonate (**170a-g**) (1.0 eq.) and di-isopropylethylamine (2.0 eq.) in ACN (0.2 M) at rt, the (1.5 eq.) was added dissolved in the minimum amount of ACN. The reaction mixture was stirred at 60 °C overnight. After evaporation of the solvent at reduced pressure, the residue was dissolved in water and DCM and the organic layer was separated. The aqueous phase was extracted with DCM three times.

The combined organic layers were washed with water and brine, dried with $MgSO_4$ anhydride and evaporated. The crude product was purified by silica gel chromatography to afford the corresponding Boc-protected compounds. For compounds **171a** and **171b** the first fraction of purification was isolated, concentrated and characterized to afford compounds **173a** and **173b**.

Compound 171a:

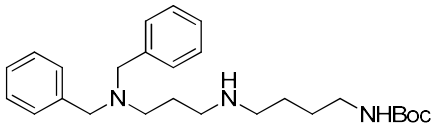

Yellow oil. (37% in two steps)R_f (EtOAc/MeOH, 9:1) = 0.06.

^{1}H NMR (300 MHz, $CDCl_3$): δ = 7.34-7.24 (m, 10H), 5.18 (s, 1H), 3.54 (s, 4H), 3.09 (s, 2H), 2.63 (t, 2H, J = 6.5 Hz), 2.49 - 2.44 (m, 4H), 1.78 - 7.72 (m, 2H), 1-57 - 1.53 (m, 4H), 1.45 (s, 9H) ppm.

^{13}C NMR (75 MHz, $CDCl_3$): δ = 128.9, 128.8, 128.2, 128.19, 126.9, 126.8, 77.4, 77.4, 77.0, 76.9, 76.7, 76.5, 58.5, 58.4, 51.4, 49.1, 48.0, 28.5, 28.4 ppm.

HRMS-ESI(+): calcd for $C_{26}H_{40}NO_2$: 426.3115, found: 426.3126 $[M+H]^+$.

Compound 173a:

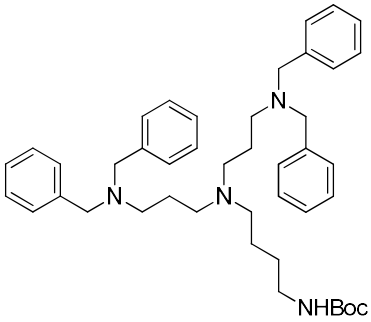

Yellow oil. (16% in two steps). R_f (EtOAc/MeOH 9:1) = 0.68.

^{1}H NMR (300 MHz, $CDCl_3$): δ = 7.43 - 7.27 (m, 20H), 4.98 (s, 1H), 3.60 (s, 8H), 3.11-3.09 (m, 2H), 2.49-2.37 (m, 10H), 1.70-1.64 (m, 4H), 1.51 (s, 9H), 1-42-1.34 (m, 2H) ppm.

HRMS-ESI(+): calcd for $C_{43}H_{59}N_4O_2$: 663.4633, found: 663.4655 $[M+H]^+$.

Compound 171b:

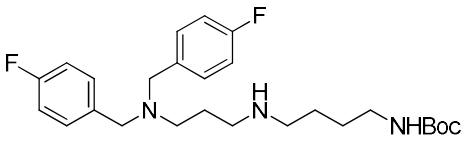

Yellow oil. (12% in two steps). R_f (EtOAc/MeOH, 9:1) = 0.08.

^{1}H NMR (300 MHz, $CDCl_3$): δ = 7.26 (dd, *J* = 8.2, 5.8 Hz, 4H), 7.00 (t, *J* = 8.6 Hz, 4H), 4.98 (s, 1H), 3.48 (s, 4H), 3.10 (d, *J* = 4.8 Hz, 2H), 2.79 - 2.59 (m, 4H), 2.46 (t, *J* = 6.3 Hz, 2H), 1.88 (t, *J* = 6.7 Hz, 2H), 1.63 (d, *J* = 7.0 Hz, 2H), 1.52 (d, *J* = 7.0 Hz, 2H), 1.43 (s, 9H) ppm.

^{13}C NMR (75 MHz, $CDCl_3$): δ = 130.9, 130.3, 129.5, 128.19, 127.7, 126.9, 78.4, 77.6, 77.0, 76.7, 75.9, 59.0, 50.7, 49.8, 47.9, 28.7, 28.3 ppm.

HRMS-ESI(+): calcd for $C_{26}H_{38}F_2N_3O_2$: 462.2927, found: 462.2926 $[M+H]^+$.

Compound 173b:

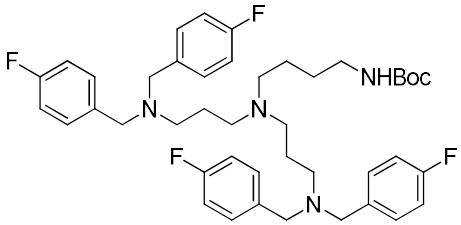

Yellow oil. (13% in two steps). R_f (Cyclohexane/EtOAc 5:5) = 0.55.

^{1}H NMR (300 MHz, $CDCl_3$): δ = 7.28 (dd, *J* = 8.4, 5.7 Hz, 8H), 6.99 (t, *J* = 8.7 Hz, 8H), 4.85 (s, 1H), 3.48 (s, 8H), 3.08 (m, 2H) , 2.35 (m, 10H), 1.57 (m, 4H), 1.45 (s, 9H), 1.37 (m, 4H) ppm.

^{13}C NMR (75 MHz, $CDCl_3$): δ = 163.21, 160.51, 155.99, 135.34, 135.30, 130.13, 130.05, 115.09, 114.86, 77.38, 77.02, 76.67, 57.52, 53.73, 51.97, 51.69, 40.53, 28.44, 28.07, 24.60, 24.40, 14.20 ppm.

HRMS-ESI(+): calcd for $C_{43}H_{55}F_4N_4O_2$: 735.4256, found: 735.4354 $[M+H]^+$.

Compound 171c:

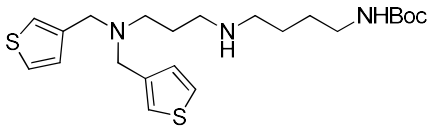

Yellow oil. (29% in two steps) R_f (EtOAc/MeOH 9:1) = 0.20.

^{1}H NMR (360 MHz, $CDCl_3$): δ = 7.28 (dd, J = 4.3, 3.1 Hz, 2H), 7.12 - 7.10 (m, 2H), 7.07 - 7.04 (m, 2H), 4.98 (br s, 1H), 3.57 (s, 4H), 3.20 - 3.03 (m, 2H), 2.61 (t, J = 6.8 Hz, 2H), 2.54 (t, J = 6.7 Hz, 2H), 2.46 (t, J = 6.7 Hz, 2H), 1.70 (p, J = 6.6 Hz, 2H), 1.53-1.42 (m, 13H) ppm.

^{13}C NMR (90 MHz, $CDCl_3$): δ = 156.2, 140.6, 128.4, 125.5, 122.3, 53.1, 51.4, 49.7, 48.2, 40.6, 28.6, 28.1, 27.7, 27.2.

HRMS-ESI(+): calcd for $C_{22}H_{36}N_3O_2S_2$: 438.2243, found: 438.2242 $[M+H]^+$.

Compound 171d:

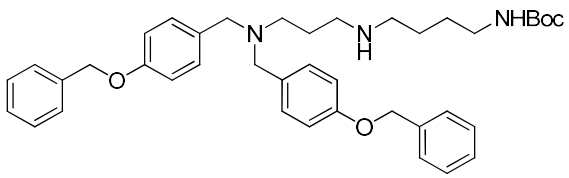

Yellow oil. (14% in two steps) R_f (EtOAc/MeOH 9:1) = 0.13.

^{1}H NMR (300 MHz, $CDCl_3$): δ = 7.48 - 7.32 (m, 10H), 7.29 - 7.22 (m, 4H), 6.92 (d, J = 8.6 Hz, 4H), 5.04 (s, 4H), 3.48 (s, 4H), 3.07 (s, 2H), 2.38-2.36 (m, 6H), 1.63-1.60 (m, 4H), 1.44 (s, 9H), 1.28-1.24 (m, 2H) ppm.

^{13}C NMR (75 MHz, $CDCl_3$): δ = 157.7, 156.0, 137.2, 132.1, 129.9, 128.5, 127.9, 127.5, 114.5, 70.0, 57.5, 28.4 ppm.

HRMS-ESI(+): calcd for $C_{40}H_{52}N_3O_4$: 638.3952, found: 638.3921 $[M+H]^+$.

Compound 171e:

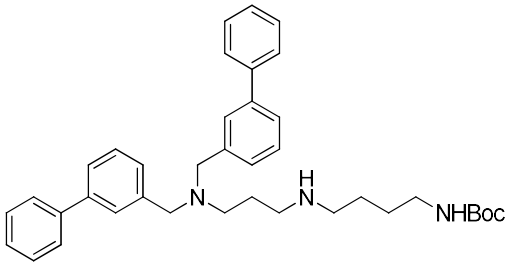

Yellow oil. (40% in two steps) R_f (EtOAc/MeOH 8:2) = 0.24.

^{1}H NMR (300 MHz, $CDCl_3$): δ = 7.69-7.23 (m, 18H), 4.75 (s, 1H), 3.63 (s, 4H), 2.95 (s, 2H), 2.58-2.20 (m, 6H), 1.76-1.70 (m, 4H), 1.44 (s, 9H), 1.37-1.23 (m, 2H) ppm.

^{13}C NMR (75 MHz, $CDCl_3$): δ = 181.3, 155.7, 141.2, 141.0, 140.3, 128.7, 128.6, 127.7, 127.5, 127.2, 127.1, 125.6, 58.4, 51.8, 28.4, 26.8 ppm.

HRMS-ESI(+): calcd for $C_{38}H_{48}N_3O_2$: 578.3741, found: 578.3731 $[M+H]^+$.

Compound 171f:

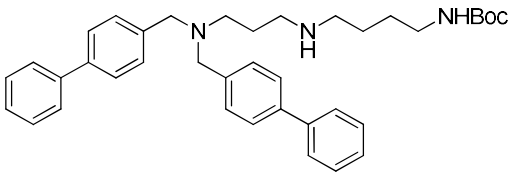

Yellow oil. (34% in two steps) R_f (EtOAc/MeOH 9:1) = 0.23.

^{1}H NMR (300 MHz, MeOD-d_4): δ = 7.66 - 7.53 (m, J = 7.5, 5.6 Hz, 8H), 7.48 - 7.36 (m, J = 8.4 Hz, 8H), 7.35 - 7.26 (m, J = 7.3 Hz, 2H), 3.58 (s, 4H), 3.04-2.88 (m, 2H), 2.60-2.39 (m, 6H), 1.78 - 1.66 (m, 2H), 1.50 - 1.32 (m, 13H) ppm.

^{13}C NMR (75 MHz, MeOD-d_4): δ = 160.7, 142.2, 141.3, 140.0, 130.7, 129.9, 128.3, 127.9, 59.2, 52.5, 50.3, 48.8, 41.1, 28.8, 27.8, 27.3 ppm.

HRMS-ESI(+): calcd for $C_{38}H_{48}N_3O_2$: 578.3741, found: 578.3733 $[M+H]^+$.

Compound 171g:

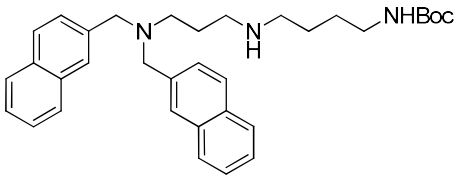

Yellow oil. (25% in two steps) R_f (EtOAc/MeOH 9:1) = 0.18.

^{1}H NMR (360 MHz, $CDCl_3$): δ = 7.86 - 7.74 (m, 8H), 7.58 - 7.51 (m, 2H), 7.51 - 7.40 (m, 4H), 4.84 (br s, 1H), 3.73 (s, 4H), 3.07 - 2.95 (m, 2H), 2.63 - 2.50 (m, 4H), 2.43 (t, J = 6.9 Hz, 2H), 1.75 (p, J = 6.5 Hz, 2H), 1.44 (s, 9H), 1.40 - 1.28 (m, 4H) ppm.

^{13}C NMR (90 MHz, $CDCl_3$): δ = 156.1, 137.5, 133.5, 132.9, 128.0, 127.8, 127.6, 127.4, 126.1, 125.7, 58.9, 51.4, 49.6, 48.0, 40.6, 28.6, 27.9, 27.5, 27.1 ppm.

HRMS-ESI(+): calcd for $C_{34}H_{44}N_3O_2$: 526.3428, found: 526.3422 $[M+H]^+$.

Compound 177a:

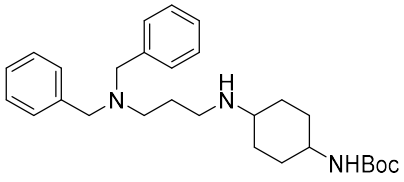

Yellowish solid, (41%). R_f (EtOAc/MeOH 9:1) = 0.19.

^{1}H NMR (250 MHz, $CDCl_3$): δ = 7.46 -7.16 (m, 10H), 4.35 (s, 1H), 3.55 (s, 4H), 3.38 (s, 1H), 2.62 (t, *J* = 6.8 Hz, 2H), 2.47 (t, *J* = 6.6 Hz, 2H), 2.28 (s, 1H), 1.99-1.95 (m, 4H), 1.85-1.81 (m, 4H), 1.71-16.8 (m, 2H), 1.44 (s, 9H) ppm.

^{13}C NMR (63 MHz, $CDCl_3$): δ = 173.3, 171.5, 139.7, 128.8, 128.2, 126.8, 95.6, 58.4, 55.6, 51.3, 45.0, 34.5, 32.2, 32.1, 31.9, 28.4, 27.1 ppm.

HRMS-ESI(+): calcd for $C_{28}H_{41}N_3O_2$: 452.3199, found: 452.3297 $[M+H]^+$.

Compound 177b:

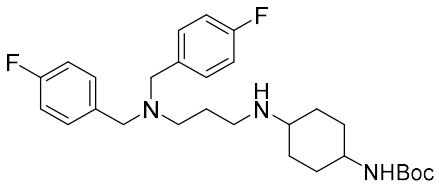

Yellow oil. (29%) R_f (EtOAc/MeOH 8:2) = 0.09.

^{1}H NMR (250 MHz, $CDCl_3$): δ = 7.11 - 7.08 (m, 4H), 6.87 - 6.81 (m, 4H), 4.21 - 4.20 (m, 1H), 3.31 (s, 2H), 3.25 (s, 1H), 2.28 (t, *J* = 6.9 Hz, 2H), 2.28 (t, *J* = 6.2 Hz, 2H), 1.74 - 1.62 (m, 6H), 1.28 (s, 9H), 1.14 - 1.10 (m, 4H) ppm.

^{13}C NMR (70 MHz, $CDCl_3$): δ = 163.9, 160.0, 155.1, 134.9, 134.9, 130.4, 130.3, 115.2, 114.9, 79.3, 57.5, 56.0, 51.1, 49.0, 44.6, 31.7, 30.4, 28.4, 25.9 ppm.

HRMS-ESI(+): calcd for $C_{28}H_{40}F_2N_3O_2$: 488.3083, found: 488.3080 $[M+H]^+$.

Compound 179b:

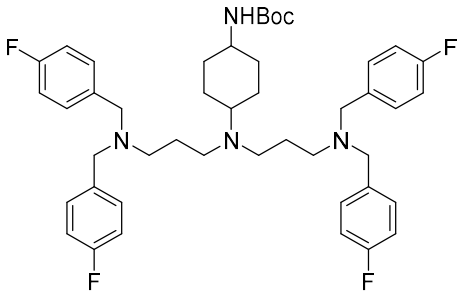

Yellow oil. (25% in two steps). R_f (Cyclohexane/EtOAc 5:5) = 0.22.

^{1}H NMR (250 MHz, $CDCl_3$): δ = 7.29 (m, 8H), 7.00 (m, 8H), 4.38 (m, 1H), 3.48 (s, 8H), 3.33 (m, 1H), 2.37 (m, 6H), 2.01 (m, 4H), 1.67 (m, 6H), 1.47 (s, 9H), 1.28 (m, 4H) ppm.

^{13}C NMR (63 MHz, $CDCl_3$): δ = 163.8, 159.9, 155.2, 135.3, 130.2, 130.1, 115.2, 114.8, 77.5, 77.0, 76.5, 57.6, 51.6, 48.7, 32.9, 28.4, 27.0, 26.5 ppm.

HRMS-ESI(+): calcd for $C_{45}H_{57}F_4N_4O_2$: 761.4448, found: 761.4440 $[M+H]^+$.

<u>General procedure for synthesis of compounds 172a, 174a-b,178h-i and 180i:</u>

Boc-protected polyamines were deprotected using an excess of 4M HCl in dioxane. The mixture was stirred overnight at room temperature and the solvent was removed under reduced pressure to afford the final product as pure hydrochloride salt.

Compound 172a:

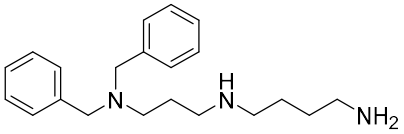

Yellowish solid, (quantitative yield).

^{1}H NMR (300 MHz, MeOD): δ = 7.67 - 7.58 (m, 10H), 3.55 (s, 4H), 2.80 - 2.76 (m, 6H), 1.76 - 1.59 (m, 6H), 1.42 - 1.37 (m, 2H) ppm.

^{13}C NMR (90 MHz, MeOD): δ = 139.2, 138.7, 128.7, 128.5, 128.5, 127.3, 126.9, 59.1, 58.5, 52.4, 49.7, 48.4, 40.8, 31.14, 27.3, 27.0 ppm.

HRMS-ESI(+): calcd for $C_{21}H_{32}N_3$: 326.2591, found: 326.2611 $[M+H]^+$.

Compound 174a:

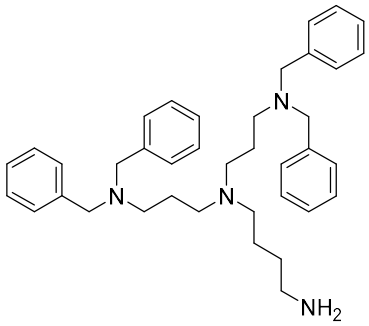

Yellowish solid. (quantitative yield).

^{1}H NMR (300 MHz, MeOD): δ = 7.76 - 7.71 (m, 20H), 3.59 (s, 8H), 2.91-2.88 (m, 8H), 1.65 - 1.52 (m, 10H), 1.36 - 1.29 (m, 2H) ppm.

^{13}C NMR (75 MHz, MeOD): δ = 140.2, 139.8, 138.2, 138.2, 129.0, 129.0, 128.8, 128.7, 126.3, 60.5, 59.5, 58.5, 55.3, 53.09, 52.9, 40.2, 31.3, 25.0, 24.2 ppm.

HRMS-ESI(+): calcd for $C_{38}H_{51}N_4$: 563.4108, found: 563.4121 $[M+H]^+$.

Compound 172b:

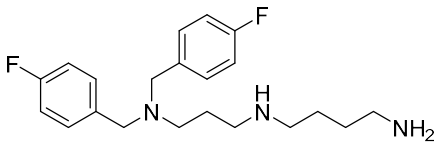

Yellowish solid. (quantitative yield).

^{1}H NMR (300 MHz, MeOD): δ = 7.70 - 7.66 (m, 4H), 7.24 (t, J = 8.4 Hz, 4H), 4.46 (s, 4H), 3.36-3.30 (m, 2H), 3.07 - 3.01 (m, 6H), 2.35 - 2.33 (m, 2H), 1.83 - 1.80 (m, 4H) ppm.

^{13}C NMR (75 MHz, MeOD): δ = 165.3, 162.0, 133.6, 133.5, 125.2, 125.1, 116.0, 115.8, 56.2, 49.3, 44.5, 38.6, 24.1, 22.8, 20.6 ppm.

HRMS-ESI(+): calcd for $C_{21}H_{30}F_2N_3$: 362.2402, found: 362.2391 $[M+H]^+$.

Compound 174b:

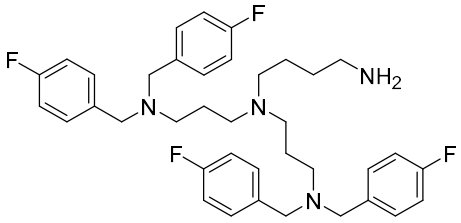

Yellowish solid. (quantitative yield).

^{1}H NMR (300 MHz, MeOD): δ = 7.50 - 7.47 (m, 8H), 7.26 - 7.23 (m, 8H), 4.43 (s, 8H), 3.19 - 3.09 (m, 12H), 2.18 - 2.13 (m, 4H), 1.75 - 1.70 (m, 4H) ppm.

^{13}C NMR (75 MHz, MeOD): δ = 165.1, 161.8, 133.4, 133.2, 124.8, 124.8, 116.5, 116.2, 66.5, 57.0, 52.4, 49.7, 49.1, 38.7, 23.8, 20.5, 18.9 ppm.

HRMS-ESI(+): calcd for $C_{38}H_{47}F_4N_4$: 635.3731, found: 635.3742 $[M+H]^+$.

Compound 172c:

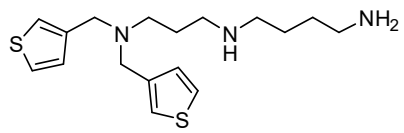

Yellowish solid. (quantitative yield).

^{1}H NMR (360 MHz, MeOD): δ = 7.88 - 7.80 (m, 2H), 7.64 - 7.57 (m, 2H), 7.35 (d, J = 4.5 Hz, 2H), 4.45 (s, 4H), 3.24 - 3.13 (m, 2H), 3.13 - 2.93 (m, 6H), 2.39 - 2.24 (m, 2H), 1.91 - 1.71 (m, 4H) ppm.

^{13}C NMR (90 MHz, MeOD): δ = 130.8, 130.5, 130.2, 128.9, 52.4, 50.3, 48.2, 45.8, 40.0, 25.5, 24.2, 22.0 ppm.

HRMS-ESI(+): calcd for $C_{17}H_{28}N_3S_2$: 338.1719; found: 338.1713 $[M+H]^+$.

Compound 172d:

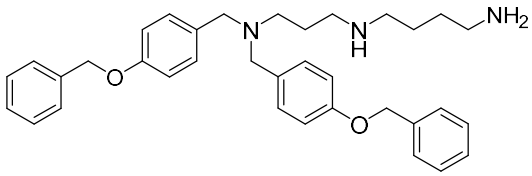

Yellowish solid, (quantitative yield).

^{1}H NMR (300 MHz, MeOD): δ = 7.45 - 7.33 (m, 14H), 7.11 - 7.08 (m, 4H), 5.14 (s, 4H), 4.35 (s, 4H), 3.04 - 2.72 (m, 6H), 2.41 - 2.38 (m, 4H), 1.83 - 1.78 (m, 4H) ppm.

^{13}C NMR (75 MHz, MeOD): δ = 162.3, 139.5, 133.7, 130.7, 129.7, 125.7, 117.8, 117.6, 72.2, 72.2, 59.3, 57.0, 44.9, 19.9, 18.4, 14.3 ppm.

HRMS-ESI(+): calcd for $C_{35}H_{44}N_3O_2$: 538.3428, found: 538.3417 $[M+H]^+$.

Compound 172e:

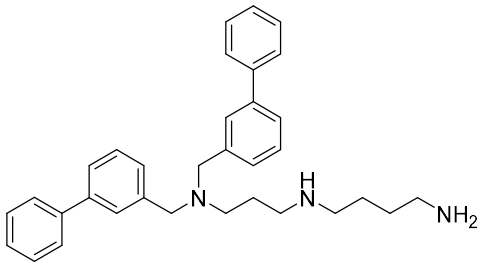

Yellowish solid, (quantitative yield).

^{1}H NMR (300 MHz, MeOD): δ = 7.68 - 7.34 (m, 18H), 4.62 (s, 4H), 3.36 - 3.32 (m, 4H), 2.98 - 2.87 (m, 2H), 2.56 - 2.53 (m, 4H), 1.86 - 1.74 (m, 4H) ppm.

^{13}C NMR (75 MHz, MeOD): δ = 142.1, 139.7, 129.8, 129.5, 128.6, 128.2, 127.5, 126.8, 66.7, 57.5, 52.7, 50.6, 49.6, 38.6, 24.1, 20.7, 19.0 ppm.

HRMS-ESI(+): calcd for $C_{33}H_{40}N_3$: 478.3217, found: 478.3179 $[M+H]^+$.

Compound 172f:

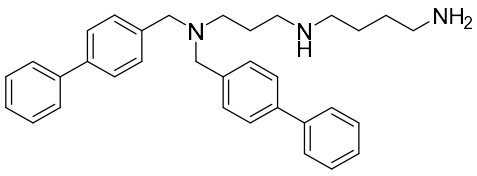

White-yellowish solid, (quantitative yield).

^{1}H NMR (360 MHz, MeOD): δ = 7.81-7.51 (m, 12H), 7.48-7.23 (m, 6H), 4.48 (s, 4H), 3.29-3.21 (m, 2H), 3.13-2.87 (m, 6H), 2.56-2.30 (m, 2H), 1.96-1.65 (m, 4H) ppm.

^{13}C NMR (90 MHz, MeOD): δ = 144.0, 140.1, 133.1, 130.0, 129.3, 129.0, 128.8, 128.0, 58.16, 50.8, 48.3, 45.9, 40.0, 25.5, 24.2, 22.0 ppm.

HRMS-ESI(+): calcd for $C_{33}H_{40}N_3$: 478.3217, found: 478.93 $[M+H]^+$.

Compound 172g:

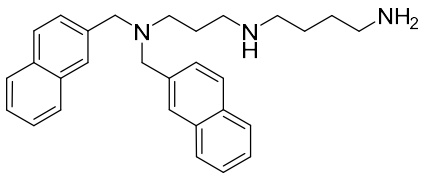

Yellowish solid, (quantitative yield).

^{1}H NMR (300 MHz, MeOD): δ = 8.15 - 8.09 (m, 2H), 8.01 - 7.85 (m, 6H), 7.68 (d, J = 7.8 Hz, 2H), 7.61 - 7.50 (m, 4H), 4.66 (s, 4H), 3.43 - 3.21 (m, 2H), 3.16 - 2.90 (m, 6H), 2.51 - 2.33 (m, 2H), 1.94 - 1.66 (m, 4H) ppm.

^{13}C NMR (75 MHz, MeOD): δ = 135.2, 134.6, 132.8, 130.4, 129.4, 128.8, 128.6, 128.0, 127.8, 58.9, 51.1, 48.3, 45.9, 40.0, 25.5, 24.2, 22.1 ppm.

HRMS-ESI(+): calcd for $C_{29}H_{36}N_3$: 426.2888, found: 426.2904 $[M+H]^+$.

Compound 178a:

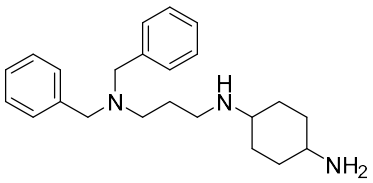

Yellowish solid, (quantitative yield).

^{1}H NMR (300 MHz, MeOD): δ = 7.60 - 7.58 (m, 4H), 7.53 - 7.51 (m, 6H), 4.45 (s, 4H), 3.28 - 3.25 (m, 2H), 3.01 - 2.99 (m, 2H), 2.31 - 2.26 (m, 2H), 2.19 - 2.16 (m, 2H), 1.53 - 1.49 (m, 2H) ppm.

^{13}C NMR (75 MHz, MeOD): δ = 139.3, 129.1, 129.1, 128.9, 127.9, 127.5, 126.5, 59.0, 58.1, 53.3, 50.51, 49.7, 33.2, 30.6, 27.3 ppm.

HRMS-ESI(+): calcd for $C_{23}H_{34}N_3$: 352.2747, found: 352.2641 $[M+H]^+$.

Compound 178b:

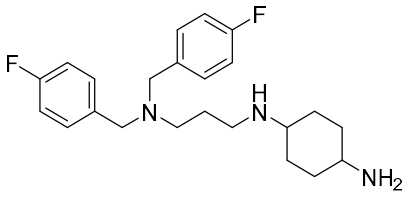

Yellowish solid, (quantitative yield).

^{1}H NMR (300 MHz, MeOD): δ = 7.75 - 7.72 (m, 4H), 7.29 - 7.25 (m, 4H), 5.01 (s, 4H), 4.55 - 4.49 (m, 3H), 3.28 - 3.25 (m, 1H), 3.15 - 3.13 (m, 2H), 2.31 - 2.24 (m, 6H), 1.62 - 1.57 (m, 4H) ppm.

^{13}C NMR (75 MHz, MeOD): δ = 165.3, 162.0, 138.5, 133.7, 133.6, 125.2, 125.2, 116.0, 115.7, 106.9, 56.2, 55.2, 41.7, 38.9, 28.0, 26.5, 20.7 ppm.

HRMS-ESI(+): calcd for $C_{23}H_{32}F_2N_3$: 388.2559, found: 388.2547 $[M+H]^+$.

Compound 180b:

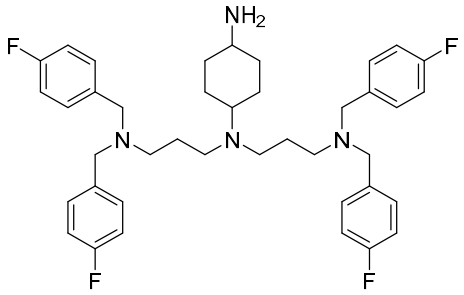

Yellowish solid, (quantitative yield).

^{1}H NMR (300 MHz, MeOD): δ = 7.69 (dd, J = 8.7, 5.2 Hz, 8H), 7.25 (t, J = 8.7 Hz, 8H), 4.51 (s, 1H), 4.47 (s, 8H), 3.27 (m, 6H), 2.53 (m, 4H), 2.22 (m, 4H), 1.74 (m, 4H), 1.31 (m, 2H) ppm.

^{13}C NMR (75 MHz, MeOD): δ = 135.2, 134.6, 132.8, 130.4, 129.4, 128.8, 128.6, 128.0, 127.8, 58.9, 51.1, 48.3, 45.9, 40.0, 25.5, 24.2, 22.1 ppm.

HRMS-ESI(+): calcd for $C_{40}H_{49}F_4N_4$: 661.3815, found: 661.3877 $[M+H]^+$.

IV. Nitrobenzoxadiazole

N-methyl-4-amino-7-nitrobenzofurazan (186):

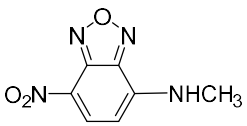

To 200 mg (1 mmol, 1 eq.) of 4-chloro-7-nitrobenzofurazan dissolved in 6 mL methanol was added 101 mg (1.5 mmol, 1.5 eq.) of methylamine hydrochloride. The reaction mixture was refluxed at 75°C under N_2 for 2h. Then 400 mg (4.8 mmol, 5 eq.) of sodium hydrogen carbonate dissolved in 6 mL of distilled water was added dropwise. After stirring overnight and cooling, red crystal of the desired compound precipitated. Red solids were filtered and washed with methanol.

Red crystal powder, (61%). R_f (Cyclohexane/EtOAc 5:5) = 0.42.

^{1}H NMR (300 MHz, DMSO): δ = 9.52 (s, 1H), 8.53 (d, J = 8.8Hz, 1H), 6.31 (d, J = 8.9Hz, 1H), 3.39 (s, 3H) ppm.

HRMS-ESI(+): calcd for $C_7H_7N_4O_3$: 195.0555, found: 195.0559 $[M+H]^+$.

Compound 187a:

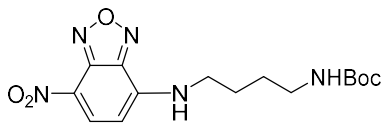

To 941 mg (5 mmol, 1 eq.) of mono-protected 1,4-butane diamine dissolved in 25 mL of acetonitrile was added 1.2 g (5 mmol,1 eq.) of cesium carbonate and 1 g (5 mmol, 1 eq.) of 4-chloro-7-nitrobenzofurazan. The mixture was refluxed at 80°C for 30 min. Solvant was removed under pressure. The product was extracted with DCM. The organic layer was washed with brine, dried over $MgSO_4$ and evaporated. Solids were recrystallized from di-isopropyl ether. Orange powder, (50%). R_f (Cyclohexane/EtOAc 3:7) = 0.74.

^{1}H NMR (300 MHz, $CDCl_3$): δ = 9.54 (s, 1H), 8.52 (d, J = 8.8Hz, 1H), 6.81 (s, 1H), 6.42 (d, J = 8.8Hz, 1H), 3.45 (m, 2H), 2.96 (m, 2H), 1.67 (m, 2H), 1.49 (m, 2H), 1.35 (s, 9H) ppm.

HRMS-ESI(+): calcd for $C_{15}H_{22}N_5O_5$: 352.1610, found: 352.1615 $[M+H]^+$.

General procedure for the preparation of compounds spermidine/spermine NBD-BOC 187a-c and 187e:

The Boc-protected compound (1 eq.) was dissolved in acetonitrile, cesium carbonate (1 eq.) and 4-chloro-7-nitrobenzofurazane (1 eq.) was added. The mixture was stirred for 30 min at 80°C.

Extraction with DCM was followed by drying over $MgSO_4$ and evaporation. The Boc-NBD intermediate was purified by column chromatography (EtOAc/Cyclohexane 5:5).

Compound 187b:

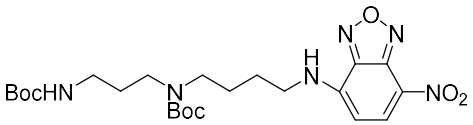

Orange oil, (54%). R_f (Cyclohexane/EtOAc 5:5) = 0.60.

^{1}H NMR (250 MHz, $CDCl_3$): δ = 8.07 (d, J = 8.7Hz, 1H) , 7.57 (s, 1H, NH), 6.88 (d, J = 8.7Hz, 1H), 3.13 (m, 2H), 2.99 (m, 2H), 2.74 (m, 4H), 1.56 (m, 2H), 1.33 (s, 1H, NH), 1.09 (m, 22H) ppm.

^{13}C NMR (90 MHz, $CDCl_3$): δ = 173.3, 173.2, 152.1, 139.2, 135.9, 131.1, 124.7, 114.0, 79.8, 79.7, 34.9, 34.3, 31.4, 30.3, 29.6, 28.4, 28.4, 25.9, 22.6, 14.0 ppm.

HRMS-ESI(+): calcd for $C_{23}H_{37}N_6O_7$: 509.2718, found: 509.2703 $[M+H]^+$.

Compound 187c:

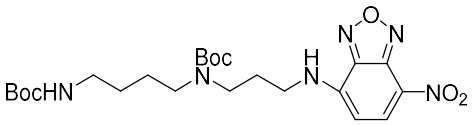

Orange oil, (29%). R_f (Cyclohexane/EtOAc 5:5) = 0.60.

^{1}H NMR (250 MHz, $CDCl_3$): δ = 8.76 (d, J = 8.7Hz, 1H), 6.47 (d, J = 8.7Hz, 1H), 4.24 (m, 2H), 2.90 (m, 2H), 2.62 (m, 4H), 1.69 (m, 6H), 1.31 (s, 18H) ppm.

^{13}C NMR (63 MHz, $CDCl_3$): δ = 175.6, 175.4, 155.5, 140.2, 138.8, 132.3, 125.7, 114.4, 79.7, 77.5, 35.4, 34.2, 33.8, 31.8, 31.4, 30.3, 29.8, 28.4, 28.3, 25.8, 23.2, 14.1 ppm.

HRMS-ESI(+): calcd for $C_{23}H_{37}N_6O_7$: 509.2718, found: 509.2726 $[M+H]^+$.

Compound 187e:

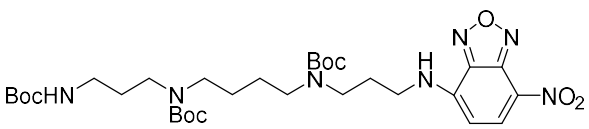

Yellow oil, (80%). R_f (Cyclohexane/EtOAc 5:5) = 0.3.

^{1}H NMR (300 MHz, $CDCl_3$): δ = 8.51 (d, *J* = 8.7Hz, 1H), 7.96 (s, 1H, NH), 6.20 (d, *J* = 8.7Hz, 1H), 3.55 (m, 2H), 3.40 (m 2H), 3.22-3.12 (m, 8H), 1.93 (m, 2H), 1.68 (m, 2H), 1.50 (m, 4H), 1.45 (s, 27H) ppm.

^{13}C NMR (75 MHz, $CDCl_3$): δ = 156.0, 155.2 151.8, 144.1, 143.9, 136.4, 126.2, 80.3, 80.0, 79.6, 38.7, 38.5, 31.7, 29.7, 28.4, 28.4, 22.7, 14.1 ppm.

HRMS-ESI(+): calcd for $C_{31}H_{52}N_7O_9$: 666.3821, found: 666.3826 $[M+H]^+$.

General procedure for the preparation/deprotection of compounds spermidine/spermine NBD 188a-c and 188e:

The protected compound was stirred for 3h in a solution of 4M HCl in dioxane. The solvent was removed under reduced pressure. Extraction was carried out with DCM and water, the organic phase was discarded and the hydrochloride salt compound in aqueous layer was then lyophilized.

Compound 188a:

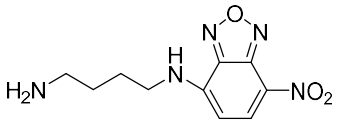

Orange powder, (quantitative yield).

^{1}H NMR (250 MHz, D_2O): δ = 8.50 (d, *J* = 9.0Hz, 1H), 6.42 (d, *J* = 9.1Hz, 1H), 3.47 (t, *J* = 4.6Hz, 5.6Hz, 2H), 1.66 - 1.55 (m, 2H), 1.48 - 1.45 (m, 2H) ppm.

HRMS-ESI(+): calcd for $C_{10}H_{14}N_5O_3$: 252.1091, found: 252.1110 $[M+H]^+$.

Compound 188b:

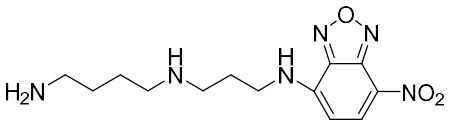

Orange powder, (quantitative yield).

^{1}H NMR (250 MHz, D_2O): δ = 8.26 (d, *J* = 9.0Hz, 1H), 6.22 (d, , *J* = 9.0Hz, 1H), 3.94 (t, *J* =4.6Hz, 5.6Hz, 2H), 3.62 (s, 2H, NH_2), 3.48 (t, *J* =4.6Hz, 5.6Hz, 2H), 3.20 – 3.18 (m, 6H), 2.13 – 2.10 (m, 2H), 1.78 - 1.74 (m, 2H) ppm.

^{13}C NMR (300 MHz, D_2O): δ = 155.89, 155.50, 152.78, 150.60, 132.03, 131.59, 58.90, 57.04, 50.68, 48.44, 36.35, 35.78, 34.62 ppm.

HRMS-ESI(+): calcd for $C_{13}H_{21}N_6O_3$: 309.1670, found: 309.1667 $[M+H]^+$.

Compound 188c:

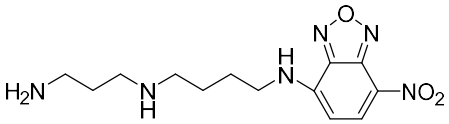

Orange powder, (quantitative yield).

^{1}H NMR (360 MHz, D_2O): δ = 8.51 (d, *J* = 9.0Hz, 1H), 6.38 (d, *J* = 9.0Hz, 1H), 3.67 - 3.65 (m, 2H), 3.13 – 3.11 (m, 6H), 2.13 - 2.10 (m, 2H), 1.91 - 1.88 (m, 4H) ppm.

^{13}C NMR (360 MHz, D_2O): δ = 170.4, 158.1, 136.9, 120.9, 102.8, 99.9, 48.0, 47.6, 47.3, 37.0, 28.1, 26.2, 23.3 ppm.

HRMS-ESI(+): calcd for $C_{13}H_{21}N_6O_3$: 309.1670, found: 309.1661 $[M+H]^+$.

Compound 188e:

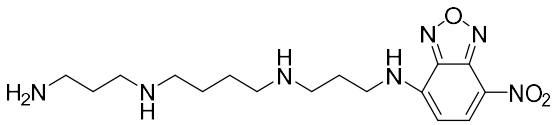

Orange powder, (quantitative yield).

^{1}H NMR (250 MHz, D_2O): δ = 7.74 (d, *J* = 9.0Hz, 1H), 7.54 (d, *J* = 9.0Hz, 1H), 4.24 - 4.19 (m, 2H), 2.90 - 2.84 (m, 2H), 2.62 -2.57 (m, 4H), 1.69 - 1.52(m, 6H), 1.31 (s, 18H) ppm.

^{13}C NMR (360 MHz, D_2O): δ = 147.4, 146.7, 140.8, 130.4, 133.0, 130.6, 120.4, 49.2, 48.9, 47.1, 46.7, 41.7, 39.6, 39.0, 30.1, 29.5, 29.2, 27.4 ppm.

Biology

I. In vitro evaluation

1. *Leishmania donovani*

Culture of *Leishmania donovani*. MHOM/ET/67/HU3, also called LV9, promastigote forms were grown in M-199 medium supplemented with 40 mM HEPES, 100 mM adenosine, 0.5 $mg.mL^{-1}$ haemin, 10% heat-inactivated fetal bovine serum (FBS) and 50 $mg.mL^{-1}$ gentamycin at 26 °C in a dark environment. Differentiation of promastigotes into axenic amastigotes was achieved by dilution of 1.10^6 promastigotes in 5 ml of axenic amastigote media M-199 (15 mM KCl; 8 mM glucose; 5 mM glutamine, 2.5% BBLTM trypticase™ peptone, 4 mM haemin, and 20% Fetal Bovine Serum). The pH was adjusted to pH 5.5. Axenic amastigotes were grown at 37°C under an atmosphere of 5% CO_2. All the experiments were performed with parasites in their logarithmic phase of growth.

In vitro evaluation of *Leishmania donovani* axenic amastigotes. Amastigote forms were suspended to yield 10^7 $cells.mL^{-1}$. The maximum final compound concentrations used were 100 mM. Triplicates were used for each concentration. Cultures were incubated at 37° C for 72h in the dark and under a 5% CO_2 atmosphere, and then the viability of the amastigotes was assessed. Parasite growth was determined by using SYBR Green I, a dye with marked fluorescence enhancement upon contact with parasite DNA. Parasites were lysed following Direct PCR-Cell Genotyping without DNA isolation protocol (Euromedex, France). 10 µL of lysed parasite solution of each well was added to 40 µL of PCR-Cell reagent containing the SYBR green I in a qPCR plate of 96 wells, and the contents were mixed. Fluorescence was measured with Mastercycler ep realplex (Eppendorf, France). Fluorescence obtained was compared to those from the range obtained with different parasite densities. The antileishmanial activity was expressed as IC_{50} in µM (concentration of drug inhibiting 50% of the parasite growth, comparatively to the controls treated with the excipient only). Miltefosine was used as reference compound.

In vitro evaluation on intramacrophage amastigotes. The mouse monocyte/macrophage cell line RAW 264.7 was maintained in DMEM supplemented with 10% heat-inactivated fetal bovine serum. RAW 264.7 cells were seeded into a 96-well microtiter plate at a density of 5.10^3 cells/well in 100 µl of DMEM. After incubation in a 5% CO_2 incubator at 37°C for 24 h, the culture medium was replaced with 100 mL of fresh DMEM containing a suspension of amastigote forms of 10^6 cells.mL^{-1}. After incubation in a 5% CO_2 incubator at 37 °C for 24 h the culture medium was replaced with 100 µL of fresh DMEM containing the test compounds for a new incubation of 48 h. The viability of the amastigotes into macrophages was then assessed using the SYBR Green I (Invitrogen, France) incorporation method. Fluorescence obtained was compared to those from the range obtained with parasite, infected cell and non-infected cell densities. Results were expressed as IC_{50}. Miltefosine was used as reference compound.

2. *Leishmannia mexicana*

Promastigotes of *L. mexicana* (MNYC/BZ/62/M379) were grown in vitro at 25°C in HOMEM medium, pH 7.4, supplemented with 10% (v:v) heat-inactivated fetal calf serum. Amastigotes of *L. mexicana* (MNYC/BZ/62/M379) were grown at 32°C in Schneider's Drosophila Medium (Gibco), pH 5.5, supplemented with 20% (v:v) heat-inactivated fetal calf serum and gentamicin sulphate at 25 $mg.ml^{-1}$.

3. *Trypanosmosa brucei*

Culture of *Trypanosoma brucei gambiense* and in vitro trypanocidal evaluation: Strain FéoITMAP/1893 was grown in a medium constituted of prepacked Iscove's modified Dulbecco's medium (Gibco, BRL) supplemented with 36 mM $NaHCO_3$, 1 mM hypoxanthine, 0.05 mM bathocuproine, 0.16 mM thymidine, 0.2 mM 2-mercaptoethanol, 1.5 mM L-cysteine, 10 % heat-inactivated foetal bovine serum, 100 IU penicillin and 100 $\mu g.mL^{-1}$ streptomycin. Two fold serial dilutions of the compounds were performed in 100 µL of the same medium in 96-well microplates. Trypanosomes were then added to each well at 4.10^4/ml in 200 µL final volume. After 72 h of incubation at 37 °C with 5% CO_2 in the dark, 20 µL of 450 µM resazurin in aqueous solution was added to each well and further incubated for 6 h at 37 °C with 5% CO_2. In living

cells, resazurin is reduced in resofurin. This conversion is monitored by measuring the absorbance at specific wavelengths of resofurin (570 nm) and resazurin (600 nm) using a microplate reader (Labsystems Multiskan MS, McLean, USA). In this evaluation, the activity was expressed in IC_{50} (concentration inhibiting the parasite growth by 50%) and the reference drug used was pentamidine di-isethionate.

4. Cytotoxicity assays

The mouse monocyte/macrophage cell line RAW264.7 was cultured in DMEM supplemented with 10% heat-inactivated fetal bovine serum. RAW 264.7 cells were suspended into a 96-well microtiter plate at a density of 5.10^3 cells/well in 100 µL of DMEM. After incubation in a 5% CO_2 incubator at 37 °C for 24 h, the culture medium was replaced with 100 µL of fresh DMEM containing the test compounds. The IC_{50} of the compounds were determined by using the Alamar Blue technics after 72 h incubation.

II. Enzymatic assays

Recombinant *T. brucei* TryR was prepared and assayed as described previously.[171] Stock solutions of the inhibitors were prepared in DMSO. The activity was measured at 25 °C in a total volume of 1 mL of 40 mM Hepes, 1 mM EDTA, pH 7.5 (Assay Buffer*) in the presence of 100 µM NADPH and 5-10 mU TryR containing 5% DMSO. The reaction was started by adding TS_2 and NADPH consumption was followed spectrophotometrically at 340 nm. To determine the percentage of inhibition, the assay contained 100 µM and 40 µM TS_2, respectively, in the absence and presence of a fixed concentration (40 µM) of inhibitor. The type of inhibition was determined by a Lineweaver-Burk plot.

[171] Persch, E.; Bryson, S.; Todoroff, N. K.; Eberle, C.; Thelemann, J.; Dirdjaja, N.; Kaiser, M.; Weber, M.; Derbani, H.; Brun, R.; Schneider, G.; Pai, E. F.; Krauth-Siegel, R. L.; Diederich, F. *ChemMedChem* **2014**, *8*, 1880.

III. Fluorescence experiments

As cells approached confluence, polyamine-NBD probes (100 µM) were added to the media and the cells were incubated from 1h to 20h. Cells were transfered on a microscope slide and viewed under a Zeiss Axiovert 135 inverted microscope by phase contrast microscopy. A FITC filter (Zeiss) was used to observe the fluorescence of compounds with the NBD group. Confocal images were obtained using a Leica TCS4D confocal laser scanning microscope.

IV. Radiolabelled experiments

Leishmania mexicana or *Leishmania donovani* promastigotes were cultivated with appropriate medium as previously described. All the experiments were performed with parasites in their logarithmic phase of growth. Promastigotes were counted using a hemocytometer. All transport assays were performed in triplicate. Three microfuge tubes per condition were prepared. Conditions varied in terms of inhibitor concentration, time of incubation, and whether a putative transport antagonist was added to the transport medium. 500 µL of a 2-butylphtalate/mineral oil (7:1) mixture was added to the bottom of each microfuge tube. Solution of radiolabeled [^{3}H]-spermidine in Assay Buffer* was prepared at a concentration 4x (40 µM) using a mixture between cold spermidine solution and [^{3}H]-spermidine. Inert oil already present in the microfuge tubes was overlayed with 100 µL of that mixture. The number of scintillation vials required should correspond to the number of microfuge tubes used in the transport experiment. Parasites were centrifuged at 1,500 x g for 10-15 min in order to obtain cell pellet. Supernatant was removed and sedimented cells were suspended in 50 mL of Assay Buffer. This washing step was repeated two more times. Then, after the last washing step, the cell pellet was suspended to afford a concentration of 1.10^8 cells/mL in Assay Buffer. Microfuge tubes containing radiolabeled buffer overlaying the inert oil were placed into the rotor of a benchtop microfuge without caps. 100µL of cell suspension were added into the aqueous layer of each tube (Figure 95).

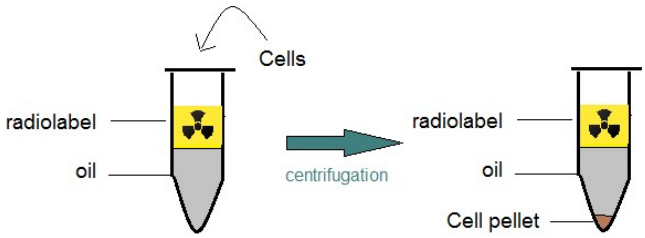

Figure 95: Radiolabeled experiment for the transport.

At fixed intervals, as determined by a timer started at the initiation of the experiment, the cells were sedimented through the inert oil layer at 16000 g for 60 s. This centrifugation step separated the cells from the aqueous layer containing the non-incorporated radiolabeled, this step terminated the transport assay. At the end of each centrifugation steps (60 s), the parasite pellet should be clearly visible at the bottom of the microfuge tube (Figure 95). Without delay, the microfuge tubes were flash frozen with liquid nitrogen. The tip of the frozen microfuge tube containing the cell was cut with a dog nail clipper and dropped into scintillation vial. 200 µL of 2% SDS were added to each scintillation vial to solubilize the cell pellets and this solution was vortexed at maximal speed for 30 min. 3-4 ml of scintillation fluid were added to each vial which were again vortexed at maximum speed overnight. Radiolabel incorporated by parasites was quantified using a liquid scintillation counter. Each sample was counted for 3 min. Additional scintillation vial were prepared in order to assess the number of counts in the radiolabeled transport cocktail (controls).

*Ingredient for 2 L of Assay Buffer: Glucose 5.1 g, HEPES 16 g, MOPS 10 g, $NaHCO_3$ 4 g, KCl 695 mg, $MgCl.6H_2O$ 125 mg, NaCl 11.4 g, $NaH_2PO_42H_2O$ 1.83 g, $CaCl_2.2H_2O$ 81.4 g, $MgSO_4.7H_2O$ 39.8 g.

Bibliography

[1] Povelones, M. L. *Mol. Biochem. Parasitol.* **2014**, *196*, 53–60.

[2] Auty, H.; Morrison, L. J.; Torr, S. J.; Lord, J. *Trends Parasitol.* **2016**, *32*, 608–621

[3] Singh Grewal, A.; Pandita, D.; Bhardwaj, S.; Lather, V. *Curr. Top. Med. Chem.* **2016**, *16*, 2245–2265.

[4] Paucar, R.; Moreno-Viguri, E.; Pérez-Silanes, S. *Curr. Med. Chem.* **2016.**

[5] Van Assche, T.; Deschacht, M.; da Luz, R. A. I.; Maes, L.; Cos, P. *Free Radic. Biol. Med.* **2011**, *51*, 337–351.

[6] Singh, V. P.; Ranjan, A.; Topno, R. K.; Verma, R. B.; Siddique, N. A.; Ravidas, V. N.; Kumar, N.; Pandey, K.; Das, P. *Am. J. Trop. Med. Hyg.* **2010**, *82*, 9–11.

[7] Dujardin, J.-C.; Campino, L.; Cañavate, C.; Dedet, J.-P.; Gradoni, L.; Soteriadou, K.; Mazeris, A.; Ozbel, Y.; Boelaert, M. *Emerg. Infect. Dis.* **2008**, *14*, 1013–1018.

[8] Liévin-Le Moal, V.; Loiseau, P. M. *FEBS J.* **2016**, *283*, 598–607.

[9] D Zilberstein; Shapira, and M. *Annu. Rev. Microbiol.* **1994**, *48*, 449–470.

[10] Hussain, H.; Al-Harrasi, A.; Al-Rawahi, A.; Green, I. R.; Gibbons, S. *Chem. Rev.* **2014**, *114*, 10369–10428.

[11] Metcalf, B. W.; Bey, P.; Danzin, C.; Jung, M. J.; Casara, P.; Vevert, J. P. *J. Am. Chem. Soc.* **1978**, *100*, 2551–2553.

[12] Stijlemans, B.; Caljon, G.; Van Den Abbeele, J.; Van Ginderachter, J. A.; Magez, S.; De Trez, C. *Front. Immunol.* **2016**, *7*, 233.

[13] Medina, N. P.; Mingala, C. N. *Ann. Parasitol.* **2016**, *62*, 11–15.

[14] Merritt, C.; Silva, L. E.; Tanner, A. L.; Stuart, K.; Pollastri, M. P. *Chem. Rev.* **2014**, *114*, 11280–11304.

[15] Lepesheva, G. I.; Waterman, M. R. *Curr. Top. Med. Chem.* **2011**, *11*, 2060–2071.

[16] Chawla, B.; Madhubala, R. *J. Parasit. Dis. Off. Organ Indian Soc. Parasitol.* **2010**, *34*, 1–13.

[17] O'Brien, T. C.; Mackey, Z. B.; Fetter, R. D.; Choe, Y.; O'Donoghue, A. J.; Zhou, M.; Craik, C. S.; Caffrey, C. R.; McKerrow, J. H. *J. Biol. Chem.* **2008**, *283*, 28934–28943.

[18] Hardy, L. W.; Matthews, W.; Nare, B.; Beverley, S. M. *Exp. Parasitol.* **1997**, *87*, 157–169.

[19] Das, B. B.; Ganguly, A.; Majumder, H. K. *Adv. Exp. Med. Biol.* **2008**, *625*, 103–115.

[20] Meshnick, S. R.; Eaton, J. W. *Biochem. Biophys. Res. Commun.* **1981**, *102*, 970–976.

[21] Ghosh, S.; Goswami, S.; Adhya, S. *Biochem. J.* **2003**, *369*, 447–452.

[22] Longoni, S. S.; Sánchez-Moreno, M.; López, J. E. R.; Marín, C. *Comp. Immunol. Microbiol. Infect. Dis.* **2013**, *36*, 499–506.

[23] Birkholtz, L.-M.; Williams, M.; Niemand, J.; Louw, A. I.; Persson, L.; Heby, O. *Biochem. J.* **2011**, *438*, 229–244.

[24] Wallace, H. M.; Fraser, A. V.; Hughes, A. *Biochem. J.* **2003**, *376*, 1–14.

[25] Thomas, T.; Thomas, T. J. *Cell. Mol. Life Sci. CMLS* **2001**, *58*, 244–258.

[26] Seiler, N.; Heby, O. *Acta Biochim. Biophys. Hung.* **1988**, *23*, 1–35.

[27] Heby, O.; Persson, L.; Rentala, M. *Amino Acids* **2007**, *33*, 359–366.

[28] Wang, C. C. *Annu. Rev. Pharmacol. Toxicol.* **1995**, *35*, 93–127.

[29] Bacchi, C. J.; Nathan, H. C.; Hutner, S. H.; McCann, P. P.; Sjoerdsma, A. *Science* **1980**, *210*, 332–334.

[30] Fairlamb, A. H.; Cerami, A. *Annu. Rev. Microbiol.* **1992**, *46*, 695–729.

[31] Menezes, D.; Valentim, C.; Oliveira, M. F.; Vannier-Santos, M. A. *Parasitol. Res.* **2006**, *98*, 99–105.

[32] Vannier-Santos, M. A.; Menezes, D.; Oliveira, M. F.; de Mello, F. G. *Microbiol. Read. Engl.* **2008**, *154*, 3104–3111.

[33] da Costa, C. F.; Coimbra, E. S.; Braga, F. G.; dos Reis, R. C. N.; da Silva, A. D.; de Almeida, M. V. *Biomed. Pharmacother.* **2009**, *63*, 40–42.

[34] Kumar, V. V.; Singh, S. K.; Sharma, (Late) S.; Bhaduri, A. P.; Gupta, S.; Zaidi, A.; Tiwari, S.; Katiyar, J. C. *Bioorg. Med. Chem. Lett.* **1997**, *7*, 675–680.

[35] Pinheiro, A. C.; Rocha, M. N.; Nogueira, P. M.; Nogueira, T. C. M.; Jasmim, L. F.; de Souza, M. V. N.; Soares, R. P. *Diagn. Microbiol. Infect. Dis.* **2011**, *71*, 273–278.

[36] Jagu, E.; Djilali, R.; Pomel, S.; Ramiandrasoa, F.; Pethe, S.; Labruère, R.; Loiseau, P. M.; Blonski, C. *Bioorg. Med. Chem. Lett.* **2015**, *25*, 207–209.

[37] Coimbra, E. S.; Almeida, C. G.; Júnior, W. V.; Dos Reis, R. C. N.; De Almeida, A. C. F.; Forezi, L. S. M.; De Almeida, M. V.; Le Hyaric, M. *ScientificWorldJournal* **2008**, *8*, 752–756.

[38] Labadie, G. R.; Choi, S.-R.; Avery, M. A. *Bioorg. Med. Chem. Lett.* **2004**, *14*, 615–619.

[39] del Olmo, E.; Alves, M.; López, J. L.; Inchaustti, A.; Yaluff, G.; Rojas de Arias, A.; San Feliciano, A. *Bioorg. Med. Chem. Lett.* **2002**, *12*, 659–662.

[40] Jagu, E.; Pomel, S.; Diez-Martinez, A.; Ramiandrasoa, F.; Krauth-Siegel, R. L.; Pethe, S.; Blonski, C.; Labruère, R.; Loiseau, P. M. *Bioorg. Med. Chem.* Accepted.

[41] Lizzi, F.; Veronesi, G.; Belluti, F.; Bergamini, C.; López-Sánchez, A.; Kaiser, M.; Brun, R.; Krauth-Siegel, R. L.; Hall, D. G.; Rivas, L.; Bolognesi, M. L. *J. Med. Chem.* **2012**, *55*, 10490–10500.

[42] Bolognesi, M. L.; Calonghi, N.; Mangano, C.; Masotti, L.; Melchiorre, C. *J. Med. Chem.* **2008**, *51*, 5463–5467.

[43] Richardson, J. L.; Nett, I. R. E.; Jones, D. C.; Abdille, M. H.; Gilbert, I. H.; Fairlamb, A. H. *ChemMedChem* **2009**, *4*, 1333–1340.

[44] O'Sullivan, M. C.; Durham, T. B.; Valdes, H. E.; Dauer, K. L.; Karney, N. J.; Forrestel, A. C.; Bacchi, C. J.; Baker, J. F. *Bioorg. Med. Chem.* **2015**, *23*, 996–1010.

[45] Oliveira, J.; Ralton, L.; Tavares, J.; Codeiro-da-Silva, A.; Bestwick, C. S.; McPherson, A.; Thoo Lin, P. K. *Bioorg. Med. Chem.* **2007**, *15*, 541–545.

[46] Tavares, J.; Ouaissi, A.; Lin, P. K. T.; Tomás, A.; Cordeiro-da-Silva, A. *Int. J. Parasitol.* **2005**, *35*, 637–646.

[47] Lin, P. K.; Pavlov, V. A. *Bioorg. Med. Chem. Lett.* **2000**, *10*, 1609–1612.

[48] Hwang, J. Y.; Kawasuji, T.; Lowes, D. J.; Clark, J. A.; Connelly, M. C.; Zhu, F.; Guiguemde, W. A.; Sigal, M. S.; Wilson, E. B.; DeRisi, J. L.; Guy, R. K. *J. Med. Chem.* **2011**, *54*, 7084–7093.

[49] W, O.; C, S.; J, B.; Jp, G.; R, B. *Trop. Med. Parasitol. Off. Organ Dtsch. Tropenmedizinische Ges. Dtsch. Ges. Tech. Zusammenarbeit GTZ* **1995**, *46*, 49–53.

[50] Bonse, S.; Santelli-Rouvier, C.; Barbe, J.; Krauth-Siegel, R. L. *J. Med. Chem.* **1999**, *42*, 5448–5454.

[51] Moloney, G. P.; Kelly, D. P.; Mack, P. *Molecules* **2001**, *6*, 230–243.

[52] Caffrey, C. R.; Steverding, D.; Swenerton, R. K.; Kelly, B.; Walshe, D.; Debnath, A.; Zhou, Y.-M.; Doyle, P. S.; Fafarman, A. T.; Zorn, J. A.; Land, K. M.; Beauchene, J.; Schreiber, K.; Moll, H.; Ponte-Sucre, A.; Schirmeister, T.; Saravanamuthu, A.; Fairlamb, A. H.; Cohen, F. E.; McKerrow, J. H.; Weisman, J. L.; May, B. C. H. *Antimicrob. Agents Chemother.* **2007**, *51*, 2164–2172.

[53] Meshnick, S. R.; Kitchener, K. R.; Le Trang, N. *Biochem. Pharmacol.* **1985**, *34*, 3147–3152.

[54] Trant, N. L.; Meshnick, S. R.; Kitchener, K.; Eaton, J. W.; Cerami, A. *J. Biol. Chem.* **1983**, *258*, 125–130.

[55] Caminos, A. P.; Panozzo-Zenere, E. A.; Wilkinson, S. R.; Tekwani, B. L.; Labadie, G. R. *Bioorg. Med. Chem. Lett.* **2012**, *22*, 1712–1715.

[56] Krauth-Siegel, R. L.; Comini, M. A. *Biochim. Biophys. Acta* **2008**, *1780*, 1236–1248.

[57] Krieger, S.; Schwarz, W.; Ariyanayagam, M. R.; Fairlamb, A. H.; Krauth-Siegel, R. L.; Clayton, C. *Mol. Microbiol.* **2000**, *35*, 542–552.

[58] Krauth-Siegel, R. L.; Bauer, H.; Schirmer, R. H. *Angew. Chem. Int. Ed.* **2005**, *44*, 690–715.

[59] Garrard, E. A.; Borman, E. C.; Cook, B. N.; Pike, E. J.; Alberg, D. G. *Org. Lett.* **2000**, *2*, 3639–3642.

[60] Czechowicz, J. A.; Wilhelm, A. K.; Spalding, M. D.; Larson, A. M.; Engel, L. K.; Alberg, D. G. *J. Org. Chem.* **2007**, *72*, 3689–3693.

[61] Duyzend, M. H.; Clark, C. T.; Simmons, S. L.; Johnson, W. B.; Larson, A. M.; Leconte, A. M.; Wills, A. W.; Ginder-Vogel, M.; Wilhelm, A. K.; Czechowicz, J. A.; Alberg, D. G. *J. Enzyme Inhib. Med. Chem.* **2012**, *27*, 784–794.

[62] Smith, H. K.; Bradley, M. *J. Comb. Chem.* **1999**, *1*, 326–332.

[63] Dixon, M. J.; Maurer, R. I.; Biggi, C.; Oyarzabal, J.; Essex, J. W.; Bradley, M. *Bioorg. Med. Chem.* **2005**, *13*, 4513–4526.

[64] Bandyopadhyay, K.; Banères, J.-L.; Martin, A.; Blonski, C.; Parello, J.; Gjerset, R. A. *Cell Cycle Georget. Tex* **2009**, *8*, 2779–2788.

[65] Alonso, V. L.; Serra, E. C. *J. Biomed. Biotechnol.* **2012**, *2012*.

[66] Zou, Y.; Wu, Z.; Sirisoma, N.; Woster, P. M.; Casero Jr., R. A.; Weiss, L. M.; Rattendi, D.; Lane, S.; Bacchi, C. J. *Bioorg. Med. Chem. Lett.* **2001**, *11*, 1613–1617.

[67] Kandpal, M.; Tekwani, B. L.; Chauhan, P. M.; Bhaduri, A. P. *Life Sci.* **1996**, *59*, PL75-80.

[68] Finlayson, R.; Pearce, A. N.; Page, M. J.; Kaiser, M.; Bourguet-Kondracki, M.-L.; Harper, J. L.; Webb, V. L.; Copp, B. R. *J. Nat. Prod.* **2011**, *74*, 888–892.

[69] Wang, J.; Kaiser, M.; Copp, B. R. *Mar. Drugs* **2014**, *12*, 3138–3160.

[70] Liew, L. P. P.; Kaiser, M.; Copp, B. R. *Bioorg. Med. Chem. Lett.* **2013**, *23*, 452–454.

[71] Ponasik, J. A.; Strickland, C.; Faerman, C.; Savvides, S.; Karplus, P. A.; Ganem, B. *Biochem. J.* **1995**, *311*, 371–375.

[72] O'Sullivan, M. C.; Zhou, Q. *Bioorg. Med. Chem. Lett.* **1995**, *5*, 1957–1960.

[73] Carter, N. S.; Fairlamb, A. H. *Nature* **1993**, *361*, 173–176.

[74] Tye, C. K.; Kasinathan, G.; Barrett, M. P.; Brun, R.; Doyle, V. E.; Fairlamb, A. H.; Weaver, R.; Gilbert, I. H. *Bioorg. Med. Chem. Lett.* **1998**, *8*, 811–816.

[75] O'Sullivan, M. C.; Zhou, Q.; Li, Z.; Durham, T. B.; Rattendi, D.; Lane, S.; Bacchi, C. J. *Bioorg. Med. Chem.* **1997**, *5*, 2145–2155.

[76] Chitkul, B.; Bradley, M. *Bioorg. Med. Chem. Lett.* **2000**, *10*, 2367–2369.

[77] Salmon, L.; Landry, V.; Melnyk, O.; Maes, L.; Sergheraert, C.; Davioud-Charvet, E. *Chem. Pharm. Bull. (Tokyo)* **1998**, *46*, 707–710.

[78] Bellevue, F. H.; Boahbedason, M.; Wu, R.; Woster, P. M.; Casero, R. A.; Rattendi, D.; Lane, S.; Bacchi, C. J. *Bioorg. Med. Chem. Lett.* **1996**, *6*, 2765–2770.

[79] Bi, X.; Lopez, C.; Bacchi, C. J.; Rattendi, D.; Woster, P. M. *Bioorg. Med. Chem. Lett.* **2006**, *16*, 3229–3232.

[80] Meiering, S.; Inhoff, O.; Mies, J.; Vincek, A.; Garcia, G.; Kramer, B.; Dormeyer, M.; Krauth-Siegel, R. L. *J. Med. Chem.* **2005**, *48*, 4793–4802.

[81] Ilhan, E.; Capan, G.; Ergenç, N.; Uzun, M.; Kiraz, M.; Kaya, D. *Farm. Soc. Chim. Ital. 1989* **1995**, *50*, 787–790.

[82] Coro, J.; Pérez, R.; Rodríguez, H.; Suárez, M.; Vega, C.; Rolón, M.; Montero, D.; Nogal, J. J.; Gómez-Barrio, A. *Bioorg. Med. Chem.* **2005**, *13*, 3413–3421.

[83] Coro, J.; Atherton, R.; Little, S.; Wharton, H.; Yardley, V.; Alvarez Jr., A.; Súarez, M.; Pérez, R.; Rodríguez, H. *Bioorg. Med. Chem. Lett.* **2006**, *16*, 1312–1315.

[84] Coro, J.; Little, S.; Yardley, V.; Suárez, M.; Rodríguez, H.; Martín, N.; Perez-Pineiro, R. *Arch. Pharm. (Weinheim)* **2008**, *341*, 708–713.

[85] Bitonti, A. J.; Dumont, J. A.; Bush, T. L.; Edwards, M. L.; Stemerick, D. M.; McCann, P. P.; Sjoerdsma, A. *Proc. Natl. Acad. Sci. U. S. A.* **1989**, *86*, 651–655.

[86] Edwards, M. L.; Snyder, R. D.; Stemerick, D. M. *J. Med. Chem.* **1991**, *34*, 2414–2420.

[87] Baumann, R. J.; Hanson, W. L.; McCann, P. P.; Sjoerdsma, A.; Bitonti, A. J. *Antimicrob. Agents Chemother.* **1990**, *34*, 722–727.

[88] Seiler, N.; Duranton, B.; Raul, F. *Prog. Drug Res. Fortschritte Arzneimittelforschung Prog. Rech. Pharm.* **2002**, *59*, 1–40.

[89] Mukhopadhyay, R.; Madhubala, R. *Pharmacol. Res.* **1993**, *28*, 359–365.

[90] Majumder, S.; Kierszenbaum, F. *Antimicrob. Agents Chemother.* **1993**, *37*, 2235–2238.

[91] Majumder, S.; Kierszenbaum, F. *Mol. Biochem. Parasitol.* **1993**, *60*, 231–239.

[92] Mukhopadhyay, R.; Madhubala, R. *Exp. Parasitol.* **1995**, *81*, 39–46.

[93] Bonnet, B.; Soullez, D.; Davioud-Charvet, E.; Landry, V.; Horvath, D.; Sergheraert, C. *Bioorg. Med. Chem.* **1997**, *5*, 1249–1256.

[94] Olmo, F.; Marín, C.; Clares, M. P.; Blasco, S.; Albelda, M. T.; Soriano, C.; Gutiérrez-Sánchez, R.; Arrebola-Vargas, F.; García-España, E.; Sánchez-Moreno, M. *Eur. J. Med. Chem.* **2013**, *70*, 189–198.

[95] Marín, C.; Clares, M. P.; Ramírez-Macías, I.; Blasco, S.; Olmo, F.; Soriano, C.; Verdejo, B.; Rosales, M. J.; Gomez-Herrera, D.; García-España, E.; Sánchez-Moreno, M. *Eur. J. Med. Chem.* **2013**, *62*, 466–477.

[96] Olmo, F.; Costas, M.; Marín, C.; Rosales, M. J.; Martín-Escolano, R.; Cussó, O.; Gutierrez-Sánchez, R.; Ribas, X.; Sánchez-Moreno, M. *J. Chemother.* **2016**, *0*, 1–11.

[97] Bond, C. S.; Zhang, Y.; Berriman, M.; Cunningham, M. L.; Fairlamb, A. H.; Hunter, W. N. *Structure* **1999**, *7*, 81–89.

[98] Hamilton, C. J.; Saravanamuthu, A.; Fairlamb, A. H.; Eggleston, I. M. *Bioorg. Med. Chem.* **2003**, *11*, 3683–3693.

[99] Hamilton, C. J.; Saravanamuthu, A.; Poupat, C.; Fairlamb, A. H.; Eggleston, I. M. *Bioorg. Med. Chem.* **2006**, *14*, 2266–2278.

[100] Salmon, L.; Landry, V.; Melnyk, O.; Maes, L.; Sergheraert, C.; Davioud-Charvet, E. *Chem. Pharm. Bull. (Tokyo)* **1998**, *46*, 707–710.

[101] Tomita, S.; Abdalla, M. O. A.; Fujiwara, S.; Yamamoto, T.; Iwase, H.; Nakao, M.; Saitoh, N. *Wiley Interdiscip. Rev. RNA* **2016**.

[102] Kowalski, A.; Pałyga, J. *Biol. Cell* **2016**, n/a-n/a.

[103] Grunstein, M. *Nature* **1997**, *389*, 349–352.

[104] Legube, G.; Trouche, D. *EMBO Rep.* **2003**, *4*, 944–947.

[105] Marmorstein, R.; Roth, S. Y. *Curr. Opin. Genet. Dev.* **2001**, *11*, 155–161.

[106] Cullis, P. M.; Wolfenden, R.; Cousens, L. S.; Alberts, B. M. *J. Biol. Chem.* **1982**, *257*, 12165–12169.

[107] Wapenaar, H.; Dekker, F. J. *Clin. Epigenetics* **2016**, *8*, 59.

[108] Roblot, G.; Wylde, R.; Martin, A.; Parello, J. *Tetrahedron* **1993**, *49*, 6381–6398.

[109] Bandyopadhyay, K.; Banères, J.-L.; Martin, A.; Blonski, C.; Parello, J.; Gjerset, R. A. *Cell Cycle Georget. Tex* **2009**, *8*, 2779–2788.

[110] Kwie, F. H. A.; Briet, M.; Soupaya, D.; Hoffmann, P.; Maturano, M.; Rodriguez, F.; Blonski, C.; Lherbet, C.; Baudoin-Dehoux, C. *Chem. Biol. Drug Des.* **2011**, *77*, 86–92.

[111] Ivens, A. C.; Peacock, C. S.; Worthey, E. A.; Murphy, L.; Aggarwal, G.; Berriman, M.; Sisk, E.; Rajandream, M.-A.; Adlem, E.; Aert, R.; Anupama, A.; Apostolou, Z.; Attipoe, P.; Bason, N.; Bauser, C.; Beck, A.; Beverley, S. M.; Bianchettin, G.; Borzym, K.; Bothe, G.; Bruschi, C. V.; Collins, M.; Cadag, E.; Ciarloni, L.; Clayton, C.; Coulson, R. M. R.; Cronin, A.; Cruz, A. K.; Davies, R. M.; Gaudenzi, J. D.; Dobson, D. E.; Duesterhoeft, A.; Fazelina, G.; Fosker, N.; Frasch, A. C.; Fraser, A.; Fuchs, M.; Gabel, C.; Goble, A.; Goffeau, A.; Harris, D.; Hertz-Fowler, C.; Hilbert, H.; Horn, D.; Huang, Y.; Klages, S.; Knights, A.; Kube, M.; Larke, N.; Litvin, L.; Lord, A.; Louie, T.; Marra, M.; Masuy, D.; Matthews, K.; Michaeli, S.; Mottram, J. C.; Müller-Auer, S.; Munden, H.; Nelson, S.; Norbertczak, H.; Oliver, K.; O'Neil, S.; Pentony, M.; Pohl, T. M.; Price, C.; Purnelle, B.; Quail, M. A.; Rabbinowitsch, E.; Reinhardt, R.; Rieger, M.; Rinta, J.; Robben, J.; Robertson, L.; Ruiz, J. C.; Rutter, S.; Saunders, D.; Schäfer, M.; Schein, J.; Schwartz, D. C.; Seeger, K.; Seyler, A.; Sharp, S.; Shin, H.; Sivam, D.; Squares, R.; Squares, S.; Tosato, V.; Vogt, C.; Volckaert, G.; Wambutt, R.; Warren, T.; Wedler, H.; Woodward, J.; Zhou, S.; Zimmermann, W.; Smith, D. F.; Blackwell, J. M.; Stuart, K. D.; Barrell, B.; Myler, P. J. *Science* **2005**, *309*, 436–442.

[112] Hammarton, T. C.; Mottram, J. C.; Doerig, C. *Prog. Cell Cycle Res.* **2003**, *5*, 91–101.

[113] Kawahara, T.; Siegel, T. N.; Ingram, A. K.; Alsford, S.; Cross, G. A. M.; Horn, D. *Mol. Microbiol.* **2008**, *69*, 1054–1068.

[114] Maity, A. K.; Saha, P. *FEMS Microbiol. Lett.* **2012**, *336*, 57–63.

[115] Sagar, V.; Zheng, W.; Thompson, P. R.; Cole, P. A. *Bioorg. Med. Chem.* **2004**, *12*, 3383–3390.

[116] Ren, Y. *Med. Chem.* **2014**, *4*.

[117] Riss, T. L.; Moravec, R. A.; Niles, A. L.; Duellman, S.; Benink, H. A.; Worzella, T. J.; Minor, L. In *Assay Guidance Manual*; Sittampalam, G. S.; Coussens, N. P.; Nelson, H.; Arkin, M.; Auld, D.; Austin, C.; Bejcek, B.; Glicksman, M.; Inglese, J.; Iversen, P. W.; Li, Z.; McGee, J.; McManus, O.; Minor, L.; Napper, A.; Peltier, J. M.; Riss, T.; Trask, O. J.; Weidner, J., Eds.; Eli Lilly & Company and the National Center for Advancing Translational Sciences: Bethesda (MD), **2004**.

[118] Cheikh-Ali, Z.; Caron, J.; Cojean, S.; Bories, C.; Couvreur, P.; Loiseau, P. M.; Desmaële, D.; Poupon, E.; Champy, P. *ChemMedChem* **2015**, *10*, 411–418.

[119] Thompson, P. R.; Wang, D.; Wang, L.; Fulco, M.; Pediconi, N.; Zhang, D.; An, W.; Ge, Q.; Roeder, R. G.; Wong, J.; Levrero, M.; Sartorelli, V.; Cotter, R. J.; Cole, P. A. *Nat. Struct. Mol. Biol.* **2004**, *11*, 308–315.

[120] Trievel, R. C.; Li, F. Y.; Marmorstein, R. *Anal. Biochem.* **2000**, *287*, 319–328.

[121] Bacchi, C. J.; Nathan, H. C.; Hutner, S. H.; McCann, P. P.; Sjoerdsma, A. *Science* **1980**, *210*, 332–334.

[122] Thibault, B.; Clement, E.; Zorza, G.; Meignan, S.; Delord, J.-P.; Couderc, B.; Bailly, C.; Narducci, F.; Vandenberghe, I.; Kruczynski, A.; Guilbaud, N.; Ferré, P.; Annereau, J.-P. *Cancer Lett.* **2016**, *370*, 10–18.

[123] Chadwick, J.; Jones, M.; Mercer, A. E.; Stocks, P. A.; Ward, S. A.; Park, B. K.; O'Neill, P. M. *Bioorg. Med. Chem.* **2010**, *18*, 2586–2597.

[124] Geall, A. J.; Blagbrough, I. S. *Tetrahedron* **2000**, *56*, 2449–2460.

[125] Blagbrough, I. S.; Geall, A. J. *Tetrahedron Lett.* **1998**, *39*, 439–442.

[126] Guminski, Y.; Grousseaud, M.; Cugnasse, S.; Brel, V.; Annereau, J.-P.; Vispé, S.; Guilbaud, N.; Barret, J.-M.; Bailly, C.; Imbert, T. *Bioorg. Med. Chem. Lett.* **2009**, *19*, 2474–2477.

[127] Audisio, D.; Messaoudi, S.; Cojean, S.; Peyrat, J.-F.; Brion, J.-D.; Bories, C.; Huteau, F.; Loiseau, P. M.; Alami, M. *Eur. J. Med. Chem.* **2012**, *52*, 44.

[128] Martin, R. J. *Vet. J. Lond. Engl. 1997* **1997**, *154*, 11–34.

[129] Huczyński, A.; Janczak, J.; Antoszczak, M.; Stefańska, J.; Brzezinski, B. *J. Mol. Struct.* **2012**, *1022*, 197–203.

[130] Augustynowicz-Kopeć, E.; Zwolska, Z.; Orzeszko, A.; Kazimierczuk, Z. *Acta Pol. Pharm.* **2008**, *65*, 435–439.

[131] Verschueren, K. H. G.; Pumpor, K.; Anemüller, S.; Chen, S.; Mesters, J. R.; Hilgenfeld, R. *Chem. Biol.* **2008**, *15*, 597–606.

[132] Fu, J.; Yang, Y.; Zhang, X.-W.; Mao, W.-J.; Zhang, Z.-M.; Zhu, H.-L. *Bioorg. Med. Chem.* **2010**, *18*, 8457–8462.

[133] Becerra, M. C.; Guiñazú, N.; Hergert, L. Y.; Pellegrini, A.; Mazzieri, M. R.; Gea, S.; Albesa, I. *Exp. Parasitol.* **2012**, *131*, 57–62.

[134] Testa, B.; Mayer, J. M. In *Hydrolysis in Drug and Prodrug Metabolism*; Verlag Helvetica Chimica Acta, **2003**; pp. 419–534.

[135] Ghosh, A. K.; Brindisi, M. *J. Med. Chem.* **2015**, *58*, 2895–2940.

[136] Vacondio, F.; Silva, C.; Mor, M.; Testa, B. *Drug Metab. Rev.* **2010**, *42*, 551–589.

[137] Le Quesne, S. A.; Fairlamb, A. H. *Biochem. J.* **1996**, *316 (Pt 2)*, 481–486.

[138] Basselin, M.; Coombs, G. H.; Barrett, M. P. *Mol. Biochem. Parasitol.* **2000**, *109*, 37–46.

[139] Xiao, Y.; McCloskey, D. E.; Phillips, M. A. *Eukaryot. Cell* **2009**, *8*, 747–755.

[140] Boido, A.; Vazzana, I.; Mattioli, F.; Sparatore, F. *Farmaco* **2003**, *58*, 33.

[141] Tetko, I. V.; Gasteiger, J.; Todeschini, R.; Mauri, A.; Livingstone, D.; Ertl, P.; Palyulin, V. A.; Radchenko, E. V.; Zefirov, N. S.; Makarenko, A. S.; Tanchuk, V. Y.; Prokopenko, V. V. *J. Comput. Aided Mol. Des.* **2005**, *19*, 453–463.

[142] Nishimura, K.; Yanase, T.; Araki, N.; Ohnishi, Y.; Kozaki, S.; Shima, K.; Asakura, M.; Samosomsuk, W.; Yamasaki, S. *J. Parasitol.* **2006**, *92*, 211–217.

[143] Lueder, D. V.; Phillips, M. A. *J. Biol. Chem.* **1996**, *271*, 17485–17490.

[144] Stoll, V. S.; Simpson, S. J.; Krauth-Siegel, R. L.; Walsh, C. T.; Pai, E. F. *Biochemistry (Mosc.)* **1997**, *36*, 6437–6447.

[145] Sullivan, F. X.; Sobolov, S. B.; Bradley, M.; Walsh, C. T. *Biochemistry (Mosc.)* **1991**, *30*, 2761–2767.7.

[146] Baumann, R. J.; Hanson, W. L.; McCann, P. P.; Sjoerdsma, A.; Bitonti, A. J. *Antimicrob. Agents Chemother.* **1990**, *34*, 722–727.

[147] Bazzini, P.; Wermuth, C. G. In *The Practice of Medicinal Chemistry (Third Edition)*; Academic Press: New York, **2008**; pp. 429–463.

[148] Mann, A. In *The Practice of Medicinal Chemistry (Third Edition)*; Academic Press: New York, **2008**; pp. 363–379.

[149] Lakanen, J. R.; Coward, J. K.; Pegg, A. E. *J. Med. Chem.* **1992**, *35*, 724–734.

[150] Järvinen, A.; Grigorenko, N.; Khomutov, A. R.; Hyvönen, M. T.; Uimari, A.; Vepsäläinen, J.; Sinervirta, R.; Keinänen, T. A.; Vujcic, S.; Alhonen, L.; Porter, C. W.; Jänne, J. *J. Biol. Chem.* **2005**, *280*, 6595–6601.

[151] Seiler, N.; Delcros, J. G.; Moulinoux, J. P. *Int. J. Biochem. Cell Biol.* **1996**, *28*, 843–861.

[152] Belting, M.; Mani, K.; Jönsson, M.; Cheng, F.; Sandgren, S.; Jonsson, S.; Ding, K.; Delcros, J.-G.; Fransson, L.-Å. *J. Biol. Chem.* **2003**, *278*, 47181–47189.

[153] Soulet, D.; Gagnon, B.; Rivest, S.; Audette, M.; Poulin, R. *J. Biol. Chem.* **2004**, *279*, 49355–49366.

[154] Mitchell, J. L. A.; Simkus, C. L.; Thane, T. K.; Tokarz, P.; Bonar, M. M.; Frydman, B.; Valasinas, A. L.; Reddy, V. K.; Marton, L. J. *Biochem. J.* **2004**, *384*, 271–279.

[155] Pegg, A. E. *Biochem. J.* **1986**, *234*, 249–262.

[156] Persson, K.; Aslund, L.; Grahn, B.; Hanke, J.; Heby, O. *Biochem. J.* **1998**, *333 (Pt 3)*, 527–537.

[157] Hamana, K.; Matsuzaki, S. *FEMS Microbiol. Lett.* **1987**, *41*, 211–215.

[158] Carrillo, C.; Canepa, G. E.; Algranati, I. D.; Pereira, C. A. *Biochem. Biophys. Res. Commun.* **2006**, *344*, 936–940.

[159] Ariyanayagam, M. R.; Fairlamb, A. H. *Mol. Biochem. Parasitol.* **1997**, *84*, 111–121.

[160] Reigada, C.; Sayé, M.; Vera, E. V.; Balcazar, D.; Fraccaroli, L.; Carrillo, C.; Miranda, M. R.; Pereira, C. A. *J. Membr. Biol.* **2016**.

[161] Balaña-Fouce, R.; Ordóñez, D.; Alunda, J. M. *Mol. Biochem. Parasitol.* **1989**, *35*, 43–50.

[162] Kandpal, M.; Tekwani, B. L. *Life Sci.* **1997**, *60*, 1793–1801.

[163] Hasne, M.-P.; Ullman, B. *J. Biol. Chem.* **2005**, *280*, 15188–15194.

[164] Wallace, H. M.; Keir, H. M. *Biochem. J.* **1982**, *202*, 785–790.

[165] Phanstiel, O.; Kaur, N.; Delcros, J.-G. *Amino Acids* **2007**, *33*, 305–313.

[166] Cullis, P. M.; Green, R. E.; Merson-Davies, L.; Travis, N. *Chem. Biol.* **1999**, *6*, 717–729.

[167] Kruczynski, A.; Pillon, A.; Créancier, L.; Vandenberghe, I.; Gomes, B.; Brel, V.; Fournier, E.; Annereau, J.-P.; Currie, E.; Guminski, Y.; Bonnet, D.; Bailly, C.; Guilbaud, N. *Leukemia* **2013**, *27*, 2139–2148.

[168] Barret, J.-M.; Kruczynski, A.; Vispé, S.; Annereau, J.-P.; Brel, V.; Guminski, Y.; Delcros, J.-G.; Lansiaux, A.; Guilbaud, N.; Imbert, T.; Bailly, C. *Cancer Res.* **2008**, *68*, 9845–9853.

[169] Opperdoes, F. R.; Coombs, G. H. *Trends Parasitol.* **2007**, *23*, 149–158.

[170] Shaked-Mishan, P.; Suter-Grotemeyer, M.; Yoel-Almagor, T.; Holland, N.; Zilberstein, D.; Rentsch, D. *Mol. Microbiol.* **2006**, *60*, 30–38.

[171] Persch, E.; Bryson, S.; Todoroff, N. K.; Eberle, C.; Thelemann, J.; Dirdjaja, N.; Kaiser, M.; Weber, M.; Derbani, H.; Brun, R.; Schneider, G.; Pai, E. F.; Krauth-Siegel, R. L.; Diederich, F. *ChemMedChem* **2014**, *8*, 1880.

ÉCOLE DOCTORALE
Sciences chimiques : molécules, matériaux, instrumentation et biosystèmes

Titre : Synthèse et évaluation biologique de dérivés polyamines en tant qu'agents antikinétoplastidés

Mots clés : Polyamine, Kinétoplastidés, *Trypanosoma, Leishmania*, Chimie Médicinale

Résumé : Ce projet d'interface Chimie/Biologie repose sur les expertises complémentaires de deux équipes. Il concerne la conception et le développement d'inhibiteurs dirigés contre les Kinétoplastidés (trypanosomes, leishmanies). Il est en effet urgent de développer de nouvelles stratégies thérapeutiques pour répondre à la chimiorésistance et à la toxicité des médicaments actuellement utilisés contre ces parasites.

Le métabolisme et le transport des polyamines étant essentiel chez les parasites, ils constituent des cibles thérapeutiques d'intérêt contre les Kinétoplastidés.

Le projet intègre la synthèse de nouveaux dérivés polyamines spécifiques des parasites, l'évaluation sur des modèles *in vitro* de leishmaniose et de trypanosomose africaine, ainsi qu'une évaluation sur trypanothione réductase. La mise au point d'une méthode de quantification du transport de polyamine a également été initiée.

Cinquante-quatre composés, répartis en trois séries chimiques, ont été synthétisés et évalués. Un grand nombre d'entre eux présentent des activités antiparasitaires de l'ordre du micromolaire et des évaluations *in vivo* sont actuellement en cours avec le composé le plus prometteur.

Title : Design, synthesis and biological evaluation of new polyamine derivatives as antikinetoplastids agents.

Keywords : Polyamine, Kinetoplastid, *Trypanosoma, Leishmania*, Medicinal Chemistry

Abstract : This project is at the interface of chemistry and biology and relies on the expertise of two different teams. This thesis involves the design and development of inhibitors directed against Kinetoplastids. It is urgent to develop new therapeutic strategies to respond to drug resistance and toxicity of currently used drugs against these parasites.
Polyamine metabolism and transporter have been demonstrated as essential for parasite grothw.

Therefore, these systems are potential drug targets for development of antikinetoplastid compounds. We chose to synthesize polyamine derivatives and evaluate their biological activity against Kinetoplatids.
Fifty-four compounds, divided into three chemical series, have been synthesized and evaluated. Many have shown a micromolar biological activity in vitro against parasite. In vivo evaluation is foreseen for the most promising derivative.

Université Paris-Saclay
Espace Technologique / Immeuble Discovery
Route de l'Orme aux Merisiers RD 128 / 91190 Saint-Aubin, France